Pont, *Chemistry Today* **2009**, *87*

Members of the Jury

- **Prof. dr. ir. Paul Van Der Meeren** (Chairman)

  Department of Applied Analytical and Physical Chemistry

  Faculty of Bioscience Engineering, Ghent University

- **Prof. dr. Ian Baxendale**

  Department of Chemistry

  University of Durham

- **Prof. dr. Timothy Noël**

  Micro Flow Chemistry and Process Technology

  Department of Chemical Engineering and Chemistry

  Eindhoven University of Technology

  Department of Organic and Macromolecular Chemistry

  Faculty of Science, Ghent University

- **dr. Bert Metten**

  Ajinomoto OmniChem, Wetteren

- **Prof. dr. ir. Sven Mangelinckx**

  Department of Sustainable Organic Chemistry and Technology

  Faculty of Bioscience Engineering, Ghent University

- **Prof. dr. ir. Bruno De Meulenaer**

  Department of Food Safety and Food Quality

  Faculty of Bioscience Engineering, Ghent University

Promoter

Prof. dr. ir. Chris Stevens

Department of Sustainable Organic Chemistry and Technology

Faculty of Bioscience Engineering, Ghent University

Dean of the Faculty

Prof. dr. ir. Guido Van Huylenbroeck

Rector of the University

Prof. dr. Anne De Paepe

UNIVERSITEIT
GENT

ir. Frederik Van Waes

Micro- and millireactor technology for challenging batch reactions in organic chemistry

Thesis submitted in fulfillment of the requirements for the degree of Doctor (PhD) in Applied Biological Sciences: Chemistry and Bioprocess Technology

Dutch translation of the title: 'Micro- en millireactortechnologie voor uitdagende batch reacties in de organische chemie'

Cover illustration: KiloFlow® (Chemtrix)

The author: The promoter:

ir. Frederik Van Waes   Prof. dr. ir. C. Stevens

Woord vooraf

Het schrijven van het woord vooraf vormt typisch het sluitstuk van een doctoraat. Ook in dit doctoraat is het woord vooraf het laatste hoofdstuk(je) dat geschreven wordt. Met dit woord vooraf sluit ik negen mooie jaren aan het 'boerekot' af. Negen jaren die voorbij gevlogen zijn. Negen jaren die uiteindelijk geleid hebben tot dit werk.

In de eerste plaats wil ik mijn promotor, prof. Chris Stevens, bedanken om mij de kans te bieden mij te verdiepen in de wereld van microreactortechnologie. Steeds kon ik bij u terecht als de chemie of technologie weer eens tegenspartelde. Bedankt voor het gestelde vertrouwen, uw motiverende input en het vele werk achter de schermen!

I also would like to thank the members of the examination committee: Prof. dr. ir. Paul Van Der Meeren, Prof. dr. Ian Baxendale, Prof. dr. Timothy Noël, dr. Bert Metten, Prof. dr. ir. Sven Mangelinckx and Prof. dr. ir. Bruno De Meulenaer for the critical reading of my thesis and the fruitful discussions. It definitely improved the quality of this work.

Iets wat me altijd zal bijblijven, is de unieke sfeer in de labo's op het 4^e en 5^e van de B-blok van het 'boerekot'. Bij de start van mijn doctoraat werd ik op het 4^e gedropt bij een aantal doorgewinterde doctoraatsstudenten. Vaak werd met enig leedvermaak (en soms ook wel wat medelijden) toegekeken hoe ik al na 15 minuten mijn volledige dagplanning overboord mocht gooien aangezien ik de rest van de dag bezig was met het uitkuisen van de microreactor. Er ging geen dag voorbij waarbij er niet gelachen werd of één of andere quizvraag de revue passeerde. Alle collega's van de afgelopen vier jaar bij naam noemen zou mij te ver leiden maar een aantal collega's verdienen een speciaal dankwoordje. Matthias, als indringer van de Sterre kwam je in ons labo terecht maar al snel ontdekte ik dat we twee passies gemeen hadden, naast chemie natuurlijk ☺: mountainbike en bouwen. Bedankt voor de ontspannende ritjes mountainbike en de vele discussies over onze bouwprojecten! Koen, één blik wisselen op de vooravond van 1 april was genoeg om ervoor te zorgen dat sommige collega's de volgende dag met enige vertraging aan hun werkdag moesten beginnen. We deelden vaak dezelfde chemische frustraties die al snel vergeten werden bij een potje snooker of minivoetbal. Merci é Koen! Tamara, de kat - hond discussie zal eeuwig blijven doorgaan vermoed ik en onze weddenschappen zal ik niet snel vergeten! Sofie, als helft van mijn meest memorabele thesisduo verdien je ook je plaatsje in dit woord vooraf. Bedankt voor je nooit aflatende enthousiasme. Koen, Wouter, Bart, Thomas, Jeroen, Karel, Nils, Kevin, Rodrigo, Eli en invallers, bedankt om met de Synthesizers elk jaar

onze ranking in de minivoetbal te verdedigen! Ans, Els, Pieter en Andy, bedankt voor de hulp bij de administratieve en technische beslommeringen.

Bert (Ajinomoto OmniChem) en Wim (Agfa-Gevaert), bedankt voor de aangename samenwerking. We hebben een aantal mooie resultaten bereikt! *Gijs (Chemtrix) and Mark (Uniqsis), thanks for answering all my questions with regard to the flow equipment and for sending me some nice illustrations.*

Een dikke merci ook aan de vrienden van het thuisfront. Alexander, we doen niets liever dan de zondagochtend door de modder crossen met de mountainbike. Na de bouw pikken we dit zeker weer op! Stefaan, bedankt voor de ontspannende partijtjes beachvolley en snooker. Lien en Stephanie, bedankt voor de gezellige (spelletjes)avonden bij een bbq'tje.

Mama en papa, bedankt voor het warme nest waarin ik mocht opgroeien en jullie onvoorwaardelijke steun. Papa, je bent een gedroomde hulp op de werf aangezien je sneller metst dan je schaduw en (zo goed als) alle hoekjes zet ☺. Mama, achter elke sterke man staat een sterke vrouw en dat is in dit geval meer dan waar! Delphine, als 'niet-wetenschappelijke' tegenpool kan ik mij geen betere zus voorstellen. Ook mijn schoonfamilie wil ik bedanken voor hun steun en gastvrijheid.

Tenslotte mag ook mijn allerliefste schat, Stefanie, niet ontbreken in dit woord vooraf. Samen een doctoraat afleggen en tussendoor ook nog eens verder werken aan ons huisje, het was niet altijd gemakkelijk maar toch zijn we erin geslaagd! Nu je doctoraat binnen is, heb je geen reden meer om tegen te pruttelen als we om 6u naar de werf moeten vertrekken ☺. Bedankt voor je steun, luisterend oor en geduld! Ik kijk er enorm naar uit om verder aan onze toekomst te bouwen, letterlijk en figuurlijk!

<div align="right">

Frederik Van Waes

September 2014

</div>

Table of contents

List of abbreviations

AiBN	azobisisobutyronitrile
AIHA	American industrial hygiene association®
BPR	back pressure regulator
BPO	benzoyl peroxide
BtH	1*H*-benzotriazole
Cbz	carbobenzyloxy
Cbz-AA	Cbz-protected amino acid
Cbz-AA-Bt	Cbz-protected, Bt-activated amino acid
CL	clogging
CPME	cyclopentyl methyl ether
CRM	complex reaction mixture
CSTR	continuous stirred tank reactor
Da	Damköhler number
DABCO	1,4-diazobicyclo[2.2.2]octane
Dibal-H	diisobutylaluminum hydride
DIPE	diisopropyl ether
DIPEA	diisopropylethylamine
DMAP	4-dimethylaminopyridine
DME	1,2-dimethoxyethane
DMSO	dimethyl sulfoxide
EDTA	ethylenediaminetetraacetic acid
EOF	electroosmotic flow
ETFE	ethylene tetrafluoroethylene
EWG	electron withdrawing group
FAME	fatty acid methyl esters
FEP	fluorinated ethylene propylene
FLLEX	flow liquid liquid extraction

Fo	Fourier number
GC	gas chromatography
HOBt	1-hydroxybenzotriazole
ID	inner diameter
IMRET	International Conference on Microreaction Technology
LC	liquid chromatography
NMP	N-methyl-2-pyrrolidone
NMR	nuclear magnetic resonance
MAO-I	monoamine oxidase inhibitor
MicroChemTec	Industrial Platform of Modular Micro Chemical Technology
MNU	N-methyl-N-nitrosourea
MR	microreactor
MsCl	methanesulfonyl chloride
MTBE	methyl t-butyl ether
OD	outer diameter
on.	overnight
PDMS	polydimethylsiloxane
PE	petroleum ether
PET	polyethylene terephthalate
PEEK	polyether ether ketone
PFA	perfluoroalkoxy
PPS	polyphenylene sulfide
PS	polymer-supported
PTC	phase transfer catalyst
PTFE	polytetrafluoroethylene
Re	Reynolds number
rt	room temperature
RT	residence time
SPSS	solid phase peptide synthesis
STBE	solketal t-butyl ether
TBABr	tetrabutylammonium bromide
TEA	triethylamine

TFA	trifluoroacetic acid
TFAA	trifluoroacetic anhydride
THF	tetrahydrofuran
TLC	thin layer chromatography
t_{mix}	mixing time
TMSOTf	trimethylsilyl trifluoromethanesulfonate

Chapter 1

Introduction and goals

Organic chemists have been using more or less the same reaction equipment over the last two centuries. The glassware used in the time of Williamson to synthesize ethers is comparable to current laboratory glassware. The round-bottom flask and the large-scale batch reactor were and are still common in the fine chemical and pharmaceutical industry. Although chemists have been able to synthesize a broad range of molecules with these traditional methods, many batch processes have important drawbacks. These can be related to energy or time efficiency, the generation of waste, the formation of side products, poor selectivity and insufficient conversion.

As the fine chemical and pharmaceutical industry is working hard towards more sustainable production and the minimization of the ecological footprint of their processes, many attempts have been made to increase the efficiency of their processes (e.g. multicomponent reactions, homogeneous and heterogeneous catalysis, etc.). Microreactor technology is a rather new type of technology which has received increased interest in the last decennia from both the chemical process industry as well as in academic research.

Watts *et al.* define microreactor technology as "the continuous processing of reactions within well defined reaction channels, where dimensions are typically of the order of less than 1000 μm".[1] Microreactor technology started in the field of inkjet printers and heat exchangers (Figure 1.1).[2] In 1997, the first International Conference on Microreaction Technology (IMRET1) took place in Frankfurt (Germany) and in 2001, the Industrial Platform of Modular Micro Chemical Technology (MicroChemTec) was founded (Figure 1.1). All these initiatives resulted in an increased interest for this emerging technology.[3]
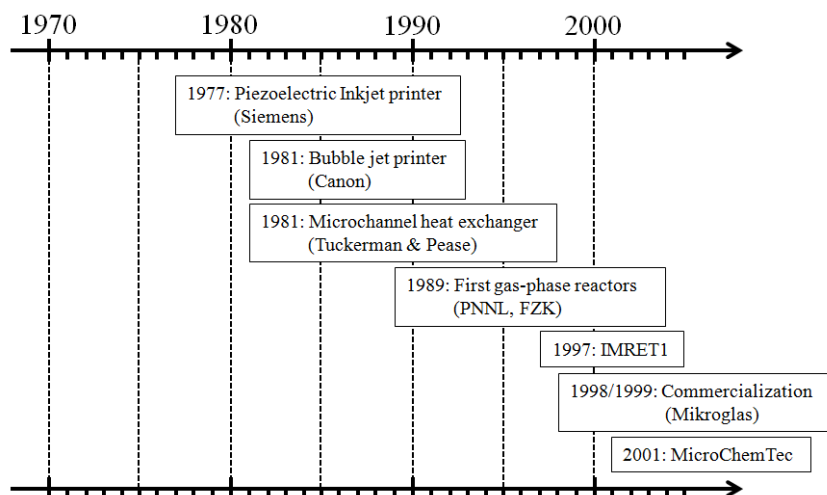
Figure 1.1. Brief history of microfluidics (adapted from Hessel and Noël)[2]

The first example of organic synthesis in a microreactor was published by Harrison *et al.* in 1997.[4,5] These authors reported the use of a microfabricated glass chip to synthesize a red dye (Scheme 1.1). Since then, numereous examples of the application of microreactors in organic synthesis have been reported in literature (Figure 1.2).[6–19]
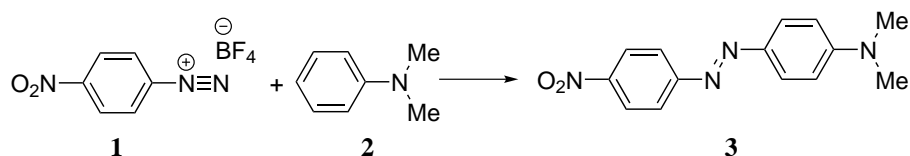
Scheme 1.1. First example of organic chemistry in a microreactor
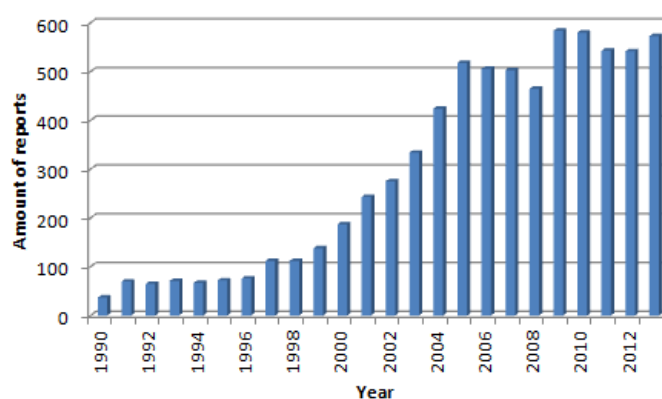
Figure 1.2. Amount of reports about microreactors (source: SciFinder®, research topic: microreactor)

Continuous processing is common in bulk chemical production but the fine chemical and pharmaceutical industry relies frequently on stirred tank reactors to perform reactions.[10,20]

Although batch technology has proven its value due to its flexibility and versatility, industrial interest in microreactor technology is growing as it provides a series of well-known advantages compared to conventional batch technology.[10,21,22]

Microreactors are characterized by a large surface-to-volume ratio, enabling efficient heating or cooling of the reaction mixture.[10,22–24] Reactions can be run at near isothermal conditions preventing the formation of hot spots or thermal runaway. Mixing is very fast due to the limited diffusion distances within the microreactor channels and the small and closed hold-up volume allows the safe manipulation of reactive and toxic reagents. Moreover, reactive and unstable intermediates can be generated and used *in situ* due to the excellent control of the reaction time. In a traditional batch environment, a chemical process is developed at small scale in the laboratory and successively conducted on a larger scale and this scale-up is often ambiguous.[25,26] The main scale-up issues are related with heat and mass transport and can result in an increased formation of byproducts and lower yields.[27] Scale-up of a continuous flow process is straightforward using the scale-out or numbering up principle.[22]

In 2005, Roberge *et al.* stated that about 44% of the reactions in the fine chemical and pharmaceutical industry could benefit from microreactor technology.[28] However, the majority of these reactions deal with solids and hence cannot be performed in a conventional microreactor due to the risk of clogging the channels. Nowadays, examples of solid handling under continuous flow conditions using acoustic irradiation have been published and dedicated microreactors, e.g. agitated cell reactors, have been developed.[29–32]

Recently, the importance of continuous processing was acknowledged by the American Chemical Society Green Chemistry Institute. They established a roundtable to encourage the integration of green chemistry and engineering into the pharmaceutical industry. The roundtable identified a list of key research areas and continuous processing was ranked as the primary key area.[33–35] Several green chemistry principles can benefit from continuous flow technology leading to a more sustainable production.[34]

As stated above, microreactor technology provides a number of significant advantages compared to traditional batch technology. In this PhD thesis, a number of generic reactions will be fundamentally studied in order to be able to perform these under microreactor conditions. The research will focus on industrially relevant reactions which are difficult to scale-up and could benefit from the intrinsic characteristics (increased mass and heat transfer, small hold-up volume, etc.) of microreactor technology.

In a first part of this thesis, the catalyst-free, continuous flow condensation of acid chlorides **4** and alcohols **5** will be evaluated (Scheme 1.2).
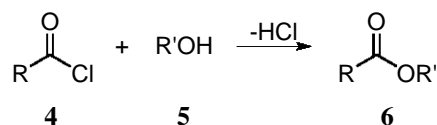
Scheme 1.2. Condensation of acid chlorides and alcohols

This straightforward reaction is well-known in batch and has already been performed under continuous flow conditions using a base to scavenge the formed HCl.[36–38] However, aqueous work up of the reaction mixture was required and hence, a lot of waste was generated leading to an increased process cost and making the process less sustainable. In order to increase the efficiency of this reaction, the catalyst-free condensation of acid chlorides and alcohols will be evaluated.

The reaction will be performed under continuous flow conditions in order to be able to use high temperature - high pressure conditions.[39–41] The influence of the reaction temperature, residence time and stoichiometric ratio will be evaluated. If possible, the reaction will be performed solventless in order to increase the overall sustainability of the process. Initial optimization experiments will be performed on a Labtrix® Start microreactor and a scale-up to the KiloFlow® reactor will be evaluated. At larger scale, efforts will be made to recuperate the formed HCl.

In a second part, the biphasic reaction between methyl sulfones and hypobromite will be evaluated (Scheme 1.3).
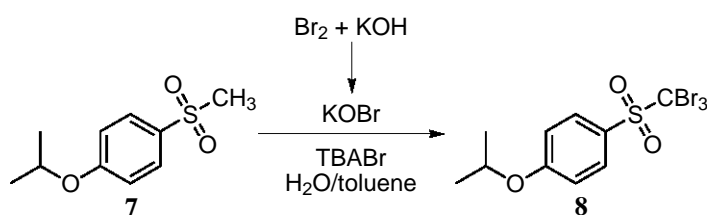
Scheme 1.3. Bromination of 4-isopropoxyphenyl methyl sulfone **7**

Industry has a lot of interest in performing this reaction under continuous flow conditions because of the instability of the hypobromite solution as well as the safety issues related with the manipulation of Br_2. Moreover, scale-up of a biphasic reaction in a batch reactor is ambiguous.

Hypobromite is formed through reaction of potassium hydroxide with Br_2 but the formed hypobromite is unstable and degrades rapidly, especially at higher temperatures (>5°C):

$$Br_2 + 2KOH \longrightarrow KBr + KOBr + H_2O \tag{1.1}$$

$$3KOBr \longrightarrow 2KBr + KBrO_3 \tag{1.2}$$

$$2KOBr \longrightarrow 2KBr + O_2 \tag{1.3}$$
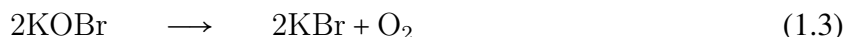
Moreover, Br_2 is a corrosive and toxic product, limiting the materials that can be used for the reactor and requiring several safety precautions. Use of a continuous flow reactor can reduce the safety hazards due to the small and closed hold-up volume. Beside, continuous flow reactors have excellent heat and mass transfer characteristics which can provide a significant improvement for a biphasic reaction.[38,42–47]

First, the KOBr-solution will be synthesized in batch and the bromination of methyl sulfones with KOBr will be evaluated under continuous flow conditions. Two different reactor systems will be tested: (1) a straightforward tube reactor and (2) a static mixer chip (Uniqsis®). The bromination reaction will be optimized in both systems by varying reaction temperature, residence time and the excess of hypobromite. Both reactor systems will be compared and subsequently, the substrate scope will be broadened to methanesulfonates and methanesulfonamides. In a second step, the formation of hypobromite under continuous flow conditions will be evaluated and coupled with the subsequent bromination reaction.

A final part of this research topic comprises the deprotection of the isopropyl ether group of compound **8** (Scheme 1.4).
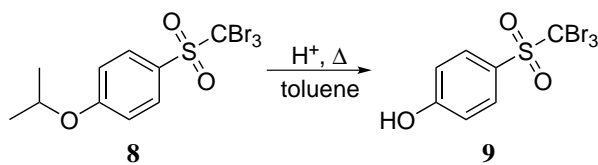
Scheme 1.4. Deprotection of the isopropyl ether group of **8**

Although an efficient batch process using triflic acid has been developed, industry has interest in a continuous flow process. In this way, the bromination reaction and the subsequent deprotection step can be telescoped. Next to CF_3SO_3H, other acids will be evaluated (CH_3SO_3H, H_2SO_4 or H_3PO_4). Special attention will go to the limited solubility of the end product **9** in toluene in order to avoid clogging of the reactor.

In a third part of this PhD research, the Simmons-Smith cyclopropanation of enamines will be explored (Scheme 1.5).
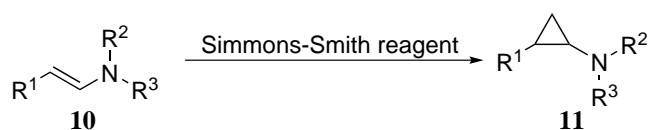
Scheme 1.5. Simmons-Smith cyclopropanation of enamines

The Simmons-Smith reaction is not widely used in industry due to the exothermic behaviour of the reaction. Moreover, several hazards are related with this reaction (e.g. Et$_2$Zn is a pyrophoric substance). Accidents related to Simmons-Smith cyclopropanations in batch are reported by both Charette and the AIHA (American Industrial Hygiene Association®).[48,49] The Simmons-Smith reaction can benefit from microreactor technology taking into account the efficient heat transfer as well as the small and closed hold-up volume.

First, the reaction will be evaluated in batch in order to find reaction conditions which can be translated to a continuous flow process. Special attention will go to the choice of the solvent and the Zn-carbenoid as precipitation of the Zn-carbenoid must be avoided at all time in order to prevent clogging of the microreactor. Once optimized, the batch reaction will be translated to a continuous flow process. The continuous flow process will be split in two steps: (1) generation of the Zn-carbenoid and (2) cyclopropanation reaction. First of all, the Zn-carbenoid will be generated in batch and the cyclopropanation reaction will be optimized under continuous flow conditions. Subsequently, both steps will be performed under continuous flow conditions.

A penultimate research topic will deal with the synthesis of *N*-vinyl-2,2-bisphosphonoaziridines **14**. In preliminary research within our research group (SynBioC, Department of Sustainable Organic Chemistry and Technology, Faculty of Bioscience Engineering, Ghent University), the synthesis of these compounds was optimized in batch starting from the corresponding 1,1-bisphosphono-2-aza-1,3-dienes **12** and it was noticed that several side products can be formed (Scheme 1.6).[50]

The synthesis of *N*-vinyl-2,2-bisphosphonoaziridines **14** will be evaluated under continuous flow conditions in order to increase the selectivity of the reaction. Special attention will go to the use of light irradiation as it is known that the intermediate triazolines **13** decompose under light irradiation.[51–53] Photochemistry benefits from microreactor technology as more efficient light penetration is obtained in the microreactor channels compared to a batch reaction flask.[54–58]
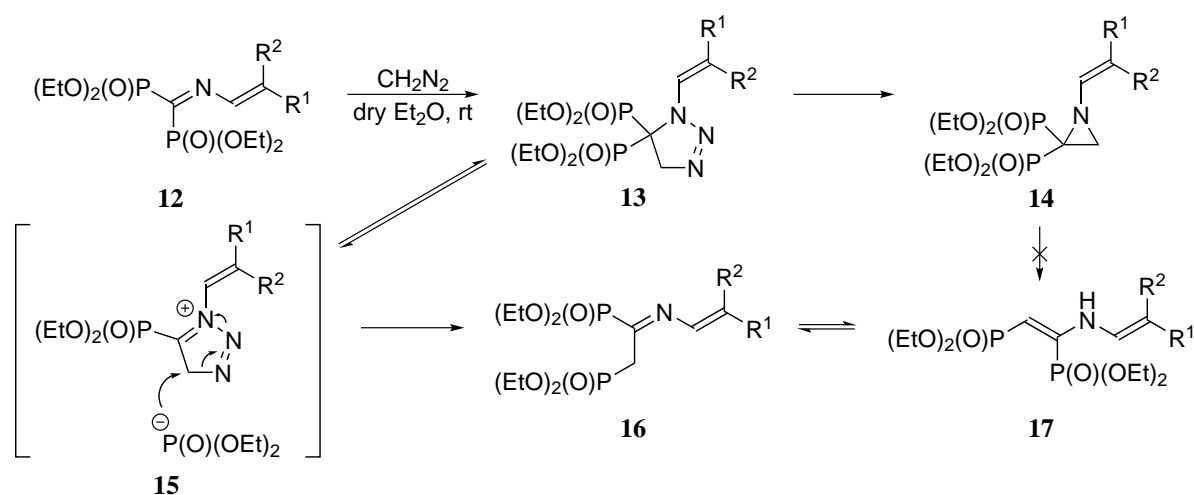
Scheme 1.6. Reaction mechanism for synthesis of *N*-vinyl-2,2-bisphosphonoaziridines **14**

In a final research topic, the activation of amino acids with 1*H*-benzotriazole (BtH) under continuous flow conditions will be evaluated. In previous research performed at our department (SynBioC, Department of Sustainable Organic Chemistry and Technology, Faculty of Bioscience Engineering, Ghent University), benzotriazole activated amino acids were efficiently coupled with heterocyclic amines using microreactor technology (Scheme 1.7).[59]
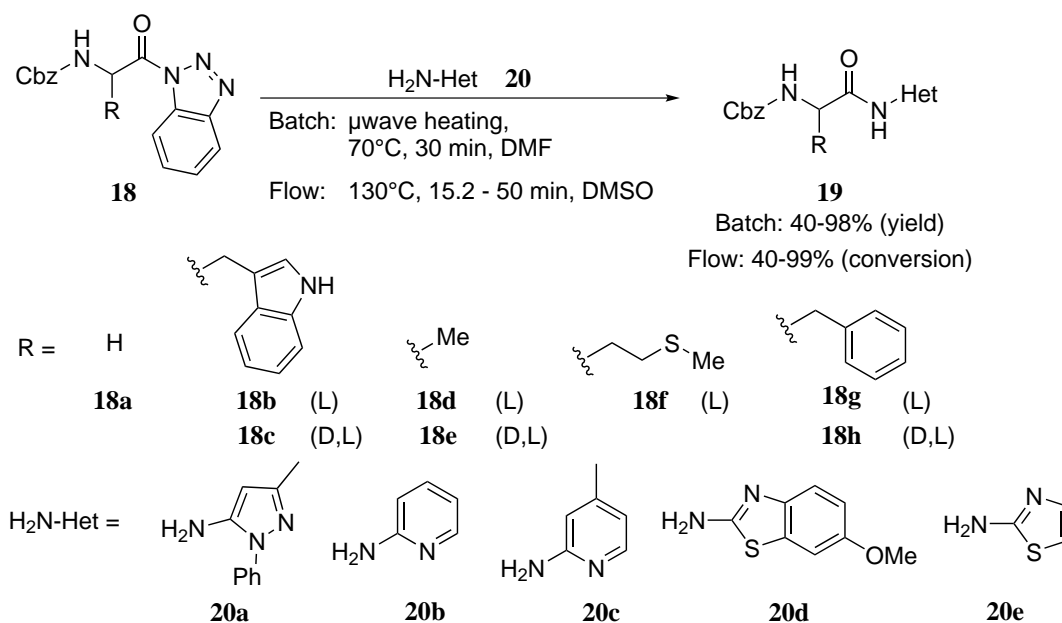
Scheme 1.7. Synthesis of (α-aminoacyl)amino-substituted heterocycles **19**[59]

The Cbz-protected amino acids were activated with benzotriazole in batch (Scheme 1.8).
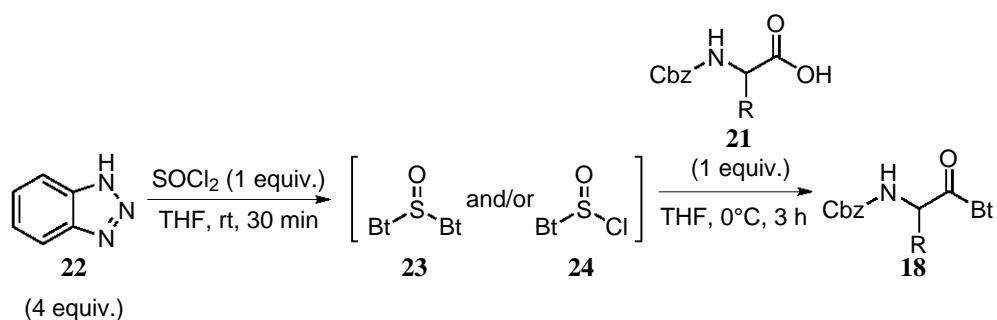
Scheme 1.8. Synthesis of *N*-protected α-aminoacylbenzotriazoles **18** in batch

In this PhD thesis, the activation of amino acids with benzotriazole will be evaluated under continuous flow conditions. Performing both activation and subsequent coupling of amino acids in a continuous flow mode makes high throughput and fully automated synthesis of peptides possible. Two activation strategies will be tested and compared (Scheme 1.9).
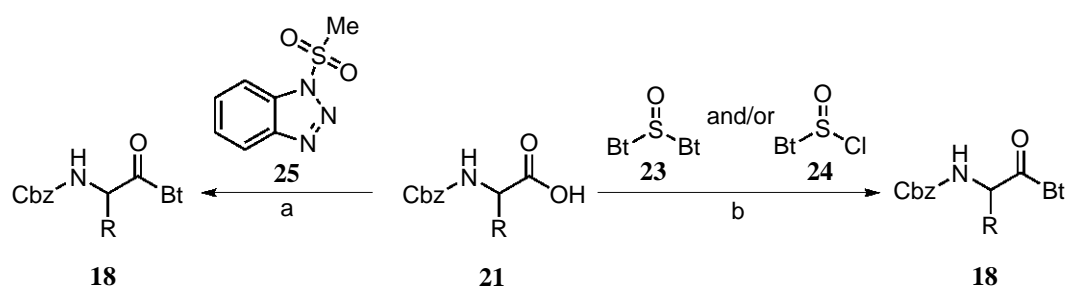
Scheme 1.9. Synthesis of *N*-protected α-aminoacylbenzotriazoles **18**

Special attention will go to the choice of the solvent in order to avoid precipitation of the formed salts and hence clogging of the microreactor. The two activation strategies will be optimized under continuous flow conditions and compared with each other. A library of activated amino acids will be synthesized and the subsequent coupling of the activated amino acids with heterocyclic amines or amino acids will be shortly evaluated.

Chapter 2

Literature overview

2.1 Introduction

The application of microstructured reactors in organic synthesis has gained significant interest in recent years in both academic research and the chemical process industry. The first microstructured system related to chemistry was described in a German patent in 1986 but it was not until 1995, after a workshop about the application of microsystems for chemical and biological transformations, that the development of microreactors expanded.[60,61] Today, numerous examples of the application of microreactors in organic synthesis have been reported in literature.[6–19] In this literature overview, a brief overview of the beneficial characteristics of flow reactors will be given, illustrated with literature examples. To narrow the scope of this literature overview, the given examples will be limited to liquid phase reactions.

2.2 Excellent mixing characteristics

The quality of mixing can have an influence on the conversion and selectivity of reactions, especially when fast reactions are considered. When a reaction proceeds faster than the time required to reach a homogeneous reaction mixture, different local stoichiometric ratios are observed, giving rise to selectivity issues. In this respect, Rys introduced the concept of disguised chemical selectivity.[62,63] Disguised chemical selectivity is obtained when the product selectivity is affected by the mixing efficiency and is not determined by the intrinsic kinetics of the (side) reaction. Only kinetic selectivity is influenced by the mixing characteristics, thermodynamic selectivity is established by the thermodynamic stabilities of the end products.[64]

Fluid flow in microchannels is laminar because of the small dimensions associated with micro- (10-500 μm ID (inner diameter)) and mesoreactors (500 μm - mm ID). The flow regime is determined by the Reynolds number (Re) and for flow in a cylindrical pipe, the Reynolds number is defined as:

$$Re = \frac{Q \cdot ID}{\nu \cdot A} \tag{2.1}$$

with

- Q = volumetric flow rate (m^3/s)
- ID = inner diameter (m)
- ν = kinematic viscosity (m^2/s)
- A = cross-sectional area (m^2)

Flow is considered laminar if Re<2100 and turbulent if Re>4000.[24] In Table 2.1, Reynolds numbers for different inner diameters and flow rates are given. In all cases, Reynolds numbers below 2100 are obtained and hence laminar flow is observed.

Table 2.1: Reynolds numbers for different micro- and mesochannels and flow rates[a]

ID	Flow rate (ml/min)					
	0.001	0.05	0.1	1	5	10
10 μm	5.54	227.03	554.06	-	-	-
500 μm	-	5.54	11.08	110.81	554.06	1108.13
1 mm	-	-	5.54	55.41	277.03	554.06

[a] Calculations based on acetone: ν = 3.83·10^{-7} m^2/s (25°C)[65]

Because of the laminar flow regime, mixing in microchannels is limited to diffusion. The mixing time (i.e. the time to diffuse halfway across a channel), t_{mix}, can be obtained by solving Fick's law:[24,66,67]

$$t_{mix} = \frac{ID^2}{4 \cdot D_{AB}}$$ (2.2)

with

- ID = inner diameter (m)
- D_{AB} = diffusion coefficient (m^2/s, typical 10^{-9} m^2/s)

However, the mixing time as obtained by Fick's law does not take into account any chemical reaction. In this respect, the Damköhler number (Da) describes the relative rate of reaction and diffusion:[24,67]

$$Da = \frac{\text{reaction rate}}{\text{diffusion rate}}$$ (2.3)

The Damköhler number can be estimated based on the Fourier number (Fo) and a coefficient (χ) depending on the reaction kinetics and stoichiometric ratios:[23,67]

$$Da = \frac{\chi}{Fo}$$ (2.4)

$$Fo = \frac{RT}{t_{mix}} \qquad (2.5)$$

with

- RT = residence time

These principles can be used to decide if enhanced mixing is required (Da>1). Several active and passive micromixers with mixing times in the range of 1 s down to a few milliseconds are available.[68–70] The selectivity of several reaction types can be enhanced taking advantage of the excellent mixing characteristics of microreactors.

2.2.1 Friedel-Crafts aminoalkylation

The Friedel-Crafts alkylation of aromatic compounds is difficult to stop at the stage of monoalkylation because the formed product is more reactive than the substrate, leading to polyalkylation. Nevertheless, selective monoalkylation of reactive aromatic substrates is possible using micromixers. Yoshida *et al.* evaluated the Friedel-Crafts reaction of several aromatic and heteroaromatic compounds with an electrochemically generated *N*-acyliminium ion **27** (Scheme 2.1).[64,71,72]
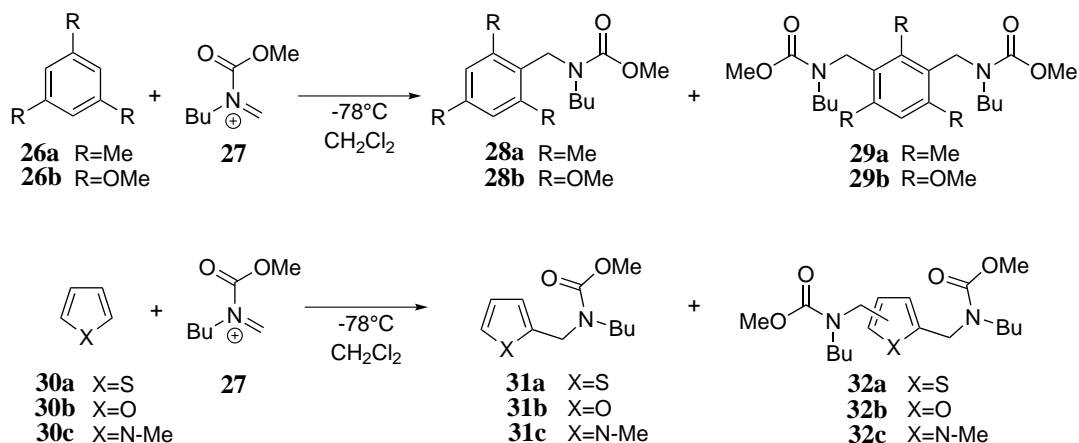
Scheme 2.1. Friedel-Crafts aminoalkylation of aromatic and heteroaromatic compounds

In the Friedel-Crafts reaction of 1,3,5-trimethylbenzene **26a**, selective monoalkylation was observed in batch (69%). However, dialkylation was expected because the monoalkylated product **28a** should be more reactive than the substrate **26a** due to the electron-donating properties of the additional alkyl group. The authors attributed the selective monoalkylation of **26a** to the protonation of the carbamate group and hence the creation of an electron-withdrawing group making the monoalkylated product **28a** less reactive than the substrate **26a**.

When more reactive substrates were used, e.g. 1,3,5-trimethoxybenzene **26b**, dialkylation was observed in batch. However, microreactor experiments revealed that also for these substrates, monoalkylation proceeds faster than the consecutive dialkylation. The reduced selectivity in batch can be attributed to disguised chemical selectivity. Due to inefficient mixing, the monoalkylated product **28b** can accumulate locally in the presence of **27**, enhancing the consecutive reaction of **28b** to **29b**. The results for the Friedel-Crafts aminoalkylation of 1,3,5-trimethoxybenzene **26b** are summarized in Table 2.2.

Table 2.2: Friedel-Crafts aminoalkylation of 1,3,5-trimethoxybenzene **26b**

Entry			**28b** (%)	**29b** (%)	**28b:29b**
1		addition of **27** to **26b**	37	32	54:46
2	Batch	addition of **26b** to **27**	33	33	50:50
3		simultaneous addition of **26b** and **27**	34	30	53:47
4		T-mixer	36	31	54:46
5	Micromixer	Split-and-recombine micromixer	50	14	78:22
6		Multilamination micromixer	92	4	96:4

Various batch strategies were evaluated but in all cases, a near 1:1 mixture of the monoalkylated **28b** and dialkylated product **29b** was obtained (Table 2.2, entries 1-3). When a T-mixer was used under microreactor conditions, the same selectivity was observed as in batch (Table 2.2, entry 4). The selectivity increased when a split-and-recombine micromixer was used (Table 2.2, entry 5). However, still a significant amount of dialkylated product **29b** was formed. The best results were obtained with a multilamination micromixer (Figure 2.1), an excellent yield (92%) and selectivity (96:4 **28b:29b**) were observed at a reaction temperature of -78°C.
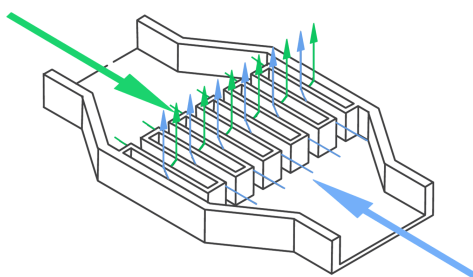
Figure 2.1. Multilamination micromixer

Subsequently, the substrate scope was expanded to heteroaromatic substrates (Table 2.3). Use of microreactor technology resulted in an increased yield and selectivity for the Friedel-Crafts reaction compared to the corresponding batch process.

Table 2.3: Friedel-Crafts aminoalkylation of heteroaromatic substrates

Entry	Substrate	Reactor	**31a - 31c** (%)	**32a - 32c** (%)
1		batch	14	27
	30a			
2		micromixer	84	0
3		batch	11	5
	30b			
4		micromixer	39	trace
5		batch	33	28
	30c			
6		micromixer	60	6

2.2.2 Hetero Diels-Alder reaction of nitroso dienophiles

The hetero Diels-Alder reaction between nitroso dienophiles **33** or **34** and a diene **35** leads to polyfunctional 3,6-dihydro-1,2-oxazine scaffolds **36**. Stevens and coworkers evaluated this cycloaddition reaction under continuous flow conditions.[73] Both aryl- **33** and acylnitroso **34** dienophiles were reacted with different dienes **35** (Scheme 2.2).
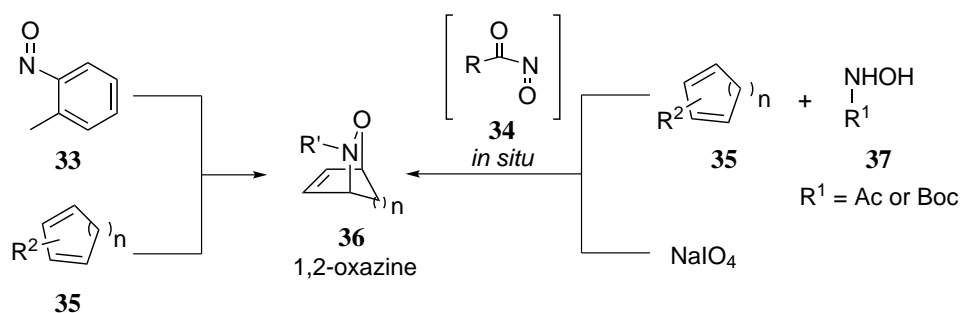
Scheme 2.2. Hetero Diels-Alder reaction of a nitroso dienophile **33** or **34** and a diene **35**

The acylnitroso dienophiles **34** were generated in situ from hydroxamic acids **37** under oxidative conditions. However, dimerization and degradation of the acylnitroso dienophiles **34** is possible if a local excess of hydroxamic acid is present.[74–77] These side reactions can be limited in a microreactor due to the efficient mixing. Moreover, the exothermic cycloaddition reaction takes advantage of the efficient heat transfer under continuous flow conditions. Several derivatives were synthesized in good to excellent yields. Table 2.4 gives an overview of the results for the

reaction of cyclohexadiene **35a** with nitroso dienophiles **33** and **34** under batch and continuous flow conditions.

Table 2.4: Diels-Alder reaction of cyclohexadiene **35a** with nitroso dienophiles **33** and **34**

Entry	Dienophile	Batch (%)	Flow (%)
1	**33**	67[78]	92
2	**34a** (R[1] = Ac)	57[79]	94
3	**34b** (R[1] = Boc)	83[80]	87

2.2.3   Selective monolithiation of dibromobiaryls

Selective monolithiation of dihalobiaryls using halogen-lithium exchange is difficult to achieve in batch.[81,82] Yoshida and coworkers investigated the continuous flow lithiation of dibromobiaryls using 2,2'-dibromobiphenyl as a model substrate (Scheme 2.3).[83,84] In a first step, they examined the batch reaction at different reaction temperatures (Table 2.5).
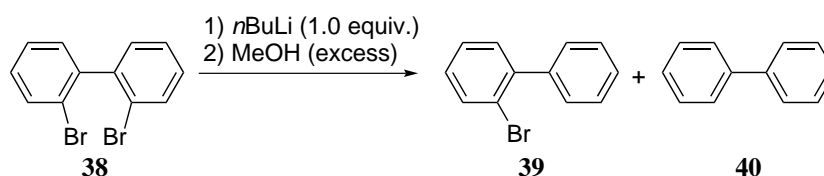
Scheme 2.3. Lithiation of 2,2'-dibromobiphenyl **38** using *n*BuLi

Table 2.5: Lithiation of 2,2'-dibromobiphenyl **38** in batch

Entry	Temperature (°C)	Reaction time (min)	Conversion (%)	**39** (%)	**40** (%)
1	-78	60	94	76	4
2	-48	10	86	69	4
3	-27	10	81	48	18
4	0	10	75	36	25
5	24	10	66	14	34

A good selectivity was obtained at a reaction temperature of -78°C but the selectivity decreased significantly with increasing temperatures. Subsequently, the reaction was evaluated under continuous flow conditions using a system built up of two T-mixers and two tube reactors (Scheme 2.4). The results of the microreactor experiments are summarized in Figure 2.2.
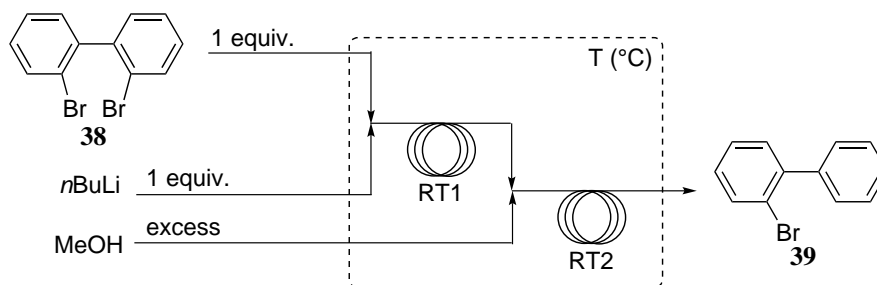
Scheme 2.4. Lithiation of 2,2'-dibromobiphenyl **38** in flow
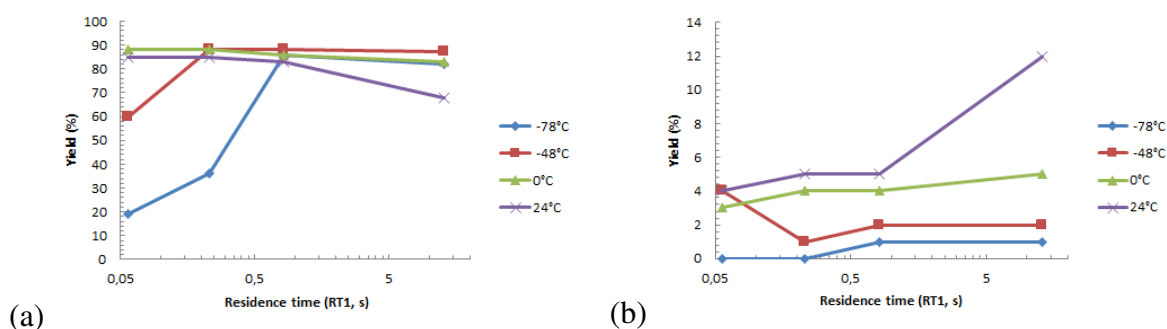
Figure 2.2. Lithiation of 2,2'-dibromobiphenyl **38** in flow: (a) yield of **39** and (b) yield of **40**

Using microreactor technology, high yields and selectivities can be obtained at remarkable higher temperatures compared to the corresponding batch process (83-88% yield at 0°C in flow compared to 76% yield at -78°C in batch). Higher reaction temperatures are possible due to the excellent heat transfer and short residence times (RT1 = 0.06 s - 13 s) associated with the continuous flow procedure. However, another crucial factor for the selective monolithiation is the efficient 1:1 mixing. Selectivity decreased with increasing inner diameter of the T-mixer for the mixing of 2,2'-dibromobiphenyl **38** and *n*BuLi or decreasing total flow rate and hence decreasing mixing rate (Table 2.6).[68]

Table 2.6: Influence of the flow rate and inner diameter of the T-mixer on the lithiation of 2,2'-dibromobiphenyl **38** at 0°C

Entry	Total flow rate (ml/min)	ID T-mixer (μm)	Conversion (%)	**39** (%)	**40** (%)
1	7.2	250	97	88	3
2	3.6	250	90	80	7
3	1.8	250	76	57	15
4	0.72	250	69	41	19
5	7.2	500	93	77	7
6	7.2	800	79	62	9

2.2.4 Glycosylation

The contact between different reagent streams can be controlled efficiently using microreactor technology. Ratner *et al.* applied this principle to reduce side product formation in a glycosylation reaction. The authors evaluated the reaction between mannosyl trichloro-acetimidate **41** (donor) and diisopropylidene galactose **42** (acceptor) with trimethylsilyl trifluoromethanesulfonate (TMSOTf) as activator (Scheme 2.5). Next to the desired end product **43**, orthoester **44** can be formed. However, using controlled contact between the different reagent streams in which the donor **41** can only reach the activator, TMSOTf, in the presence of the acceptor **42**, the undesired orthoester formation is limited (Figure 2.3).[24,85,86]
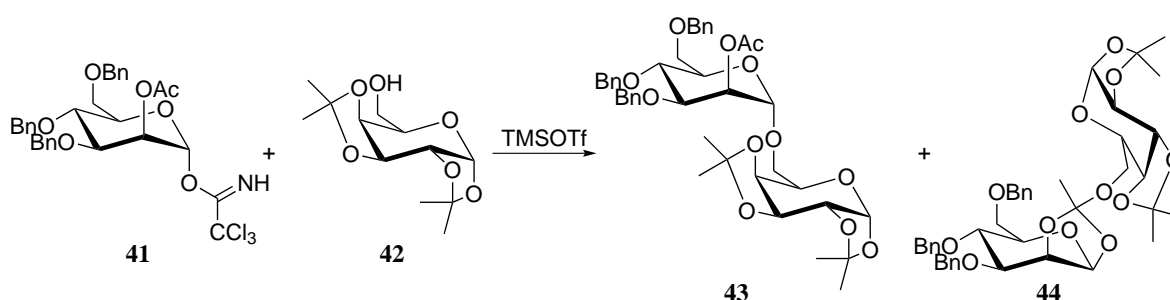
Scheme 2.5. Glycosylation reaction
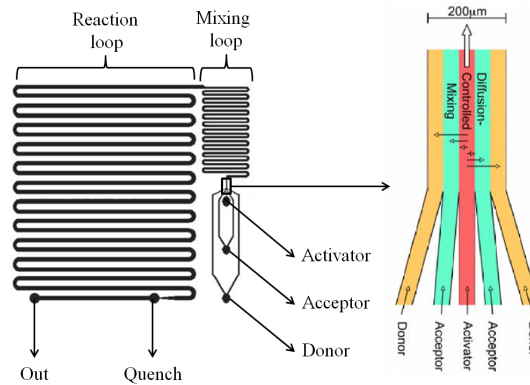
Figure 2.3. Glycosylation reaction using controlled contact between the different reagents

2.3 Unique heat transfer properties

Continuous flow reactors exhibit unique heat transfer properties due to the high surface-to-volume ratio. This enables fast and efficient heating or cooling of the reaction mixture whereby reactions can be run under near isothermal conditions. A comparison of typical values for the surface-to-volume ratio of micro- and mesoreactors and batch reactors is given in Table 2.7. Thermal conductivity values for microreactor construction materials are given in Table 2.8.

Table 2.7: Typical values for the surface-to-volume ratio of different reactors[10,22–24]

Reactor	Surface-to-volume ratio (m^2 m^{-3})
Microreactor (10 - 500 μm ID)	5 000 - 50 000
Mesoreactor (500 μm - mm ID)	100 - 10 000
Round bottom flask (100 ml)	100
Round bottom flask (250 ml)	80
Batch reactor (1 m^3)	6

The excellent heat transfer characteristics of a microreactor allow for an efficient control of the reaction temperature. In this way, possible runaway reactions can be controlled and the formation of unwanted side products can be prevented. Batch reactors typically provide a relative broad temperature profile, possibly leading to the formation of side products if multiple reaction pathways are possible. In microreactors, the reaction can be run under near isothermal conditions, restricting the reaction outcome to the desired product. Figure 2.4 compares the temperature profiles of a batch reactor and a microreactor and its influence on the formation of side products.

Table 2.8: Typical thermal conductivity values for microreactor construction materials

Construction material	Thermal conductivity (W m K^{-1})
Teflon	0.1
Glass	1.05
Stainless steel	10
Silicon	150
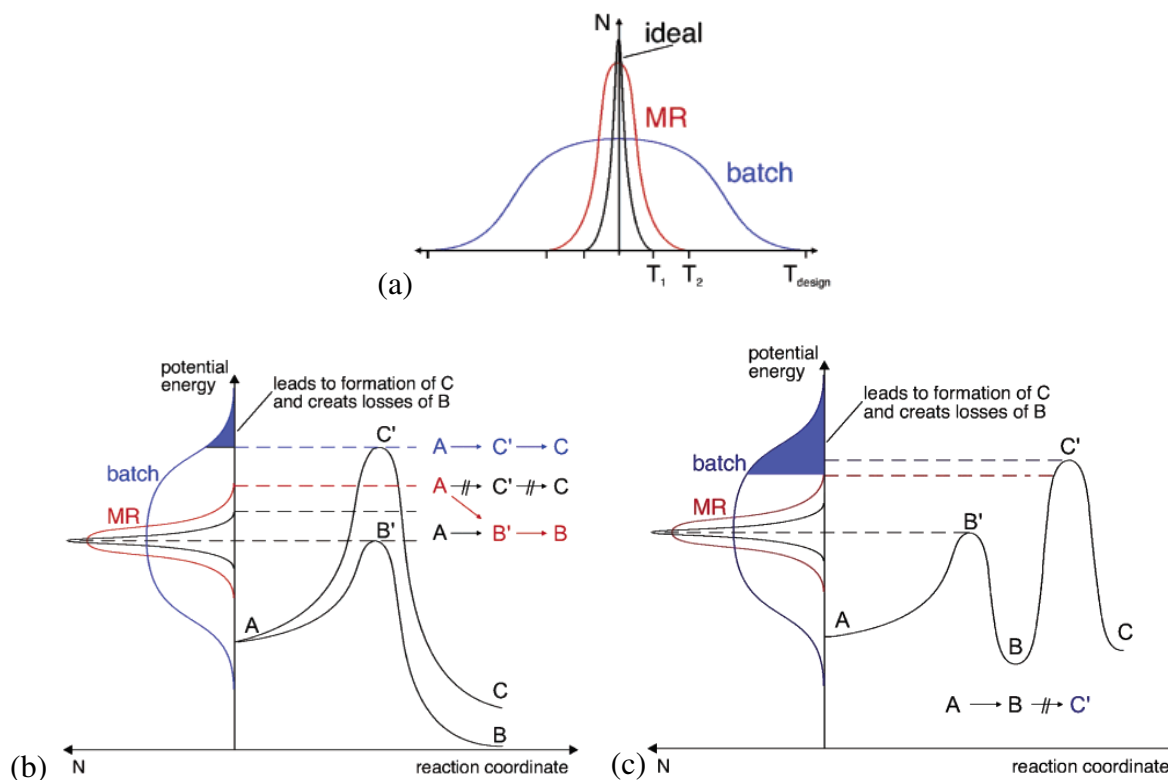
Figure 2.4. Influence of the temperature profile on the formation of side products: (a) Ideal temperature distribution and actual temperature distribution for a batch and microreactor (MR), (b) Influence of the temperature profile on two competing reaction pathways, (c) Influence of the temperature profile on consecutive reactions. The broad temperature profile of the batch reactor allows the formation of the unwanted side product C whereas the formation of C is prevented in the microreactor.[87]

2.3.1 Nitration

Nitration reactions are often dangerous to perform on an industrial scale due to the exothermic nature of the reaction with risk for a runaway reaction and the possible generation of explosive side products. Renaud *et al.* investigated the potentially hazardous nitration of 3-methylpyrazole **45** in a microreactor (Scheme 2.6).[88] The nitration of 3-methylpyrazole **45** proceeds via the intermediate *N*-nitropyrazole **46** which rearranges to 3-methyl-4-nitropyrazole **47**. However, at higher temperatures (>80°C), unstable and potentially explosive dinitropyrazole derivatives **48** are generated.
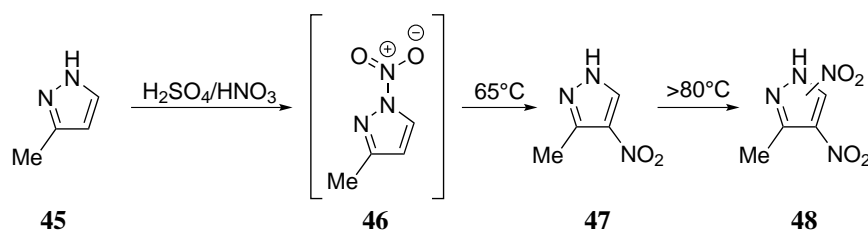
Scheme 2.6. Nitration of 3-methylpyrazole **45**

This process could be run safely in a microreactor due the excellent temperature control, avoiding the generation of the dinitropyrazole derivatives **48**. When the nitration of 3-methyl-pyrazole **45** was performed in a microreactor at 65°C and 90 min residence time, a throughput of 0.82 g/h and an isolated yield of 88% was obtained.

2.3.2 Grignard reaction

The Grignard reaction is a very fast and exothermic reaction. Roberge *et al.* evaluated the Grignard reaction between phenylethylmagnesium bromide **49** and 2-chloropropionyl chloride **50** using microreactor technology (Scheme 2.7).[89]
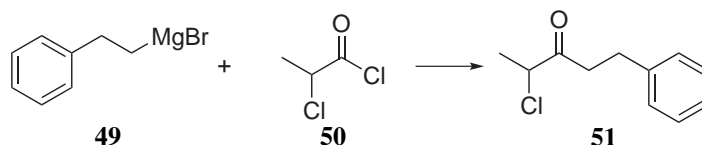
Scheme 2.7. Grignard reaction between phenylethylmagnesium bromide **49** and 2-chloropropionyl chloride **50**

Theoretical simulations and experimental results showed that hot spots are formed in the mixing zone of the microreactor for this fast and exothermic reaction despite the excellent heat transfer characteristics attributed to microreactors. To suppress hot spot formation and hence product

degradation and side reactions, the solution of phenylethylmagnesium bromide **49** was split and mixed with the 2-chloropropionyl chloride **50** solution over multiple injection points. Using this approach, the yield was increased from 35% to 50%.

Other examples include a Grignard exchange reaction to synthesize pentafluorophenyl-magnesium bromide and the selective addition of Grignard reagents to aldehydes and ketones at room temperature.[90,91]

2.3.3 Dibal-H reduction of esters to aldehydes

The partial reduction of esters with Dibal-H (diisobutylaluminum hydride) forms a straightforward synthetic method towards the corresponding aldehydes (Scheme 2.8).[92]
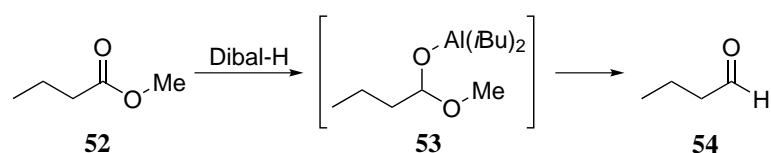
Scheme 2.8. Reduction of methyl butyrate **52**

In order to prevent a significant increase of the reaction temperature, a slow addition of the Dibal-H solution is required in batch which leads to extended dosage times when scaling-up is considered. Taking advantage of the heat transfer characteristics of a microreactor, this reaction could be run with the same selectivity at temperatures that were 25°C higher than the batch reaction temperature (Figure 2.5).
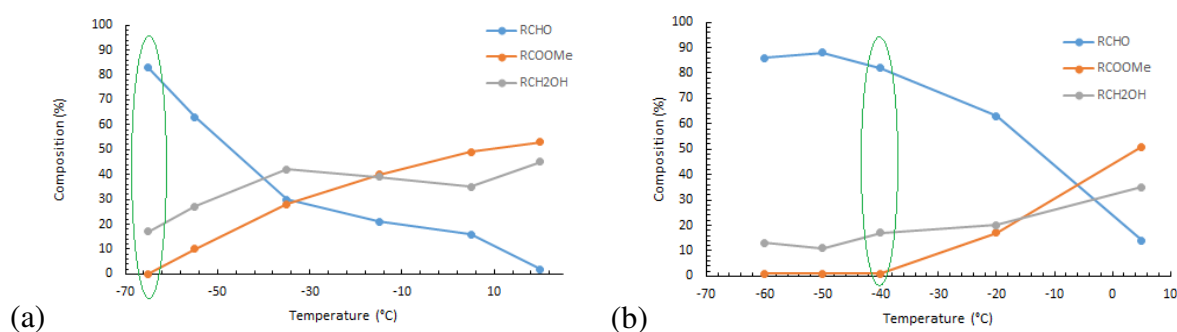
Figure 2.5. Dibal-H reduction of methyl butyrate **52** (a) in batch and (b) in flow

2.4 Excellent control of the reaction time

In a flow reactor, the reaction time corresponds to the residence time in the reactor which in turn is determined by the total flow rate of the reagents and the internal volume of the reactor. In this way, the reaction time can be effectively controlled by tuning the flow rates of the reagents for a given internal volume. Using microreactor technology, extremely short residence times (milliseconds to seconds) are possible and a narrow residence time distribution is obtained. The excellent control of the reaction time allows to work with very reactive intermediates: the reactive species can be generated and used in a subsequent reaction before decomposition occurs. In this respect, Yoshida *et al.* introduced the concept of flash chemistry: extremely fast reactions with highly reactive and unstable intermediates.[93–95] Excellent control of the reaction time, together with fast mixing and efficient temperature control allows the handling of these reactive and unstable intermediates in microreactor systems.

2.4.1 Moffatt-Swern oxidation

Via the Moffatt-Swern oxidation, primary and secondary alcohols are converted into the corresponding aldehydes and ketones but several side products can be formed (Scheme 2.9).[96,97]
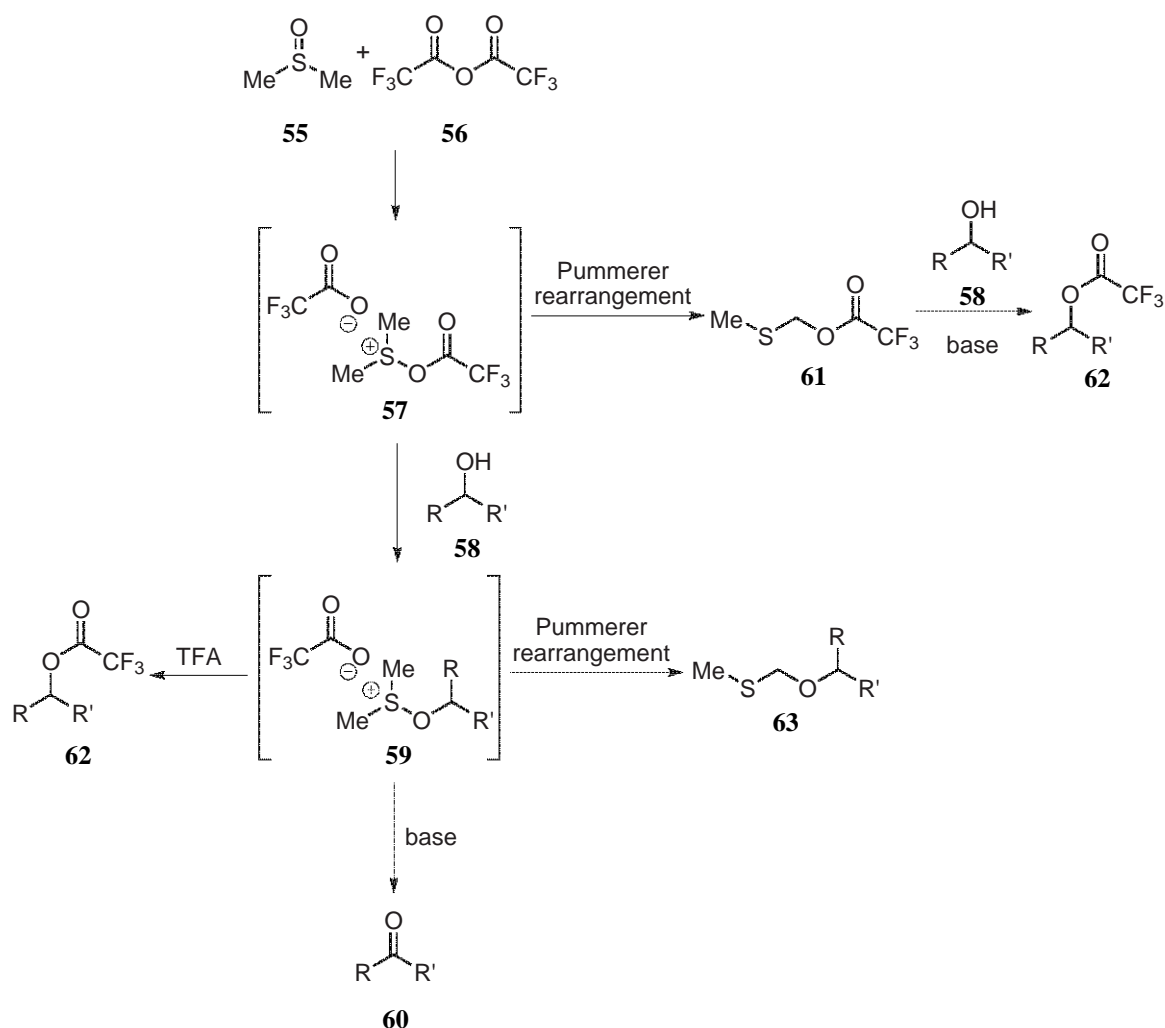
Scheme 2.9. Moffatt-Swern oxidation of primary and secondary alcohols

In the Moffatt-Swern oxidation, DMSO **55** is activated with trifluoroacetic anhydride **56** (TFAA) to form the trifluoroacetoxydimethylsulfonium salt **57**. This intermediate **57** is only stable at temperatures below -30°C.[98,99] At higher temperatures, Pummerer rearrangement of **57** to **61** takes place, which in turn can react with the alcohol **58** to form the acylated alcohol **62**. Therefore, this synthesis is typically performed below -50°C in batch. In a second step, the alcohol **58** is added to form the alkoxydimethylsulfonium salt **59**. In the presence of a base, intermediate **59** is converted into the desired aldehyde or ketone **60**. However, Pummerer rearrangement of **59** to the methylthiomethyl ether **63** can occur and reaction of **59** with trifluoroacetic acid (TFA) gives **62**.[100]

Yoshida *et al.* examined this reaction using a microreactor built up of multilamination micromixers and stainless steel tube reactors (Scheme 2.10).[93,94,100] Table 2.9 summarizes the results for the Moffatt-Swern oxidation of cyclohexanol **58a**.
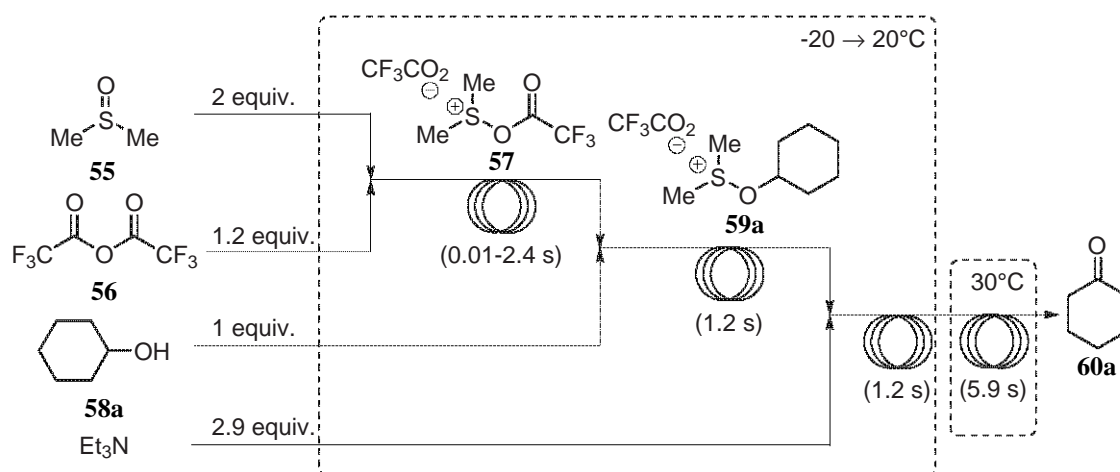
Scheme 2.10. Microreactor set-up for the Moffatt-Swern oxidation of cyclohexanol **58a**

Table 2.9: Moffatt-Swern oxidation of cyclohexanol **58a**

Entry	Reactor	T (°C)	Time	Yield (%) 60a	63a	62a
1		-20	2.4 s	88	6	5
2	Microreactor	0	0.01 s	89	7	1
3		20	0.01 s	88	5	2
4	Batch	-70	10 min	83	10	5
5		-20	10 min	19	2	70

The oxidation of cyclohexanol **58a** proceeded smoothly to give the corresponding ketone **60a** in good yield and selectivity at -20°C with a residence time of 2.4 s in the first tube reactor (Table 2.9, entry 1). If this residence time was lowered to 0.01 s, the reaction could even be performed at room temperature with comparable yield and selectivity (Table 2.9, entry 3). When the reaction was performed in batch, cryogenic conditions were required in order to obtain good results (Table 2.9, entry 4). Raising the temperature to -20°C had a dramatic effect on the selectivity of the reaction (Table 2.9, entry 5).

According to Yoshida *et al.*, the high selectivity of the Moffatt-Swern oxidation at room temperature can be attributed to the short residence time, precise temperature control and fast mixing possible with microreactor technology. However, Kemperman and coworkers concluded that the high selectivity is mainly caused by the short residence times and is not influenced by the type of micromixer.[101] The same results were obtained for the Moffatt-Swern

oxidation of benzyl alcohol **58b** when using a multilamination micromixer or a simple T-mixer. Nevertheless, fast mixing is required taking into account the short residence times.

Kemperman *et al.* also evaluated premixing DMSO **55** with the alcohol **58** prior to mixing it with TFAA **56**. In this way, the trifluoroacetoxydimethylsulfonium salt **57** that was formed, was immediately intercepted by the alcohol, thereby preventing Pummerer rearrangement of **57**. Similar or better yields and selectivities were obtained using this approach.[101]

Rutjes *et al.* used multivariate screening to optimize the Moffatt-Swern oxidation of benzyl alcohol **58b**. After optimization, the reaction could be performed at 70°C with a yield of 96% when the alcohol **58b** and DMSO **55** were premixed.[102]

2.4.2 Generation of unstable organometallic intermediates

Yoshida *et al.* studied the lithiation of *o*-dibromobenzene **64** and subsequent trapping of the generated *o*-bromophenyllithium **65** with an electrophile.[93,94,103] In batch, this reaction is performed at -110°C or below in order to prevent the formation of benzyne **67** through elimination of LiBr. This elimination already takes place at a temperature of -78°C and gives rise to undesired side products (Scheme 2.11).[104–107]
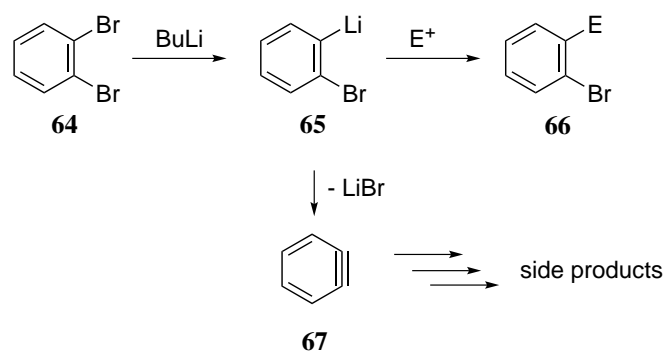
Scheme 2.11. Selective lithiation of *o*-dibromobenzene

The reaction was optimized using *n*BuLi to generate *o*-bromophenyllithium **65** and MeOH to trap the lithiated intermediate. Various residence times and temperatures were evaluated and the optimal conditions were found to be -78°C and 0.8 s for the generation of *o*-bromophenyllithium **65** (Scheme 2.12).
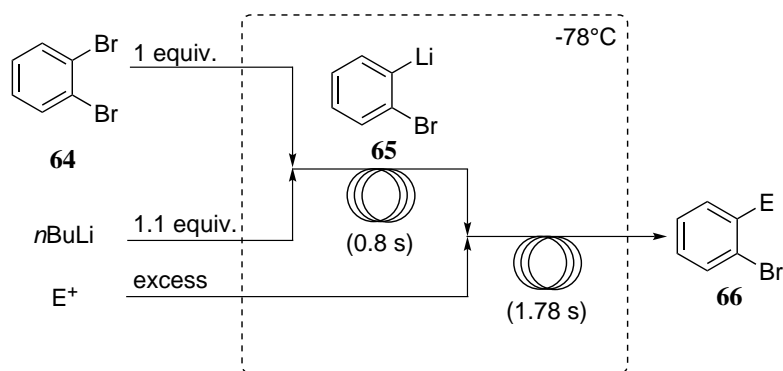
Scheme 2.12. Selective lithiation of *o*-dibromobenzene **64** using a microreactor

Using these optimized conditions, dibromobenzene **64** was converted into different substituted bromobenzenes **66** using various electrophiles (methyl triflate, chlorodimethylsilane, trimethyl-silyl triflate, aldehydes and ketones) with yields ranging from 68% to 81%.[103]

Subsequently, the developed procedure was extended to substitute both bromine atoms with electrophiles.[93,94,103] The second Br-Li exchange was performed at a temperature of 0°C because the generated aryllithium intermediate should be more stable than *o*-bromophenyllithium **65** (Scheme 2.13). After optimization, several disubstituted benzenes **68** could be obtained in yields ranging from 53% to 74%.
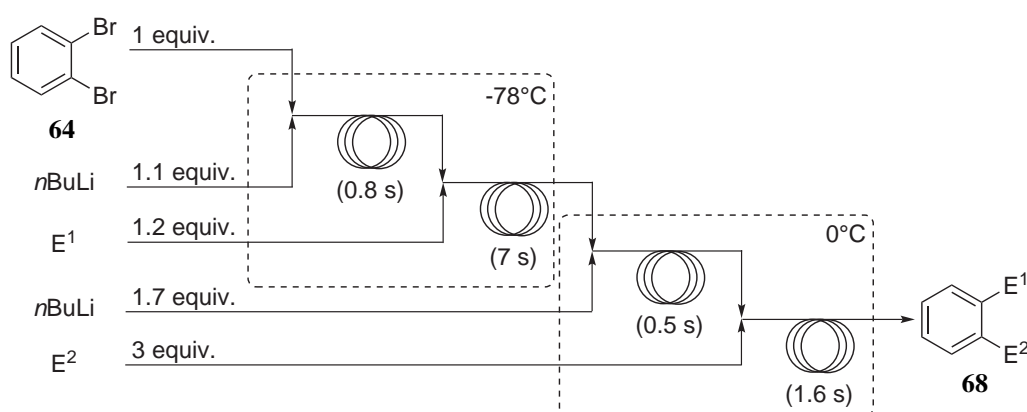
Scheme 2.13. Selective, sequential lithiation of *o*-dibromobenzene **64** using a microreactor

Another example of the use of unstable organometallic intermediates in flow is the generation of aryllithium compounds bearing electrophilic functional groups. These compounds are difficult to synthesize due to their high reactivity towards the electrophilic groups (e.g. alkoxycarbonyl, nitro and cyano groups).[94] The generation of aryllithium compounds with electrophilic functional groups has been reported in batch at low temperatures (-100°C) for carboxylic acid,

cyano, *o*-nitro and amide functional groups but with alkoxycarbonyl groups, these compounds dimerize rapidly by self-condensation (Scheme 2.14).[108–111]
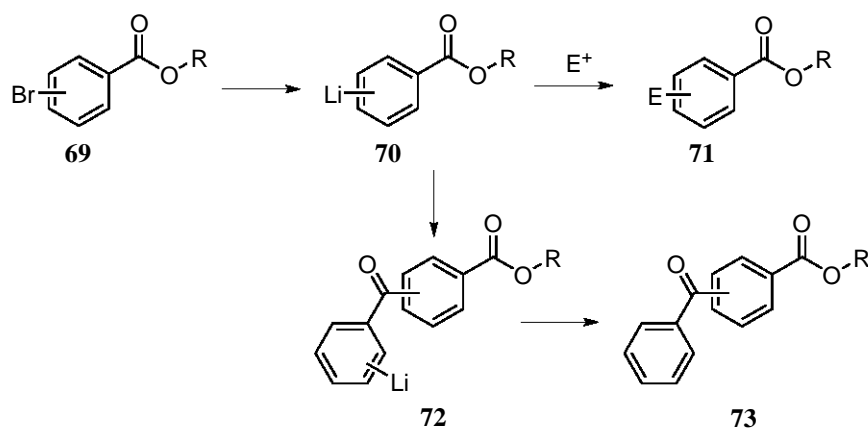
Scheme 2.14. Generation of aryllithium compounds bearing an alkoxycarbonyl group

Yoshida and coworkers performed some batch experiments at -78°C for the generation of aryllithiums with an alkoxycarbonyl group at the *ortho-*, *meta-* or *para*-position.[112,113] The results are summarized in Table 2.10. *Ortho-*, *meta-* and *para-tert*-butoxycarbonyl aryllithiums can be generated at low temperature due to the sterically demanding *tert*-butyl group (Table 2.10, entries 1, 5 and 9). Aryllithium compounds with an isopropoxycarbonyl group in *ortho*-position could also be generated although the yield was moderate (Table 2.10, entry 2). When less sterically hindered alkoxycarbonyl groups (ethoxy- and methoxycarbonyl) were used, the desired aryllithium compounds could not be generated.

Table 2.10: Generation of aryllithium compounds bearing an alkoxycarbonyl group in batch
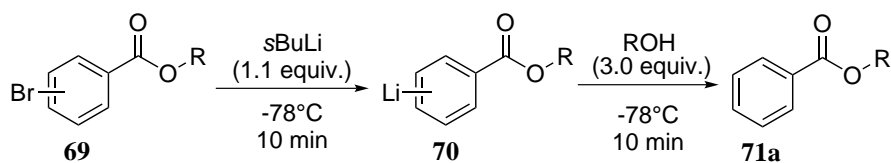
Entry	Position of Br	R	Conversion (%)	71a(%)
1	*ortho*	*tert*-butyl	100	61
2	*ortho*	isopropyl	100	12
3	*ortho*	ethyl	100	0
4	*ortho*	methyl	100	0
5	*para*	*tert*-butyl	98	35
6	*para*	isopropyl	74	trace
7	*para*	ethyl	82	0
8	*para*	methyl	42	0
9	*meta*	*tert*-butyl	96	40
10	*meta*	isopropyl	80	5
11	*meta*	ethyl	73	trace
12	*meta*	methyl	56	0

Subsequently, the lithiation of **69** with *s*BuLi was evaluated under microflow conditions taking advantage of the residence time control (Scheme 2.15).[112]
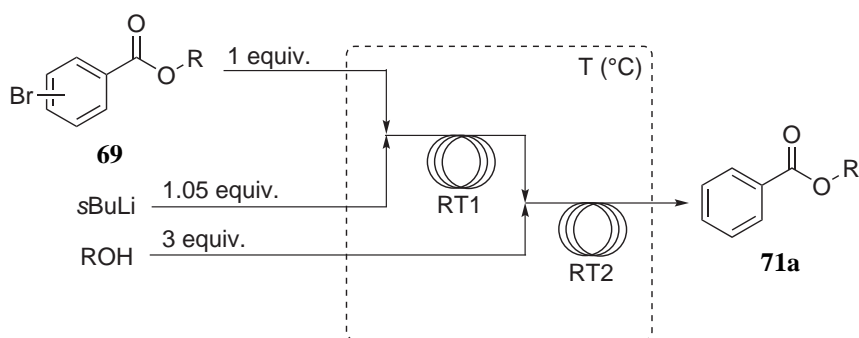
Scheme 2.15. Generation of aryllithium compounds bearing an alkoxycarbonyl group in flow

It is possible to generate *o*-alkoxycarbonyl phenyllithium compounds in excellent to good yields by optimizing the reaction temperature and residence time.[112,113] The stability of the phenyllithium compounds increases in the order methoxycarbonyl < ethoxycarbonyl < isopropoxycarbonyl < *tert*-butoxycarbonyl. At lower temperatures and shorter residence times, incomplete Br/Li-exchange results in lower yields while higher temperatures and longer residence times give lower yields due to decomposition of the generated phenyllithium compounds.

Subsequently, the generation of *p*-alkoxycarbonyl phenyllithium compounds was investigated.[113] *p-tert*-Butoxycarbonyl phenyllithium could be generated over a broad range of temperatures and residence times. However, the generation of *p*-isopropoxycarbonyl phenyllithium via Br/Li-exchange appeared to be difficult. For these compounds, less steric hindrance is present compared to *p-tert*-butoxycarbonyl phenyllithium and compared to *o*-alkoxycarbonyl phenyllithium compounds, no coordination between the carbonyl oxygen atom and lithium is possible.

When I/Li-exchange was used, *p*-alkoxycarbonyl phenyllithium compounds could be generated in excellent to good yields using the appropriate temperature and residence time. For the generation of *m*-alkoxycarbonyl phenyllithium compounds, the same results were observed as for *p*-alkoxycarbonyl phenyllithium compounds.[113]

Finally, the substrate scope was extended to cyano- and nitro-substituted aryllithium compounds. Cyano-substituted phenyllithium compounds could be generated at 0 - 20°C whilst nitro-substituted phenyllithium compounds were generated at -28 - 0°C.[114,115] The key advantage of microreactor technology in these reactions is the short residence time combined with excellent mixing and efficient temperature control.

2.4.3 Aldol condensation

Efficient control of the residence time can prevent the formation of unwanted side products due to consecutive reactions (Figure 2.6).
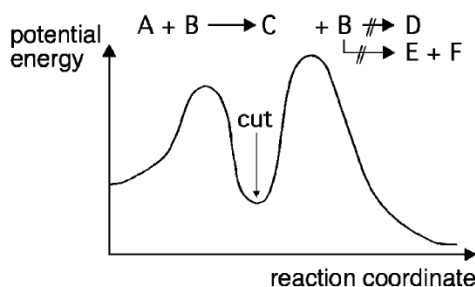
Figure 2.6. Control of the reaction time in order to prevent the formation of side products[87]
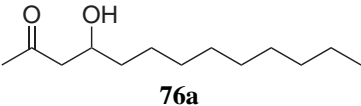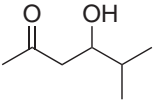
Fukase *et al.* applied this principle to perform a biphasic aldol reaction (Scheme 2.16). A microreactor built up of two micromixers was used and the reaction mixture was quenched with aq. HCl in a T-mixer.[116,117]
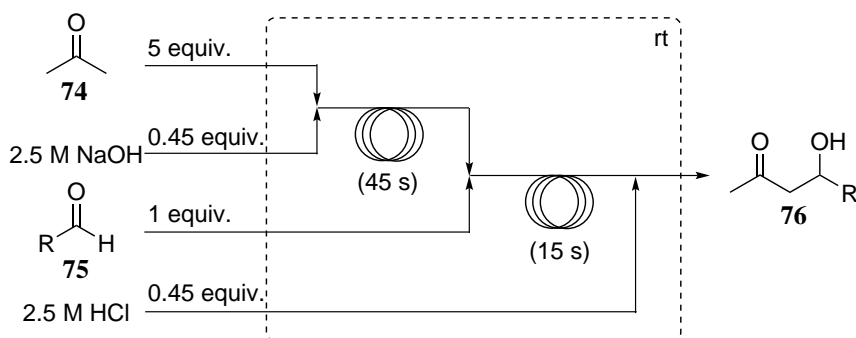
Scheme 2.16. Biphasic aldol reaction

When this reaction was performed in batch at considerable scale, different bottlenecks appeared: (1) mixing of the biphasic reaction mixture and (2) prolonged reaction times. In batch, one of the main problems was the polymerization of the aldehyde **75** or aldol product **76** due to the basic reaction conditions and prolonged reaction times. Performing the aldol reaction in flow can prevent the formation of polymers due to the application of short residence times and immediate neutralization of the reaction mixture. Different ketones **76** could be synthesized in good to excellent yields (Table 2.11).[116]

Table 2.11: Synthesis of ketones **76** via the aldol reaction

Entry	Ketone **76**	Batch Yield (%)	Microreactor Yield (%)
1	**76a**	<20	74
2	**76b**	69	95

2.5 Increased safety features

Microreactor technology enables the safe use of toxic or explosive reagents because of the small and confined reaction volume. Hazardous reagents can be synthesized and used in situ, avoiding the manipulation of these reagents. Moreover, strong exothermic reactions can be performed safely in a microreactor. The efficient heat transfer allows precise temperature control and hence, possible runaway reactions can be run with reduced risks.

2.5.1 Diazomethane

Diazomethane is a versatile and valuable building block in organic chemistry and can be used for a plethora of reactions (e.g. methylations, cycloadditions, etc.).[118] However, several safety hazards are related with diazomethane.[119–122] Diazomethane is a toxic, carcinogenic, shock-sensitive and explosive gas and hence, special safety features have to be undertaken.

Warr *et al.* described a continuous batch process for the safe generation of diazomethane on an industrial scale.[123,124] Diazomethane was generated by adding a DMSO-solution of diazald (*N*-methyl-*N*-nitroso-*p*-toluenesulfonamide) and an aqueous KOH-solution simultaneously to a stirred reactor. The level of the reaction mixture was kept constant by continually draining the reactor. Diazomethane was removed from the reaction mixture by purging the reaction mixture with nitrogen. Subsequently, the generated diazomethane was transferred to the reagent solution (e.g. benzoic acid in dimethoxyethane). With this setup, 90-93 g/h diazomethane could be produced while the maximum amount of diazomethane present at any moment was 0.11 g.

Stark *et al.* reported the first microreactor procedure for the methylation of benzoic acid **78** using diazomethane generated from diazald **77a**.[125] Two different reactors were evaluated for

the generation of diazomethane: (1) a commercial microreactor with integrated mixing elements and (2) a straightforward tube reactor (Scheme 2.17).
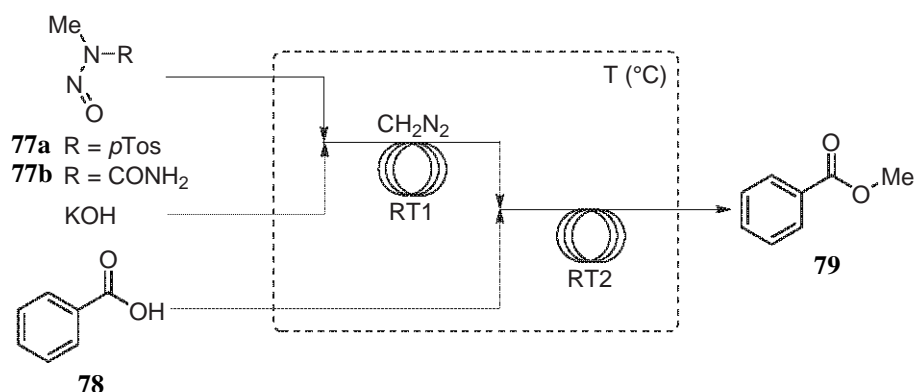
Scheme 2.17. Generation of diazomethane and subsequent methylation of benzoic acid **78**

First, the reaction was evaluated in batch to find an optimal solvent system which maximizes yield and avoids precipitation and hence clogging of the microreactor. After solvent screening, diazald **77a** and benzoic acid **78** were dissolved in carbitol (2-(2-ethoxyethoxy)ethanol) while KOH was dissolved in isopropanol. As expected, shorter residence times could be obtained in the commercial microreactor system (RT1=5 s) compared to the capillary reactor (RT1=50 s) in order to obtain the same yield. Yields were constant over a broad temperature range (0-50°C) but started to decrease slightly at higher temperatures. Using a stoichiometric ratio **77a**:KOH:**78** 1:1.5:4, methyl benzoate **79** was obtained with a yield of 65% in both flow systems.

Maggini *et al.* described a procedure analogous to the one of Stark *et al.* in which diazomethane was generated from *N*-methyl-*N*-nitrosourea (MNU) **77b** instead of diazald **77a** (Scheme 2.17).[126] A liquid-liquid two-phase system was used in a Corning flow reactor with integrated mixing elements. A solution of MNU **77b** in a 1:1 mixture diethyl ether:carbitol was mixed with an aqueous KOH-solution to generate diazomethane and the resulting reaction mixture was mixed with a solution of benzoic acid **78** in EtOH. Using the optimized conditions (**77b**:KOH:**78** 1:1.3:3, 25°C, RT1=28.4 s, RT2=5.8 s), methyl benzoate **79** was obtained in 97% yield.

Baxendale and coworkers used polymer-supported diazald and KO*t*Bu to generate diazomethane (Scheme 2.18).[127] A solution of KO*t*Bu was passed through a column of polymer-supported diazald and the resulting reaction mixture was quenched with H_2O. Subsequently, the biphasic mixture was separated using a FLLEX module (Flow Liquid Liquid EXtraction) resulting in an organic diazomethane solution and an aqueous waste stream. However, this method was not elaborated further due to low conversion and high pressure drops.
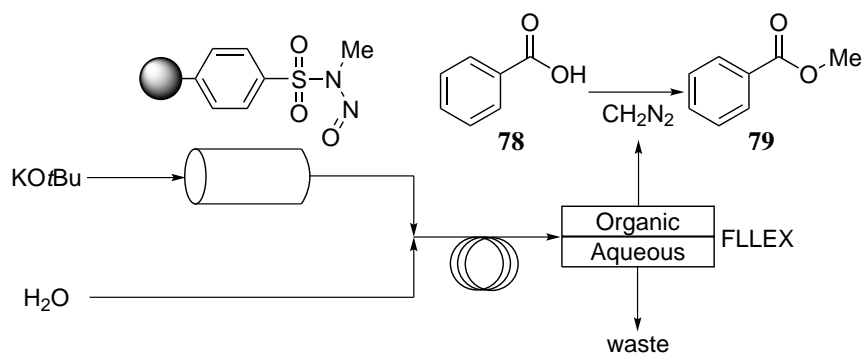
Scheme 2.18. Generation and separation of diazomethane using a FLLEX module
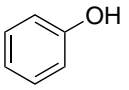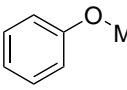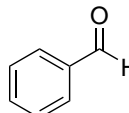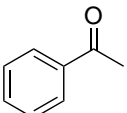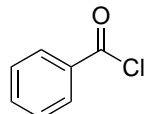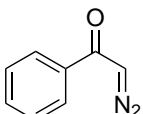
The use of membrane technology for diazomethane reactions was further explored by Kim and coworkers.[128] They developed a dual-channel microreactor with a PDMS (polydimethyl-siloxane) membrane which allows efficient generation, separation and reaction of diazomethane (Scheme 2.19).
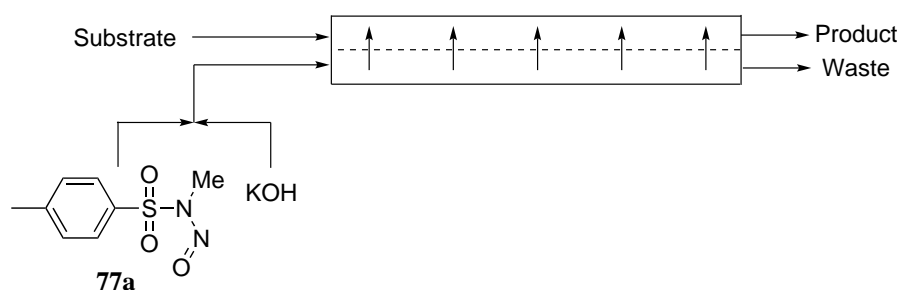
Scheme 2.19. Generation, separation and reaction of diazomethane using a dual-channel microreactor

Diazomethane was generated by mixing a solution of diazald **77a** in DMF with an aqueous KOH-solution containing a phase transfer catalyst (PTC). Subsequently, diazomethane was selectively transported through the PDMS membrane to the other channel where it reacted with the substrate. Excellent conversions were obtained for the reaction of diazomethane with different substrates at room temperature (Table 2.12).

Table 2.12: Generation, separation and reaction of diazomethane using a dual-channel microreactor

Entry	Substrate	Product	Yield (%)
1	**80**	**81**	>99
2	**82**	**83**	>99
3	**84**	**85**	81
4	**86**	**87**	90
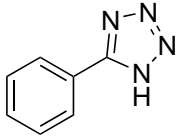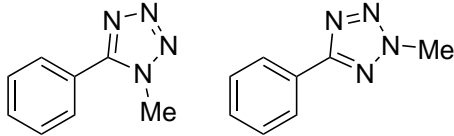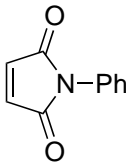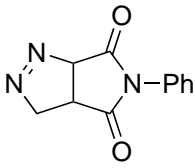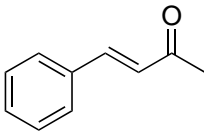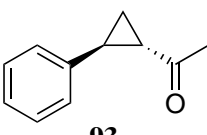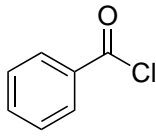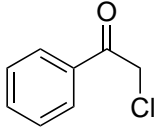
The excellent yield of the Arndt-Eistert reaction with benzoyl chloride **86** indicated that no water passed through the PDMS membrane and hence anhydrous diazomethane was separated from the reaction mixture (Table 2.12, entry 4). However, the output was limited due to the small internal volume of the reactor (60 μl) and some organic solvents (THF, Et_2O or $CHCl_3$) caused swelling of the PDMS polymer. These limitations prompted Kappe and coworkers to investigate this reaction using a tube-in-tube reactor.[129] The inner tube of the reactor served as a gaspermeable membrane (Scheme 2.20).
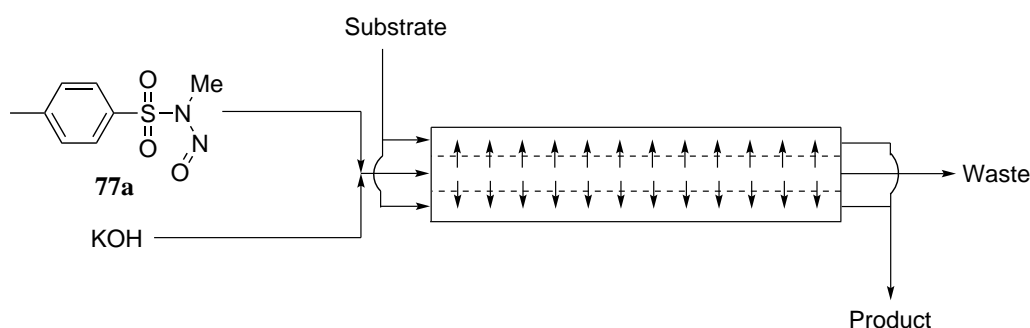
Scheme 2.20. Generation, separation and reaction of diazomethane using a tube-in-tube reactor

Quantitative conversion of benzoic acid **78** was obtained when a solution of diazald in MeOH and a solution of KOH in MeOH:H_2O (1:1) were mixed in the inner tube and a solution

of benzoic acid **78** in THF was passed through the outer tube with a stoichiometric ratio diazald:KOH:substrate 2:4:1. All three reagent streams were passed through the tube-in-tube reactor at the same flow rate corresponding with a residence time of 16 min for the methylation reaction. Next to benzoic acid **78**, substituted benzoic acids were converted into the corresponding methyl benzoates in excellent yields. The tube-in-tube reactor was also evaluated for the methylation of 5-phenyltetrazole **88**, the cycloaddition of diazomethane to *N*-phenylmaleimide **90**, the synthesis of cylopropanes and the Arndt-Eistert reaction (Table 2.13).

Table 2.13: Generation, separation and reaction of diazomethane using a tube-in-tube reactor

Entry	Substrate	Product	Yield (%)
1	**88**	**89a** **89b**	97[a]
2	**90**	**91**	76
3	**92**	**93**	59
4	**86**	**94**	91[b]

[a]**89a**:**89b** 12:85 [b]After quench with 6 M HCl

2.5.2   HCN and HN$_3$

HCN and HN$_3$ are extremely toxic and low boiling substances requiring rigorous safety precautions. However, these compounds can be generated safely from the corresponding salts using microreactor technology taking advantage of the small and closed hold-up volume.

This approach was used by Stevens and coworkers to synthesize diamino-1H-isochromen-1-ones **96** through a multicomponent reaction between 2-formylbenzoic acid **95**, an aromatic amine and HCN generated from KCN and HOAc (Scheme 2.21).[130]
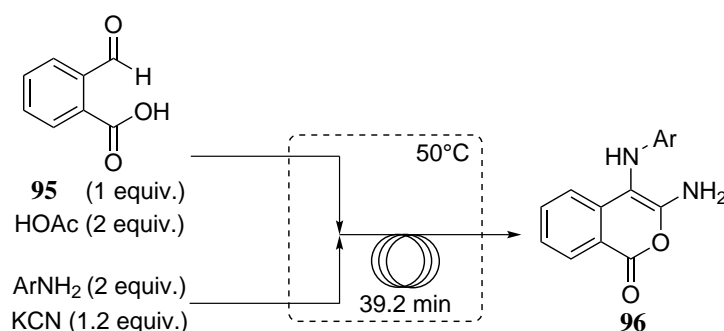
Scheme 2.21. Synthesis of diamino-1H-isochromen-1-ones **96** through a multicomponent reaction

Several aromatic amines were converted into the corresponding diamino-1H-isochromen-1-ones **96** in yields ranging from 49 to 75%. These diamino-1H-isochromen-1-ones were subsequently converted into the corresponding 1H-isochromeno[3,4-d]imidazol-5-ones under continuous flow conditions.[131] The same microreactor setup as for the generation of diamino-1H-isochromen-1-ones **96** was used to synthesize acetone cyanohydrin starting from acetone, KCN and HOAc.[132] Stevens *et al.* also evaluated this approach in the Kiliani reaction (Scheme 2.22).
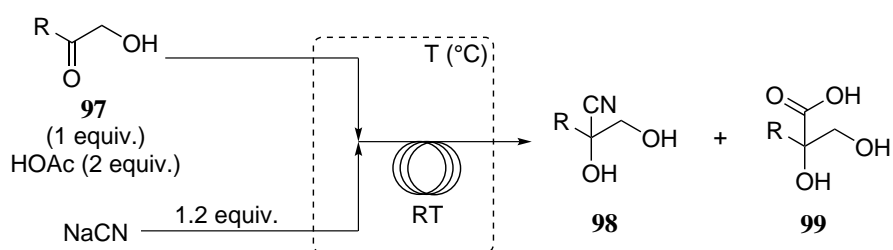
Scheme 2.22. Kiliani reaction

Depending on the choice of the solvent, reaction temperature and residence time, selective conversion to either the corresponding cyanohydrin **98** or α-hydroxycarboxylic acid **99** was obtained. In batch, the conversion of the starting material was limited and selective conversion was not possible (Table 2.14).[133]

Table 2.14: Kiliani reaction on dihydroxyacetone **97a**

Entry	Method	Ratio H$^+$/CN$^-$	RT (min)	T (°C)	Solvent	98a[a] (%)	99a[a] (%)
1	Batch	1.1	120	25	MeOH	50	-
2	Batch	1.1	180	60	MeOH:H$_2$O (3:1)	60	40
3	Flow	1.1	117.5	25	MeOH	>98	-
4	Flow	1.8	23.5	50	MeOH	>99	-
5	Flow	0.1	47	60	MeOH:H$_2$O (3:1)	-	>99

[a] Conversion determined via ^{13}C-NMR

Kappe *et al.* used hydrazoic acid to convert nitriles into 5-substituted 1*H*-tetrazoles **100** via a Huisgen 1,3-dipolar cycloaddition (Scheme 2.23).[134–136]
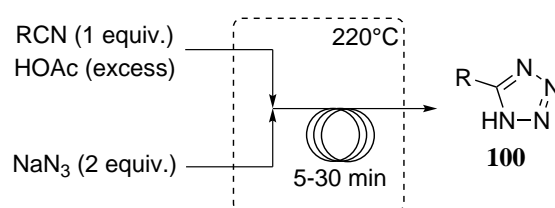
Scheme 2.23. Synthesis of 5-substituted 1*H*-tetrazoles **100**

Hydrazoic acid was generated in situ from NaN$_3$ and HOAc and subsequently reacted with the nitriles under high temperature (220°C) and high pressure (34 bar) conditions. The 5-substituted 1*H*-tetrazoles **100** were obtained in excellent yields (75-98%) with residence times ranging from 5 to 30 min. If this reaction is performed in batch, several safety precautions are required. Hydrazoic acid is a toxic and explosive compound and gas-phase mixtures of HN$_3$ in N$_2$ as low as 8% are reported to be explosive.[137] Moreover, liquid HN$_3$ is extremely shock-sensitive so condensation on cold surfaces has to be avoided. Using continuous flow technology, these hazards are significantly reduced due to the absence of a headspace and the small reaction volume, limiting the amount of hydrazoic acid present at any time.

HN$_3$ was also used to synthesize *N*-(2-azidoethyl)acylamides **102** (Scheme 2.24). HN$_3$ was generated through solvolysis of TMSN$_3$ with MeOH because the starting 2-oxazolines **101** were susceptible to hydrolysis in aqueous reaction media.[136,138]
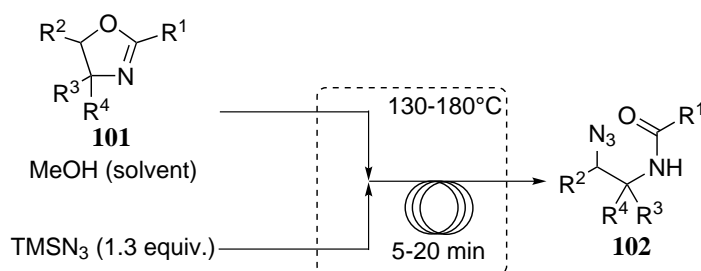
Scheme 2.24. Synthesis of *N*-(2-azidoethyl)acylamides **102**

Different *N*-(2-azidoethyl)acylamides **102** were synthesized in good to excellent yield (59-95%) with throughputs of around 0.5 kg/day. In a subsequent step, the *N*-(2-azidoethyl)acyl-amides **102** were hydrogenated to the corresponding *N*-(2-aminoethyl)acylamides.

2.5.3 Azides

Azides are valuable and versatile intermediates in organic synthesis.[139,140] However, azides are explosive compounds and can decompose in the presence of acids or certain metal salts. Moreover, organic azides are shock and heat sensitive and decompose under UV light irradiation.[141,142] These compounds can be manipulated safely using microreactor technology taking advantage of the small and closed hold-up volume.[143]

Baxendale *et al.* developed a continuous flow process for the synthesis of aryl azides **104** starting from the corresponding anilines **103** (Scheme 2.25). The reaction mixture was purified inline by passing it through a column with polymer-supported sulfonic acid and subsequently through a column with polymer-supported dimethylamine. Several aryl azides were synthesized with excellent conversions.[144,145] The same synthetic approach to aryl azides was reported by Bacchi *et al.*[146]
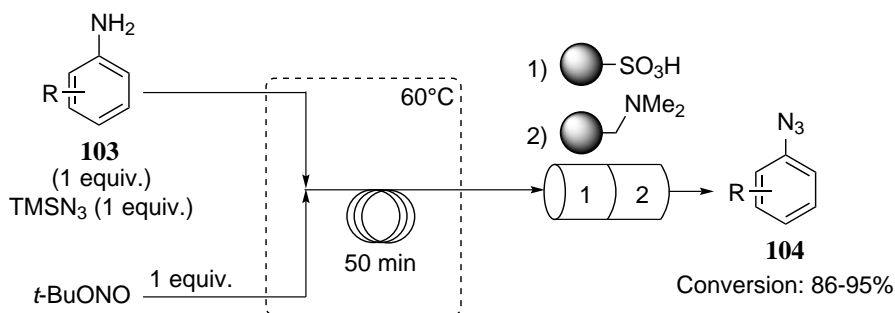
Scheme 2.25. Synthesis of aryl azides **104**

Williams and coworkers published the synthesis of alkyl azides under continuous flow conditions by reacting the corresponding alkyl halides with NaN_3.[137] The high reaction temperature and the use of toxic NaN_3 prompted Rutjes and coworkers to evaluate an alternative approach. They reported the continuous flow synthesis of benzyl azide using a diazotransfer reagent (imidazole-1-sulfonyl azide hydrochloride).[147,148]

Ley *et al.* used azide ion exchange resins to convert alkyl bromides **105** into the corresponding azides **106** in near quantitative yield (Scheme 2.26).[144,149]
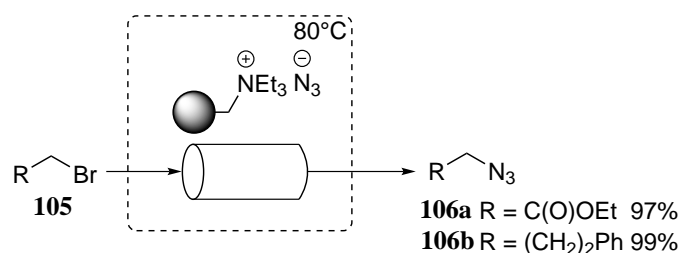
Scheme 2.26. Synthesis of alkyl azides **106**

Azides have been extensively used under continuous flow conditions in various reaction types: tetrazole synthesis,[150] 1,2,3-triazole synthesis,[145,146,151–156] Curtius rearrangement,[157–161] and Staudinger aza-Wittig reaction[144].

2.5.4 Nitration

As discussed previously, nitration reactions are often dangerous when performed on an industrial scale due to the exothermic nature of the reaction. Many research groups evaluated the continuous flow nitration of a broad range of substrates.[162–173] Nitration reactions can be performed safely under continuous flow conditions due to the excellent heat transfer and confined reaction volume, preventing runaway reactions or the accumulation of potentially dangerous intermediates. Moreover, the exothermic neutralization of the reaction mixture requires slow addition of the quenching reagent in batch while in flow, the reaction mixture can be quenched immediately inline, avoiding long neutralization times.

Nitration reactions can be performed safely on a considerable scale using microreactor technology. Zheng *et al.* described the nitration of a pyridine derivative on a kg-scale (Scheme 2.27).[171]
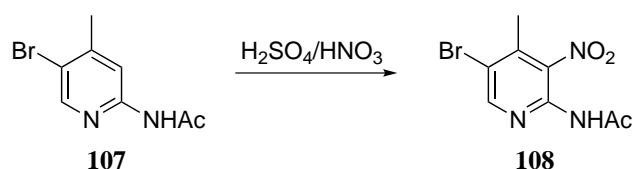
Scheme 2.27. Nitration of pyridine **107**

When the reaction is performed in batch at 25-33°C, the nitropyridine **108** can be isolated in 52-55% yield. However, an exotherm of 156 kJ/mol is observed which can lead to an adiabatic temperature rise of 76°C. Hence, safety precautions are required at large scale in order to prevent a possible runaway reaction. After optimization in a microreactor, the reaction could be run at 50-55°C with a throughput of 28 kg/day and an isolated yield of 59%.

2.6 Scale-up

The scale-up of reactions under continuous flow conditions can be based on two principles:[22]

1. **Scale-out:** Scale-out can be achieved by either extending the product collection time or increasing the throughput via simultaneously increasing the flow rates of the individual reagents and the length or size of the channels of the reactor.

2. **Numbering up:** With the numbering up principle, several reactors are operated in parallel. However, this strategy requires complex online monitoring and uniform fluid distribution to each reactor.[67]

2.6.1 Large-scale synthesis of pristane

Pristane **113** (2,6,10,14-tetramethylpentadecane) is an isoprenoid isolated from the basking shark (*Cetorhinus maximus*) and has been used as an adjuvant for monoclonal antibody production. Pristane **113** can be synthesized starting from farnesol **109** through oxidation, alkylation, dehydration and hydrogenation (Scheme 2.28).[117,174,175]
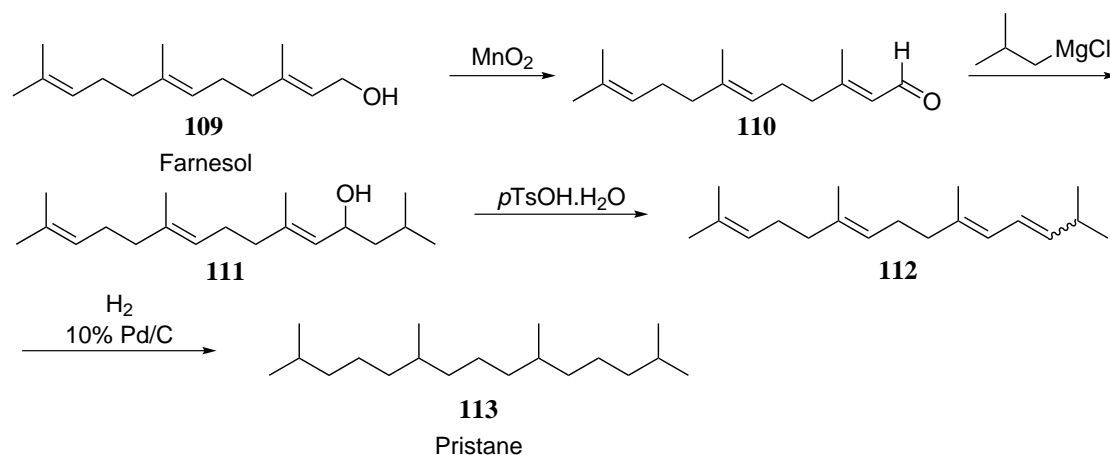
Scheme 2.28. Synthesis of pristane **113** starting from farnesol **109**

Small-scale synthesis of pristane **113** was readily performed in batch. However, when scaling up the batch process, dehydration of the alcohol **111** to **112** seemed to be the bottleneck. On a 100 mg scale, diene **112** was obtained as a mixture of (*E*)- and (*Z*)-isomers in 55% yield. When the scale was increased to 100 g, various side product were observed due to cyclization or alkyl migration reactions. Moreover, these side products were hard to separate from the desired diene **112**.[117,174,175]

Fukase *et al.* explored microreactor technology to perform the dehydration step (Scheme 2.29). A micromixer was used to mix the substrate **111** and *p*TsOH and the reaction mixture was quenched at room temperature with a sat. NaHCO$_3$ solution.[117,174,175] After optimization, diene **112** was obtained without the formation of side products. Starting from farnesol **109**, a yield of 80% was reached.
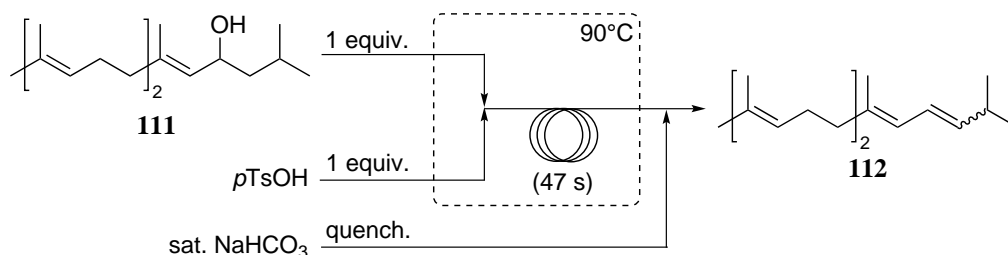
Scheme 2.29. Continuous flow step in the large scale synthesis of pristane

In a next step, the developed procedure was scaled-up. After the synthesis of the alcohol **111** on a kg-scale in batch, the dehydration was performed in flow. Ten micromixers were arranged in parallel and the dehydration was performed on a 8-kg-scale over a period of 3 to 4 days. After hydrogenation in batch, pristane **113** was obtained in an overall yield of 50-55%.

2.6.2 Phenyl boronic acid process

Aryl and alkyl boronic acids are versatile synthetic building blocks in organic synthesis. These compounds can be generated through addition of a Grignard reagent to a boronic acid precursor (Scheme 2.30). In batch, the formation of side products is controlled by (1) working at low temperatures (<-25°C), (2) slow addition of the Grignard reagent and (3) the use of dilute solutions.[176]
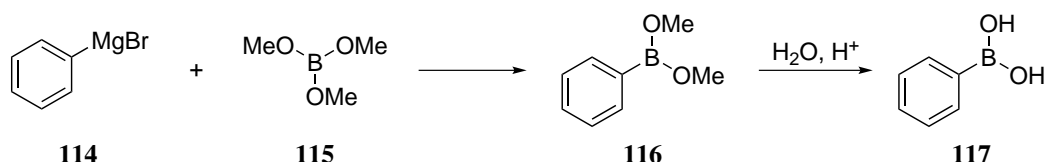
Scheme 2.30. Synthesis of phenyl boronic acid **117**

In the industrial batch procedure, a yield of 65% was obtained. Hessel *et al.* translated this batch process into a continuous flow process with enhanced process characteristics. A minimixer was used in combination with a stainless steel tube reactor. After optimization, a yield of 89% was obtained with a residence time of 10 s and a reaction temperature of 10°C. Compared to the batch process, significantly less side products were formed, resulting in an increased selectivity and hence easier product purification. With the developed continuous flow system, a production of 20 tons per year could be reached.

2.6.3 Effective production of the biodiesel additive STBE

STBE (solketal *t*-butyl ether) is a promising fuel additive as it improves engine performance.[177] Stevens and coworkers developed an industrial relevant continuous flow process for the synthesis of STBE with a throughput of several kg/h.[178] STBE was synthesized in two steps from glycerol (Scheme 2.31).
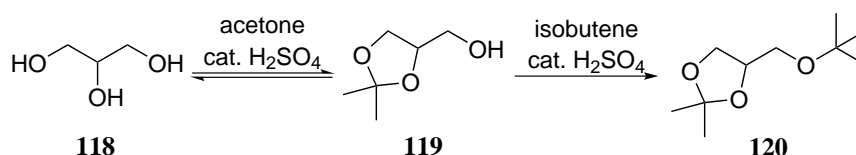
Scheme 2.31. Synthesis of STBE **120** starting from glycerol **118**

The synthesis of solketal under continuous flow conditions was optimized by evaluating the influence of the reaction temperature, the excess of acetone and the concentration of sulfuric acid. Moreover, it was noticed that the flow rate had a significant impact on the conversion.

A threefold increase of the flow rate resulted in an increase of the conversion from 69% to 98% and hence a throughput of 11 kg/h solketal was reached. In the subsequent acid catalysed etherification with isobutene, high yields (>85%) were obtained with as little as 1 equivalent of isobutene and very short residence times (41 s), leading to a throughput of 12 kg/h. Recently, a heterogeneously catalysed continuous flow process for the conversion of glycerol to solketal was reported.[179,180]

2.7   Conclusion

In this literature overview, some selected examples of chemical reactions that benefit from the intrinsic characteristics of microreactors have been discussed. Micro- and mesoreactors provide significant advantages compared to traditional batch equipment: (1) increased mass and heat transfer, (2) excellent mixing, (3) reaction time control, (4) increased safety features and (5) straight-forward scale-up. Reactions which are not possible in batch or require rigorous safety precautions can be performed in flow taking advantage of the intrinsic properties of continuous flow equipment.

Chapter 3

Results and discussion

3.1 Condensation of acid chlorides and alcohols using continuous flow

3.1.1 Introduction

Esters form an important class of organic compounds and are widely used within the food, cosmetic and pharmaceutical industry. Esters find application as flavor or fragrance (e.g. isoamyl acetate, banana fragrance), solvent (e.g. ethyl acetate), polymer (e.g. PET, polyethylene terephthalate), plasticizer (e.g. bis(2-ethylhexyl) phthalate), natural surfactant (e.g. sucrose esters), etc. The ester functionality can also be used as protection strategy for hydroxyl or carboxylic acid moieties.[36] A lot of synthetic methods are known in literature, including some continuous flow procedures. These continuous flow procedures include Fischer-type esterification,[181–183] the use of mixed anhydrides,[37] phase transfer catalyzed reactions,[38,43] the use of lipases,[184–187] heterogeneous catalysis[181,188] and the use of novel process windows (Scheme 3.1).[189,190] Two research groups described the use of acid chlorides for an esterification reaction in flow. Wiles *et al.* described the acetylation and benzoylation of phenol and 4-nitrophenol in flow using an EOF-based borosilicate glass microreactor (EOF: electroosmotic flow).[37] However, the substrate scope was limited to these two phenolic compounds and Et$_3$N was used to scavenge the formed HCl. Recently, Šinkovec *et al.* studied the phase transfer catalyzed reaction between of 4-*t*-butylphenol and 4-methoxybenzoyl chloride with NaOH. Tetrabutylammonium bromide (TBABr) was used as phase transfer catalyst (Scheme 3.1).[38]

In the framework of our research to use microreactor technology to develop reactions which benefit from continuous processing, we evaluated the catalyst-free condensation of acid chlorides with alcohols under continuous flow conditions.[73,130–133,178,191–196] The reaction between an acid chloride and an alcohol is a well-known reaction in batch and is typically performed in the presence of a catalyst. Among the base catalysts used for this reaction, the most common are pyridine, Et$_3$N, 4-dimethylaminopyridine (DMAP) and 1,4-diazo-bicyclo[2.2.2]octane (DABCO).[36,197,198] Beside these bases, some inorganic catalysts are reported in literature, e.g. LiClO$_4$,[199] Al$_2$O$_3$,[200–202] TiO$_2$[203] and BiCl$_3$.[204]
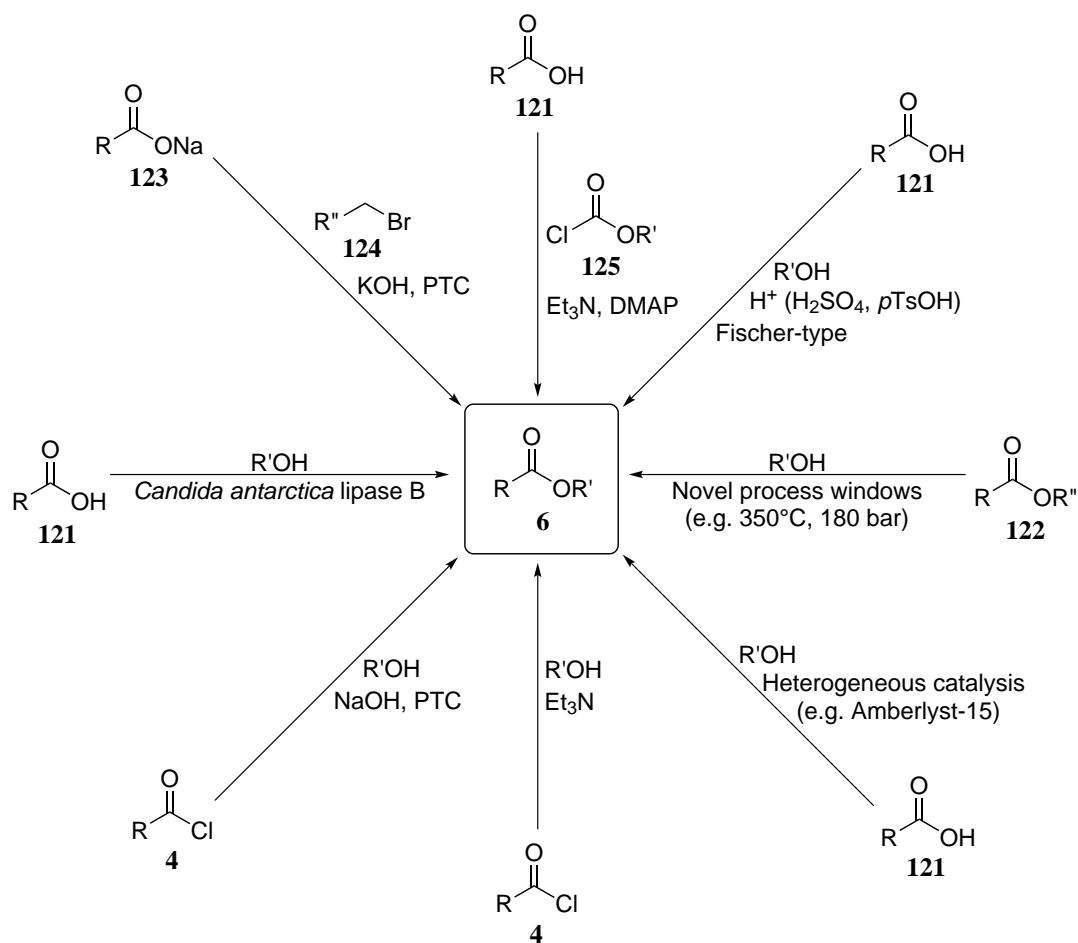
Scheme 3.1. Overview of known synthesis methods of esters under continuous flow conditions

Strazzolini *et al.* reported a catalyst-free procedure for the condensation of acid chlorides and alcohols.[205] However, a competition between alkyl halide and ester formation was observed. Ranu *et al.* reported a solvent-free and catalyst-free procedure.[206] Different alcohols were reacted with acetyl or propanoyl chloride giving the corresponding esters with an isolated yield between 88% and 93%. The scale of their reactions was restricted to 5 mmol and the substrate scope was limited to aliphatic acid chlorides. Moreover, as much as 20% excess of acid chloride was used and most of their research focussed on the use of acid anhydrides which makes the method less atom efficient in comparison with the use of acid chlorides (Scheme 3.2).

Taking these considerations into account, we evaluated the catalyst-free condensation of acid chlorides and alcohols using continuous flow in order to develop an industrially relevant, practical, efficient, fast and green procedure.
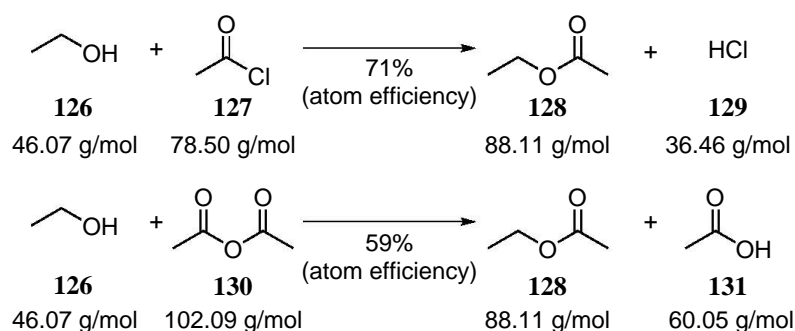
Scheme 3.2. Comparison of acid chlorides and acid anhydrides with regard to atom efficiency

3.1.2 Batch experiments

In preliminary batch experiments, the condensation of equimolar amounts of benzoyl chloride (BzCl) and ethanol was carried out at room temperature in diethyl ether. Only a trace of ethyl benzoate was detected after 21 hours. However, this benzoate was isolated in quantitative yield when benzoyl chloride was reacted with an excess of ethanol (10 equiv.) for 200 min. A similar condensation of benzoyl chloride with an excess of methanol (10 equiv.) gave quantitatively methyl benzoate after 15 min.

3.1.3 Optimization in flow

To evaluate the condensation of acid chlorides and alcohols under continuous flow conditions, the reaction between benzoyl chloride and methanol was chosen as a generic reaction. This reaction was optimized in a Labtrix® Start microreactor with an internal volume of 10 μl (Figure 3.1).
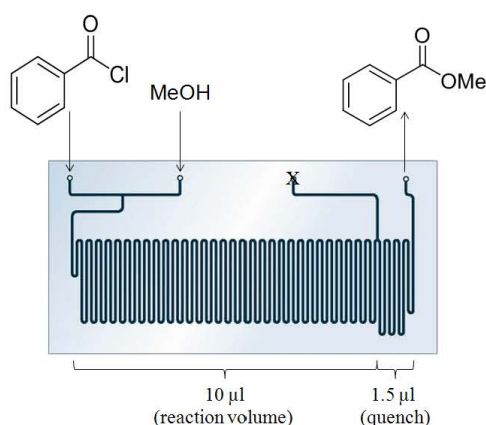
Figure 3.1. Condensation of benzoyl chloride and MeOH using a Labtrix® Start microreactor

In a first series of experiments, the reaction temperature, residence time (RT) and stoichiometric ratio of both reagents were varied and the results were evaluated qualitatively using IR (Figure 3.2).
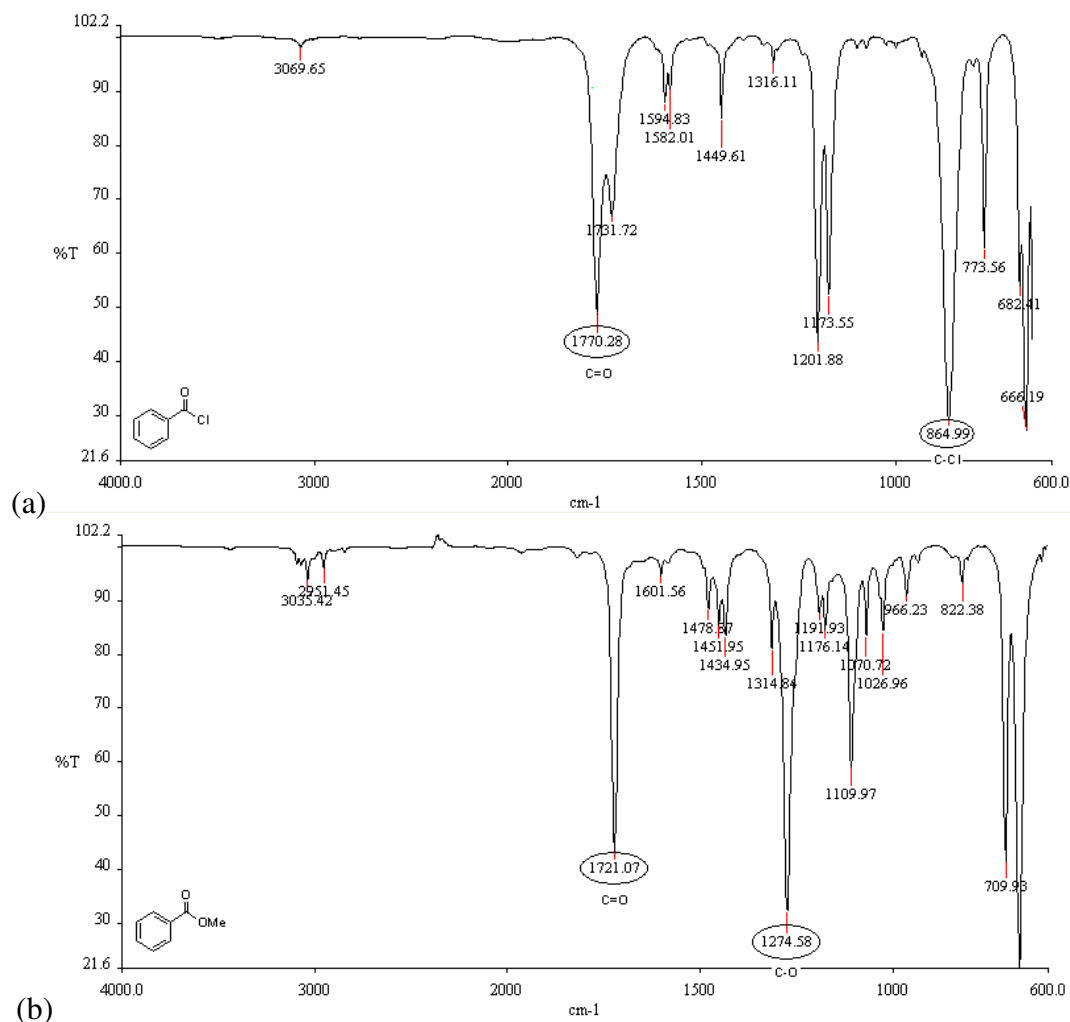
Figure 3.2. IR-spectrum of (a) benzoyl chloride and (b) methyl benzoate

Initial experiments were performed in Et$_2$O as solvent. A 5 M solution of benzoyl chloride and a 10 M solution of MeOH were mixed in the microreactor chip at the same flow rate leading to a stoichiometric ratio MeOH:BzCl of 2:1. Using a reaction temperature of 20°C and a residence time of 100 or 200 s, about half of the benzoyl chloride was converted into methyl benzoate based on IR. However, gas bubbles were observed in the microreactor chip as no BPR (back pressure regulator) was used. Gas bubbles can be formed due to liberation of the formed HCl-gas or due to the exothermic nature of the reaction leading to boiling of the solvent. When the reaction temperature was increased to 50°C in combination with a BPR of 10 bar, no increase of the conversion was observed.

Next, the condensation was evaluated solventless. Both reagents were pumped neat through the microreactor chip and after a steady state period, a sample was collected and evaluated qualitatively via IR (Table 3.1).

Table 3.1: Solventless condensation of benzoyl chloride with MeOH: qualitative evaluation

Entry	T	BPR	MeOH	RT[a] (s)		
	(°C)	(bar)	(equiv.)	100	200	300
1	50	-	1	+	+	ND
2	50	-	1.5	+	ND	ND
3	50	-	2	+	++	ND
4	50	-	3	ND	++	ND
5	80	10	1	ND	+++	+++
6	80	10	1.2	ND	+++	+++
7	80	10	1.3	ND	ND	++++
8	80	10	1.5	ND	++++	ND
9	80	10	2	++++	++++	ND
10	90	10	1	ND	ND	+++

[a] +: moderate conversion → ++++: excellent conversion

ND: not determined

From these experiments, it was clear that the reaction temperature was preferable above the atmospheric boiling point of methanol (T_b = 65°C). Good conversions were obtained with a reaction temperature of 80°C whereas the conversion was limited at 50°C. In the experiments performed without BPR, no gas bubbles were observed although conversions of about 50% were obtained. Therefore, the previously observed gas bubbles when using Et_2O at 20°C without BPR were most probably caused by boiling of the solvent due to the liberated heat during the reaction. The most important solventless experiments (Table 3.1, entries 5-10) were reconfirmed and the conversion was determined by GC (Table 3.2).

Table 3.2: Solventless condensation of benzoyl chloride with MeOH: quantitative evaluation[a]

T	RT	MeOH (equiv.)					
(°C)	(s)	1	1.1	1.2	1.3	1.5	2
80	100	-	-	-	-	-	97
80	200	-	-	96	-	98	98
80	300	95	-	99	100	-	-
90	300	96	-	-	-	-	-
100	300	-	99	-	-	-	-

[a] Conversion determined via GC

Full conversion of benzoyl chloride was obtained with a residence time of 300 s, a reaction temperature of 80°C and as little as 1.3 equivalents of MeOH. At lower residence times, traces of benzoyl chloride were detected in the reaction mixture, even if the ratio MeOH:BzCl was increased. In an attempt to achieve full conversion with a stoichiometric ratio beneath 1.3, the reaction temperature was increased to 90 or 100°C. Excellent conversions (99%) were obtained with a reaction temperature of 100°C and 1.1 equivalents of MeOH but traces of benzoyl chloride were still visible in the reaction mixture.

Using the optimized conditions for the condensation of benzoyl chloride and MeOH (80°C, 300 s, 1.3 equivalents of MeOH), the microreactor was run for 5.6 h in order to determine the isolated yield. The work up of the reaction mixture was very straightforward: after evaporation of the excess MeOH, pure methyl benzoate was obtained with an isolated yield of 96%.

In a next series of experiments, the optimized conditions for the condensation of benzoyl chloride and methanol were used for the condensation of benzoyl chloride and ethanol (Table 3.3).

With a reaction temperature of 80°C, the stoichiometric ratio EtOH:BzCl had to be above 1.3:1 in order to obtain good conversions. This was probably due to the fact that a temperature of 80°C is close to the atmospheric boiling point of EtOH ($T_b = 78°C$) while at this temperature, MeOH was superheated. Increasing the reaction temperature to 110°C led to full conversion with 1.3 equivalents of EtOH. Excellent conversions (99%) were obtained with a stoichiometric ratio EtOH:BzCl of 1.1:1 when the reaction temperature was raised to 130°C or 140°C.

Table 3.3: Solventless condensation of benzoyl chloride with EtOH[a]

T	RT	EtOH (equiv.)			
(°C)	(s)	1.1	1.3	1.5	2
80	300	-	88	93	98
100	300	-	99	-	-
110	300	95	100	-	-
130	300	99	-	-	-
130	400	99	-	-	-
140	300	99	-	-	-
140	400	99	-	-	-

[a] Conversion determined via GC

When benzoyl chloride was reacted with *i*PrOH instead of EtOH, the conversion was poor at a reaction temperature of 80°C, even with 2 equivalents of *i*PrOH (Table 3.4). Raising the reaction temperature furnished again good conversions. For the condensation of benzoyl chloride and *i*PrOH, the optimized conditions were a reaction temperature of 120°C, a residence time of 300 s and 1.3 equivalents of *i*PrOH.

Table 3.4: Solventless condensation of benzoyl chloride with *i*PrOH[a]
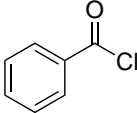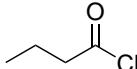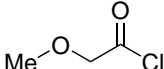
T	RT	*i*PrOH (equiv.)		
(°C)	(s)	1.3	1.5	2
80	300	-	-	61
100	300	92	95	-
110	300	99	100	-
120	300	100	-	-

[a] Conversion determined via GC

3.1.4 Substrate scope

Using the optimized conditions for the different alcohols, other acid chlorides were converted into their corresponding esters (Table 3.5).

Table 3.5: Condensation of acid chlorides with alcohols under continuous flow conditions

Entry	Acid chloride	Alcohol	RT (s)	T (°C)	Alcohol (equiv.)	Conversion[a] (%)
1		MeOH	300	80	1.3	100
2	**86**	EtOH	300	110	1.3	100
3		*i*PrOH	300	120	1.3	100
4		MeOH	300	80	1.3	100
5	**132**	EtOH	300	110	1.3	100
6		*i*PrOH	300	120	1.3	100
7		MeOH	300	80	1.3	91
8	**133**	EtOH	300	110	1.3	97
9		*i*PrOH	300	120	1.3	100

[a] Conversion determined via GC

Both aliphatic and aromatic acid chlorides reacted with low molecular weight alcohols to the corresponding esters with excellent conversions. When more challenging acid chlorides were used (benzyl chloroformate or methyl malonyl chloride), a complex reaction mixture was obtained. With these reactive substrates, different reaction products were formed, especially under the rather harsh microreactor conditions used for the esterification.

To extend the scope of the reaction, the continuous flow procedure was evaluated for solid acid chlorides and alcohols in solution. In a first attempt, a solution of a solid acid chloride (4-bromobenzoyl chloride) was reacted with neat MeOH, using different concentrations of the acid chloride and different solvents (dioxane, CH_2Cl_2 or MeCN) (Table 3.6).

In the first trials, high concentrations of 4-bromobenzoyl chloride were used in order to establish a good flow ratio between both reagent streams. However, when CH_2Cl_2 (5 M) or dioxane (4 M) was used, clogging of the microreactor channels (width = 300 μm, depth = 60 μm) was observed (Table 3.6, entries 1-2). Lowering the concentration to 3.25 M in dioxane or MeCN resulted in less than 5% conversion, even if up to 3 equivalents of MeOH were used (Table 3.6, entries 3-6). Subsequently, the concentration of the solution was lowered to 0.5 M in order to overcome possible mixing problems due to the viscosity of the 4-bromobenzoyl chloride solution (Table 3.6, entry 7). However, the conversion of the acid chloride was still limited to 10%. No further attempts were undertaken to increase the conversion.

Table 3.6: Condensation of 4-bromobenzoyl chloride with MeOH at 80°C

Entry	Solvent	Concentration (M)	MeOH (equiv.)	Conversion[a] (%)
1	CH_2Cl_2	5	2	clogging
2	dioxane	4	2	clogging
3	dioxane	3.25	1.3	<5
4	dioxane	3.25	2	<5
5	dioxane	3.25	3	<5
6	MeCN	3.25	2	<5
7	MeCN	0.5	2	10

[a] Conversion determined via GC

Subsequently, a solid alcohol (*p*-cresol) in solution was reacted with neat benzoyl chloride (Table 3.7).

Table 3.7: Condensation of benzoyl chloride with *p*-cresol

Entry	Solvent	Concentration (M)	*p*-cresol (equiv.)	T (°C)	RT (s)	Conversion[a] (%)
1	MeCN	2	1.3	80	300	25
2	MeCN	2	1.3	100	300	63
3	MeCN	2	1.3	120	300	78
4	MeCN	2	1.3	140	400	94
5	MeCN	2	2	140	400	98
6	dioxane	2	1.3	120	300	20

[a] Conversion determined via GC

The alcohol was dissolved in dioxane or MeCN with a concentration of 2 M. An initial experiment was conducted in MeCN at a reaction temperature of 80°C, a residence time of 300 s and 1.3 equivalents of *p*-cresol (Table 3.7, entry 1). However, these conditions resulted in a limited conversion of only 25%. The conversion increased (78%) by raising the temperature to 120°C (Table 3.7, entries 2-3). A further increase of the reaction temperature (140°C) in combination with an increased residence time of 400 s led to a conversion of 94% (Table 3.7, entry 4). Almost quantitative conversion was obtained if 2 equivalents of MeOH were used

instead of 1.3 (Table 3.7, entry 5). Dioxane was also evaluated as a solvent but appeared to be less suited in comparison to MeCN (compare entries 3 and 6, Table 3.7). The optimized conditions were also evaluated for the condensation of butyryl chloride with *p*-cresol, resulting in a conversion of 99%.

At last, the condensation of a solid acid chloride (4-bromobenzoyl chloride) with a solid alcohol (*p*-cresol) was evaluated when both reagents were dissolved in MeCN. The reactions were performed at a temperature of 140°C and a residence time of 400 s (Table 3.8).

Table 3.8: Condensation of 4-bromobenzoyl chloride (R(CO)Cl) with *p*-cresol (R'OH)

Entry	Concentration R(CO)Cl (M)	Concentration R'OH (M)	R'OH (equiv.)	Conversion[a] (%)
1	1	1	1.3	55
2	1	1	2	63
3	0.5	0.5	2	33
4	1.5	1.5	2	79
5	2	2	2	74
6	1.5	3	2	55

[a] Conversion determined via GC

Initial experiments revealed that 2 equivalents of *p*-cresol are needed in order to obtain reasonable conversions (Table 3.8, entries 1-2). Varying the concentration of both solutions finally led to the optimized conditions in which both reagents were dissolved in MeCN with a concentration of 1.5 M. A conversion of 79% could be obtained (Table 3.8, entry 4).

3.1.5 Scale-up in flow

In order to investigate the applicability of this reaction on an industrial scale, the developed mmol procedure was scaled-up. The optimized conditions for the condensation of benzoyl chloride and MeOH (80°C, 300 s, 1.3 equivalents of MeOH) were tested with a mesoreactor with an internal volume of 6.5 ml (KiloFlow® from Chemtrix) (Figure 3.3).

Labtrix® Start

KiloFlow®

10 µl

6.5 ml
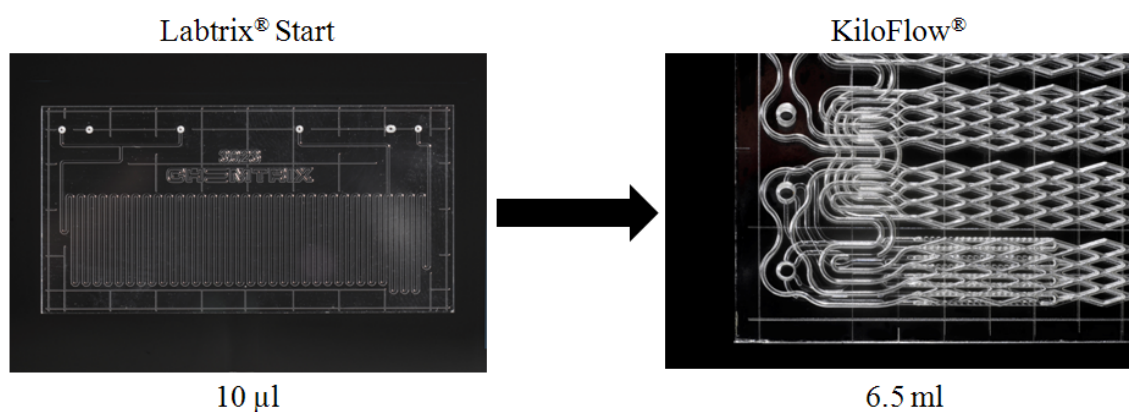
Figure 3.3. Scale-up of the developed mmol procedure from the Labtrix® Start microreactor to the KiloFlow® reactor

The condensation of benzoyl chloride and MeOH was run for several hours on the KiloFlow® reactor in order to monitor the yield during the course of the operation. After reaching steady state, the experiment was run for 4 h and samples were collected over a period of one hour. The work up of the reaction mixture was very straightforward. Pure methyl benzoate was obtained after evaporation of the excess MeOH. The isolated yield for each of the 4 samples was determined individually. Excellent and stable isolated yields were obtained during the course of the operation (Figure 3.4). The use of this system led to a capacity of 1.5 kg/day of methyl benzoate with an isolated yield of 98%.
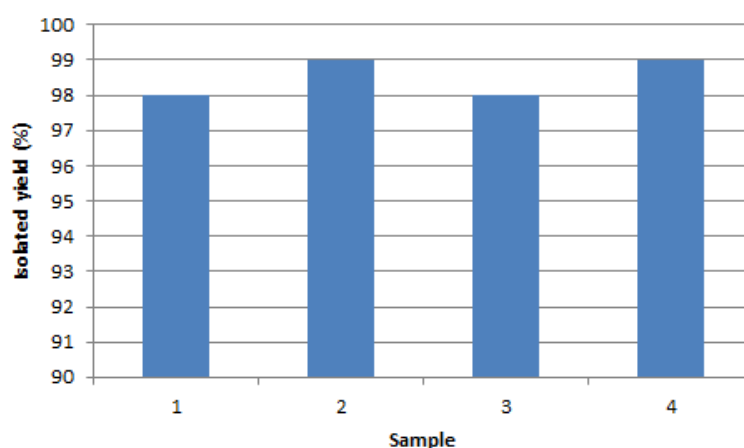
Figure 3.4. Condensation of benzoyl chloride with MeOH on the KiloFlow® reactor

The formed HCl could be captured in two separate steps: (1) during collection of the reaction mixture and (2) after collection of the reaction mixture (Figure 3.5).
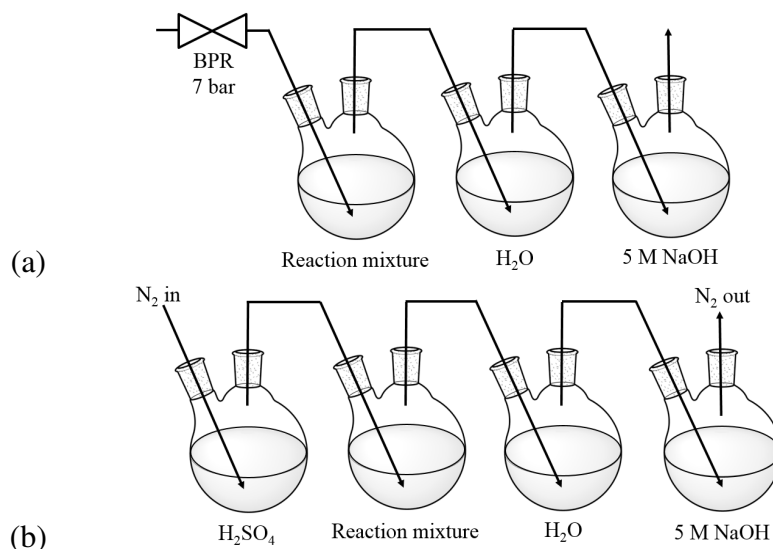
Figure 3.5. Recuperation of the formed HCl: (a) during collection, (b) after collection

In a first step, HCl was captured during the collection of the reaction mixture by connecting the collection flask with two subsequent flasks (Figure 3.5a). The first flask contained pure water while the second flask contained 5 M NaOH. Due to a pressure build up in the headspace of the closed collection flask while collecting the sample, the headspace was forced through both aqueous solutions trapping any HCl present. Titration revealed that the HCl vapour was predominantly trapped in the pure water phase. About 31% of the formed HCl was trapped in the first flask while the amount of HCl collected in the 5 M NaOH solution could be neglected.

In a second step, HCl was captured after collection of the reaction mixture (Figure 3.5b). The collected reaction mixture was purged with dry N_2 for one hour and the gas stream was directed through pure water and 5 M NaOH . Titration of both aqueous layers revealed again that the amount of HCl trapped in the 5 M NaOH solution was negligible. About 15% of the formed HCl was trapped in the water in the second step. In total, about 46% of the formed HCl could be captured as an aqueous solution. The remaining HCl could not be captured from the reaction mixture and was lost during removal of the excess MeOH under reduced pressure.

3.1.6   Conclusions

The developed catalyst-free continuous flow procedure provides a green alternative for the existing methods of esterification of acid chlorides. Both aliphatic and phenolic hydroxyl groups reacted with different acid chlorides with formation of the corresponding esters in excellent conversions and very short reaction times (300 - 400 s). The reaction was performed solventless

for liquid reagents but required a solvent for solid reagents in order to prevent clogging of the microreactor channels. Upscaling the reaction resulted in a productivity of 2.2 g/min of methyl benzoate with an isolated yield of 98% and recuperation of the formed HCl.

3.2 Continuous flow bromination of methyl sulfones and methane-sulfonates

3.2.1 Introduction

The halomethyl sulfonyl group is incorporated in several active biocides which find application in the protection of paints, leather treatment liquids, coolants, metal cutting fluids, etc. against bacterial or fungal deterioration.[207–209] The AMICAL™ Preservatives of The Dow Chemical Company for example, are useful for controlling microbial degradation in adhesives, paper coatings, plastics, textiles and coatings. The active ingredient is diiodomethyl *p*-tolyl sulfone **134** (Figure 3.6).[210]
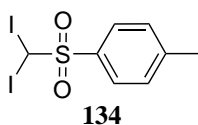
Figure 3.6. Diiodomethyl *p*-tolyl sulfone **134**

Smith described the use of diiodomethyl *p*-tolyl sulfone **134** for the treatment of fungal or yeast infections of the skin.[211] Halomethyl sulfonyl derivatives have also potential as herbicide or fungicide to protect agricultural products or as antifouling paints for ships and fishing nets.[212–214] Further, trihalomethyl sulfonyl derivatives find application in the graphics industry where they are used as polymerization initiator in lithographic printing plates (Figure 3.7).[215–218]
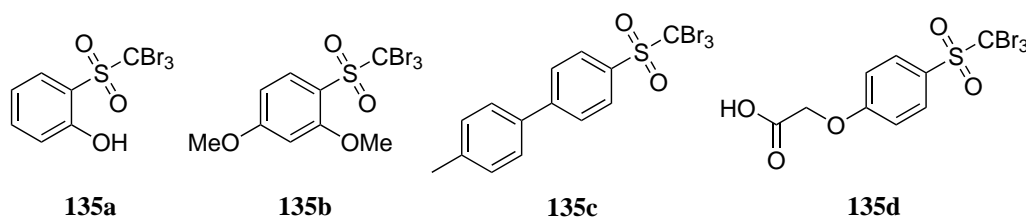
Figure 3.7. Trihalomethyl sulfones as polymerization initiator in printing plates

Several methods for the synthesis of trihalomethyl phenyl sulfones are described in literature. The reaction of thiols or disulfides with halofluoromethanes and subsequent oxidation feature the desired sulfones.[219–221] Farrar described the synthesis of trichloro- and tribromomethyl phenyl sulfones starting from phenylthioacetic acid and sodium hypohalite.[222] Ochal *et al.* synthesized bromodichloromethyl 4-chlorophenyl sulfone from chlorobenzene.[223] This group also developed the synthesis of trihalomethyl phenyl sulfones using chlorination with sodium hypochlorite or bromination with sodium hypobromite or bromine chloride.[224,225]

Due to interest from industry, we evaluated the continuous flow synthesis of tribromomethyl sulfones and tribromomethanesulfonates using the biphasic reaction between methyl sulfones or methanesulfonates and hypobromite. Potassium hypobromite is formed by reaction of potassium hydroxide with bromine:

$$Br_2 + 2KOH \quad \longrightarrow \quad KBr + KOBr + H_2O \tag{3.1}$$

However, potassium hypobromite is unstable and degrades rapidly towards KBr, $KBrO_3$ and O_2:

$$3KOBr \quad \longrightarrow \quad 2KBr + KBrO_3 \tag{3.2}$$

$$2KOBr \quad \longrightarrow \quad 2KBr + O_2 \tag{3.3}$$
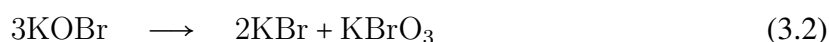
In order to prevent degradation in batch, the KOBr-solution is kept at low temperature (0-5°C) for a limited period of time. Moreover, bromine is a corrosive product and manipulation of bromine requires several safety precautions.

Performing the synthesis of hypobromite and the subsequent bromination of methyl sulfones or methanesulfonates in continuous flow is industrially relevant and could have several advantages over the batch process. A continuous flow process is inherently safer than the corresponding batch process due to the small internal volume associated with the continuous flow reactors. This safety feature is important when working with toxic reagents. Under continuous flow conditions, hypobromite can be synthesized and immediately used in situ in order to prevent degradation. Moreover, continuous flow reactors have excellent heat and mass transfer characteristics which can provide a significant improvement for biphasic reactions.[38,42–47] Finally, scaling-up a continuous flow process is very straightforward by the numbering-up concept compared to the scale-up of batch procedures which is often ambiguous.[25]

3.2.2 Batch reaction

Because of its industrial relevance, the reaction between 4-isopropoxyphenyl methyl sulfone **7** and KOBr was chosen as generic reaction for the evaluation of the bromination of methyl sulfones (Scheme 3.3). The reaction was first evaluated in batch based on an industrial procedure. The bromination reaction was performed in a biphasic water/toluene system with tetrabutylammonium bromide (TBABr) as a phase transfer catalyst.
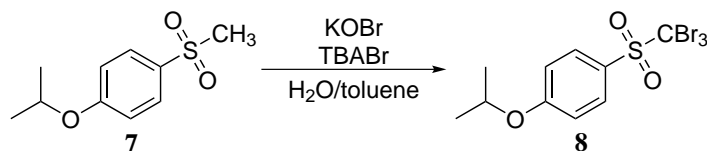
Scheme 3.3. Bromination of 4-isopropoxyphenyl methyl sulfone **7**

The KOBr-solution was prepared by dropping Br_2 to an aqueous solution of KOH at 0°C. This solution was subsequently added dropwise to a solution of 4-isopropoxyphenyl methyl sulfone **7** and TBABr in toluene at 38°C. The reaction required 22 h to reach completion. After work up, the end product, tribromomethyl 4-isopropoxyphenyl sulfone **8**, was obtained with an isolated yield of 94%. Only the tribrominated derivative was observed and no further purification was required.

3.2.3   Optimization in flow

Two different flow reactor systems were evaluated for the optimization of the bromination reaction: (1) a tube reactor (Figure 3.8a) and (2) a static mixer (Figure 3.8b). In the initial flow experiments, a 1 M KOBr solution was prepared in batch by adding Br_2 to a 5.9 M KOH solution.

(a)

(b)
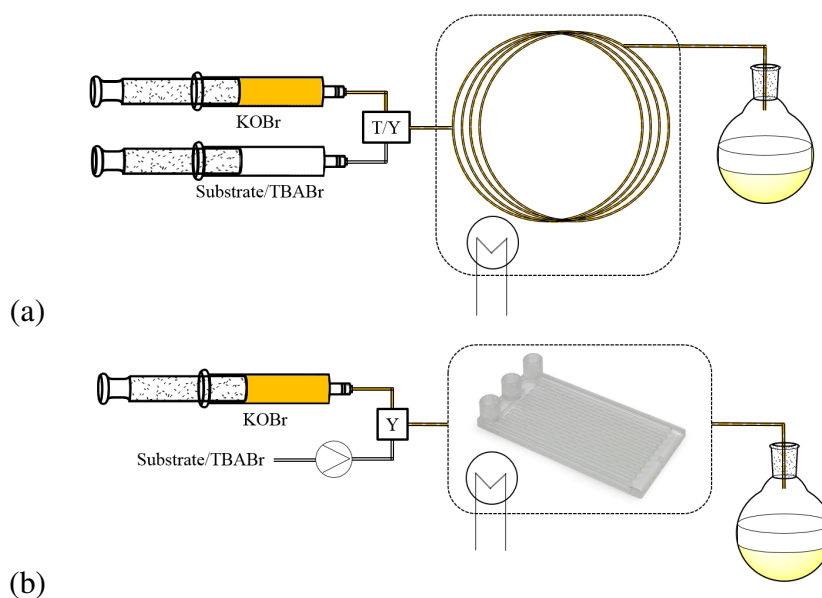
Figure 3.8. Schematic representation of the continuous flow setup: (a) tube reactor, (b) Uniqsis® static mixer

3.2.3.1   Tube reactor

The first flow reactor was a tube reactor built up of PFA-tubing with a volume of 3 ml and a T- or Y-connector to combine both reagent streams (Figure 3.8a). Several reaction parameters were evaluated: reaction temperature, residence time, equivalents of PTC and equivalents of KOBr. Besides this, the type of mixer (T- or Y-connector) had an influence on the conversion. The reaction mixtures were analyzed by HPLC-UV. In order to calculate the reaction mixture composition, a standardisation curve was prepared for both the starting material **7** and end product **8** (Figure 3.9).
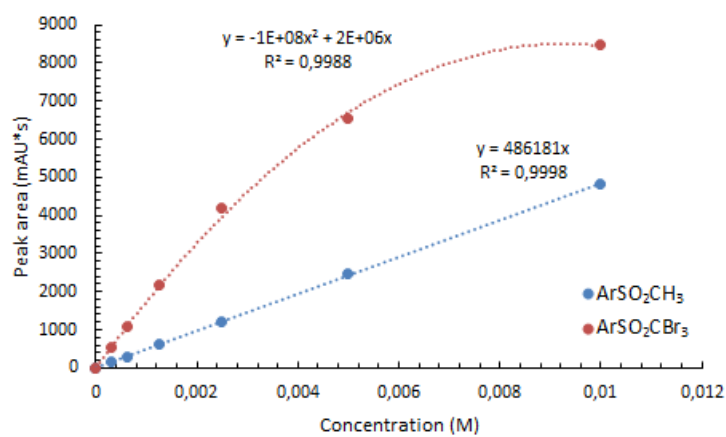
Figure 3.9. Standardisation curve for 4-isopropoxyphenyl methyl sulfone **7** ($ArSO_2CH_3$) and tribromomethyl 4-isopropoxyphenyl sulfone **8** ($ArSO_2CBr_3$) (HPLC-UV, 254.8 nm)

For the calculation of the reaction mixture composition, peak areas (HPLC-UV, 254.8 nm) were converted into concentrations and subsequently, the concentrations were expressed relatively (%).

The results for this series of optimization experiments are summarized in Table 3.9. Both reagent solutions were pumped at the same flow rate through the tube reactor in order to obtain a good flow ratio and hence efficient mixing. During the reaction, a dibrominated side product is formed due to incomplete conversion of the starting material **7**. For the calculation of the amount of the dibrominated intermediate, the standardisation curve for the end product was used because no standardisation curve for this intermediate could be prepared as no dibrominated product was available.

Table 3.9: Overview of the results for the bromination reaction in the tube reactor

Entry	T (°C)	RT (min)	PTC (equiv.)	KOBr[a] (equiv.)	T/Y mixer	RCH_3 (%)	$RCHBr_2$ (%)	$RCBr_3$ (%)
1	40	15	0.5	3.3	T	95	2	3
2	40	30	0.5	3.3	T	91	2	7
3	50	30	0.5	3.3	T	75	4	21
4	60	30	0.5	3.3	T	61	4	35
5	60	30	0.5	6.7	T	60	2	38
6	60	30	0.5	6.7	Y	39	2	59
7	60	30	1	6.7	Y	44	2	54
8	70	30	0.5	6.7	Y	27	2	71
9	70	60	0.5	6.7	Y	35	2	63

[a]A solution of 0.3 M (resp. 0.15 M) starting material was used for the reaction with 3.3 (resp. 6.7) equiv. KOBr

Starting with a reaction temperature of 40°C, a residence time of 15 min, 0.5 equiv. TBABr and a small excess of 3.3 equiv. KOBr, predominantly starting material was detected (Table 3.9, entry 1). If the residence time was prolonged to 30 min, again mainly starting material was observed (Table 3.9, entry 2). In a next step, the reaction temperature was gradually increased to 60°C, leading to better conversions (Table 3.9, entries 2-4). Next, a series of experiments was performed with 6.7 equiv. KOBr, leading to a slight decrease of the amount of the dibrominated intermediate (Table 3.9, entry 5). Changing the T-connector for a Y-connector led to a plug flow with smaller plugs and hence a larger interfacial area. For the T-connector, 2 interfaces were present over a length of 28 mm while for the Y-connector 2 interfaces were present over a length of 4 mm (Figure 3.10).
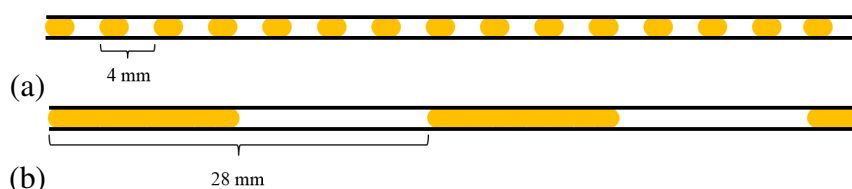
Figure 3.10. Plug flow for the (a) Y-connector and (b) T-connector

Assuming a spherical interface between the aqueous and organic phase, the interfacial area was estimated as follows:

$$\text{Interfacial area (m}^2 \text{ m}^{-3}) = \frac{x \cdot \frac{4 \cdot \pi \cdot (\frac{\text{ID}}{2})^2}{2}}{1 \cdot \pi \cdot (\frac{\text{ID}}{2})^2} \tag{3.4}$$

with

- x = number of interfaces
- ID = internal diameter (m)
- l = length (m)

Calculating the interfacial area for the plug flow with the T-connector, resp. Y-connector, resulted in values of 143 m^2 m^{-3}, resp. 1000 m^2 m^{-3}. A significant increase in the interfacial area was observed when a Y-connector was used instead of a T-connector, resulting in higher conversions for the Y-connector (Table 3.9, entry 6). Using stoichiometric amounts of PTC instead of 0.5 equivalents had no effect on the composition of the reaction mixture (Table 3.9, entry 7). Next, the reaction temperature was raised to 70°C resulting in a higher conversion of the starting material **7** (Table 3.9, entry 8). In an attempt to further increase the conversion of the starting material **7**, the residence time was increased to 60 min without any positive effect on the conversion (Table 3.9, entry 9). With a straightforward tube reactor, full conversion of the substrate **7** was not possible.

3.2.3.2   Uniqsis® static mixer chip

In a next series of experiments, the optimization procedure was repeated on a glass static mixer chip (Uniqsis®) (Figure 3.8b). The most optimal conditions for the tube reactor (Table 3.9, entry 8) were used as a starting point for the evaluation of the bromination reaction in the static mixer. In a first step, the influence of the flow rate (and thus residence time) on the conversion was evaluated (Figure 3.11). However, because more efficient mixing was expected in the static mixer compared to the tube reactor due to the integrated mixing elements, experiments were started with a residence time of 15 min.
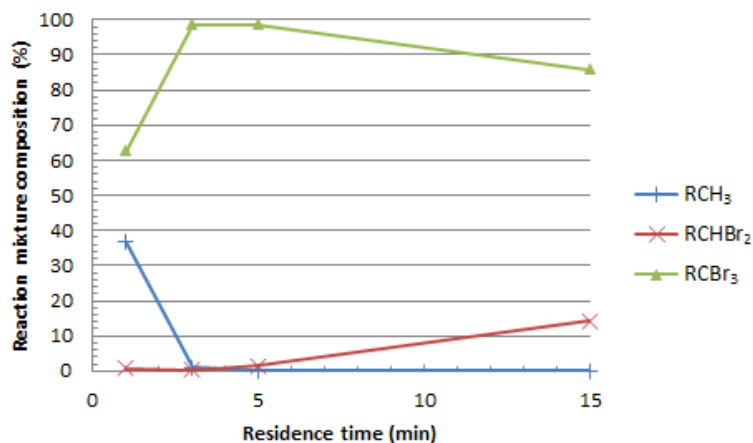
Figure 3.11. Influence of the residence time on the reaction mixture composition. Conditions: 70°C, 6.7 equiv. KOBr, 0.5 equiv. TBABr. Reaction mixture composition based on HPLC-UV (254.8 nm).

Starting the experiments with a residence time of 15 min, 86% end product **8** was detected on HPLC-UV. Decreasing the residence time to 5 min resulted in full conversion of the starting material **7** and only traces of the dibrominated intermediate were detected. A further decrease of the residence time to 3 min led to almost full conversion (99%) of the starting material **7** into the tribrominated derivative **8**. In an attempt to increase the throughput, a residence time of 1 min was evaluated. However, this residence time was too short to reach full conversion. Based on these observations, an optimum in the residence time was observed. If the residence time is too low (flow rate too high), the reaction could not reach full conversion. If the residence time is too high (flow rate too low), less efficient mixing was observed.

In a next step, the influence of the reaction temperature on the conversion was determined (Figure 3.12). In order to obtain full conversion of the starting material into the tribrominated derivative, a reaction temperature of 85°C was required.
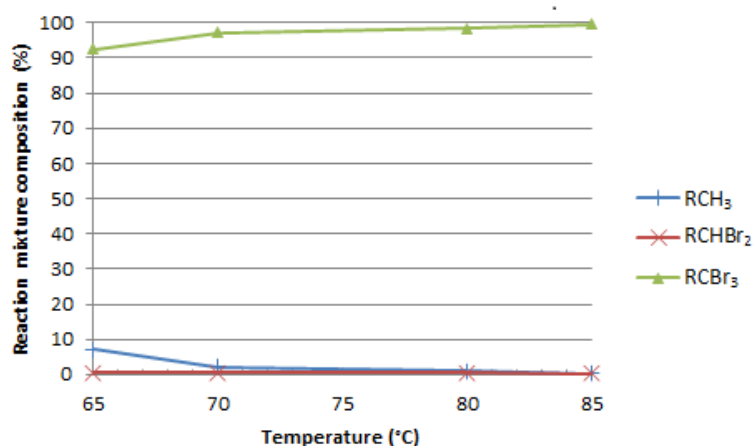
Figure 3.12. Influence of the reaction temperature on the reaction mixture composition. Conditions: 3 min residence time, 6.7 equiv. KOBr, 0.5 equiv. TBABr. Reaction mixture composition based on HPLC-UV (254.8 nm).

Finally, the amount of KOBr was reduced (Figure 3.13). Full conversion of the starting material **7** was observed with as little as 4 equivalents of KOBr. Lower amounts of KOBr resulted in incomplete conversion.
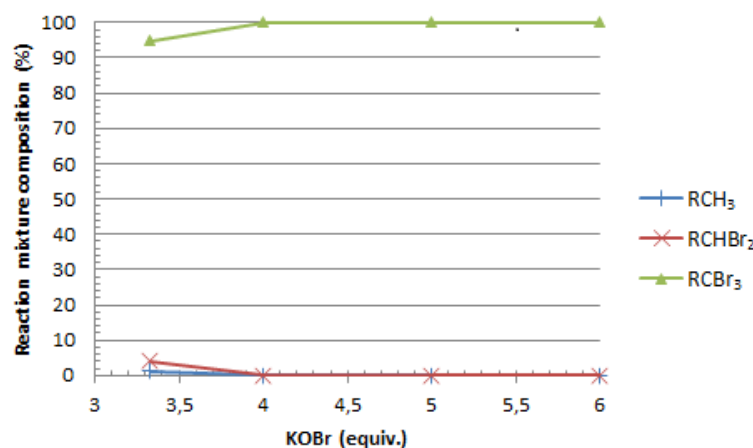
Figure 3.13. Influence of the amount of KOBr on the reaction mixture composition. Conditions: 3 min residence time, 85°C, 0.5 equiv. TBABr. Reaction mixture composition based on HPLC-UV (254.8 nm).

When both continuous flow systems were compared, the Uniqsis® glass static mixer was superior to the tube reactor. The mixing characteristics of the static mixer resulted in the formation of an emulsion, a dispersion of the toluene phase in the aqueous phase was observed. Hence, very efficient contact between the aqueous and toluene phase was obtained, resulting in

full conversion of the starting material **7** under the optimized conditions. In order to estimate the interfacial area of the emulsion, it was assumed that toluene was dispersed in the aqueous phase as spheres with a diameter corresponding to about half of the nominal diameter of the channels of the static mixer chip (1 mm). Hence, spheres with a radius of 0.25 mm were obtained. The interfacial area of the toluene phase could be estimated as follows:

$$\text{Interfacial area (m}^2\text{ m}^{-3}{}_{\text{toluene}}) = \frac{4 \cdot \pi \cdot r^2}{\frac{4}{3} \cdot \pi \cdot r^3} \tag{3.5}$$

with r = radius of the dispersed toluene spheres.

Hence the interfacial area of the toluene phase was estimated as 12000 m^2 m^{-3}. As the toluene phase comprised only 45% of the total volume of the reaction mixture (F_{KOBr} = 0.33 ml/min, $F_{\text{substrate/TBABr}}$ = 0.27 ml/min), the interfacial area, expressed as surface area per unit of reaction volume, was estimated as 5400 m^2 m^{-3}.

In the tube reactor, a plug flow was observed with a smaller interfacial area in comparison to the formed emulsion in the Uniqsis® system. In the tube reactor, a longer residence time and more KOBr were required for the conversion of the starting material and full conversion of the starting material **7** could not be reached.

3.2.4   Substrate scope
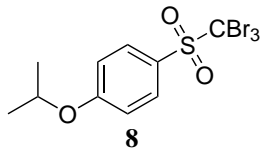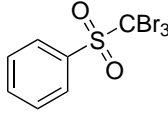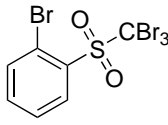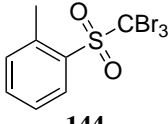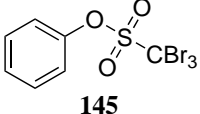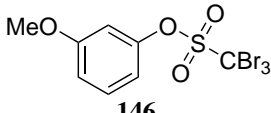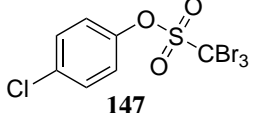
The Uniqsis® static mixer was used to synthesize a library of tribromomethyl sulfones and the substrate scope was broadened to methanesulfonates. First of all, several non-commercial methyl sulfones and methanesulfonates were synthesized in good to excellent yields (Schemes 3.4 and 3.5).[225,226]
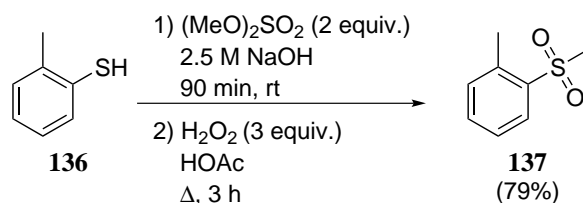
Scheme 3.4. Synthesis of methyl 2-methylphenyl sulfone **137**

Subsequently, the bromination reactions were evaluated in flow using the previously optimized conditions (static mixer, 85°C, 3 min, 4 equivalents of KOBr) and the results of these flow experiments are summarized in Table 3.10. For comparison purposes, the reactions were also performed in batch. Unless otherwise stated, no purification of the end product was necessary.
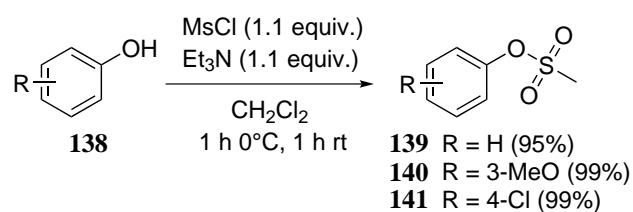
Scheme 3.5. Synthesis of methanesulfonates **139-141**

Table 3.10: Overview of synthesized tribromomethyl sulfones and tribromomethanesulfonates

| Entry | Compound | FLOW | | BATCH |
		Isolated yield (%)	Calculated throughput (g/day)	Isolated yield (%)
1	**8**	quantitative	53	94
2	**142**	87	40	82
3	**143**	48[a]	26	49
4	**144**	77[b]	37	69
5	**145**	87[b]	41	88
6	**146**	83[b]	42	84
7	**147**	84[b]	43	89

[a]Purification: recrystallization

[b]Purification: column chromatography

Excellent and comparable yields were obtained for the tribromination of methyl sulfones and methanesulfonates using batch or flow conditions. In batch, no further purification of the end product was necessary after work up of the reaction mixture whereas purification was sometimes required for the flow experiments. Lower yields were mainly caused by losses during work up of the reaction mixture.

The optimized flow procedure was also evaluated for the bromination of *N*-aryl methanesulfon-amides. These starting materials (*N*-phenyl methanesulfonamide **148**, *N*-3-chlorophenyl methanesulfonamide **149** and *N*-2,4-dimethylphenyl methanesulfonamide **150**) were obtained in batch via mesylation of the corresponding anilines (Scheme 3.6).
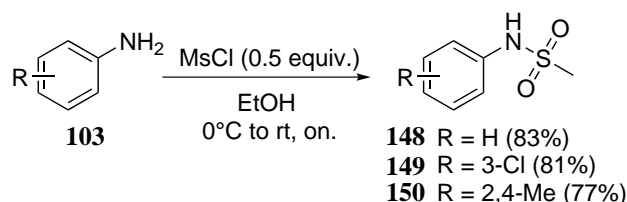
Scheme 3.6. Synthesis of *N*-aryl methanesulfonamides **148**-**150**

However, bromination of the aromatic system was observed for these substrates. Table 3.11 gives an overview of the products detected in the reaction mixtures based on ^{1}H-NMR.

Table 3.11: Bromination of *N*-aryl methanesulfonamides

3.2.5 Synthesis of KOBr in flow

In order to combine the synthesis of hypobromite with the subsequent bromination reaction, we focused on the continuous flow synthesis of KOBr starting from Br_2 and a KOH solution. The flow rates of Br_2 and the KOH-solution were determined by the stoichiometric ratio and residence time required for the subsequent bromination reaction. A first attempt to synthesize KOBr in flow was made after optimization of the bromination of 4-isopropoxyphenyl methyl sulfone **8** in the tube reactor. The reaction conditions with the highest conversion of **7** were used to determine the flow rate of Br_2 and the KOH solution. Pure bromine (2.5 μl/min) and a 5.9 M KOH solution (0.05 ml/min) were mixed in a T-mixer before entering a tube reactor of 0.5 ml at 0°C (Scheme 3.7).
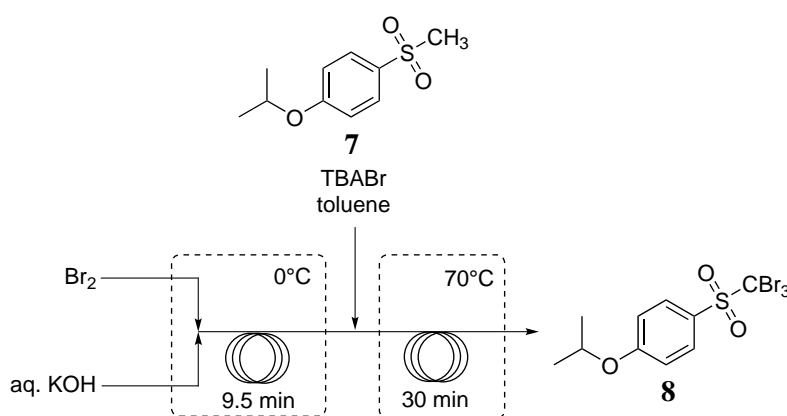
Scheme 3.7. Continuous flow synthesis of KOBr

After the T-mixer, inefficient mixing was observed (plug flow of bromine and the KOH-solution) resulting in insufficient formation of KOBr for the subsequent bromination reaction. Only 30% **8** was detected in the reaction mixture based on HPLC-UV. Probably the large difference in flow rate between both reagents caused this inefficient mixing (flow ratio Br_2:KOH 1:20).

After optimizing the bromination reaction on the static mixer, a second attempt to synthesize KOBr in flow was made. The optimized conditions in the static mixer required a flow of 0.33 ml/min of a 1 M KOBr solution which in turn required a flow of 17 μl/min Br_2 and 0.313 ml/min aq. KOH. Because previous results were not satisfying when neat Br_2 was used, Br_2 was diluted with a suitable solvent in order to obtain a better flow ratio. Several solvents were considered but initial experiments were performed with CH_2Cl_2 because problems were expected with toluene (side reactions) or Et_2O (solubility issues regarding TBABr).

Taking into account the desired stoichiometric ratios (4 equiv. KOBr, 20 equiv. KOH) and flow rates (0.165 ml/min for both solutions), the concentrations of the solutions were determined as 2 M Br_2 in CH_2Cl_2 and 12 M KOH in H_2O. When equal amounts of both solutions were added together in a flask, a colour change of both the organic and aqueous phase was observed. This colour change indicated KOBr formation but the formation of white flakes was observed. Probably, the KOH solution was too concentrated because adding H_2O dissolved these flakes. Repeating the batch experiment with a less concentrated KOH-solution (6.67 M) and a more concentrated Br_2 solution (2.43 M) in a 3:2 volume ratio, KOBr formation was observed in a clear two-phase system. With this approach, less KOH was used (16 equiv.). Subsequently, these conditions were translated into a continuous flow process (Figure 3.14 and Table 3.12).
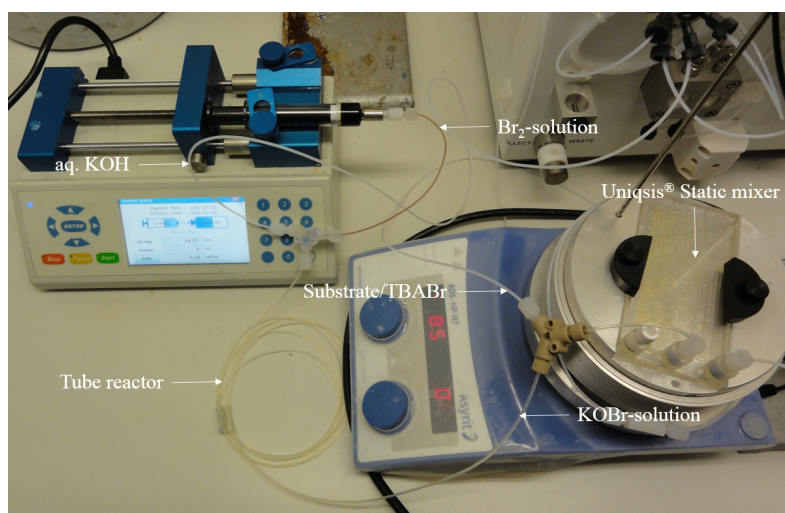
Figure 3.14. Photographic overview of the reactor setup for the synthesis of KOBr in flow

Table 3.12: Synthesis of KOBr in flow
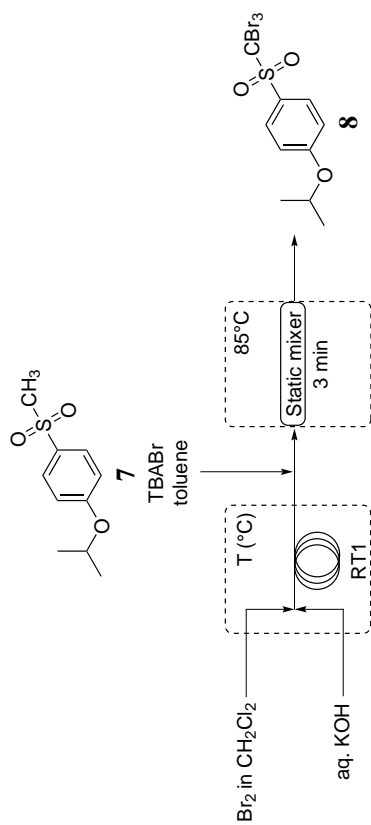
Entry	Br$_2$ (M)	KOH (M)	7 (M)	Br$_2$ (equiv.)	KOH (equiv.)	Br$_2$ (ml/min)	KOH (ml/min)	7/TBABr (ml/min)	RT1 (min)	T (°C)	Conversion[a] (%)
1	2.43	6.67	0.3	4	16	0.132	0.198	0.27	4.5	0	clogging
2	3.9	5.33	0.3	4	16.5	0.0825	0.25	0.27	1.2	rt	78
3	4.9	6	0.3	5	18.5	0.0825	0.25	0.27	1.2	rt	clogging
4	2.25	5	0.15	4	24	0.08	0.22	0.3	1.3	rt	91
5	2.8	5	0.15	5	24	0.08	0.22	0.3	1.3	rt	>99

[a]Conversion determined via ^{1}H-NMR

Using a concentrated KOH-solution in flow resulted in clogging of the tubing (Table 3.12, entries 1 and 3) whereas no precipitation was observed in batch. When 4 equivalents of Br_2 and 16.5 equivalents of KOH were used, 78% conversion was obtained (Table 3.12, entry 2). Increasing the amount of Br_2 and KOH resulted in excellent conversions (Table 3.12, entries 4-5). In these successful experiments, an old and almost empty bottle of bromine was used. When a new bottle of bromine was used, numerous repetitions of the same reaction conditions resulted in recuperation of the yellow KOBr-solution and limited conversion of the starting material **7** (<20%). So, in first instance, the influence of possible contaminants was evaluated. Contamination with syringe needles was mimicked by 'reacting' fresh Br_2 with syringe needles over a period of 24 h. Again, irreproducible results were obtained (conversions ranging from 60 to 80%). Adding traces of $FeBr_3$ or $FeBr_2$ to the Br_2-solution also did not solve the problem. A possible radical reaction mechanism was excluded by adding a radical initiator, benzoyl peroxide (BPO) or azobisisobutyronitrile (AiBN), to the solution of Br_2 without success. Subsequently, other solvents were evaluated: CH_3CN, $ClCH_2CH_2Cl$ and *t*BuOH. In all cases, hypobromite was formed when mixing both solutions observing the colour change of both the aqueous and organic phase but the use of CH_3CN resulted in clogging of the tube reactor due to precipitate formation and the conversion of **7** was limited (<15%) if $ClCH_2CH_2Cl$ or *t*BuOH were used. Increasing the amount of phase transfer catalyst was also unsuccessful.

Finally, it was observed that with the use of a two-phase system for the generation of KOBr, an unstable emulsion was formed when mixing the biphasic hypobromite solution with the solution of the starting material in the static mixer. Despite the static mixing elements, plug flow between the aqueous and organic phase was sometimes observed resulting in decreased interfacial area and hence lower conversions. Due to these variations in the observed flow regime, irreproducible results were obtained.

In an attempt to avoid the use of an extra solvent and simultaneously increasing the mixing efficiency when significantly different flow rates for both reagents were used, a glass static mixer was used to prepare the KOBr-solution starting from a 5.9 M KOH-solution and pure Br_2. Efficient mixing of the bromine and KOH-solution was observed but a white precipitate was formed during the reaction, leading to blockage of the mixer chip. Decreasing the concentration of the KOH-solution to 5 M, and hence the equivalents of KOH, did not solve this problem.

At last, a continuous stirred tank reactor (CSTR) was used to prepare the KOBr-solution. Bromine and the KOH-solution were pumped in a vial containing a rotating stirring bar.

Bromine reacted immediately with the KOH-solution, resulting in the instantaneous formation of hypobromite. When a 5.9 M KOH solution was used, a turbid reaction mixture was obtained. Lowering the concentration of the KOH-solution to 5 M solved the problem and resulted in a transparent, yellow KOBr-solution. As a proof of concept, this flow setup was used to brominate 4-isopropoxyphenyl methyl sulfone **7** (Figures 3.15-3.17).
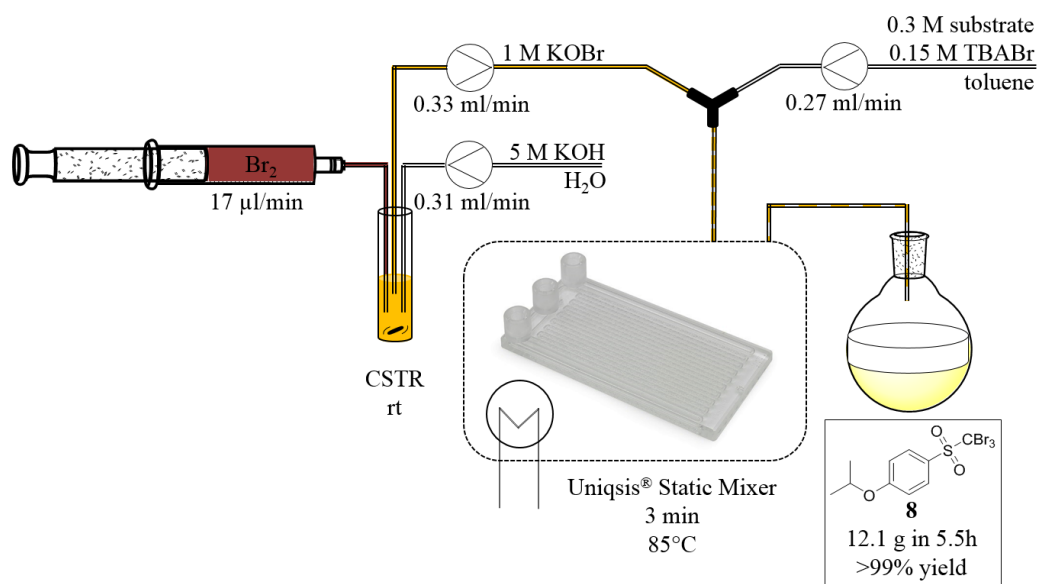
Figure 3.15. Schematic overview of the continuous production of hypobromite and subsequent bromination
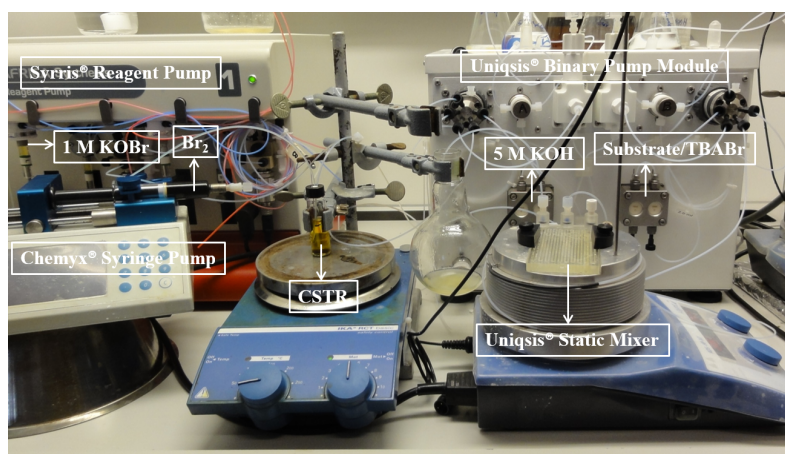
Figure 3.16. Photographic overview of the continuous production of hypobromite and subsequent bromination
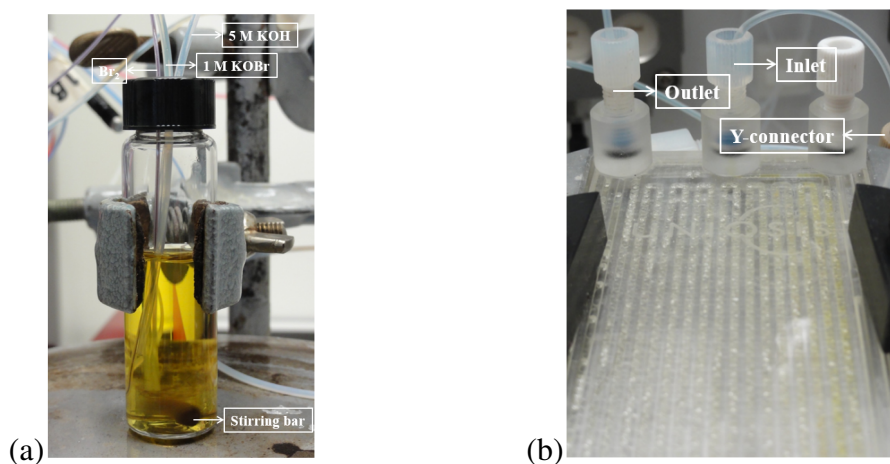
Figure 3.17. (a) Detail of the CSTR, (b) detail of the mixer chip

After reaching steady state, the reactor was run for 5.5 h and the isolated yield was determined over different time intervals (Table 3.13). The work up and purification of the end product was very straightforward since only dilution of the reaction mixture with Et$_2$O and washing with water was required. Stable and excellent isolated yields were obtained during the course of the operation and only the tribrominated derivative **8** was observed.

Table 3.13: Isolated yields during the course of the operation

Time interval (min)	Isolated yield (%)
0-60	98
60-120	quantitative
120-180	quantitative
180-240	quantitative
240-330	quantitative

Compared to the batch process, the continuous flow bromination in a glass static mixer was much faster due to the formation of an emulsion and hence efficient heat and mass transfer in the biphasic system. Moreover, the formation of hypobromite could be directly coupled to the subsequent bromination reaction. Using this experimental setup, a safe, efficient and scalable bromination was possible with a production of up to 53 g/day.

3.2.6 Deprotection of tribromomethyl 4-isopropoxyphenyl sulfone

Besides the bromination of 4-isopropoxyphenyl methyl sulfone **7** using KOBr, we evaluated shortly the subsequent deprotection of the isopropyl ether group of **8** to form the corresponding alcohol **9** (Scheme 3.8).
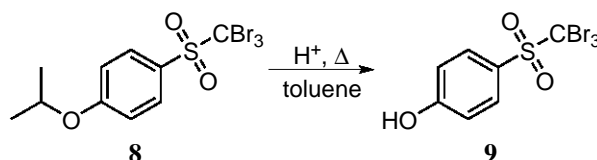
Scheme 3.8. Deprotection of the isopropyl ether group of **8**

In the industrial batch process, the volume of the organic phase of the bromination reaction is reduced *in vacuo* after aqueous work up. Subsequently, a catalytic amount of CF_3SO_3H is added and the end product, tribromomethyl 4-hydroxyphenyl sulfone **9**, precipitates from the reaction mixture. Despite this efficient batch process, industry has interest in a continuous flow process in which other acids are used (H_2SO_4, CH_3SO_3H or H_3PO_4). Preliminary batch experiments revealed that several hours at elevated temperatures (120°C) are required to deprotect **8** with H_2SO_4.

H_2SO_4, CH_3SO_3H and H_3PO_4 were evaluated in a continuous flow process. A 0.2 M solution of **8** in toluene was mixed with a neat acid in a T-mixer and the reaction mixture was subsequently heated to the desired reaction temperature in a tube reactor. For the calculation of the conversion, peak areas (HPLC-UV, 254.8 nm) were converted into concentrations based on a standardisation curve (Figure 3.18). The results are summarized in Table 3.14.
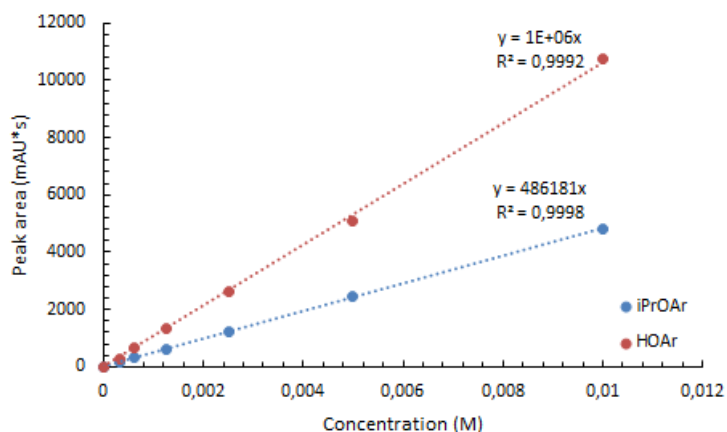
Figure 3.18. Standardisation curve for tribromomethyl 4-isopropoxyphenyl sulfone **8** (*i*PrOAr) and tribromomethyl 4-hydroxyphenyl sulfone **9** (HOAr) (HPLC-UV, 254.8 nm)

Table 3.14: Deprotection of the isopropyl ether group of **8** using H_2SO_4, CH_3SO_3H or H_3PO_4
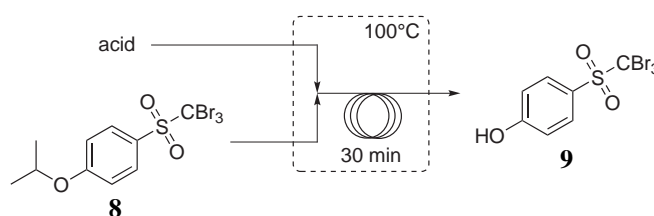
Entry	Acid	**8** (ml/min)	Acid (ml/min)	Acid (equiv.)	Conversion (%)
1	H_2SO_4	0.096	0.0041	4	81
2	CH_3SO_3H	0.091	0.0094	4	92
3	H_3PO_4	0.096	0.0040	4	0
4[a]	CH_3SO_3H	0.050	0.050	1	0

[a] 0.2 M CH_3SO_3H in DMSO

Good conversions were obtained with H_2SO_4 and CH_3SO_3H (Table 3.14, entries 1-2). However, several unidentified side products were formed during the reaction, resulting in an impure end product. Although the deprotection of ethers with H_3PO_4 was reported in the literature,[227] all starting material was recovered in the attempted deprotection of **8** with H_3PO_4 (Table 3.14, entry 3). To eliminate possible mixing effects due to the significantly different flow rates using neat acid, a 0.2 M solution of CH_3SO_3H in DMSO (CH_3SO_3H is not soluble in toluene) was mixed with the starting material at the same flow rate (Table 3.14, entry 4). However, no conversion of the starting material was observed.

In a subsequent step, the deprotection of **8** with CF_3SO_3H was evaluated in flow. In batch, rapid precipitation of the end product was observed after adding CF_3SO_3H at a reaction temperature of 60°C and the reaction was completed within 1 h. Due to this fast batch reaction, preliminary flow experiments were run with much shorter residence times than those applied in the deprotection with H_2SO_4, CH_3SO_3H or H_3PO_4. These preliminary flow experiments were run at 100°C and clogging of the tubing at the end of the reactor, where the reaction mixture was cooled, was observed due to precipitation of the end product **9**. To counter this problem, the reaction mixture was mixed with DMSO before cooling, in order to dissolve all the formed tribromomethyl 4-hydroxyphenyl sulfone **9**. The results for these experiments are summarized in Table 3.15. Excellent conversions were obtained for the deprotection of the isopropyl ether group of tribromomethyl 4-isopropoxyphenyl sulfone **8** and in contrast to the deprotection with H_2SO_4 or CH_3SO_3H, no side products were detected based on HPLC-UV. However, stoichiometric amounts of CF_3SO_3H were required whereas the batch process used only a catalytic amount.

Table 3.15: Deprotection of tribromomethyl 4-isopropoxyphenyl sulfone **8** using CF_3SO_3H
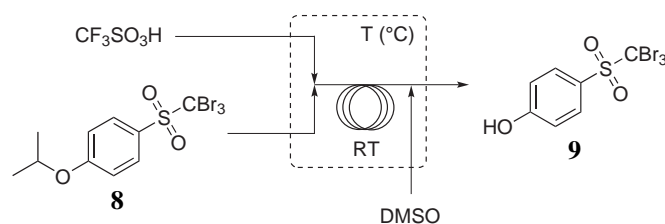
Entry	**8** (ml/min)	Acid (μl/min)	Acid (equiv.)	T (°C)	RT (min)	Conversion (%)
1	0.1989	1.1	0.3	90	1	42
2	0.0995	0.5	0.3	100	2	39
3	0.1965	3.5	1	100	1	95
4	0.0983	1.7	1	100	2	97

In a batch reactor, the formed propene escapes from the reaction mixture and the end product **153** precipitates. Hence, the equilibrium of the reaction is shifted to the right (Le Chatelier's principle). In flow, homogeneous reaction conditions were obtained and propene stays in solution as no headspace is available in the tubing. Probably, this explains why the reaction doesn't not work in flow with catalytic amounts of CF_3SO_3H whereas in batch, excellent yields were obtained.

3.2.7   Conclusions

The developed continuous flow bromination of methyl sulfones and methanesulfonates forms an industrially relevant procedure for the synthesis of tribromomethyl sulfones and tribromomethanesulfonates. Different brominated methyl sulfones and methanesulfonates were synthesized in excellent isolated yields. If *N*-aryl methanesulfonamides were used, bromination of the aromatic system was observed. When both evaluated reactor systems were compared, the static mixer was superior to the tube reactor due to the formation of an emulsion. The bromination reaction was completed in the static mixer in as less as 3 min compared to 22 h for the corresponding batch process and only a small excess of potassium hypobromite was required. Using a continuous stirred tank reactor, hypobromite could be prepared continuously and subsequently used for the bromination reaction. Quantitative conversion of the starting material was obtained and throughputs of up to 53 g/day could be reached. In this way, a very efficient and safe continuous flow method for the bromination of methyl sulfones and methanesulfonates was developed.

Subsequently, the deprotection of the isopropyl ether group of tribromomethyl 4-isopropoxy-phenyl sulfone **8** was evaluated. Use of CF_3SO_3H in stoichiometric amounts resulted in almost full and selective conversion of the starting material **8** to the corresponding alcohol **9**. However, the original batch procedure was superior to the developed continuous flow process due to the use of catalytic amounts of CF_3SO_3H and the straightforward product isolation in high isolated yields.

3.3 Simmons-Smith cyclopropanation of enamines

3.3.1 Introduction

The aminocyclopropane unit is an important structure found in several natural products and biologically active compounds with interesting properties.[228] Belactosin A **154**, for example, is a *Streptomyces* metabolite with antitumor activity (Figure 3.19).[229–232]
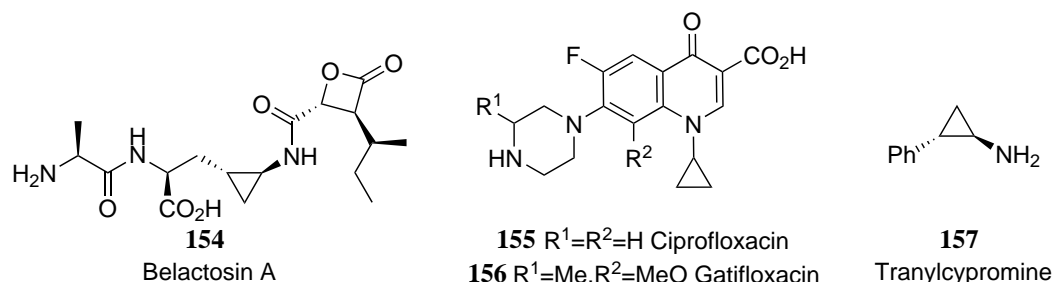
Figure 3.19. Biologically active compounds containing the amincocyclopropane unit

The class of aminocyclopropyl containing fluoroquinolones (e.g. ciprofloxacin **155**, gatifloxacin **156**) is used for the treatment of bacterial infections (e.g. tuberculosis).[233–235] Tranylcypromine **157** (*trans*-2-phenylcyclopropylamine) is a monoamine oxidase inhibitor (MAO-I) and is used as an antidepressant (Parnate® or Jatrosom®).[236,237] Also other cyclopropylamines exhibit MAO-I activity.[238–241] MAO-I's are useful in the treatment of psychiatric and neurological disorders like Parkinson's disease, Alzheimer's dementia, depression syndrome and panic disorders.[242] Beside this MAO-I activity, cyclopropylamines are also known to inhibit cytochrome P-450 enzymes.[243,244] These enzymes are involved in the metabolism of a broad range of substrates.

During the last few decades, a lot of methods have been developed for the synthesis of aminocyclopropanes. Most of the reported methods start from enamines to form the aminocyclopropyl moiety through cyclopropanation of the enamine double bond with a carbene. These methods include Simmons-Smith cyclopropanation[245–250] or cyclopropanation using diazo compounds,[251–255] pyridinium ylide complexes[256,257] or other carbenes.[258,259] Other synthetic methods involve the reduction of nitrocyclopropanes,[260,261] Curtius rearrangement of intermediate cyclopropanecarboxylates,[262–265] *N*-cyclopropylation of amines,[266,267] amidocyclopropanation of alkenes,[268–270] intramolecular cyclization of amine derivatives[271–273] and Ti-mediated syntheses.[274–277]

In the framework of our research into the use of microreactor technology to develop reactions which pose problems to scale-up in batch, we studied the continuous flow synthesis of cyclopropylamines using the Simmons-Smith reaction starting from the corresponding enamines.[73,130–133,178,191–196] Although the Simmons-Smith cyclopropanation of enamines is known in batch, this reaction has never been evaluated using microreactor technology. To the best of our knowledge, only two examples were reported concerning continuous flow cyclopropanation reactions. Sokolova *et al.* evaluated the cyclopropanation of styrene with ethyl diazoacetate using a Ru-PyBox monolithic miniflow reactor.[278,279] Casarubios *et al.* reported the continuous flow cyclopropanation of ethyl crotonate with dimethylsulfoxonium methylide (Corey's ylide).[280]

Industry has great interest in performing the Simmons-Smith reaction under continuous flow conditions due to the hazards associated with this reaction. Accidents related to Simmons-Smith cyclopropanations in batch were reported by both Charette and the AIHA (American Industrial Hygiene Association®).[48,49] Performing the exothermic Simmons-Smith reaction in flow is inherently safer than the corresponding batch procedure due to the small internal volume and excellent heat transfer associated with microreactor technology. Straightforward scale-up of the Simmons-Smith reaction using microreactor technology (scale-out or numbering up) makes this cyclopropanation procedure also attractive.
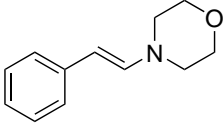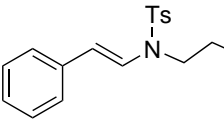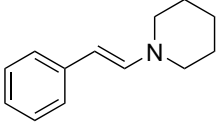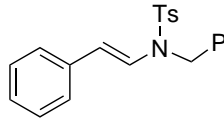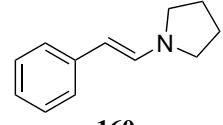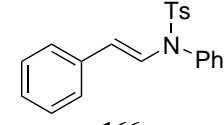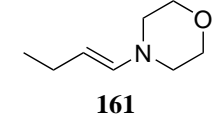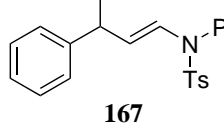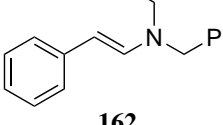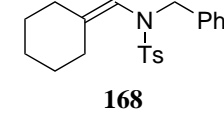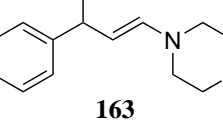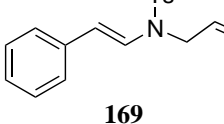
3.3.2 Synthesis of enamines

The enamines were synthesized using standard imination procedures starting from the corresponding aldehydes and secondary amines:

1. $MgSO_4$ (3.5 equiv.), $CHCl_3$, 1 h, 0°C[281]

2. Dean-Stark, *p*TsOH (0.01 equiv.), toluene, reflux, o.n.

3. K_2CO_3 (0.15 equiv.), neat, rt, on.[282]

Table 3.16 gives an overview of the synthesized enamines. An *E*-configuration was observed for the enamines (^{1}H-NMR).

Table 3.16: Overview of the synthesized enamines

Enamine	Method	Yield (%)	Enamine	Method	Yield (%)
158	MgSO$_4$	82	**164**	Dean-Stark	80
159	MgSO$_4$	74	**165**	Dean-Stark	81
160	MgSO$_4$	72	**166**	Dean-Stark	58
161	K$_2$CO$_3$	44	**167**	Dean-Stark	43
162	MgSO$_4$	82	**168**	Dean-Stark	72
163	MgSO$_4$	90	**169**	Dean-Stark	45

3.3.3 Simmons-Smith cyclopropanation in batch

The original Simmons-Smith reaction, reported by H.E. Simmons and R.D. Smith in 1958, made use of a Zn-Cu couple to generate a carbenoid.[283,284] Different modifications of the Simmons-Smith reaction have been reported and nowadays, Et$_2$Zn is used for the generation of the Zn-carbenoid.[285–287] The Simmons-Smith cyclopropanation proceeds via a butterfly mechanism (Scheme 3.9). Due to the concerted mechanism, the reaction is stereospecific.
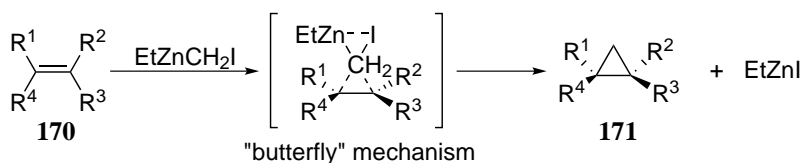
Scheme 3.9. Simmons-Smith cyclopropanation

In order to be able to perform the Simmons-Smith cyclopropanation in flow, a homogeneous reaction mixture is required. Taylor *et al.* described the Simmons-Smith cyclopropanation of Stork enamines using a Zn-Cu couple.[246] King *et al.* generated $Zn(CH_2I)_2$ in benzene to cyclopropanate different Stork enamines **172** in moderate to good yields (Scheme 3.10).[247] An analogous experiment in toluene resulted however in the formation of a white suspension during the generation of the carbenoid, which could lead to clogging of the microreactor (Scheme 3.11).
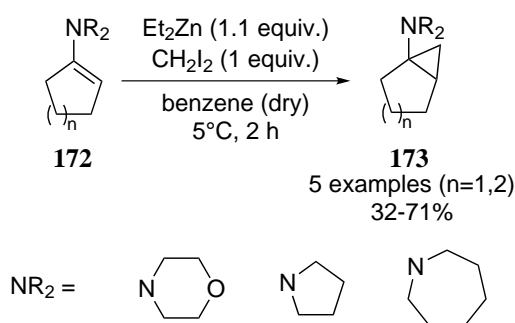
Scheme 3.10. Cyclopropanation of enamines as described by King *et al.*[247]
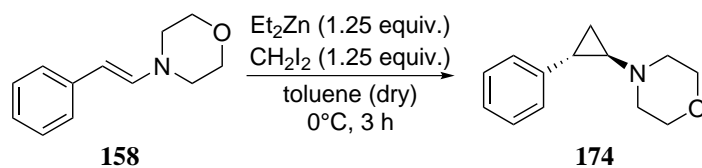
Scheme 3.11. Cyclopropanation with $Zn(CH_2I)_2$ in toluene

Different approaches can be used to generate a homogeneous solution of the Zn-carbenoid:

1. A solvent which complexes the Zn-carbenoid: e.g. THF

2. A ligand which complexes the Zn-carbenoid in a non-complexing solvent: 1,2-dimethoxy-ethane (DME) in CH_2Cl_2

3. A modified carbenoid in a non-complexing solvent: $CF_3CO_2ZnCH_2I$ (Shi's carbenoid) in CH_2Cl_2

These three approaches were evaluated in the Simmons-Smith cyclopropanation of enamines (Scheme 3.12). All experiments were performed in anhydrous solvents.
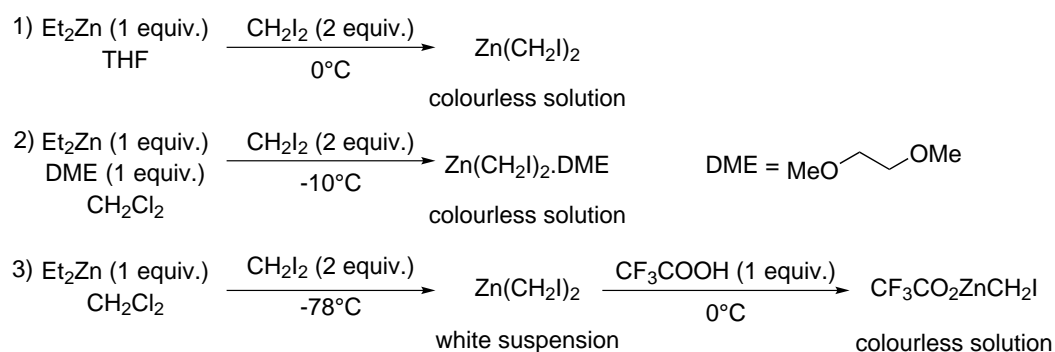
Scheme 3.12. Overview of the Zn-carbenoids used for the Simmons-Smith cyclopropanation

In a first series of batch experiments, the generated Zn-carbenoids were evaluated in the cyclopropanation of *N*-styrylmorpholine **158**, *N*-styrylpiperidine **159** and *N*-styrylpyrrolidine **160** (Table 3.17).

Table 3.17: Evaluation of the different Zn-carbenoids
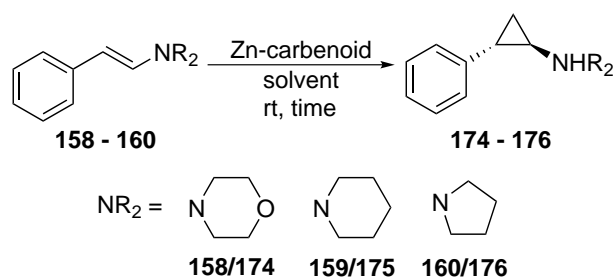
Entry	Substrate	Zn-carbenoid	Zn-carbenoid (equiv.)	Solvent (dry)	Time (h)	Conversion[a] (%)
1	**158**	$Zn(CH_2I)_2$.DME	5	CH_2Cl_2	24	90
2	**158**	$Zn(CH_2I)_2$	2	THF	3	91
3	**158**	$Zn(CH_2I)_2$	2	THF	5	100
4	**158**	$CF_3CO_2ZnCH_2I$	2	CH_2Cl_2	5	96
5	**159**	$Zn(CH_2I)_2$	2	THF	5.5	100
6	**159**	$CF_3CO_2ZnCH_2I$	2	CH_2Cl_2	2.5	100
7	**160**	$CF_3CO_2ZnCH_2I$	2	CH_2Cl_2	2.75	100

[a] Conversion determined via ^{1}H-NMR

The cyclopropanation of *N*-styrylmorpholine **158** with $Zn(CH_2I)_2$.DME in CH_2Cl_2 led to 90% conversion within one day using 5 equivalents of the carbenoid (Table 3.17, entry 1). Moreover, using $Zn(CH_2I)_2$ in THF or $CF_3CO_2ZnCH_2I$ in CH_2Cl_2 led to excellent conversions within acceptable timeframes with as little as 2 equivalents of the carbenoid (Table 3.17, entries 2-4).

These two Zn-carbenoids were evaluated further using *N*-styrylpiperidine **159**, resulting in complete conversion of the enamine (Table 3.17, entries 5 and 6). In these experiments, Shi's carbenoid seemed to be the most potent carbenoid because complete conversion was reached within 2.5 h in contrast to 5.5 h with $Zn(CH_2I)_2$. As a result, Shi's carbenoid was also evaluated in the cyclopropanation of *N*-styrylpyrrolidine **160** (Table 3.17, entry 7). Again, complete conversion was obtained after 2.75 h. Due to the relatively fast reactions and high conversions of the enamines, $CF_3CO_2ZnCH_2I$ was selected as the Zn-carbenoid for the cyclopropanation of enamines.

Although excellent conversions of the enamines were obtained with $CF_3CO_2ZnCH_2I$, the isolation of the formed cyclopropyl derivatives constituted a major challenge. Despite the quantitative conversions, isolated yields were moderate (<60%). Different work up and purification strategies to isolate **174** were evaluated (Table 3.18).
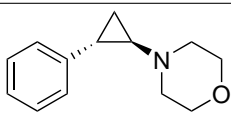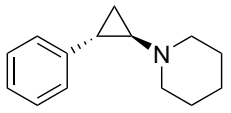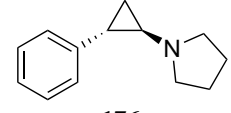
Firstly, aqueous work up combined with column chromatography was evaluated to isolate **174**. The use of sat. $NaHCO_3$ resulted in the formation of an emulsion and limited yields (22-39%) were obtained with 2 M NaOH or sat. Na_2EDTA (Table 3.18, entries 1-3). When sat. K_2CO_3 was added to the reaction mixture, the aqueous layer turned turbid. Nevertheless, a clear phase separation was visible and after column chromatography, the end product **174** was isolated with a yield of 57% (Table 3.18, entry 4). Use of vacuum distillation instead of column chromatography to purify the crude cyclopropyl derivative resulted in an impure end product (Table 3.18, entries 5-6). Attempts to form the HCl-salt of **174** failed (Table 3.18, entry 7). Straightforward evaporation of the reaction mixture and addition of dry Et_2O to precipitate the Zn-salts and dissolve the end product failed as did evaporation and subsequent column chromatography (Table 3.18, entries 8-9). No end product was collected when solid K_2CO_3 was added to the reaction mixture followed by vacuum distillation (Table 3.18, entry 10). Addition of MeOH to decompose the Zn-complex and Et_3N to neutralize any traces of acid, followed by addition of dry Et_2O to precipitate the formed salts additionally failed (Table 3.18, entry 11). When column chromatography was used after quenching the reaction mixture with MeOH and Et_3N, the end product **174** was obtained in 50% yield (Table 3.18, entry 12).

Table 3.18: Work up and purification strategies for **174**

Entry	Work up	Remarks	Purification	Remarks
1	sat. NaHCO$_3$	emulsion	-	-
2	2 M NaOH	-	column chromatography	Y=39%
3	sat. Na$_2$EDTA	-	column chromatography	Y=22%
4	sat. K$_2$CO$_3$	turbid aqueous layer clear phase separation	column chromatography	Y=57%
5	5 M NaOH	-	vacuum distillation	impure end product
6	sat. K$_2$CO$_3$	turbid aqueous layer clear phase separation	vacuum distillation	impure end product
7	sat. Na$_2$EDTA	-	HCl-salt formation	no precipitation
8	evaporation	-	addition of dry Et$_2$O	no precipitation
9	evaporation	-	column chromatography (normal phase or reversed phase)	impure end product
10	4 equiv. K$_2$CO$_3$	-	vacuum distillation	no product collected
11	40 equiv. MeOH + 4 equiv. Et$_3$N evaporation	-	addition of dry Et$_2$O	no precipitation
12	40 equiv. MeOH + 4 equiv. Et$_3$N evaporation	-	column chromatography	Y=50%

To verify if degradation reactions contribute to the low isolated yields, **174** was dissolved in MeOH and stirred at room temperature for 24 h. No degradation of the cyclopropyl derivative was observed. An experiment in which the cyclopropyl derivative **174** was dissolved in CH_2Cl_2 or Et_2O and subsequently washed with H_2O revealed that a lot of product (35%) was lost during the aqueous work up. Despite the large product loss, the best isolated yield was obtained when aqueous work up with a minimal amount of a sat. K_2CO_3 solution was combined with purification through column chromatography. Using 2 equivalents of $CF_3CO_2ZnCH_2I$ in CH_2Cl_2, three derivatives were obtained in moderate yield (Table 3.19).

Table 3.19: Synthesis of cyclopropylamines with Shi's carbenoid in batch

Substrate	Cyclopropyl derivative	Yield (%)
158	**174**	57
159	**175**	36
160	**176**	47

In a next step, the Simmons-Smith cyclopropanation of enamines with an electron withdrawing group (EWG) on nitrogen was evaluated in batch. As mentioned before, these enamines were prepared by reacting a tosylated primary amine with an aldehyde in a Dean-Stark apparatus. In a first series of batch experiments, the cyclopropanation reaction of *N*-styryl-*N*-tosylpropylamine **164** was evaluated at room temperature (Table 3.20).

Table 3.20: Evaluation of different Zn-carbenoids for the cyclopropanation of **164** in batch
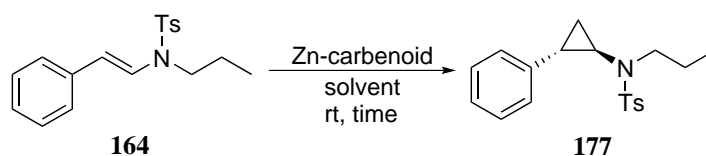
Entry	Zn-carbenoid	Zn-carbenoid (equiv.)	Solvent (dry)	Time (h)	Conversion[a] (%)
1	$CF_3CO_2ZnCH_2I$	2	CH_2Cl_2	2.5	65
2	$CF_3CO_2ZnCH_2I$	2	CH_2Cl_2	6	87
3	$CF_3CO_2ZnCH_2I$	3	CH_2Cl_2	6	100
4	$Zn(CH_2I)_2$	3	THF	5.5	0
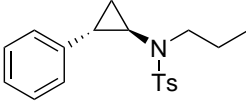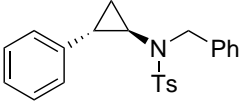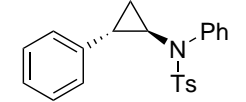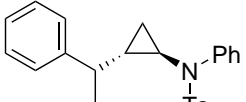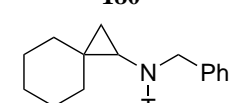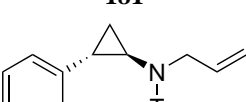
[a] Conversion determined via ^{1}H-NMR

Compared to the previously tested enamines **158** - **160** (Table 3.17), the Simmons-Smith cyclopropanation of enamines with an EWG on nitrogen was more difficult. The use of 2 equivalents of Shi's carbenoid led to only 87% conversion after 6 h (Table 3.20, entry 2). However, full conversion was obtained within 6 h with 3 equivalents of $CF_3CO_2ZnCH_2I$ (Table 3.20, entry 3). On the other hand, $Zn(CH_2I)_2$ in THF did not react at all with this less reactive enamine (Table 3.20, entry 4).

The optimized reaction conditions (Table 3.20, entry 3) were used to synthesize different cyclopropylamines with an EWG on nitrogen (Table 3.21).

Full conversion of **164** and **165** to the corresponding cyclopropylamines **177** and **178** was obtained with 3 equivalents of Shi's carbenoid and these compounds could be isolated in excellent yields via recrystallization after aqueous work up (Table 3.21, entries 1-2). Cyclopropanation of **166** to synthesize **179** resulted in a lower conversion after 6 h reaction (Table 3.21, entry 3). Although an excellent conversion was observed for the cyclopropanation of **167**, the cyclopropylamine **180** was isolated in a moderate yield after recrystallization (Table 3.21, entry 4). Synthesis of the spiro compound **181** via Simmons-Smith cyclopropanation of **168** failed, probably due to steric hindrance (Table 3.21, entry 5). When **169** was used in the Simmons-Smith cyclopropanation with 3 equivalents of $CF_3CO_2ZnCH_2I$, a mixture of products was observed due to partial cyclopropanation of both double bonds (Table 3.21, entry 6). In an attempt to cyclopropanate both double bonds completely, the reaction was repeated overnight with 10 equivalents of Shi's carbenoid. However, again a complex reaction mixture of different cyclopropanated products was obtained and it was not possible to separate these products.

Table 3.21: Batch synthesis of cyclopropylamines with an EWG on nitrogen
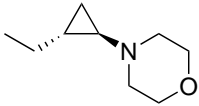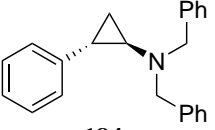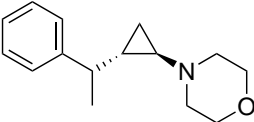
Entry	Substrate	Cyclopropyl derivative	Conversion[a] (%)	Yield (%)
1	**164**	**177**	100	70
2	**165**	**178**	100	80
3	**166**	**179**	71	-
4	**167**	**180**	99	39
5	**168**	**181**	20	-
6	**169**	**182**	CRM[b]	-

[a] Conversion determined via ^{1}H-NMR

[b] Complex reaction mixture

Finally, the optimized reaction conditions for the enamines with an EWG on nitrogen (3 equivalents of $CF_3CO_2ZnCH_2I$) were also tested on the enamines **158**-**160**. Using 3 equivalents of Shi's carbenoid instead of 2 equivalents led to complete conversion of the enamines **158**-**160** within 30-45 min compared to several hours in the original experiments. Using 3 equivalents of Shi's carbenoid and a reaction time of 45 min, three more cyclopropanation reactions were performed (Table 3.22). Only **184** could be isolated in a moderate yield (Table 3.22, entry 2).

Table 3.22: Batch synthesis of cyclopropylamines with 3 equivalents of $CF_3CO_2ZnCH_2I$

Substrate	Cyclopropylamine	Yield (%)
161	**183**	CRM
162	**184**	65
163	**185**	CRM

3.3.4 Simmons-Smith cyclopropanation in flow

In a first series of continuous flow experiments, a solution of Shi's carbenoid (0.2 M in CH_2Cl_2) was prepared in batch and used as such for the cyclopropanation of enamines under continuous flow conditions. Syringe pumps were used to pump the reagents with the desired flow rate through a tube reactor. In these experiments, it was of utmost importance to avoid contact of the carbenoid solution with air during manipulation of the syringes. Otherwise, precipitate formation in the syringe or reactor was observed, leading to clogging of the tubing. A schematic representation of the reactor for the initial flow experiments is depicted in Scheme 3.13.
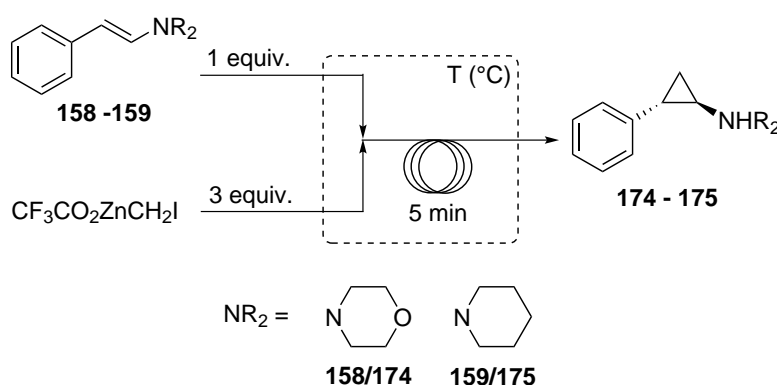
Scheme 3.13. Schematic overview of the tube reactor for the initial flow experiments

In these preliminary flow experiments, a residence time of 5 min was used in combination with 3 equivalents of $CF_3CO_2ZnCH_2I$. Different reaction temperatures were evaluated and the conversion was determined via ^{1}H-NMR (Table 3.23).

Table 3.23: Evaluation of the Simmons-Smith reaction in flow

Entry	Substrate	T (°C)	Conversion[a] (%)
1	**158**	21	86
2	**158**	30	95
3	**158**	35	100
4	**159**	35	94
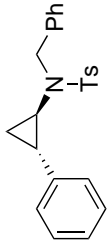
[a] Conversion determined via ^{1}H-NMR

After optimization of the reaction temperature, full conversion of *N*-styrylmorpholine **158** to **174** could be obtained within 5 min at 35°C (Table 3.23, entry 3). Applying these reaction conditions to *N*-styrylpiperidine **159** revealed again excellent conversion (94%) to the cyclopropyl derivative **175** (Table 3.23, entry 4).

In a subsequent step, the formation of Shi's carbenoid in flow was evaluated. The original experimental batch procedure (Scheme 3.12, method 3) could not be translated to flow due to the formation of an intermediate suspension. Therefore, three other experimental procedures were evaluated in batch and compared to the original one (Table 3.24). Because of the straightforward work up of the cyclopropylamine **178**, the formed carbenoids were evaluated in the cyclopropanation of *N*-styryl-*N*-tosylbenzylamine **165**.

Changing the addition order of trifluoroacetic acid (TFA) and diiodomethane formed a turbid reaction mixture which was not suited for flow experiments (Table 3.24, entry 2). When a solution of 2 equivalents of TFA and 1 equivalent of CH_2I_2 in CH_2Cl_2 was added to a solution of Et_2Zn in CH_2Cl_2, the reaction mixture turned turbid (Table 3.24, entry 3). However, the turbidity disappeared again after a few minutes. Finally, addition of a solution of TFA (1 equiv.) and CH_2I_2 (1 equiv.) to Et_2Zn in CH_2Cl_2 formed a colourless solution. After reaction with *N*-styryl-*N*-tosylbenzylamine **165**, the corresponding cyclopropyl derivative **178** could be isolated with a yield comparable to that of the original method when 3 equivalents of the formed carbenoid were used (Table 3.24, entry 4).

Table 3.24: Evaluation of the synthesis of Shi's carbenoid in batch

Entry	Procedure	Observation	178 (%)
1	Original procedure: 1) $Et_2Zn + CH_2Cl_2$ 2) Add 2 equiv. CH_2I_2 at -78°C + 15' 0°C 3) Add 1 equiv. CF_3CO_2H at 0°C + 15' 0°C	1) Colourless solution 2) White suspension 3) Colourless solution	80
2	1) $Et_2Zn + CH_2Cl_2$ 2) Add 1 equiv. CF_3CO_2H at 0°C + 15' 0°C 3) Add 2 equiv. H_2I_2 at 0°C + 15' 0°C	1) Colourless solution 2) Turbid reaction mixture 3) -	-
3	1) $Et_2Zn + CH_2Cl_2$ 2) Add solution of CH_2I_2 (2 equiv.) and CF_3CO_2H (1 equiv.) in CH_2Cl_2 at 0°C	1) Colourless solution 2) Turbidity disappeared	67
4	1) $Et_2Zn + CH_2Cl_2$ 2) Add solution of CH_2I_2 (1 equiv.) and CF_3CO_2H (1 equiv.) in CH_2Cl_2 at 0°C	1) Colourless solution 2) Colourless solution	70

To form Shi's carbenoid in flow, a 0.4 M solution of Et_2Zn in CH_2Cl_2 was mixed with a 0.4 M solution of CH_2I_2 and TFA in CH_2Cl_2 in a T- or Y-connector before entering a tube reactor at 0°C (Scheme 3.14). The formation of $CF_3CO_2ZnCH_2I$ under continuous flow conditions was evaluated for the cyclopropanation of **165** because of the straightforward work up of **178**. However, due to the lower reactivity of enamines with an EWG on nitrogen, experiments were performed with a residence time of 1 h for the cyclopropanation reaction. Several attempts to form Shi's carbenoid in flow resulted in clogging of the first tube reactor. Use of a T-mixer and a tube reactor with a larger internal diameter for the generation of $CF_3CO_2ZnCH_2I$ combined with ultrasound irradiation, resulted again in clogging of the tubing. Premixing the enamine **165** with Et_2Zn and subsequent formation of the carbenoid also resulted in clogging of the first tube reactor.
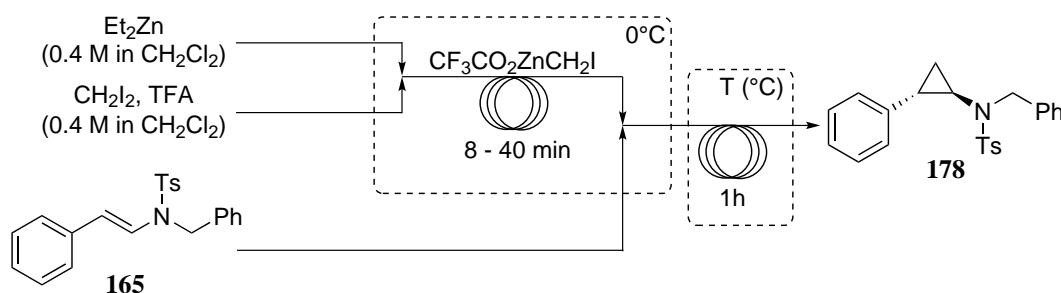
Scheme 3.14. Synthesis of $CF_3CO_2ZnCH_2I$ under continuous flow conditions

In a next step, THF was used for the continuous flow synthesis of $CF_3CO_2ZnCH_2I$ and subsequent cyclopropanation of **165**. No clogging of the tubing occurred and a clear reaction mixture was obtained. However, no conversion of the starting material **165** was observed at different reaction temperatures (21 and 40°C). In order to account for the lower reactivity of enamines with an EWG on nitrogen, the same reaction conditions were evaluated for the cyclopropanation of **158**, although without succes. When $Zn(CH_2I)_2$ in THF was used, a clear reaction mixture was obtained without clogging of the tube reactors but either a complex reaction mixture (cyclopropanation of **158**) or no conversion (cyclopropanation of **165**) was observed.
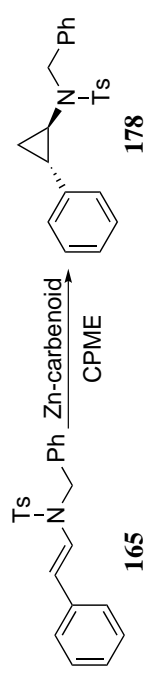
Recently, Sugimura and coworkers evaluated the Simmons-Smith cyclopropanation of silyl enol ethers using a Zn/Cu-couple and CH_2I_2 in different solvents.[288] They observed that the use of cyclopentyl methyl ether (CPME) resulted in remarkable better conversions compared to other solvents (Table 3.25).

Table 3.25: Cyclopropanation of silyl enol ethers **186** in different solvents[288]
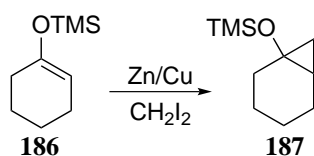
Entry	Solvent	Conversion (after 2 h, %)
1	1,4-dioxane	1
2	methyl *t*-butyl ether (MTBE)	10
3	diisopropyl ether (DIPE)	4
4	Et$_2$O	7
5	cyclopentyl methyl ether (CPME)	19
6	1,2-dimethoxyethane (DME)	2
7	THF	9

As a consequence, CPME was evaluated for the Simmons-Smith cyclopropanation of **165** in batch (Table 3.26).

Use of Shi's carbenoid in CPME resulted in limited conversions of the enamine **165** after prolonged reaction times (Table 3.26, entries 1-2). When Zn(CH$_2$I)$_2$ was used to cyclopropanate **165**, higher conversions were obtained but the formation of a precipitate was observed (Table 3.26, entries 3-4). When CPME was added in stoichiometric amounts (with respect to Et$_2$Zn) to CH$_2$Cl$_2$, only traces of the cyclopropyl derivative **178** were detected (Table 3.26, entry 5). Finally, Zn(CH$_2$I)$_2$ was evaluated in CH$_2$Cl$_2$ with 1 equivalent of CPME but the formed Zn-carbenoid was insoluble in this solvent mixture.

Table 3.26: Cyclopropanation of **165** in CPME

$$\text{165} \xrightarrow[\text{CPME}]{\text{Zn-carbenoid}} \text{178}$$

Entry	Zn-carbenoid	Solvent (dry)	T (°C)	Time (h)	Conversion[a] (%)	Remarks
1	$CF_3CO_2ZnCH_2I$	CPME	rt	20	0	-
2	$CF_3CO_2ZnCH_2I$	CPME	40	24	28	-
3	$Zn(CH_2I)_2$	CPME	rt	20	60	precipitation
4	$Zn(CH_2I)_2$	CPME	40	20	76	precipitation
5	$CF_3CO_2ZnCH_2I$	CH_2Cl_2 + 1 equiv. CPME	rt	5	traces	-
6	$Zn(CH_2I)_2$	CH_2Cl_2 + 1 equiv. CPME	-	-	-	$Zn(CH_2I)_2$ not soluble

[a] Conversion determined via ^{1}H-NMR

When CH_2Cl_2 was used as a non-complexing solvent under continuous flow conditions, there was a high risk for clogging of the tube reactor during the generation of $CF_3CO_2ZnCH_2I$. On the other hand, use of a complexing solvent (THF) resulted in the recuperation of the enamine or a complex reaction mixture. To find the right balance between reactivity and solubility of the formed Zn-carbenoid, different solvent mixtures of CH_2Cl_2 and THF were evaluated in batch. The cyclopropanation of **158** at room temperature with 3 equivalents of $CF_3CO_2ZnCH_2I$ was used to evaluated these solvent mixtures due to the relatively short reaction time. The conversion was determined via ^{1}H-NMR during the course of the reaction (Figure 3.20).
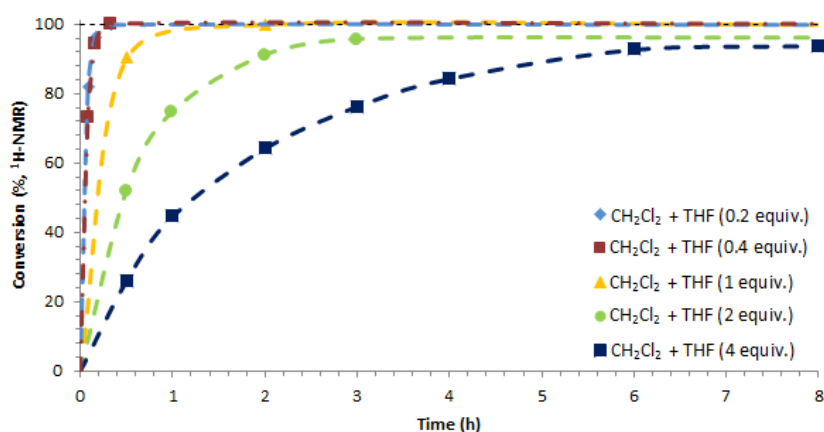
Figure 3.20. Simmons-Smith cyclopropanation of **158** in batch with $CF_3CO_2ZnCH_2I$ in CH_2Cl_2:THF solvent mixtures (equivalents of THF expressed relatively to Et_2Zn)

Precipitation of $CF_3CO_2ZnCH_2I$ was never observed using a mixture of CH_2Cl_2:THF and the more THF was used, the slower the reaction proceeded and the lower the final conversion obtained. However, using CH_2Cl_2 with 0.2 or 0.4 equivalents of THF resulted in complete conversion within 15 min after the addition of the enamine (Figure 3.21).
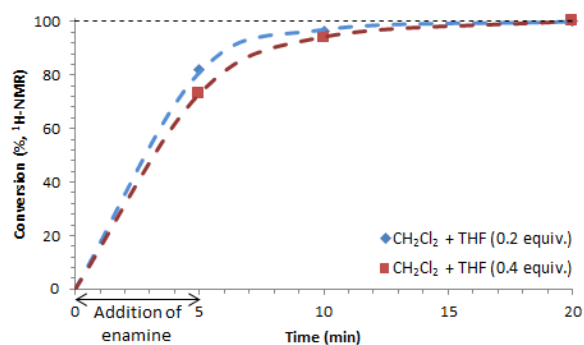
Figure 3.21. Simmons-Smith cyclopropanation of **158** in batch with $CF_3CO_2ZnCH_2I$ in CH_2Cl_2 with 0.2 or 0.4 equivalents of THF (equivalents of THF expressed relatively to Et_2Zn)

Subsequently, CH_2Cl_2 + 0.4 equivalents of THF was used in a next series of flow experiments (Figure 3.15 and Table 3.27).
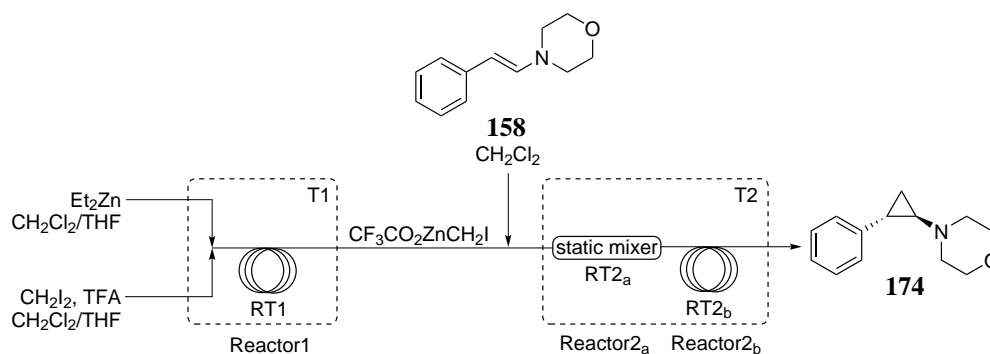
Scheme 3.15. Reactor setup to cyclopropanate **158** using CH_2Cl_2 + 0.4 equivalents of THF (equivalents of THF expressed relatively to Et_2Zn)

Table 3.27: Cyclopropanation of **158** using CH_2Cl_2 + 0.4 equivalents of THF (equivalents of THF expressed relatively to Et_2Zn)

	Entry	Et_2Zn (M)	CH_2I_2/TFA (M)	**158** (M)	$CF_3CO_2ZnCH_2I$ (equiv.)	Reactor1 (ml)	RT1 (min)	$RT2_a$ (min)	$Reactor2_b$ (ml)	$RT2_b$ (min)	T1 (°C)	T2 (°C)	Conversion[a] (%)
Teflon AF-2400	1	0.4	0.4	0.068	3	1.9	4.75	2	0.2	0.25	rt	rt	62
	2	0.4	0.4	0.068	3	1.9	4.75	2	0.2	0.25	rt	30	92
	3	0.4	0.4	0.068	3	1.9	11.88	5	0.2	0.63	rt	30	100
PFA-tubing	4	0.4	0.4	0.068	3	2	5	2	0.2	0.25	rt	30	95
	5	0.4	0.4	0.068	3	0.5	1.25	2	0.2	0.25	rt	30	100
	6	0.4	0.4	0.136	1.5	0.5	1.25	2	0.2	0.25	rt	30	67
	7	0.4	0.4	0.136	1.5	0.5	1.25	2	0.2	0.25	0	30	64
	8	0.4	0.4	0.136	1.5	0.5	3.125	5	0.2	0.63	rt	30	82
	9	0.4	0.4	0.136	1.5	0.5	3.125	5	0.2	0.63	rt	35	84
	10	0.4	0.4	0.136	1.5	0.5	3.125	5	0.2	0.63	rt	40	87
	11	0.4	0.4	0.136	1.5	0.25	3.125	10	0.2	1.26	rt	30	78
	12	0.4	0.4	0.100	2	0.5	3.125	5	0.2	0.63	rt	35	91
	13	0.4	0.4	0.100	2	0.5	6.25	10	0.2	1.26	rt	35	CRM
	14	0.4	0.4	0.136	1.5	0.5	4.35	7.11	5.2	23.11	rt	30	>98
	15	0.8	0.8	0.272	1.5	0.5	4.35	7.11	5.2	23.11	rt	30	96
	16	0.8	0.8	0.272	1.5	0.5	4.35	7.11	5.2	23.11	rt	35	100

[a] Conversion determined via ^1H-NMR

Two types of tube reactors were evaluated for the generation of $CF_3CO_2ZnCH_2I$. The first tube reactor was made of gaspermeable tubing (Teflon AF-2400) in order to remove ethane from the reaction mixture (Table 3.27, entries 1-3). Ethane was formed due to reaction of CF_3CO_2H with Et_2Zn. The Teflon AF-2400 tubing was placed under a constant N_2-flush. Using this approach, an initial experiment resulted in 62% conversion (Table 3.27, entry 1). Raising the reaction temperature of the cyclopropanation reaction from rt to 30°C resulted in an increase of the conversion to 92% (Table 3.27, entry 2). Complete conversion of **158** was obtained by prolonging the reaction time of the cyclopropanation reaction to 5.63 min (Table 3.27, entry 3).

The other tube reactor for the synthesis of $CF_3CO_2ZnCH_2I$ was constructed of PFA-tubing (Table 3.27, entries 4-16). Performing an analogous experiment as with the gaspermeable tubing (Table 3.27, entry 2), a comparable conversion of 95% was obtained (Table 3.27, entry 4). Full conversion was obtained by decreasing the reaction time for the generation of $CF_3CO_2ZnCH_2I$ to 1.25 min (Table 3.27, entry 5). Use of 1.5 equivalents of $CF_3CO_2ZnCH_2I$ instead of 3 equivalents, resulted in a moderate conversion of 67% (Table 3.27, entry 6) and performing the generation of $CF_3CO_2ZnCH_2I$ at a lower temperature did not improve the conversion (Table 3.27, entry 7). However, increasing the reaction time for both the generation of $CF_3CO_2ZnCH_2I$ and the cyclopropanation of **158**, resulted in an increased conversion of 82% (Table 3.27, entry 8). Subsequently, a conversion of 87% was obtained by increasing the reaction temperature for the cyclopropanation reaction to 40°C (Table 3.27, entries 9-10). Doubling of the reaction time for the cyclopropanation reaction while maintaining the reaction time for the generation of $CF_3CO_2ZnCH_2I$ gave a comparable conversion (Table 3.27, entries 8 and 11). Use of 2 equivalents of $CF_3CO_2ZnCH_2I$ instead of 1.5 equivalents resulted in an increase of the conversion (Table 3.27, entries 9 and 12). A subsequent increase of the reaction time resulted in the formation of a complex reaction mixture (Table 3.27, entry 13). However, excellent conversions (>98%) were obtained with 1.5 equivalents of $CF_3CO_2ZnCH_2I$ if the reaction time for the cyclopropanation of **158** was prolonged to 30 min (Table 3.27, entry 14). In a final experiment, the throughput of the reaction was doubled by doubling the concentrations of the starting material solutions. After increasing the reaction temperature to 35°C, full conversion of **158** was obtained (Table 3.27, entries 15-16).

Use of the right solvent mixture allowed the generation of $CF_3CO_2ZnCH_2I$ in a continuous flow setup. Moreover, the cyclopropanation reaction proceeded with excellent conversion with as little as 1.5 equivalents of the generated carbenoid. A theoretical throughput of around 9 g/day of **174** could be reached.

As in the original batch experiments, isolation of the synthesized cyclopropylamine **174** was difficult. Next to the different methods to work up the reaction mixture as depicted in Table 3.18, a few more methods were evaluated:

- Aqueous work up with 30% NH_4OH, sat. NH_4Cl, H_2O or brine
- Continuous extraction of the aqueous phase with CH_2Cl_2 or Et_2O
- Salt formation with pTsOH or oxalic acid
- Use of a pyridine resin (poly(4-vinylpyridine))

All these attempts failed or resulted in limited crude yields (20-40%). Remarkably, when the Simmons-Smith cyclopropanation was performed in CH_2Cl_2 + 0.4 equivalents of THF (with respect to Et_2Zn), aqueous work up of the reaction mixture and subsequent evaporation of the organic solvent resulted in a solid material although the end product **174** is an oil. Moreover, the mass of the obtained solid material was much larger than the theoretical mass of the end product. Probably, this solid material contained the end product in combination with some Zn-salts. Several attempts to extract the cyclopropylamine **174** from this solid material failed.

3.3.5   Conclusions

Different Zn-carbenoids could be used in the Simmons-Smith cyclopropanation of enamines. However, in view of continuous flow applications, Shi's carbenoid, $CF_3CO_2ZnCH_2I$, was chosen to cyclopropanate different enamines in batch. Several derivatives were cyclopropanated with excellent conversions but the isolation of the synthesized cyclopropylamines was difficult. Different work up strategies resulted in limited isolated yields. Enamines with an EWG on nitrogen were less reactive and required longer reactions times in order to reach full conversion. However, the corresponding cyclopropyl derivatives were isolated in good yields.

Preliminary experiments regarding the continuous flow cyclopropanation of enamines, in which Shi's carbenoid was synthesized in batch, revealed excellent conversions within short residence times. In order to be able to synthesize $CF_3CO_2ZnCH_2I$ in flow, the original experimental procedure was adapted succesfully. The generation of Shi's carbenoid and subsequent Simmons-Smith cyclopropanation of **158** were performed in flow with excellent conversions with as little as 1.5 equivalents of $CF_3CO_2ZnCH_2I$. However, isolation of the synthesized cyclopropylamine **174** remained the main bottleneck.

3.4 Aziridination of bisphosphonoazadienes

3.4.1 Introduction

Bisphosphonates form an important class of compounds widely used in the treatment of bone diseases such as osteoporosis (Figure 3.22). Two classes of bisphosphonates are distinguished according to their mode of action with the aminobisphosphonates being the most potent class. These aminobisphosphonates are also known to exhibit antitumor activity. [289–293]
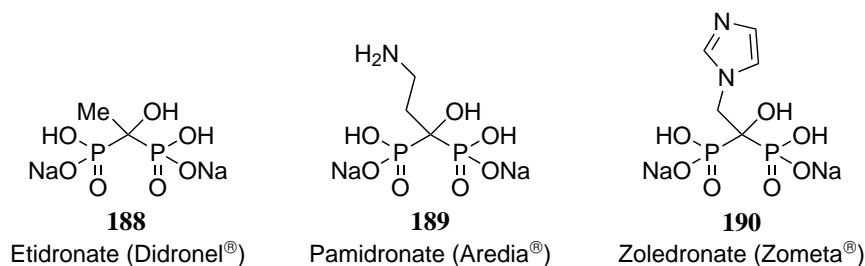
Figure 3.22. Bisphosphonates used in the treatment of bone diseases

Our research group (SynBioC, Department of Sustainable Organic Chemistry and Technology, Faculty of Bioscience Engineering, Ghent University) developed the synthesis of *N*-vinyl-2,2-bisphosphonoaziridines **14** by treatment of 1,1-bisphosphono-2-aza-1,3-dienes **12** with diazomethane. [50] The reaction proceeds via an intermediate triazoline **13**. Depending on the substituents of the 1,1-bisphosphono-2-aza-1,3-diene **12**, two side products (**16** and **17**) can be formed (Scheme 3.16 and Table 3.28).
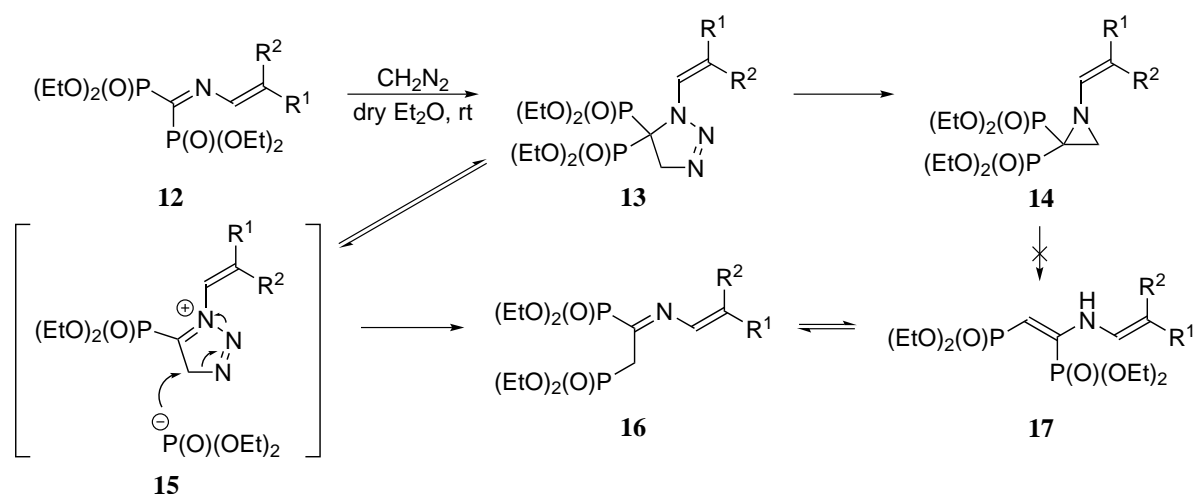
Scheme 3.16. Reaction mechanism for the aziridination of **12**

Table 3.28: Overview of the results for the aziridination of **12**

Substrate **12**	R^1	R^2	Time (h)	**14** (%)	**16/17** (%)	Ratio[a] **16:17**
12a	Me	Me	44	63	14	80:20
12b	Et	Et	44	68	14	86:14
12c	(CH$_2$)$_5$		90	67	17	77:23
12d	Ph	Me	15	79	9	100:0
12e	Ph	Ph	15	79	12	100:0
12f	Cl	Ph	15	72	19	100:0

[a] Ratio determined via ^{31}P-NMR

The intermediate 1,2,3-triazoline **13** is formed by a 1,3-dipolar cycloaddition of diazomethane to the C=N bond of the 1,1-bisphosphono-2-aza-1,3-diene **12** and is the precursor for the aziridine **14** and imine **16**. The formed imine **16** can rearrange to the corresponding enamine **17**.

It is known that 1,2,3-triazolines decompose under light irradiation.[51–53] We evaluated shortly the influence of light irradiation on the selectivity of the reaction of 1,1-bisphosphono-2-aza-1,3-dienes **12** with diazomethane. The reaction was evaluated under continuous flow conditions due to the more efficient light penetration in the microreactor channels and higher surface-to-volume ratios compared to a batch reaction flask.[54–58] To reduce the amount of possible side products, compound **12d** was used in the aziridination reaction (Scheme 3.17).
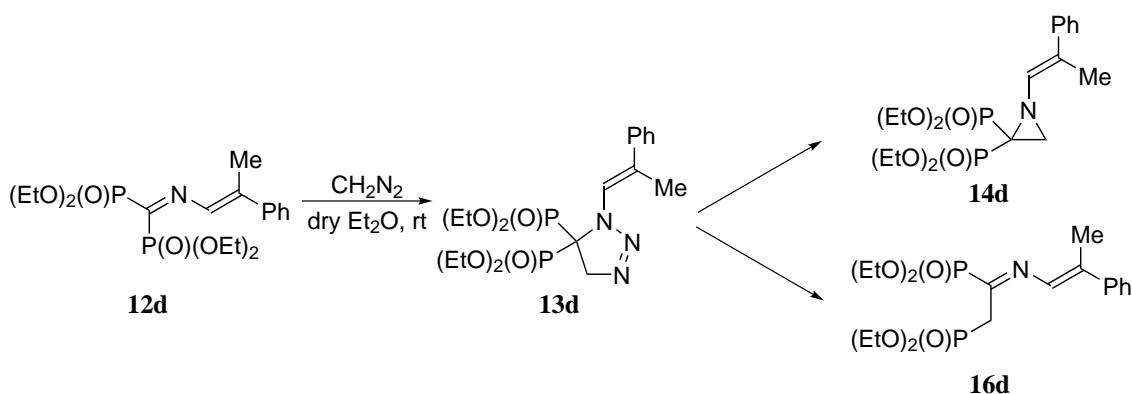
Scheme 3.17. Aziridination of 1,1-bisphosphono-2-aza-1,3-diene **12d**

3.4.2 Results and discussion

The starting material, 1,1-bisphosphono-2-aza-1,3-diene **12d**, was synthesized in batch via known literature procedures (Scheme 3.18).[294,295]
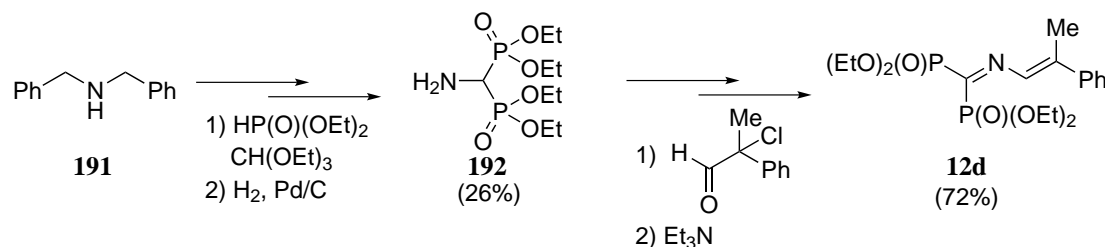
Scheme 3.18. Synthesis of 1,1-bisphosphono-2-aza-1,3-diene **12d**

The flow experiments were performed with a Labtrix® Start microreactor and the microreactor chip was illuminated with an ordinary light bulb (45W). All experiments were performed in dry Et_2O with a residence time of 10 min (Table 3.29). Diazomethane was synthesized starting from diazald and was obtained as a solution in Et_2O.

Table 3.29: Overview of the flow experiments

	Entry	CH_2N_2 (M)	**12d** (M)	CH_2N_2 (μl/min)	**12d** (μl/min)	T (°C)	CH_2N_2 (equiv.)	Conversion[a] (%)
without $h\nu$	1	0.35	0.035	0.5	0.5	21	10	-
	2	0.35	0.035	0.5	0.5	40	10	trace
	3	0.35	0.035	0.5	0.5	60	10	trace
$h\nu$	4	0.35	0.035	0.5	0.5	60	10	37
	5	0.35	0.01	0.22	0.78	60	10	34
	6	0.35	0.01	0.36	0.64	60	20	53
	7	0.35	0.01	0.5	0.5	60	35	71

[a] Conversion determined via ^{31}P-NMR

Initial flow experiments were performed without light irradiation (Table 3.29, entries 1-3). However, only traces of the aziridine **14d** were observed at reaction temperatures of 40 and 60°C. When the reactor chip was illuminated, a conversion of 37% was observed and no side product **16d** was detected (Table 3.29, entry 4). In order to eliminate possible concentration effects, an experiment was repeated with a less concentrated solution of the starting material

and a comparable conversion was obtained (Table 3.29, entries 4 and 5). If the excess CH_2N_2 was increased, a selective conversion of **12d** to **14d** of 71% was obtained (Table 3.29, entry 7).

In these flow experiments under light irradiation, the formation of the side product **16d** was never observed. A comparable batch experiment with light irradiation revealed complete conversion of the starting material **12d** after 1h to a mixture of **14d** and **16d** in a ratio 88:12 **14d**:**16d**. In order to take into account the effect of the large excess diazomethane used in one of the flow experiments (Table 3.29, entry 7), a batch experiment with 35 equivalents of CH_2N_2 was performed. Complete conversion of the starting material was obtained in this batch experiment and again a mixture of **14d** and **16d** was obtained (91:9 **14d**:**16d**).

3.4.3 Conclusions

Despite the formation of side products in batch, selective conversion of 1,1-bisphosphono-2-aza-1,3-diene **12d** to the corresponding aziridine **14d** was possible under continous flow conditions using light irradiation. Up to now, a selective conversion of 71% was reached. Further research is necessary to optimize the photodecomposition of the intermediate triazoline to the corresponding aziridine.

3.5 Continuous flow Bt-activation of amino acids

3.5.1 Introduction

Numerous methods for the coupling of amino acids in peptide chemistry are described in literature.[296–301] One of the known activation strategies, reported extensively by Katritzky and coworkers, involves the use of 1*H*-benzotriazole (BtH).[302,303] The activation of amino acids with BtH requires only the protection of the aminogroup while other functional groups are tolerated.[303] Moreover, benzotriazolides (*N*-acylbenzotriazoles) are stable and crystalline compounds which makes them easy to handle. BtH has been used as an efficient coupling reagent in the synthesis of peptides as well as derivatives thereof (glycopeptides, peptide alcohols, etc.).[303–306] The BtH-group has also proven its value in the synthesis of various classes of organic heterocycles due to its excellent leaving group characteristics.[302,307,308] Oligopeptidoylamino-substituted heterocycles are of considerable interest in the pharmaceutical and agrochemical industry due to their broad range of biological activity. However, synthesis of these compounds requires usually prolonged and often harsh conditions involving high temperatures and long reaction times.[309–315]

In previous research at our department (SynBioC, Department of Sustainable Organic Chemistry and Technology, Faculty of Bioscience Engineering, Ghent University), Bt-activated amino acids were efficiently coupled with heterocyclic amines using microreactor technology (Scheme 3.19).[59]
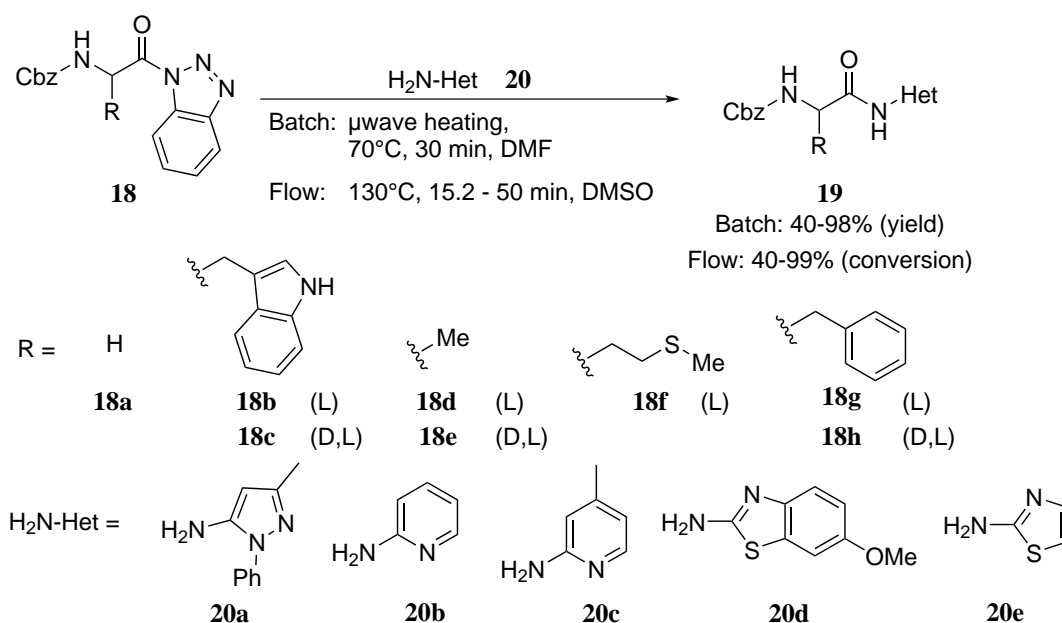
Scheme 3.19. Synthesis of (α-aminoacyl)amino-substituted heterocycles

The original reported batch procedure makes use of microwave heating to efficiently heat the reaction mixture.[316] Several (α-aminoacyl)amino-substituted heterocycles were synthesized under the optimized continuous flow conditions. The Cbz-protected amino acids were activated with benzotriazole in batch (Scheme 3.20). In this project, we investigated the benzotriazole activation of amino acids under continuous flow conditions. Performing both activation and coupling of amino acids in a continuous flow mode makes high throughput and the fully automated synthesis of peptides possible.
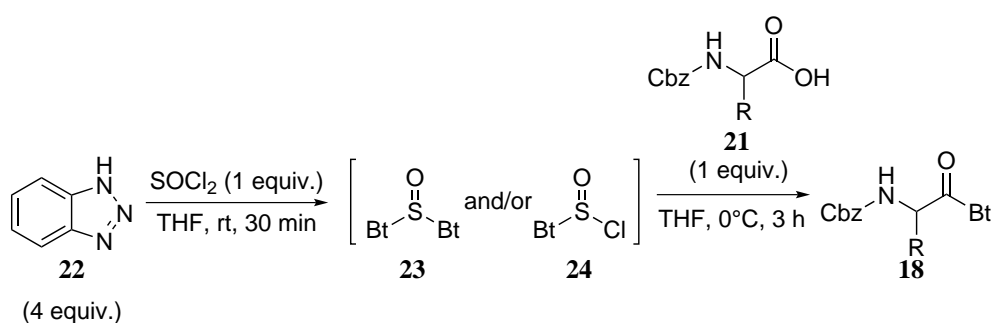
Scheme 3.20. Synthesis of *N*-protected α-aminoacylbenzotriazoles **18** in batch

An analogous continuous flow synthesis strategy was reported by Ley *et al.* (Scheme 3.21).[317]
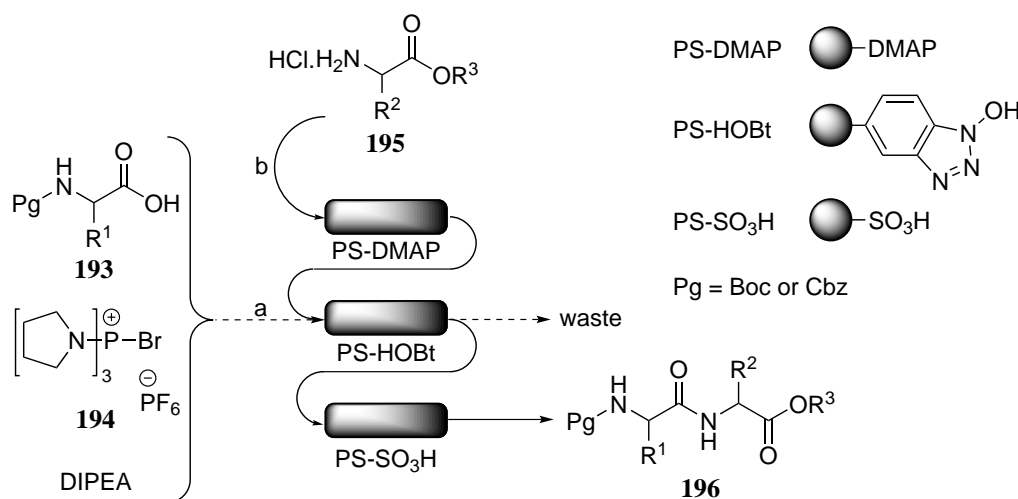
Scheme 3.21. Synthesis of dipeptides using polymer-supported (PS) reagents[317]

The peptide bond was formed in two steps using polymer-supported reagents. In a first step, a solution of a *N*-protected (Boc or Cbz) amino acid, diisopropylethylamine (DIPEA) and a phosphonium coupling reagent was passed through a column with polymer-supported HOBt (1-hydroxybenzotriazole), resulting in the formation of a polymer-supported and activated amino acid. In a second step, this column was switched inline in a serie of columns containing

polymer-supported DMAP and sulfonic acid. A second amino acid was passed through the three columns (DMAP - HOBt - SO$_3$H) resulting in the formation of a dipeptide. Several dipeptides were synthesized in good yields (61-83%). The developed procedure was elaborated to Fmoc-protected amino acids and the synthesis of tripeptides. Other methods to synthesize peptides in microreactors are described in literature.[318-320]

3.5.2 Cbz-protection

Cbz-protected amino acids were commercially available or were synthesized according to the procedure described by Pehere and Abell.[321] An aqueous mixture of K$_2$CO$_3$ and NaHCO$_3$ was used to control the pH of the solution during the addition of CbzCl (Table 3.30).

Table 3.30: Overview of the isolated yields for the Cbz-protection in batch

Entry	Substrate **197**	R	Yield (%)
1	L-Trp **197b**		86
2	D,L-Trp **197c**		85
3	L-Ala **197d**	Me	90
4	D,L-Ala **197e**	Me	92
5	L-Met **197f**	S–Me	80
6	L-Phe **197g**		85
7	D,L-Phe **197h**		82

3.5.3 Bt-activation of amino acids

Two different methods are available for the Bt-activation of amino acids: (1) BtMs (1-(methanesulfonyl)benzotriazole) and (2) BtH - SOCl$_2$.

3.5.3.1 Activation with BtMs

BtMs **25** was synthesized through reaction of benzotriazole with methanesulfonyl chloride (MsCl) (Scheme 3.22).[322]
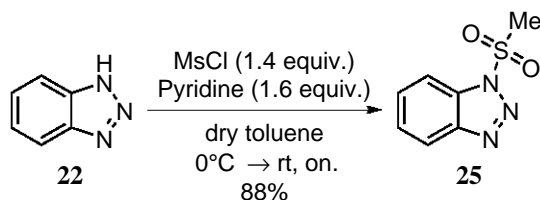
Scheme 3.22. Synthesis of BtMs **25** in batch

In a first step, a series of batch experiments was performed in different solvents (THF, MeCN and NMP (*N*-methyl-2-pyrrolidone)) based on a procedure reported by Katritzky *et al.* (Table 3.31).[323]

Table 3.31: Preliminary batch experiments for the activation with BtMs **25**

Entry	Solvent	T (°C)	Yield (%)
1	THF	Δ	18
2	THF (dry)	Δ	57
3	MeCN (dry)	70	53
4	MeCN (dry)	Δ	55
5	NMP (dry)	70	CRM

A clear reaction mixture was observed for all three solvents. Use of THF resulted in a limited isolated yield of 18% (Table 3.31, entry 1) while comparable yields were obtained with dry THF or dry MeCN (Table 3.31, entries 2-4). When dry NMP was used, a complex reaction mixture was observed on ^{1}H-NMR (Table 3.31, entry 5).

In a next series of experiments, the Bt-activation was evaluated under continuous flow conditions (Labtrix® Start microreactor) in dry MeCN. In order to accurately determine the conversion of the starting material, the optimization experiments were performed with Cbz-L-Trp **21b** and a standardisation curve was prepared for both the starting material **21b**

and end product **18b** (Figure 3.23). The results for this series of optimization experiments are summarized in Table 3.32.
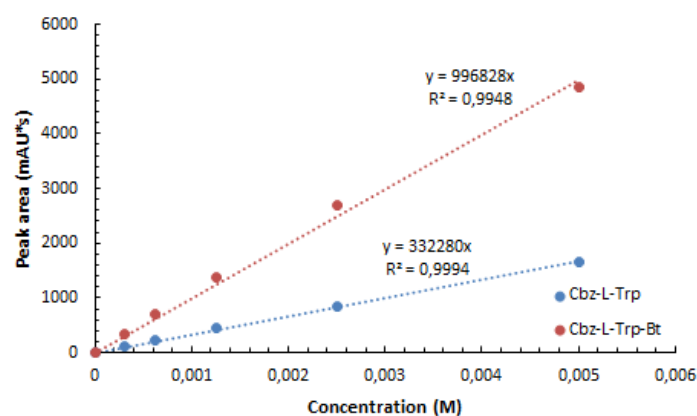
Figure 3.23. Standardisation curve for Cbz-L-Trp **21b** and Cbz-L-Trp-Bt **18b** (HPLC-UV, 254.8 nm)

Table 3.32: Optimization of the Bt-activation of Cbz-L-Trp **21b** in flow

Entry	T (°C)	BtMs (equiv.)	RT (min)	Conversion (%)
1	80	1	10	46
2	90	1	10	56
3	100	1	10	52
4	120	1	10	63
5	90	1.25	10	74
6	90	1.25	15	81
7	90	1.25	20	67
8	100	1.25	5	56
9	100	1.25	10	74
10	100	1.25	15	63
11	100	1.25	20	58

In a first series of flow experiments, the influence of the reaction temperature was evaluated (Table 3.32, entries 1-4). An increase of the reaction temperature generally resulted in an increase of the conversion although the effect was moderate. At higher temperatures, more free BtH was seen in the LC-MS spectrum, indicating a higher degree of degradation at higher reaction temperatures. In a next step, an excess of BtMs was used and both the reaction temperature and residence time were varied (Table 3.32, entries 5-11). Using an excess of BtMs resulted in a considerable increase of the conversion (Table 3.32, entries 2 and 5, 3 and 9). The highest conversion was obtained with a residence time of 15 min at 90°C (Table 3.32, entry 6). A further increase of the reaction time resulted in a decrease of the conversion (Table 3.32, entry 7). A lower conversion was obtained at higher reaction temperatures when an excess of BtMs was used (Table 3.32, entries 6 and 10, 7 and 11). In all these flow experiments, a limited amount (around 6%) of unidentified side products were detected on LC-MS. However, no correlation between side product formation and the reaction temperature or residence time was observed. A maximum conversion of 81% was reached for the activation of Cbz-L-Trp **21b** using 1.25 equivalents of BtMs combined with a residence time of 15 min at 90°C. In a next step, the activation with BtH - SOCl$_2$ was evaluated.

3.5.3.2 Activation with BtH - SOCl$_2$

As for the activation with BtMs **25**, a series of batch experiments with different solvents was performed for the activation of amino acids with BtH - SOCl$_2$ in order to determine suitable reaction conditions for the continuous flow experiments (Scheme 3.23 and Table 3.33). This Bt-activation was performed according to procedures developed by Katritzky *et al.*[302]
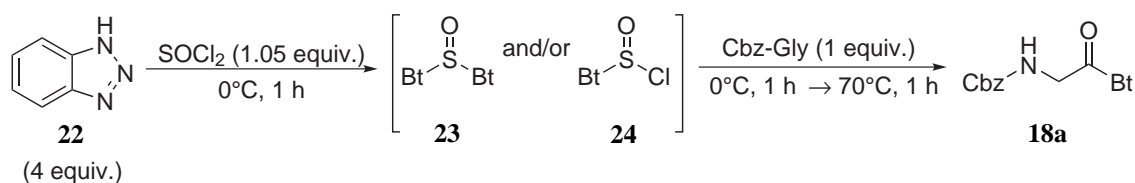
Scheme 3.23. Activation of Cbz-Gly **21a** with BtH - SOCl$_2$

Table 3.33: Evaluation of different solvents for the activation of **21a** with BtH - SOCl$_2$

Entry	Solvent	Yield (%)	Remarks
1	dry THF	76	turbid reaction mixture
2	dry CH$_2$Cl$_2$	76	turbid reaction mixture
3	dry MeCN	77	turbid reaction mixture
4	dry NMP	-	clear reaction mixture

Use of THF, CH$_2$Cl$_2$ or MeCN resulted in the formation of a turbid reaction mixture due to the precipitation of BtH.HCl, although good and comparable isolated yields were obtained (Table 3.33, entries 1-3). A clear reaction mixture without precipitation of the formed salts was observed with NMP. However, isolation of the end product **18a** was difficult due to the high boiling point of NMP (T$_b$ = 202°C). Evaporation of the solvent *in vacuo* was not possible and distillation of the solvent under high vacuum conditions (2 mbar) resulted in a complex residue. In an aqueous work up procedure, no phase separation was visible. Due to these problems related to the isolation of the Bt-activated amino acid or precipitation of the formed salts, solvent mixtures (THF:NMP and MeCN:NMP) were evaluated for the activation of Cbz-L-Trp **21b** with BtH - SOCl$_2$ (Table 3.34).

Table 3.34: Evaluation of solvent mixtures for the activation of **21b** with BtH - SOCl$_2$

Entry	Solvent mixture	Remarks
1	MeCN:NMP (1:1)	clear reaction mixture
2	MeCN:NMP (2:1)	clear reaction mixture
3	MeCN:NMP (4:1)	clear reaction mixture
4	MeCN:NMP (6:1)	clear reaction mixture
5	MeCN:NMP (9:1)	tubid reaction mixture
6	THF:NMP (1:1)	clear reaction mixture
7	THF:NMP (2:1)	clear reaction mixture
8	THF:NMP (4:1)	turbid reaction mixture

In order to limit the use of NMP, the solvent mixture with the lowest amount of NMP without the formation of a turbid reaction mixture was looked for. With MeCN, lower amounts of NMP could be used before a turbid reaction mixture was observed (Table 3.34). When the Bt-

activation of Cbz-L-Trp **21b** was evaluated in MeCN:NMP (6:1), near quantitative conversion (99%) was reached after 10 min at 0°C. Therefore, this solvent mixture was used in subsequent flow experiments.

The Bt-activation of amino acids under continuous flow conditions was optimized with **21b** as starting material (Scheme 3.24 and Table 3.35). These experiments were performed in a PFA tube reactor at 0°C in MeCN:NMP (6:1).
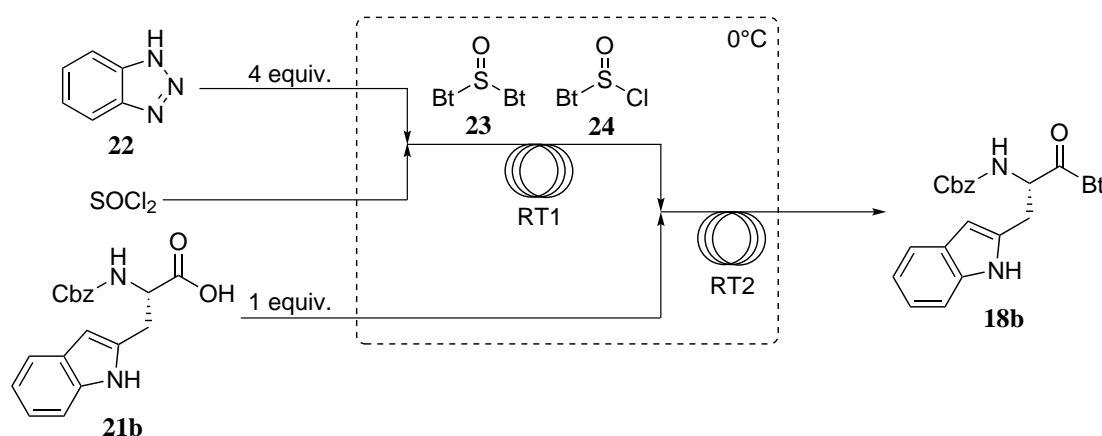
Scheme 3.24. Activation of Cbz-L-Trp **21b** with BtH - $SOCl_2$ under continuous flow conditions

Table 3.35: Activation of Cbz-L-Trp **21b** with BtH - $SOCl_2$ under continuous flow conditions

Entry	RT_1[a] (min)	RT_2[a] (min)	$SOCl_2$ (equiv.)	Conversion (%)
1	2	1	1.2	83
2	4	2	1.2	84
3	10	5	1.2	89
4	2	1	1.5	94

[a] Scheme 3.24

Changing the residence time in both tube reactors had little influence on the conversion (Table 3.35, entries 1-3). Comparable conversions were obtained with residence times varying from 2 min (resp. 1 min) to 10 min (resp. 5 min) for the first (resp. second) tube reactor. Increasing the excess of $SOCl_2$ led to an excellent conversion (Table 3.35, entry 4). Work up of the reaction mixture was very straightforward. The end product **18b** precipitated when the reactor output was collected in H_2O. However, traces of NMP were still present in the crude reaction product. In order to remove these solvent traces, the precipitate was washed with H_2O.

Subsequently, different amino acids were activated using the optimized continuous flow procedure. Table 3.36 gives an overview of the crude yield (before the removal of traces of NMP) and purified yield (after complete removal of NMP) for the synthesized derivatives. Each time, a sample was collected over a period of 30 min and the crude yield and purified yield were determined. Isolated yields obtained in batch by Cukalovic are also displayed.[59] No racemization was observed based on comparison of the optical rotation of the synthesized derivatives with literature data.[324,325]

Table 3.36: Bt-activation of amino acids under continuous flow conditions

| Entry | Compound **18** | FLOW | | | BATCH |
		Crude yield (%)	Purified yield (%)	Calculated throughput (g/day)	Yield (%)
1	Cbz-Gly-Bt **18a**	quantitative	99	50	98
2	Cbz-L-Trp-Bt **18b**	91	85	60	58
3	Cbz-D,L-Trp-Bt **18c**	94	87	62	66
4	Cbz-L-Ala-Bt **18d**	85	80	42	67
5	Cbz-D,L-Ala-Bt **18e**	82	76	40	61
6	Cbz-L-Met-Bt **18f**	97	71	44	66
7	Cbz-L-Phe-Bt **18g**	99	94	61	82
8	Cbz-D,L-Phe-Bt **18h**	99	97	63	64

In order to monitor the yield during the course of the operation, the continuous flow procedure was run for several hours for the Bt-activation of three different derivatives. Samples were collected over a period of one hour and the isolated yield of each sample was determined (Figure 3.24). Comparable isolated yields were obtained during the course of the operation, indicating stable continuous flow conditions.
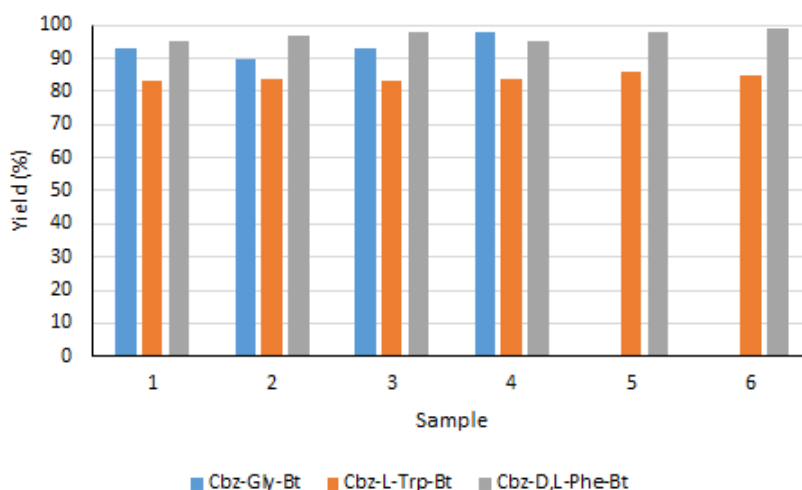
Figure 3.24. Isolated yield during the course of the operation

3.5.4 Coupling of amino acids via α-aminoacylbenzotriazoles

3.5.4.1 Coupling of Cbz-D,L-Phe-Bt and 2-aminopyridine

In order to evaluate the influence of the solvent on the coupling of α-aminoacylbenzotriazoles with heterocyclic amines, the coupling between Cbz-D,L-Phe-Bt **18h** and 2-aminopyridine **20b** was evaluated in MeCN:NMP (6:1) and compared with the results obtained in previous research.[59] Cukalovic optimized this reaction in DMSO and the optimized flow conditions are depicted in Scheme 3.25.[59]
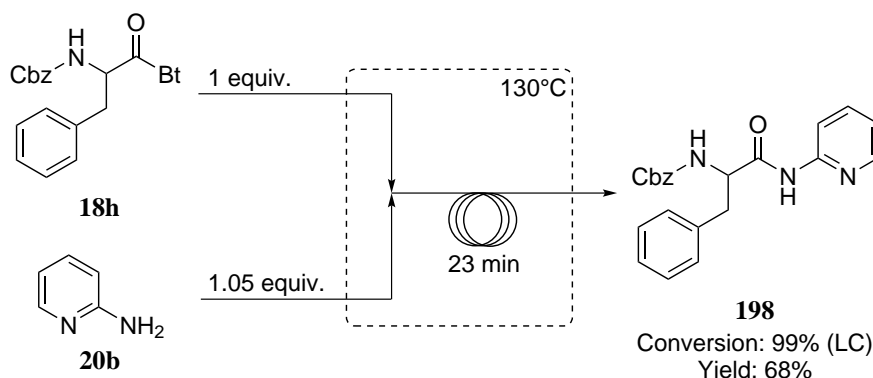
Scheme 3.25. Coupling of Cbz-D,L-Phe-Bt **18h** and 2-aminopyridine **20b** under continuous flow conditions as optimized by Cukalovic[59]

As discussed by Cukalovic, the conversion of the reaction can be easily monitored via LC-MS as the benzotriazole moiety (free in solution after the reaction) and the α-aminoacylbenzotriazole starting material exhibit the same absorption at 254.8 nm. The reaction temperature of 130°C was set as the optimal temperature; lower temperatures gave rise to lower conversions whereas a number of side products were observed at higher reaction temperatures.[59] Starting from

these reaction conditions, the coupling of Cbz-D,L-Phe-Bt **18h** and 2-aminopyridine **20b** was evaluated in MeCN:NMP (6:1) in order to telescope the activation of amino acids with the subsequent coupling reaction (Table 3.37). Both reagent solutions were pumped at the same flow rate through the KiloFlow® reactor.

Table 3.37: Coupling of Cbz-D,L-Phe-Bt **18h** and 2-aminopyridine **20b** under continuous flow conditions in MeCN:NMP (6:1)

Entry	**18h** (M)	**20b** (equiv.)	RT (min)	Conversion (%)
1	0.05	1.05	10.16	47
2	0.05	1.05	15.5	57
3	0.05	1.05	20.33	64
4	0.05	1.2	10.16	51
5	0.05	1.2	20.33	68
6	0.05	1.2	29.5	84
7	0.025	1.2	10.16	36
8	0.025	1.2	20.33	53
9	0.025	1.2	29.5	65

The experiments were performed with dilute solutions due to the limited solubility of the starting material **18h** in MeCN:NMP (6:1) and heating of the reagent solution was required in order to dissolve all Cbz-D,L-Phe-Bt **18h**. The first series of experiments with 1.05 equivalents of 2-aminopyridine **20b** resulted in moderate conversions of 47 - 64% depending on the residence time (Table 3.37, entries 1-3). Increasing the equivalents of 2-aminopyridine **20b** resulted in slightly higher conversions (Table 3.37, entries 4-5). However, a conversion of 84% was reached with a residence time of around 30 min (Table 3.37, entry 6). Decreasing the concentration of the starting material solutions resulted in poorer conversions (Table 3.37, entries 7-9).

Despite the increase of the residence time and the larger excess of 2-aminopyridine **20b**, the conversions obtained were worse than the near quantitative conversion obtained by Cukalovic when DMSO was used as solvent.[59]

3.5.4.2 Coupling of Cbz-L-Trp and L-Pro-OMe.HCl

Subsequently, the synthesis of a dipeptide (coupling between Cbz-L-Trp **18b** and L-Pro-OMe.HCl **199**) under continuous flow conditions was evaluated. First, the reaction was performed in batch with an excellent isolated yield (92%) (Scheme 3.26).
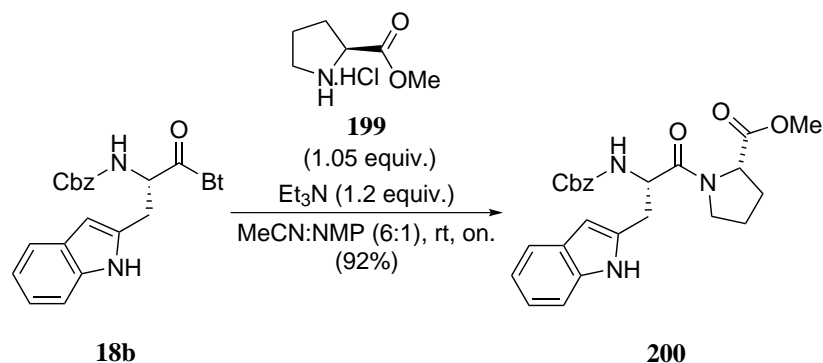
Scheme 3.26. Coupling of Cbz-L-Trp-Bt **18b** and L-Pro-OMe.HCl **199** in batch

Subsequently, the reaction was investigated under continuous flow conditions (Labtrix® Start microreactor) (Scheme 3.27 and Table 3.38).
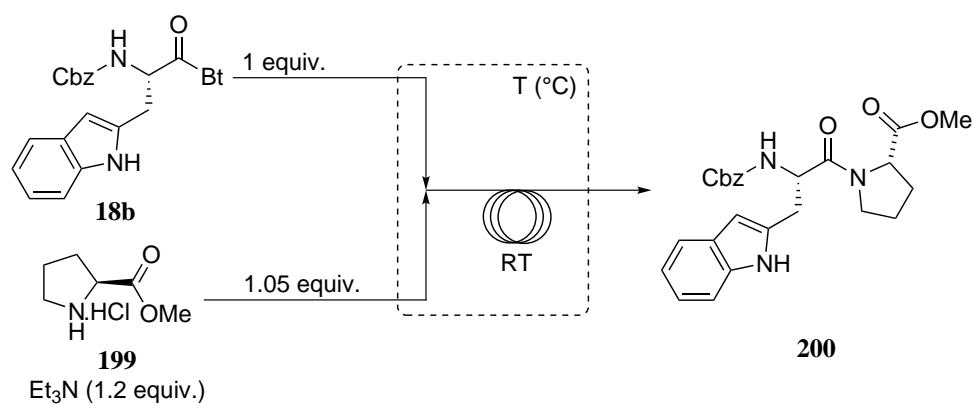
Scheme 3.27. Coupling of Cbz-L-Trp-Bt **18b** and L-Pro-OMe.HCl **199** under continuous flow conditions

Optimization of the reaction temperature and residence time finally led to near quantitative conversion (99%) (Table 3.38, entry 6). Subsequently, the optimized flow conditions were scaled-up to the KiloFlow® reactor and the reaction was run for 150 min after reaching steady state. After aqueous work up, the end product **200** was obtained with an isolated yield of 89% and a calculated throughput of 0.3 g/h. However, due to the high reaction temperature, racemization was observed and the end product was obtained as two diastereoisomers in a ratio ~6:1 LL:LD.

Table 3.38: Coupling of Cbz-L-Trp-Bt **18b** and L-Pro-OMe.HCl **199** under continuous flow conditions in MeCN:NMP (6:1)

Entry	T^a (°C)	RT^a (min)	Conversion (%)
1	50	10	45
2	70	10	62
3	90	10	77
4	110	10	84
5	130	10	90
6	130	30	99

[a] Scheme 3.27

3.5.5 Conclusions

Two methods were evaluated for the Bt-activation of amino acids: (1) BtMs and (2) BtH - SOCl$_2$. If the right solvent was used, both methods could be used under continuous flow conditions without precipitate formation. After optimization of the Bt-activation of Cbz-L-Trp **21b** with BtMs, a limited conversion of 81% was reached. However, activation with BtH - SOCl$_2$ in MeCN:NMP (6:1) resulted in an excellent conversion (94%). Moreover, work up of the reaction mixture was very straightforward. Several derivatives were synthesized in good isolated yields (76-99%).

Performing the coupling of a Bt-activated amino acid with a heterocyclic amine in MeCN:NMP (6:1) resulted in poorer conversions as compared to previous research in which DMSO was evaluated as solvent. On the other hand, the synthesis of a dipeptide in this solvent mixture went smoothly although racemization was observed due to the high reaction temperature applied.

Chapter 4

Experimental part

4.1 General experimental methods

4.1.1 Solvents

Diethyl ether (Et_2O), tetrahydrofuran (THF) and toluene were distilled from sodium or sodium benzophenone ketyl, while dichloromethane was distilled from calcium hydride prior to use. MeCN and NMP were dried over molecular sieves. Methanol was dried by distillation over magnesium/iodine. Petroleum ether refers to the 40-60°C boiling fraction.

4.1.2 Column chromatography

Purification of the reaction mixtures was performed by column chromatography in a glass column with silica gel (Aldrich, particle size 35-70 μm, pore diameter ca. 6 nm) or on a Reveleris® X2 Flash Chromatography System. Solvent systems were determined via thin layer chromatography (TLC) on glass plates coated with silica gel (Merck, Kieselgel 60F$_{254}$, precoated 0.25 mm). Compounds were revealed by UV light or $KMnO_4$ oxidation.

4.1.3 Gas chromatography

GC analysis was performed on an Agilent 6980 Series gas chromatograph, connected to a FID detector (H_2 gas), using an Alltech EC-5 capillary column (30 m x 0.25 mm) with a film thickness of 0.25 μm and helium as the carrier gas.

4.1.4 Liquid chromatography

LC and LC-MS analysis was performed on a Agilent 1200 Series liquid chromatograph with a reverse phase LC-column (Eclipse plus C18 column (50 x 4.6 mm, particle size: 3.5 μm) or Supelco Ascentis Express C18 column (30 x 4.6 mm, particle size: 2.7 μm)) with UV/VIS detector and 5 mM NH_4OAc in H_2O and MeCN as eluents. MS analysis was performed on an Agilent 1100 Series LC/MSD type SL mass spectrometer with electrospray ionization (ESI 70 eV) and using a mass selective detector (quadrupole).

4.1.5 Mass spectrometry

Low resolution mass spectra were recorded via injection on an Agilent 1100 Series LC/MSD type SL mass spectrometer with electrospray ionization (ESI 70 eV) and using a mass selective detector (quadrupole). When crude reaction mixtures were analyzed, the mass spectrometer was preceded by a HPLC reversed phase column with a diode array UV/VIS detector. High resolution mass spectra were obtained with an Agilent Technologies 6210 Time-of-Flight Mass Spectrometer (TOFMS), equipped with ESI/APCI-multimode source.

4.1.6 NMR spectroscopy

High resolution ^{1}H-NMR (300 or 400 MHz), ^{13}C-NMR (75 or 100.6 MHz) and ^{31}P-NMR (121 MHz) spectra were recorded on a Jeol Eclipse FT 300 NMR spectrometer or a Bruker Avance III Nanobay 400 MHz spectrometer at room temperature. Peak assignments were obtained with the aid of DEPT, COSY, HSQC and/or HMBC spectra. The compounds were diluted in deuterated solvents with tetramethylsilane (TMS) as internal standard.

4.1.7 Infrared spectroscopy

Infrared spectra were recorded on a Perkin Elmer Spectrum BX FT-IR Spectrometer. All compounds were analyzed in neat form with an ATR (Attenuated Total Reflectance) accessory. Only selected absorbances (ν_{max}, cm^{-1}) were reported.

4.1.8 Elementary analysis

Elementary analyses were obtained by means of a Perkin Elmer series II CHNS/O elementary analyzer 2400.

4.1.9 Melting point

Melting points of crystalline compounds were determined using a Büchi B-540 apparatus or a Kofler bench, type WME Heizbank of Wagner & Munz.

4.2   Condensation of acid chlorides and alcohols using continuous flow

All alcohols and acid chlorides are commercially available. Liquid reagents were used in neat form and if necessary, distilled prior to use. Solid reagents were dissolved in dioxane, CH_2Cl_2 or MeCN.

4.2.1   Labtrix® Start

Small-scale reactions were performed using a Labtrix® Start system (Chemtrix) fitted with a glass microreactor chip of 10 μl internal volume and 2 x 1000 μl gas-tight syringes (SGE) (Figure 4.1).
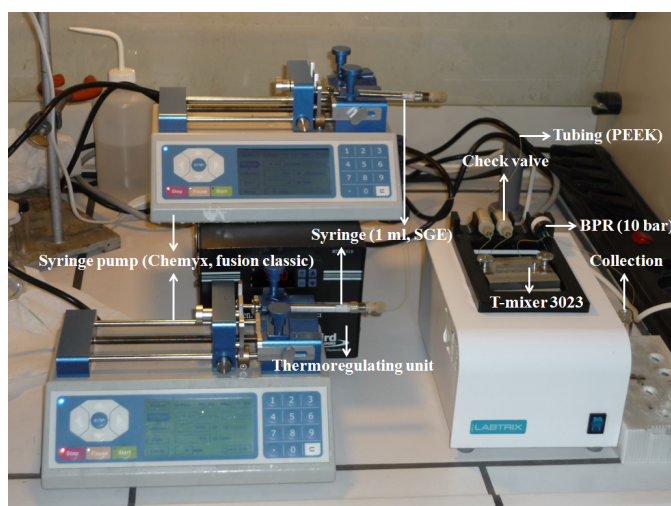
Figure 4.1. Labtrix® Start microreactor

The syringes were connected to the microreactor chip with PEEK tubing (ID = 150 μm, OD = 360 μm). A check valve prevented back flow of the liquid. The microreactor chip (T-mixer 3023) consisted of 10 μl reaction volume and 1.5 μl quench volume (Figure 4.2). A thermoregulating unit controlled the cooling or heating of the reaction volume.
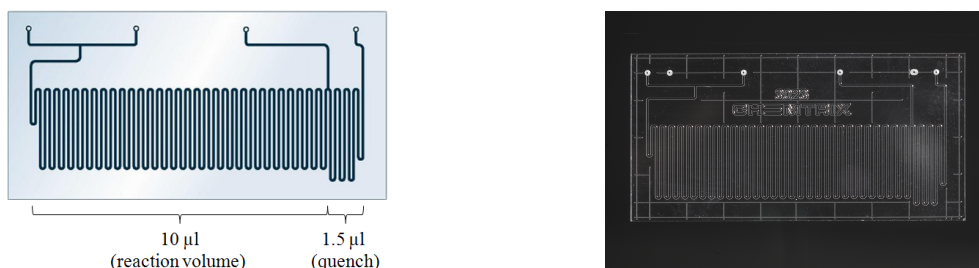
Figure 4.2. T-mixer 3023

A back pressure regulator (BPR) of 10 bar was used to keep all reagents in solution at elevated temperatures. Before performing the reaction, the microreactor was rinsed with the alcohol or solvent under investigation. Subsequently, the microreactor was primed with the alcohol and acid chloride using a total flow rate of 15-20 μl/min for 5-6 min. Finally, both reagents were pumped through the microreactor with a flow rate corresponding to the desired stoichiometric ratio and residence time. The flow rate was calculated using the following equations:

$$RT \; = \; \frac{IV}{F_1 + F_2} \tag{4.1}$$

$$ratio \; = \; \frac{C_2 \cdot F_2}{C_1 \cdot F_1} \tag{4.2}$$

$$C \; = \; \frac{\rho}{MW} \quad \text{(liquid reagents, neat)} \tag{4.3}$$

with

- RT = residence time (min)
- IV = internal volume (ml)
- F = flow rate (ml/min)
- ratio = stoichiometric ratio
- C = concentration (mmol/ml)
- ρ = density (g/ml)
- MW = molecular weight (g/mmol)

After a steady state period (50-65 min depending on the total flow rate, total volume of 100 μl), a sample was collected to be analyzed by GC. The formed esters are well known compounds and their spectral data corresponded to the data reported in literature.

4.2.2 KiloFlow®

Scale-up of the condensation of benzoyl chloride and methanol was performed using a KiloFlow® system (Chemtrix) with an internal reactor volume of 6.5 ml (Figure 4.3).
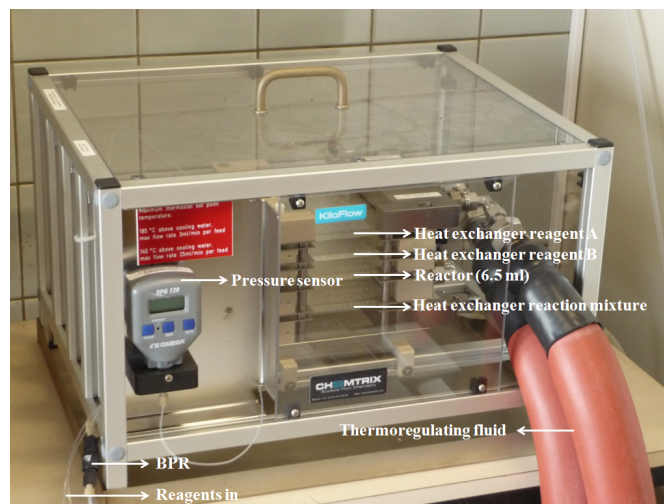
Figure 4.3. KiloFlow® reactor

A HPLC pump (FLOM HPLC pump AI-12 series) was used to pump the reagents through the reactor. Before being mixed in the reactor plate, both reagent streams were heated to the reaction temperature by flowing separately through a heat exchanger. The heating of the reagent streams and reaction mixture was controlled by a thermoregulating unit (Lauda). The reactor plate contained an integrated static mixer (SOR, staggered oriented ridges) to obtain efficient mixing of both reagent streams (Figure 4.4). After the reactor plate, a heat exchanger cooled the reaction mixture to ambient temperature by the use of running tap water. A BPR of 7 bar was used to keep all reagents in the liquid phase (Figure 4.5).
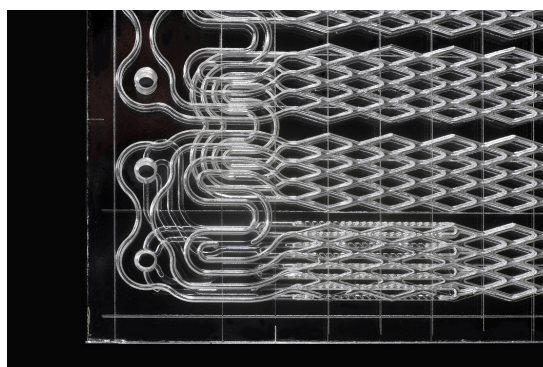
Figure 4.4. KiloFlow® reactor plate with integrated SOR-mixer
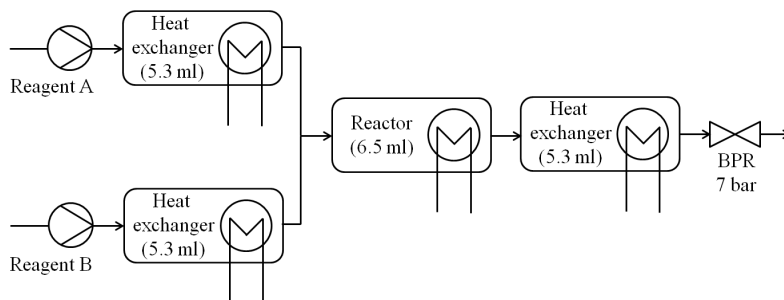
Figure 4.5. Schematic representation of the KiloFlow® reactor

After rinsing the reactor with methanol, the reactor was primed with benzoyl chloride and methanol for 15 min at a total flow rate of 2.6 ml/min (F_{MeOH} = 0.82 ml/min, F_{BzCl} = 1.78 ml/min). Subsequently, both reagents were pumped through the mesoreactor with the desired total flow rate of 1.3 ml/min (F_{MeOH} = 0.41 ml/min, F_{BzCl} = 0.89 ml/min) and thus a residence time in the reactor module of 5 min and a ratio MeOH:BzCl of 1.3:1. After reaching steady state (15 min), collection was started. The experiment was run for 4 hours and samples were collected over a period of one hour. The work up of the reaction mixture was very straightforward: excess MeOH was removed *in vacuo*. Excellent and stable isolated yields were obtained during the course of the operation (Figure 4.7). Spectral data were in agreement with the literature. Formed HCl was captured as depicted in Figure 4.6. In both steps of the HCl-recuperation, 300 ml H_2O and 250 ml 5 M NaOH were used to trap the HCl. The concentrations of the solutions were determined via titration with 2 M NaOH or 6 M HCl with phenolphthalein as indicator.
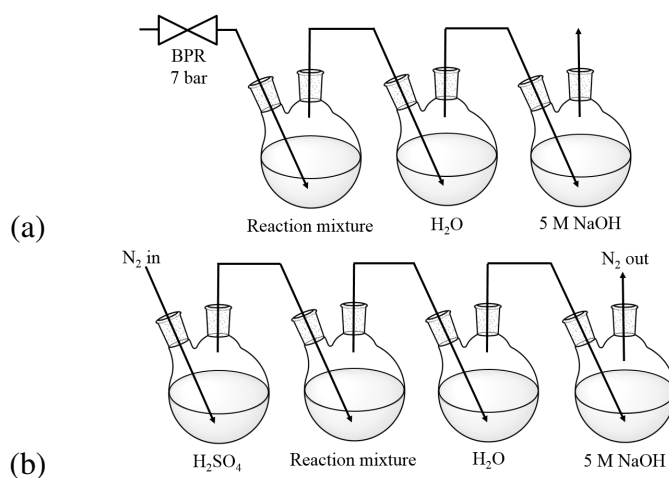
Figure 4.6. Recuperation of the formed HCl: (a) during collection, (b) purging with dry N_2
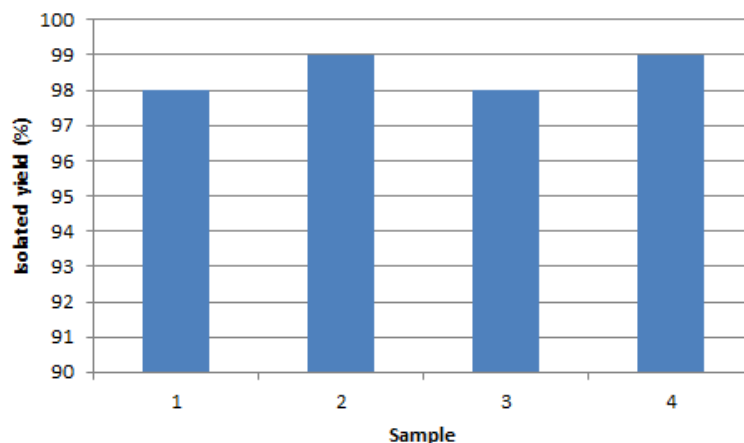
Figure 4.7. Condensation of benzoyl chloride with MeOH on the KiloFlow® reactor

An overview of the technical specifications of the used reactors is given in Table 4.1.

Table 4.1: Technical specifications of the used reactors

	Labtrix® Start	KiloFlow®
Channel dimensions	300 μm x 60 μm	1.4 mm x 1 mm
Wetted materials	Glass, PEEK, PTFE, Techtron	Glass, PEEK, PFA, PPS, perfluoroelastomer
Type of mixer	T-mixer	SOR-mixer

PEEK = polyether ether ketone, PTFE = polytetrafluoroethylene,

PFA = perfluoroalkoxy, PPS = polyphenylene sulfide

4.3 Continuous flow bromination of methyl sulfones and methanesulfonates

All reagents were obtained from commercial suppliers or synthesized based on literature procedures except for 4-isopropoxyphenyl methyl sulfone **7**, which was provided by Agfa Gevaert NV.

4.3.1 Batch procedures

4.3.1.1 Synthesis of methyl 2-methylphenyl sulfone

The procedure described by Borys *et al.* was used to synthesize methyl 2-methylphenyl sulfone **137**.[225] 4.32 g **136** (34.8 mmol, 1 equiv.) was dissolved in 20 ml 2.5 M NaOH and 6.6 ml $(MeO)_2SO_2$ (69.6 mmol, 2 equiv.) was added dropwise. After the addition of $(MeO)_2SO_2$, 2.5 M NaOH was added until pH>7. The reaction mixture was stirred at room temperature for 90 min and subsequently extracted twice with Et_2O. The combined organic layers were dried with $MgSO_4$ and the solvent was removed under reduced pressure. The residue was dissolved in HOAc (25 ml) and heated to reflux (118°C) after which 10.4 ml 30% H_2O_2 was added (3 equiv.). The reaction mixture was stirred at reflux temperature for 3 h. After cooling to room temperature, the reaction mixture was extracted twice with CH_2Cl_2. The combined organic layers were washed with sat. $NaHCO_3$ untill no more gas evolution was observed. The organic layer was dried with $MgSO_4$ and the solvent was removed *in vacuo*. After purification through column chromatography (PE:EtOAc 7:3), 4.69 g methyl 2-methylphenyl sulfone **137** (27.6 mmol) was obtained as a white solid (79%). Spectral data were in agreement with the literature.[326]

4.3.1.2 Synthesis of *N*-aryl methanesulfonamides

The synthesis of *N*-aryl methanesulfonamides **148**-**150** was based on a procedure described by Jafarpour *et al.*[226] Aniline (8.17 g, 87.75 mmol, 2 equiv.) was dissolved in 100 ml EtOH. The reaction mixture was cooled to 0°C and 3.4 ml methanesulfonyl chloride (43.87 mmol, 1 equiv.) was added. Subsequently, the reaction mixture was stirred overnight at room temperature. After evaporation of the solvent under reduced pressure, the residue was dissolved in CH_2Cl_2 and washed twice with 6 M HCl and once with brine. The organic layer was dried with $MgSO_4$ and the solvent was removed *in vacuo*. After recrystallization from MeOH, 6.23 g *N*-phenyl methanesulfonamide **148** (36.4 mmol) was obtained as a pale white solid (83%). Spectral data of all synthesized *N*-aryl methanesulfonamides were in agreement with the literature.[327]

4.3.1.3 Synthesis of methanesulfonates

To a stirred solution of 5 g phenol (53.12 mmol, 1 equiv.) and 5.9 g Et_3N (58.4 mmol, 1.1 equiv.) in CH_2Cl_2, 6.7 g methanesulfonyl chloride (58.4 mmol, 1.1 equiv.) was added dropwise at 0°C. The reaction mixture was stirred 1 h at 0°C and 1 h at rt and subsequently diluted with EtOAc. The organic phase was washed with water and dried with $MgSO_4$. After evaporation of the solvent under reduced pressure, 8.69 g phenyl methanesulfonate **139** (50.46 mmol) was isolated (95%). Spectral data of all synthesized methanesulfonates were in agreement with the literature.[328,329]

4.3.1.4 Synthesis of tribromomethyl 4-isopropoxyphenyl sulfone

13.08 g KOH (233.23 mmol, 20 equiv.) was dissolved in 30 ml H_2O and the solution was cooled to 0°C. Subsequently, 2.4 ml Br_2 (46.65 mmol, 4 equiv.) was added dropwise resulting in the formation of a yellow KOBr solution. Meanwhile, 2.5 g 4-isopropoxyphenyl methyl sulfone **7** (11.7 mmol, 1 equiv.) and 1.88 g TBABr (5.83 mmol, 0.5 equiv.) were dissolved in 40 ml toluene. The reaction mixture was heated to 50-60°C in order to dissolve all TBABr. In a next step, the KOBr solution was added dropwise to the solution of the starting material and phase transfer catalyst at 38°C over a period of 7 min. Subsequently, the reaction mixture was stirred vigorously over a period of 22 h at 38°C. Et_2O and H_2O were added to the reaction mixture after which the organic phase was washed with H_2O and brine. The organic phase was dried with $MgSO_4$ and the solvent was evaporated under reduced pressure. 4.98 g tribromomethyl 4-isopropoxyphenyl sulfone **8** (11.04 mmol) was isolated (94%). The synthesis of the other derivatives was analogous. No further purification of the end products was necessary.

Tribromomethyl 4-isopropoxyphenyl sulfone 8
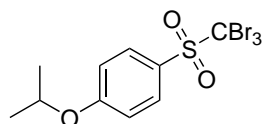
^{1}H-NMR (400 MHz, CDCl$_3$): δ 1.41 (6H, d, J = 6.07 Hz, 2 x CH$_3$); 4.70 (1H, septet, J = 6.07 Hz, C$\underline{H}$(CH$_3$)$_2$); 7.00 - 7.04 (2H, m, 2 x CH$_{arom}$); 8.11 - 8.14 (2H, m, 2 x CH$_{arom}$). **^{13}C-NMR (100.6 MHz, CDCl$_3$):** δ 21.79 (2 x CH$_3$), 51.82 (C$_q$Br$_3$); 70.99 ($\underline{C}$H(CH$_3$)$_2$); 115.24 (2 x CH$_{arom}$); 118.12 (C$_q$S); 135.97 (2 x CH$_{arom}$); 164.18 (C$_q$O). **IR (cm^{-1}):** ν_{max} 1152, 1346 (RSO$_2$R). **MS (70 eV): m/z (%)** 468 ([M+NH$_4$]$^+$, 100); 470 ([M+NH$_4$]$^+$, 100). **Melting point:** T$_m$ = 126°C. **Chromatography:** PE:EtOAc (95:5) R$_f$ = 0.10. **HRMS (ESI or APCI):** no ionization observed. **Elementary analysis:** degradation of compound. **Yield:** 94% (white crystals).

4.3.2   Continuous flow procedures

4.3.2.1   Bromination - synthesis of KOBr in batch

Equipment - tube reactor

A schematic representation of the tube reactor is given in Figure 4.8.
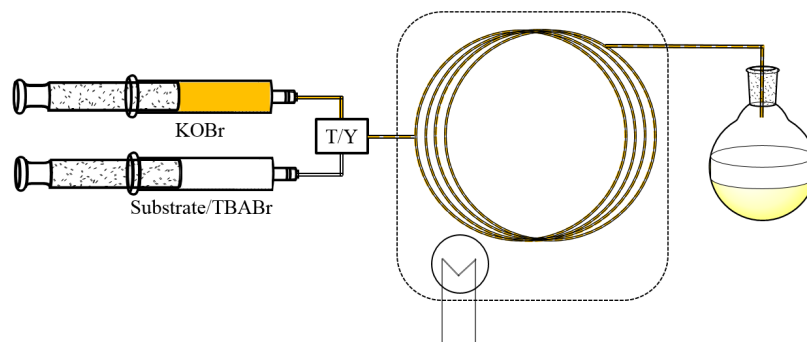
Figure 4.8. Schematic representation of the tube reactor

The reagent solutions were pumped through the mesoreactor using a syringe pump (Chemyx Syringe Pump (type Fusion Touch or Fusion Classic) or Harvard PHD 22/2000 Advance Syringe Pump). The connection of the syringes with the mixing unit occured with an ETFE (ethylene tetrafluoroethylene) Luer Lock and PFA-tubing (internal diameter: 0.020", outer diameter: 1/16"). Mixing occured in an ETFE T- or PEEK Y-connector. The mesoreactor was built up of PFA-tubing with an internal diameter of 0.020" (0.50 mm) and a total volume of 3 ml. The mesoreactor was heated to the desired reaction temperature in an oil bath.

Equipment - static mixer

A schematic representation of the glass static mixer setup is given in Figure 4.9.
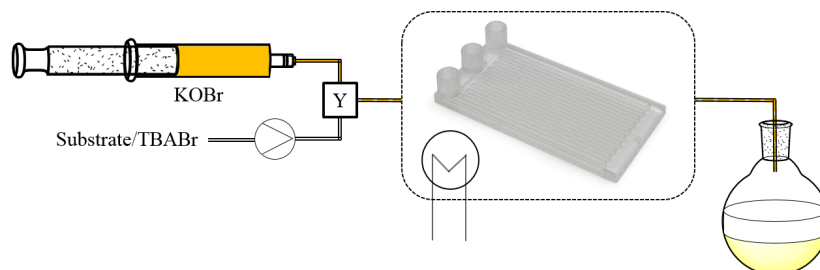
Figure 4.9. Schematic representation of the glass static mixer setup

The KOBr solution was pumped through the Uniqsis® mixer chip with a Chemyx Syringe Pump (type Fusion Touch) while the Uniqsis® Binary Pump Module was used to pump the solution of the starting material and phase transfer catalyst. The connection of the syringe with the PEEK Y-connector occured with an ETFE Luer Lock and PFA-tubing (internal diameter: 0.020", outer diameter: 1/16"). In the normal setup of the glass static mixer, both reagent solutions are heated to the reaction temperature before they are mixed in the static mixer unit. In order to prevent degradation of the KOBr solution by heating the solution before it is mixed with the starting material, both reagent solutions were mixed in a PEEK Y-connector and the Y-connector is connected to the outlet of the mixer chip by PFA-tubing (internal diameter: 0.020", outer diameter: 1/16"). In this way, both reagent solutions were mixed in the Y-connector and entered directly the static mixer zone of the chip, which was heated to the desired reaction temperature. One of the normal inlets of the chip served as outlet while the other normal inlet was closed (Figure 4.10). The channels of the mixer chip had a nominal internal diameter of 1 mm and in this setup, the reagents were passed through 1.6 ml static mixer zone and 0.2 ml residence time unit without static mixing elements.
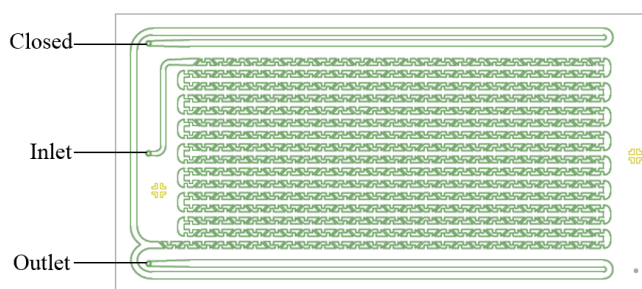
Figure 4.10. Detail of the Uniqsis® mixer chip

Experimental procedure

The following solutions were prepared in advance:

1. A 1 M KOBr solution was prepared by dropping 1.28 ml Br_2 into 25 ml of a 5.9 M aq. KOH solution at 0°C.

2. A solution of 0.3 M substrate and 0.15 M TBABr was prepared by dissolving 2.57 g 4-isopropoxyphenyl methyl sulfone **7** (12 mmol) and 1.93 g TBABr (6 mmol) in toluene until a total volume of 40 ml was obtained. The solution was heated to 50-60°C in order to dissolve all TBABr and was pumped at this temperature through the reactor.

The glass static mixer was rinsed by pumping water and toluene through the reactor. Subsequently, the reactor was heated to 85°C and both reagent solutions were pumped through

the mixer block at a total flow rate of 0.6 ml/min (F_{KOBr} = 0.33 ml/min, $F_{substrate/TBABr}$ = 0.27 ml/min) and thus a residence time of 3 min and a ratio KOBr:substrate of 4:1. After reaching steady state (11 min), a sample was collected for 45 min and the sample was subsequently diluted with water and Et_2O. The organic phase was dried with $MgSO_4$ and the solvent was removed under reduced pressure. 1.64 g tribromomethyl 4-isopropoxyphenyl sulfone **8** (3.6 mmol) was isolated (quantitative yield). No further purification of the end product was necessary.

The synthesis of the other derivatives was analogous. Each time, a sample was collected for 40 to 45 min and worked up. In some cases, the end product needed further purification (recrystallization from MeOH or column chromatography).

Tribromomethyl phenyl sulfone 142
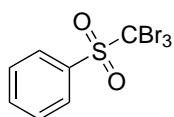
^{1}H-NMR (400 MHz, CDCl$_3$): δ 7.62 - 7.67 (2H, m, 2 x CH$_{arom}$); 7.78 - 7.83 (1H, m, CH$_{arom}$); 8.24 - 8.27 (2H, m, 2 x CH$_{arom}$). **^{13}C-NMR (100.6 MHz, CDCl$_3$):** δ 50.55 (C$_q$Br$_3$); 128.56 (C$_{q,arom}$); 128.82 (2 x CH$_{arom}$); 133.64 (2 x CH$_{arom}$); 135.76 (CH$_{arom}$). **IR (cm^{-1}):** ν_{max} 1152, 1334 (RSO$_2$R). **MS (70 eV): m/z (%)** 410 ([M+NH$_4$]$^+$, 100); 412 ([M+NH$_4$]$^+$, 100). **Melting point:** T$_m$ = 149°C. **Chromatography:** PE:EtOAc (95:5) R$_f$ = 0.14. **HRMS (ESI or APCI):** no ionization observed. **Elementary analysis:** degradation of compound. **Yield:** 87% (pale white crystals).

Tribromomethyl 2-bromophenyl sulfone 143

Purification: recrystallization from MeOH
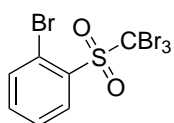
^{1}H-NMR (400 MHz, CDCl$_3$): δ 7.56 - 7.61 (2H, m, 2 x CH$_{arom}$); 7.86 - 7.90 (1H, m, CH$_{arom}$); 8.45 - 8.50 (1H, m, CH$_{arom}$). **^{13}C-NMR (100.6 MHz, CDCl$_3$):** δ 50.74 (C$_q$Br$_3$); 125.69 (C$_{q,arom}$); 127.43 (CH$_{arom}$); 128.40 (C$_{q,arom}$); 136.45 (CH$_{arom}$); 137.10 (CH$_{arom}$); 138.19 (CH$_{arom}$). **IR (cm^{-1}):** ν_{max} 1158, 1343 (RSO$_2$R). **MS (70 eV): m/z (%)** 490 ([M+NH$_4$]$^+$, 100); 488 ([M+NH$_4$]$^+$, 65); 492 ([M+NH$_4$]$^+$, 65). **Melting point:** T$_m$ = 109°C. **Chromatography:** PE:EtOAc (95:5) R$_f$ = 0.12. **HRMS (ESI or APCI):** no ionization observed. **Elementary analysis:** degradation of compound. **Yield:** 48% (brownish solid).

Tribromomethyl 2-methylphenyl sulfone 144

Purification: column chromatography (PE:EtOAc 70:30)
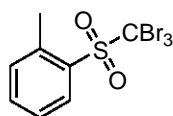
^{1}H-NMR (400 MHz, CDCl$_3$): δ 2.91 (3H, s, CH$_3$); 7.41 - 7.45 (2H, m, 2 x CH$_{arom}$); 7.65 (1H, txd, J_1 = 7.6 Hz, J_2 = 1.3 Hz, CH$_{arom}$); 8.32 (1H, ~d, J = 8.1 Hz, CH$_{arom}$). **^{13}C-NMR (100.6 MHz, CDCl$_3$):** δ 22.62 (CH$_3$), 52.50 (C$_q$Br$_3$); 126.19 (CH$_{arom}$); 127.04 (C$_q$S); 133.50 (CH$_{arom}$); 135.76 (CH$_{arom}$); 136.29 (CH$_{arom}$); 143.48 (<u>C</u>$_q$CH$_3$). **IR (cm^{-1}):** ν_{max} 1155, 1332 (RSO$_2$R). **MS (70 eV): m/z (%)** 424 ([M+NH$_4$]$^+$, 100); 426 ([M+NH$_4$]$^+$, 100). **Melting point:** T$_m$ = 102°C. **Chromatography:** PE:EtOAc (95:5) R$_f$ = 0.17. **HRMS (ESI or APCI):** no ionization observed. **Elementary analysis:** degradation of compound. **Yield:** 77% (pale white solid).

Phenyl tribromomethanesulfonate 145

Purification: column chromatography (PE:EtOAc 97.5:2.5)
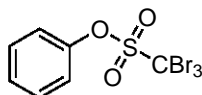
^{1}H-NMR (400 MHz, CDCl$_3$): δ 7.33 - 7.37 (1H, m, CH$_{arom}$); 7.41 - 7.46 (4H, m, 4 x CH$_{arom}$). **^{13}C-NMR (100.6 MHz, CDCl$_3$):** δ 37.82 (C$_q$Br$_3$); 121.37 (2 x CH$_{arom}$); 127.75 (CH$_{arom}$); 129.92 (2 x CH$_{arom}$); 151.06 (C$_q$OS). **IR (cm^{-1}):** ν_{max} 1192, 1379 (ROSO$_2$R). **MS (70 eV):** no ionization observed. **Chromatography:** PE:EtOAc (95:5) R$_f$ = 0.25. **HRMS (ESI or APCI):** no ionization observed. **Yield:** 87% (brownish liquid).

3-Methoxyphenyl tribromomethanesulfonate 146

Purification: column chromatography (PE:EtOAc 97.5:2.5)
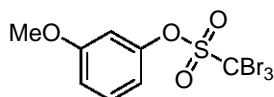
^{1}H-NMR (400 MHz, CDCl$_3$): δ 3.83 (3H, s, CH$_3$O); 6.89 (1H, dxd, J_1 = 8.32 Hz, J_2 = 2.32 Hz, CH$_{arom}$); 6.95 (1H, t, J = 2.32 Hz, CH$_{arom}$); 7.02 (1H, dxd, J_1 = 8.32 Hz, J_2 = 2.32 Hz, CH$_{arom}$); 7.33 (1H, t, J = 8.32 Hz, CH$_{arom}$). **^{13}C-NMR (100.6 MHz, CDCl$_3$):** δ 37.84 (C$_q$Br$_3$); 55.66 (CH$_3$O); 107.50 (CH$_{arom}$); 113.42 (CH$_{arom}$); 113.55 (CH$_{arom}$); 130.23 (CH$_{arom}$); 151.70 (C$_q$OS); 160.60 (C$_q$OCH$_3$). **IR (cm^{-1}):** ν_{max} 1181, 1385 (ROSO$_2$R). **MS (70 eV):** no ionization observed. **Melting point:** T$_m$ = 97°C. **Chromatography:** PE:EtOAc (95:5) R$_f$ = 0.37. **HRMS (ESI or APCI):** no ionization observed. **Elementary analysis:** degradation of compound. **Yield:** 83% (white solid).

4-Chlorophenyl tribromomethanesulfonate 147

Purification: column chromatography (PE:EtOAc 95:5)
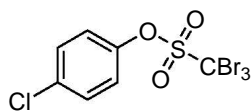
^{1}H-NMR (400 MHz, CDCl$_3$): δ 7.36 - 7.44 (4H, m, 4 x CH$_{arom}$).
^{13}C-NMR (100.6 MHz, CDCl$_3$): δ 37.47 (C$_q$Br$_3$); 122.83 (2 x CH$_{arom}$); 130.04 (2 x CH$_{arom}$); 133.52 (C$_q$Cl); 149.50 (C$_q$OS). **IR (cm^{-1}):** ν_{max} 1194, 1391 (ROSO$_2$R). **MS (70 eV):** no ionization observed. **Melting point:** T$_m$ = 58°C. **Chromatography:** PE:EtOAc (95:5) R$_f$ = 0.22. **HRMS (ESI or APCI):** no ionization observed. **Elementary analysis:** degradation of compound. **Yield:** 84% (pale white solid).

4.3.2.2   Bromination - synthesis of KOBr in flow

Equipment

A schematic representation of the experimental setup for the continuous synthesis of hypobromite and the subsequent bromination reaction is given in Figure 4.11.
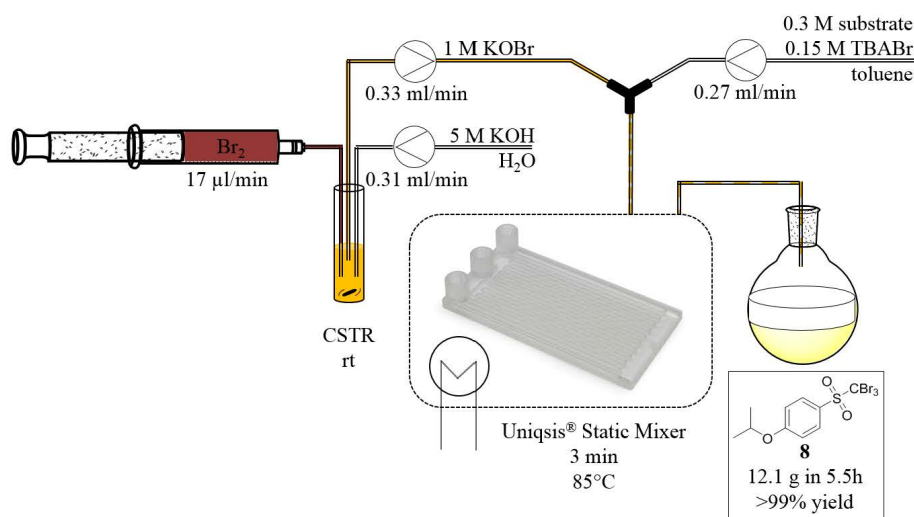
Figure 4.11. Continuous synthesis of hypobromite and subsequent bromination

A Chemyx Syringe Pump (type Fusion Touch) was used to pump Br$_2$ through FEP-tubing (FEP = fluorinated ethylene propylene) (internal diameter: 150 μm, outer diameter: 1/32") to the CSTR. 5 M aq. KOH was pumped through PFA-tubing (internal diameter: 0.020", outer diameter: 1/16") to the CSTR with the Uniqsis® Binary Pump Module. Once formed, the KOBr solution was pumped to the Uniqsis® static mixer with a Syrris® Reagent Pump. Before entering the static mixer, the KOBr solution was mixed with the solution of the starting material and PTC (pumped with the Uniqsis® Binary Pump Module) in a PEEK Y-connector in order to prevent degradation of the KOBr solution before it was mixed with the starting material. The setup of the mixer block is described earlier (Figure 4.10).

Experimental procedure

The following solutions were prepared in advance:

1. 5 M KOH in H_2O

2. 0.3 M 4-isopropoxyphenyl methyl sulfone **7** and 0.15 M TBABr in toluene. The solution was heated to 50-60°C in order to dissolve all TBABr and was pumped at this temperature through the reactor.

The glass static mixer was rinsed by pumping water and toluene through the reactor. Subsequently, the reactor was heated to 85°C. Bromine (17 μl/min) and the KOH solution (0.31 ml/min) were pumped in a vial at room temperature containing a rotating stirring bar. Hence, a 1 M KOBr solution was obtained. After building up a buffer volume, the KOBr solution was pumped through the mixer block together with the solution containing the substrate and PTC at a total flow rate of 0.6 ml/min (F_{KOBr} = 0.33 ml/min, $F_{substrate/TBABr}$ = 0.27 ml/min) and thus a residence time of 3 min and a ratio KOBr:substrate of 4:1. The complete system was run for 30 min before collection started. Isolated yields were determined at different time intervals. Each time, the sample was diluted with water and Et_2O. Subsequently, the organic phase was dried with $MgSO_4$ and the solvent was removed under reduced pressure. Table 4.2 gives an overview of the isolated yields during the course of the operation. No further purification of the end product was necessary.

Table 4.2: Isolated yields during the course of the operation

Time interval (min)	Isolated yield (%)
0-60	98
60-120	quantitative
120-180	quantitative
180-240	quantitative
240-330	quantitative

4.3.2.3   Deprotection of tribromomethyl 4-isopropoxyphenyl sulfone

Equipment

A schematic representation of the reactor is given in Figure 4.12.
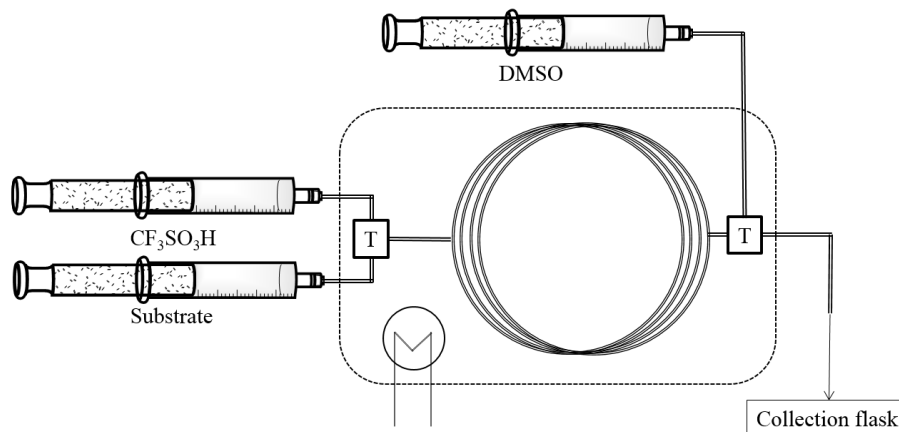
Figure 4.12. Schematic representation of the tube reactor used for the deprotection of the isopropyl ether group

The reagent solutions were pumped through the tube reactor using a syringe pump (Chemyx Syringe Pump (type Fusion Touch or Fusion Classic) or Harvard PHD 22/2000 Advance Syringe Pump). The connection of the syringes with the ETFE T-connectors occured with an ETFE Luer Lock and PFA-tubing (internal diameter: 0.020", outer diameter: 1/16"). The mesoreactor was built up of PFA-tubing with an internal diameter of 0.020" (0.50 mm) and a total volume of 0.2 ml. The mesoreactor was heated to the desired reaction temperature in an oil bath.

Experimental procedure

First, the tube reactor was rinsed by pumping toluene through the reactor and subsequently, the reactor was heated to 100°C. Both reagent solutions (CF_3SO_3H (neat) and 0.2 M tribromomethyl 4-isopropoxyphenyl sulfone **8** in toluene) were pumped through the reactor at a total flow rate of 0.1 ml/min (F_{acid} = 1.7 μl/min, $F_{substrate}$ = 98.3 μl/min) and thus a residence time of 2 min and a ratio CF_3SO_3H:**8** of 1:1. At the end of the reactor, the reaction mixture was mixed with DMSO in a T-connector (F_{DMSO} = 0.1 ml/min). After reaching steady state (6 min), a sample was collected for 5 min. After collection, the sample was neutralized with 2 M NaOH and the organic phase was analyzed via HPLC-UV. HPLC-UV peak areas were converted into concentration using a standardisation curve and hence the conversion was determined.

4.4 Simmons-Smith cyclopropanation of enamines

4.4.1 Batch procedures

4.4.1.1 Tosylation of primary amines

Method 1

Benzylamine (9.1 g, 85 mmol, 1 equiv.) was dissolved in 200 ml CH_2Cl_2 and 29.5 ml Et_3N (212 mmol, 2.5 equiv.) was added. The reaction mixture was cooled to 0°C and 15.4 g *p*-toluenesulfonyl chloride (81 mmol, 0.95 equiv.) was added portionwise (8 equal portions). Subsequently, the reaction temperature was raised to room temperature and the mixture was stirred overnight at room temperature. The reaction mixture was diluted with 500 ml Et_2O and washed twice with 500 ml 1 M HCl and once with brine. The organic phase was dried with $MgSO_4$ and the solvent was removed *in vacuo*. After recrystallization from EtOH, *N*-benzyl-*p*-toluenesulfonamide was obtained as white crystals (92%). *N*-allyl-*p*-toluenesulfonamide (white crystals, 76%) and *N*-propyl-*p*-toluenesulfonamide (white crystals, 93%) were obtained via the same procedure. Spectral data were in agreement with the literature.[330,331]

Method 2

The synthesis of *N*-phenyl-*p*-toluenesulfonamide was based on a literature procedure described by Golshani *et al.*[226] Aniline (5.0 g, 53.7 mmol, 2 equiv.) was dissolved in 55 ml EtOH and 5.1 g *p*-toluenesulfonyl chloride (26.8 mmol, 1 equiv.) was added. The reaction mixture was stirred overnight at room temperature. Subsequently, the solvent was removed under reduced pressure. The residue was purified through column chromatography (PE:EtOAc 8:1) and *N*-phenyl-*p*-toluenesulfonamide was obtained as white crystals (81%). Spectral data were in agreement with the literature.[332]

4.4.1.2 Synthesis of enamines

MgSO₄

The synthesis of enamines with $MgSO_4$ was based on a procedure reported by Darsigny *et al.*[281] In a typical experiment, the aldehyde (1 equiv.) was dissolved in $CHCl_3$ and the solution was cooled to 0°C. Subsequently, $MgSO_4$ (3.5 equiv.) and the secondary amine were added (1.2 equiv.). After 1 h at 0°C, the reaction mixture was filtered and the solvent was removed under reduced pressure. The obtained enamine was purified through recrystallization from dry MeOH or vacuum distillation. Spectral data of the synthesized enamines were in comparison with literature or are stated underneath.[281,333]

4-(3-Phenylbut-1-en-1-yl)morpholine 163
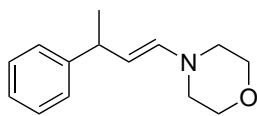
^{1}H-NMR (400 MHz, CDCl$_3$): δ 1.35 (3H, d, J=7.1 Hz, C$\underline{H}_3$CH); 2.77 (4H, t, J=4.9 Hz, 2 x CH$_2$N); 3.41 (1H, quintet, J=7.1 Hz, CH$_3$C$\underline{H}$); 3.69 (4H, t, J=4.9 Hz, 2 x CH$_2$O); 4.64 (1H, dd, J$_1$=13.9 Hz, J$_2$=7.1 Hz, C$\underline{H}$=CHN); 5.82 (1H, d, J=13.9 Hz, CH=C$\underline{H}$N); 7.13 - 7.29 (5H, m, 5 x CH$_{arom}$). **^{13}C-NMR (100.6 MHz, CDCl$_3$):** δ 22.86 ($\underline{C}$H$_3$CH); 40.41 (CH$_3\underline{C}$H); 49.41 (2 x CH$_2$N); 66.50 (2 x CH$_2$O); 108.14 ($\underline{C}$H=CHN); 125.77 (CH$_{arom}$); 126.99 (2 x CH$_{arom}$); 128.27 (2 x CH$_{arom}$); 138.66 (CH=$\underline{C}$HN); 147.55 (C$_q$). **IR (cm^{-1}):** ν_{max} 1116 (CH$_2$-O), 698 (phenyl). **MS (70 eV): m/z (%)** 218 ([M+H]$^+$, 100). **HRMS (ESI):** calculated for C$_{14}$H$_{19}$NO: 218.1539 [M+H]$^+$, experimental: 218.1534 [M+H]$^+$. **Yield:** 90% (yellow oil).

K$_2$CO$_3$

The synthesis of enamines with K$_2$CO$_3$ was based on a literature procedure described by Schamp *et al.*[282] Morpholine (5.8 g, 67 mmol, 1 equiv.) and 1.4 g K$_2$CO$_3$ (10 mmol, 0.15 equiv.) were mixed in a reaction flask and cooled to -5°C. Subsequently, 3 ml freshly distilled butyraldehyde (33.5 mmol, 0.5 equiv.) were added and the reaction mixture was stirred overnight at room temperature. The reaction mixture was filtered and the crude product was purified through vacuum distillation (1.8 mbar, 34°C). The enamine, 4-(but-1-en-1-yl)morpholine **161** was obtained as a colourles oil (44%). Spectral data were in agreement with the literature.[334]

Dean-Stark

In a typical experiment, the tosylated amine (1.1 equiv.) and aldehyde (1 equiv.) were dissolved in toluene and *p*-toluenesulfonic acid (0.01 equiv.) was added. The reaction mixture was refluxed over a period of 24 h in a Dean-Stark apparatus. Subsequently, the reaction mixture was washed with sat. NaHCO$_3$ and the organic phase was dried with MgSO$_4$. After filtration, the solvent was removed under reduced pressure. The crude product was purified through column chromatography. Spectral data were in comparison with literature or are stated underneath.[335]

N-Propyl-*N*-styryl-*p*-toluenesulfonamide 164
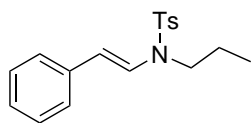
¹H-NMR (300 MHz, CDCl₃): δ 0.95 (3H, t, J=7.5 Hz, CH₂CH₃); 1.68 (2H, sextet, J=7.5 Hz, CH₂CH₃); 2.39 (3H, s, CH₃Cq); 3.37 (2H, t, J=7.5 Hz, NCH₂); 5.72 (1H, d, J=14.9 Hz, CH=CHN); 7.13 - 7.20 (1H, m, CHarom); 7.24 - 7.29 (6H, m, 6 x CHarom); 7.40 (1H, d, J=14.9

Hz, CH=CHN); 7.67 (2H, d, J=8.3 Hz, 2 x CHarom). **¹³C-NMR (75 MHz, CDCl₃):** δ 11.31 (CH₂CH₃); 20.41 (CH₂CH₃); 21.63 (CH₃Cq); 47.25 (NCH₂); 110.70 (CH=CHN); 125.47 (2 x CHarom); 126.46 (CHarom); 126.80 (CH=CHN); 126.98 (2 x CHarom); 128.80 (2 x CHarom); 129.96 (2 x CHarom); 136.25 (Cq); 136.61 (Cq); 143.88 (CqCH₃). **IR (cm⁻¹):** ν_{max} 1161 (SO₂). **MS (70 eV): m/z (%)** 316 ([M+H]⁺, 100). **Melting point:** T$_m$ = 80°C. **Chromatography:** PE:EtOAc (8:1) R$_f$ = 0.42. **HRMS (ESI):** calculated for C₁₈H₂₁NO₂S: 316.1366 [M+H]⁺, experimental: 316.1381 [M+H]⁺. **Yield:** 81% (white crystals).

N-Benzyl-*N*-styryl-*p*-toluenesulfonamide 165
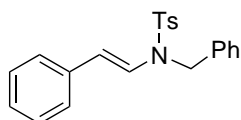
¹H-NMR (400 MHz, CDCl₃): δ 2.41 (3H, s, CH₃Cq); 4.64 (2H, s, CH₂Cq); 5.64 (1H, d, J=14.6 Hz, CH=CHN); 7.10 - 7.33 (12H, m, 12 x CHarom); 7.47 (1H, d, J=14.6 Hz, CH=CHN); 7.71 (2H, d, J=8.3 Hz, 2 x CHarom). **¹³C-NMR (75 MHz, CDCl₃):** δ 21.56 (CH₃Cq);

49.45 (CH₂Cq); 112.07 (CH=CHN); 125.40 (2 x CHarom); 126.40 (CHarom); 126.58 (CH=CHN); 126.86 (2 x CHarom); 127.00 (2 x CHarom); 127.52 (CHarom); 128.59 (2 x CHarom); 128.65 (2 x CHarom); 129.95 (2 x CHarom); 135.27 (Cq); 135.92 (Cq); 136.27 (Cq); 144.04 (CH₃Cq). **IR (cm⁻¹):** ν_{max} 1355 (SO₂), 1162 (SO₂). **MS (70 eV): m/z (%)** 364 ([M+H]⁺, 100). **Melting point:** T$_m$ = 118°C. **Chromatography:** PE:EtOAc (9:1) R$_f$ = 0.21. **HRMS (ESI):** calculated for C₂₂H₂₁NO₂S: 364.1366 [M+H]⁺, experimental: 364.1376 [M+H]⁺. **Yield:** 80% (white crystals).

N-Phenyl-*N*-(3-phenylbut-1-en-1-yl)-*p*-toluenesulfonamide 167
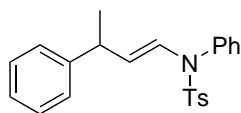
¹H-NMR (300 MHz, CDCl₃): δ 1.29 (3H, d, J=7.1 Hz, CH₃CH); 2.43 (3H, s, CH₃Cq); 3.43 (1H, ~quintet, J=7.1 Hz, CH₃CH); 4.6 (1H, dd, J₁=13.8 Hz, J₂=7.1 Hz, CH=CHN); 6.94 - 7.33 (13H, m, 12 x

CHarom + CH=CHN); 7.53 (2H, d, J=8.3 Hz, 2 x CHarom). **¹³C-NMR (75 MHz, CDCl₃):** δ 21.72 (CH₃Cq); 22.16 (CH₃CH); 40.10 (CH₃CH); 117.67 (CH=CHN); 126.22 (CHarom); 127.07 (2 x CHarom); 127.59 (2 x CHarom); 128.48 (2 x CHarom); 128.64 (CHarom); 128.92 (CH=CHN); 129.51 (2 x CHarom); 129.67 (2 x CHarom); 130.25 (2 x CHarom); 135.99 (Cq); 136.93 (Cq); 143.90 (CqCH₃); 146.08 (CHCq). **IR (cm⁻¹):** ν_{max} 1346 (SO₂), 1164 (SO₂). **MS (70 eV): m/z (%)** 378 ([M+H]⁺, 100). **Melting point:** T$_m$ = 91°C. **Chromatography:** PE:EtOAc (8:1) R$_f$

= 0.32. **HRMS (ESI):** calculated for $C_{23}H_{23}NO_2S$: 378.1522 [M+H]$^+$, experimental: 378.1536 [M+H]$^+$. **Yield:** 43% (yellow powder).

N-Benzyl-*N*-cyclohexylidenemethyl-*p*-toluenesulfonamide 168
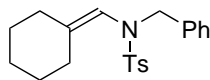
^{1}H-NMR (300 MHz, CDCl$_3$): δ 1.05 (2H, ~quintet, J=5.6 Hz, C$\underline{H}_2$(CH$_2$)$_2$C$_q$); 1.30 - 1.39 (4H, m, 2 x C$\underline{H}_2$CH$_2$C$_q$); 1.95 (2H, t, J=5.2 Hz, CH$_2$C$\underline{H}_2$C$_q$); 2.05 (2H, t, J=5.8 Hz, CH$_2$C$\underline{H}_2$C$_q$); 2.45 (3H, s, CH$_3$C$_q$); 4.16 (2H, s, NCH$_2$); 4.92 (1H, s, CHN); 7.21 - 7.29 (5H, m, 5 x CH$_{arom}$); 7.33 (2H, d, J=8.3 Hz, 2 x CH$_{arom}$); 7.70 (2H, d, J=8.3 Hz, 2 x CH$_{arom}$). **^{13}C-NMR (75 MHz, CDCl$_3$):** δ 21.54 ($\underline{C}$H$_3$C$_q$); 26.23 ($\underline{C}$H$_2$CH$_2$C$_q$); 26.49 ($\underline{C}$H$_2$(CH$_2$)$_2$C$_q$); 27.97 ($\underline{C}$H$_2$CH$_2$C$_q$); 28.83 (CH$_2$$\underline{C}H_2C_q$); 33.25 (CH$_2$$\underline{C}H_2C_q$); 54.72 (NCH$_2$); 116.82 (CHN); 127.58 (CH$_{arom}$); 127.63 (2 x CH$_{arom}$); 128.21 (2 x CH$_{arom}$); 129.17 (2 x CH$_{arom}$); 129.57 (2 x CH$_{arom}$); 135.18 (SC$_q$); 136.05 ($\underline{C}_q$CH$_2$); 143.34 ($\underline{C}_q$CH$_3$); 149.41 ($\underline{C}_q$CHN). **IR (cm^{-1}):** ν_{max} 1342 (SO$_2$), 1163 (SO$_2$). **MS (70 eV): m/z (%)** 356 ([M+H]$^+$, 100). **Melting point:** T$_m$ = 115°C. **Chromatography:** PE:EtOAc (8:1) R$_f$ = 0.41. **HRMS (ESI):** calculated for $C_{21}H_{25}NO_2S$: 356.1679 [M+H]$^+$, experimental: 356.1685 [M+H]$^+$. **Yield:** 72% (yellow powder).

N-Allyl-*N*-styryl-*p*-toluenesulfonamide 169
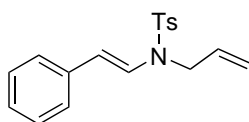
^{1}H-NMR (300 MHz, CDCl$_3$): δ 2.42 (3H, s, CH$_3$C$_q$); 4.13 (2H, dt, J$_1$=5.5 Hz, J$_2$=1.7 Hz, NCH$_2$); 5.16 - 5.28 (2H, m, CH=C$\underline{H}_2$); 5.64 - 5.77 (1H, m, C$\underline{H}$=CH$_2$); 5.75 (1H, d, J=14.6 Hz, C$\underline{H}$=CHN); 7.14 - 7.21 (1H, m, CH$_{arom}$); 7.27 - 7.33 (6H, m, 6 x CH$_{arom}$); 7.43 (1H, d, J=14.6 Hz, CH=C$\underline{H}$N); 7.7 (2H, ~d, J=8.3 Hz, 2 x CH$_{arom}$). **^{13}C-NMR (75 MHz, CDCl$_3$):** δ 21.53 ($\underline{C}$H$_3$C$_q$); 48.09 (NCH$_2$); 111.24 ($\underline{C}$H=CHN); 117.99 (CH=$\underline{C}$H$_2$); 125.37 (2 x CH$_{arom}$); 126.37 (CH$_{arom}$); 126.51 (CH=$\underline{C}$HN); 126.98 (2 x CH$_{arom}$); 128.65 (2 x CH$_{arom}$); 129.87 (2 x CH$_{arom}$); 131.50 ($\underline{C}$H=CH$_2$); 136.10 (C$_q$); 136.39 (C$_q$); 143.96 ($\underline{C}_q$CH$_3$). **IR (cm^{-1}):** ν_{max} 1350 (SO$_2$), 1155 (SO$_2$). **MS (70 eV): m/z (%)** 314 ([M+H]$^+$, 100). **Melting point:** T$_m$ = 57°C. **Chromatography:** PE:EtOAc (8:1) R$_f$ = 0.32. **HRMS (ESI):** calculated for $C_{18}H_{19}NO_2S$: 314.1209 [M+H]$^+$, experimental: 314.1218 [M+H]$^+$. **Yield:** 45% (white powder).

4.4.1.3 Simmons-Smith cyclopropanation

In a typical experiment, 4 ml Et$_2$Zn (1 M in hexanes, 4 mmol, 3 equiv.) was dissolved in 10 ml dry CH$_2$Cl$_2$. The reaction mixture was placed under a N$_2$-atmosphere and cooled to -78°C. Diiodomethane (0.64 ml, 8 mmol, 6 equiv.) was added dropwise and the reaction mixture was subsequently heated to 0°C and stirred at this temperature for 15 min. A white suspension was

formed. Trifluoroacetic acid (0.31 ml, 4 mmol, 3 equiv.) was added at 0°C and the reaction mixture was again stirred for 15 min at this temperature. During this period, a clear and colourless reaction mixture was obtained. A solution of 250 mg *N*-styrylmorpholine **158** (1.32 mmol, 1 equiv.) in 2 ml dry CH_2Cl_2 was added at 0°C after which the reaction mixture was allowed to warm to room temperature. After 45 min (6 h for the enamines with an EWG on nitrogen), 2 ml sat. K_2CO_3 was added. The organic phase was separated and the aqueous phase was extracted with CH_2Cl_2. The combined organic layers were dried with $MgSO_4$. After filtration and evaporation of the solvent under reduced pressure, a viscous yellow oil was obtained. This oil was purified through column chromatography (PE:EtOAc 95:5 + 2% Et_3N) after which 153 mg *N*-(2-phenylcyclopropyl)morpholine **174** was obtained as a yellow oil (57%).

N-(2-Phenylcyclopropyl)morpholine 174
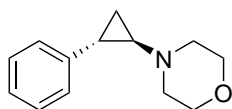
¹H-NMR (300 MHz, CDCl₃): δ 0.87 - 0.92 (1H, m, C$\underline{H}_aH_b$); 1.03 - 1.10 (1H, m, CH$_a\underline{H}_b$); 1.81 - 1.86 (1H, m, CHN); 1.95 (1H, ddd, J_1=9.4 Hz, J_2=6.1 Hz, J_3=3.3 Hz, CHC$_q$); 2.57 (4H, t, J=4.4 Hz, 2 x CH$_2$N); 3.62 (4H, t, J=4.4 Hz, 2 x CH$_2$O); 6.97 - 7.02 (2H, m, 2 x CH$_{arom}$); 7.06 - 7.12 (1H, m, CH$_{arom}$); 7.16 - 7.23 (2H, m, 2 x CH$_{arom}$). **¹³C-NMR (75 MHz, CDCl₃):** δ 15.86 (CH$_a$H$_b$); 23.99 ($\underline{C}$HC$_q$); 48.74 (CHN); 53.10 (2 x CH$_2$N); 66.57 (2 x CH$_2$O); 125.35 (CH$_{arom}$); 125.73 (2 x CH$_{arom}$); 127.96 (2 x CH$_{arom}$); 141.60 (C$_q$). **IR (cm⁻¹):** ν_{max} 1115 (CH$_2$-O), 696 (phenyl). **MS (70 eV): m/z (%)** 204 ([M+H]⁺, 100). **Chromatography:** PE:EtOAc (9:1) R$_f$ = 0.09. **HRMS (ESI):** calculated for $C_{13}H_{17}N$: 204.1383 [M+H]⁺, experimental: 204.1380 [M+H]⁺. **Yield:** 57% (yellow oil).

N-(2-Phenylcyclopropyl)piperidine 175
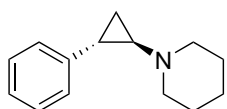
¹H-NMR (300 MHz, CDCl₃): δ 0.88 - 0.94 (1H, m, C$\underline{H}_aH_b$); 1.06 - 1.12 (1H, m, CH$_a\underline{H}_b$); 1.38 - 1.46 (2H, m, NCH$_2$CH$_2$C$\underline{H}_2$); 1.50 - 1.58 (4H, m, 2 x NCH$_2$C$\underline{H}_2$CH$_2$); 1.75 - 1.80 (1H, m, CHN); 1.97 (1H, ddd, J_1=9.2 Hz, J_2=5.6 Hz, J_3=3.3 Hz, CHC$_q$); 2.52 - 2.60 (4H, m, 2 x NCH$_2$); 7.00 - 7.05 (2H, m, 2 x CH$_{arom}$); 7.07 - 7.13 (1H, m, CH$_{arom}$); 7.17 - 7.23 (2H, m, 2 x CH$_{arom}$). **¹³C-NMR (75 MHz, CDCl₃):** δ 16.44 (CH$_a$H$_b$); 24.43 (NCH$_2$CH$_2\underline{C}$H$_2$); 24.52 ($\underline{C}$HC$_q$); 25.83 (2 x NCH$_2$CH$_2$CH$_2$); 49.65 (CHN); 54.31 (2 x NCH$_2$); 125.37 (CH$_{arom}$); 125.93 (2 x CH$_{arom}$); 128.08 (2 x CH$_{arom}$); 142.24 (C$_q$). **IR (cm⁻¹):** ν_{max} 695 (phenyl). **MS (70 eV): m/z (%)** 202 ([M+H]⁺, 100). **Chromatography:** PE:EtOAc (9:1) R$_f$ = 0.25. **HRMS (ESI):** calculated for $C_{14}H_{19}N$: 202.1590 [M+H]⁺, experimental: 202.1590 [M+H]⁺. **Yield:** 36% (yellow oil).

N-(2-Phenylcyclopropyl)pyrrolidine 176
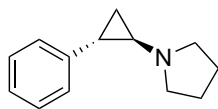
^{1}H-NMR (300 MHz, CDCl$_3$): δ 0.87 - 0.93 (1H, m, C$\underline{H}_a$H$_b$); 1.08 -1.15 (1H, m, CH$_a\underline{H}_b$); 1.70 - 1.76 (4H, m, 2 x NCH$_2$C$\underline{H}_2$); 1.78 - 1.83 (1H, m, CHN); 1.99 (1H, ddd, J$_1$=9.1 Hz, J$_2$=5.8 Hz, J$_3$=3.3 Hz, CHC$_q$); 2.62 - 2.67 (4H, m, 2 x NC$\underline{H}_2$CH$_2$); 6.98 - 7.02 (2H, m, 2 x CH$_{arom}$); 7.05 - 7.10 (1H, m, CH$_{arom}$); 7.14 - 7.21 (2H, m, 2 x CH$_{arom}$). **^{13}C-NMR (75 MHz, CDCl$_3$):** δ 16.06 (CH$_a$H$_b$); 23.31 (2 x NCH$_2\underline{C}$H$_2$); 23.86 ($\underline{C}$HC$_q$); 46.02 (CHN); 53.27 (2 x N$\underline{C}$H$_2$CH$_2$); 125.14 (CH$_{arom}$); 125.72 (2 x CH$_{arom}$); 127.85 (2 x CH$_{arom}$); 141.86 (C$_q$). **IR (cm^{-1}):** ν_{max} 696 (phenyl). **MS (70 eV): m/z (%)** 188 ([M+H]$^+$, 100). **Chromatography:** PE:EtOAc (9:1) R$_f$ = 0.09. **HRMS (ESI):** calculated for C$_{13}$H$_{17}$N: 188.1434 [M+H]$^+$, experimental: 188.1435 [M+H]$^+$. **Yield:** 47% (brown oil).

N,N-Dibenzyl-2-phenylcyclopropan-1-amine 184
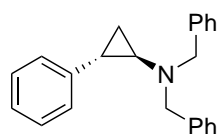
^{1}H-NMR (400 MHz, CDCl$_3$): δ 0.92 - 0.97 (1H, m, CHCH$_a$H$_b$); 1.00 - 1.05 (1H, m, CHCH$_a$H$_b$); 1.79 - 1.83 (1H, m, CHC$_q$); 2.02 (1H, ddd, J$_1$=6.9 Hz, J$_2$=4.3 Hz, J$_3$=3.2 Hz, CHN); 3.66 (2H, d, J=13.5 Hz, 2 x NC$\underline{H}_a$H$_b$); 3.77 (2H, d, J=13.5 Hz, 2 x NCH$_a\underline{H}_b$); 6.76 - 6.79 (2H, m, 2 x CH$_{arom}$); 7.08 - 7.12 (1H, m, CH$_{arom}$); 7.15 - 7.20 (2H, m, 2 x CH$_{arom}$); 7.22 - 7.32 (10H, m, 10 x CH$_{arom}$). **^{13}C-NMR (100.6 MHz, CDCl$_3$):** δ 17.56 (CH$\underline{C}$H$_a$H$_b$); 26.39 ($\underline{C}$HC$_q$); 47.58 (CHN); 58.48 (2 x NCH$_a$H$_b$); 125.36 (CH$_{arom}$); 125.76 (3 x CH$_{arom}$); 126.88 (CH$_{arom}$); 127.98 (2 x CH$_{arom}$); 128.09 (4 x CH$_{arom}$); 129.40 (4 x CH$_{arom}$); 138.67 (2 x C$_q$); 142.05 ($\underline{C}_q$CH). **IR (cm^{-1}):** ν_{max} 692 (phenyl). **MS (70 eV): m/z (%)** 314 ([M+H]$^+$, 100). **Melting point:** T$_m$ = 60°C. **Chromatography:** PE:EtOAc (9:1) R$_f$ = 0.5. **HRMS (ESI):** calculated for C$_{23}$H$_{23}$N: 314.1903 [M+H]$^+$, experimental: 314.1935 [M+H]$^+$. **Yield:** 65% (pale white powder).

N-(2-Phenylcyclopropyl)-*N*-propyl-*p*-toluenesulfonamide 177
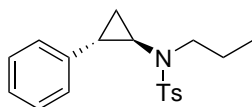
^{1}H-NMR (300 MHz, CDCl$_3$): δ 0.90 (3H, t, J=7.4 Hz, C$\underline{H}_3$CH$_2$); 1.18 - 1.25 (1H, m, CHC$\underline{H}_a$H$_b$); 1.52 (1H, ddd, J$_1$=10.0 Hz, J$_2$=5.9 Hz, J$_3$=4.2 Hz, CHCH$_a\underline{H}_b$); 1.62 (2H, sextet, J=7.4 Hz, CH$_3$C$\underline{H}_2$); 2.07 (1H, ddd, J$_1$=7.7 Hz, J$_2$=4.2 Hz, J$_3$=3.3 Hz, NCH); 2.34 - 2.41 (4H, m, CH$_3$C$_q$ + CHC$_q$); 3.10 (1H, dt, J$_1$=14.3 Hz, J$_2$=7.4 Hz, NC$\underline{H}_a$H$_b$); 3.21 (1H, dt, J$_1$=14.3 Hz, J$_2$=7.4 Hz, NCH$_a\underline{H}_b$); 7.03 - 7.07 (2H, m, 2 x CH$_{arom}$); 7.17 - 7.30 (5H, m, 5 x CH$_{arom}$); 7.63 (2H, d, J = 8.3 Hz, 2 x CH$_{arom}$). **^{13}C-NMR (75 MHz, CDCl$_3$):** δ 11.44 ($\underline{C}$H$_3$CH$_2$); 16.08 (NCH$\underline{C}$H$_a$H$_b$); 21.50 ($\underline{C}$H$_3$C$_q$); 21.73 (CH$_3\underline{C}$H$_2$); 25.10 ($\underline{C}$HC$_q$); 40.20 (NCH); 52.89 (NCH$_a$H$_b$); 126.08 (2 x CH$_{arom}$); 126.25 (CH$_{arom}$); 127.66 (2 x CH$_{arom}$); 128.42 (2 x CH$_{arom}$); 129.50 (2 x CH$_{arom}$); 135.28 (C$_q$S);

140.04 (CH$\underline{C}_q$); 143.31 (CH$_3\underline{C}_q$). **IR (cm^{-1}):** ν_{max} 1343 (SO$_2$), 1161 (SO$_2$). **MS (70 eV): m/z (%)** 330 ([M+H]$^+$, 100). **Melting point:** T$_m$ = 63°C. **Chromatography:** PE:EtOAc (9:1) R$_f$ = 0.37. **HRMS (ESI):** calculated for C$_{19}$H$_{23}$NO$_2$S: 330.1522 [M+H]$^+$, experimental: 330.1528 [M+H]$^+$. **Yield:** 70% (yellow crystals).

N-Benzyl-*N*-(2-phenylcyclopropyl)-*p*-toluenesulfonamide 178
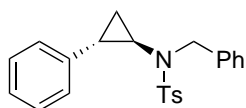
^{1}H-NMR (400 MHz, CDCl$_3$): δ 1.05 - 1.10 (1H, m, CHC$\underline{H}_a$H$_b$); 1.33 (1H, ddd, J$_1$=9.9 Hz, J$_2$=5.9 Hz, J$_3$=4.2 Hz, CHCH$_a\underline{H}_b$); 2.03 - 2.11 (2H, m, CHC$\underline{H}$N); 2.41 (3H, s, CH$_3$); 4.19 (1H, d, J=14.5 Hz, NC$\underline{H}_a$H$_b$); 4.45 (1H, d, J=14.5 Hz, NCH$_a\underline{H}_b$); 6.80 - 6.83 (2H, m, 2 x CH$_{arom}$); 7.12 - 7.33 (10H, m, 10 x CH$_{arom}$); 7.64 - 7.67 (2H, m, 2 x CH$_{arom}$). **^{13}C-NMR (100.6 MHz, CDCl$_3$):** δ 16.03 (CH$\underline{C}$H$_a$H$_b$); 22.71 (CH$_3$); 24.64 ($\underline{C}$HCHN or CHN); 40.87 ($\underline{C}$HCHN or CHN); 54.89 (N$\underline{C}$H$_a$H$_b$); 126.03 (2 x CH$_{arom}$); 126.13 (CH$_{arom}$); 127.69 (CH$_{arom}$); 127.73 (2 x CH$_{arom}$); 128.22 (2 x CH$_{arom}$); 128.46 (2 x CH$_{arom}$); 128.73 (2 x CH$_{arom}$); 129.61 (2 x CH$_{arom}$); 134.98 ($\underline{C}_q$S); 136.96 (CH$_a$H$_b\underline{C}_q$); 139.91 ($\underline{C}_q$CH); 143.54 ($\underline{C}_q$CH$_3$). **IR (cm^{-1}):** ν_{max} 1343 (SO$_2$), 1164 (SO$_2$). **MS (70 eV): m/z (%)** 378 ([M+H]$^+$, 100). **Melting point:** T$_m$ = 108°C. **Chromatography:** PE:EtOAc (9:1) R$_f$ = 0.21. **HRMS (ESI):** calculated for C$_{23}$H$_{23}$NO$_2$S: 378.1522 [M+H]$^+$, experimental: 378.1530 [M+H]$^+$. **Yield:** 80% (white powder).

N-Phenyl-*N*-(2-(1-phenylethyl)cyclopropyl)-*p*-toluenesulfonamide 180
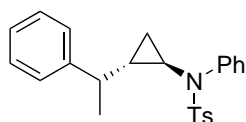
^{1}H-NMR (300 MHz, CDCl$_3$): δ 0.58 - 0.65 (1H, m, C$\underline{H}_a$H$_b$); 0.85 - 0.91 (1H, m, CH$_a\underline{H}_b$); 1.26 (3H, d, J=7.4 Hz, CHC$\underline{H}_3$); 1.41 - 1.49 (1H, m, CHC$\underline{H}$CHN); 2.16 (1H, ~quintet, J=7.4 Hz, C$\underline{H}$CH$_3$); 2.38 - 2.45 (4H, m, CH$_3$C$_q$ + CHN); 7.03 - 7.30 (12H, m, 12 x CH$_{arom}$); 7.51 (2H, d, J=8.3 Hz, 2 x CH$_{arom}$). **^{13}C-NMR (75 MHz, CDCl$_3$):** δ 15.02 (CH$_a$H$_b$); 21.71 ($\underline{C}$H$_3$C$_q$ + CH$\underline{C}$H$_3$); 29.64 (CH$\underline{C}$HCHN); 38.52 (CHN); 42.56 ($\underline{C}$HCH$_3$); 126.32 (CH$_{arom}$); 127.21 (2 x CH$_{arom}$); 127.42 (CH$_{arom}$); 127.91 (2 x CH$_{arom}$); 128.26 (2 x CH$_{arom}$); 128.43 (2 x CH$_{arom}$); 128.72 (2 x CH$_{arom}$); 129.42 (2 x CH$_{arom}$); 134.40 (C$_q$); 141.58 (C$_q$); 143.71 ($\underline{C}_q$CH$_3$); 145.51 (CH$\underline{C}_q$). **IR (cm^{-1}):** ν_{max} 1348 (SO$_2$), 1164 (SO$_2$). **MS (70 eV): m/z (%)** 392 ([M+H]$^+$, 100). **Melting point:** T$_m$ = 127°C. **Chromatography:** PE:EtOAc (9:1) R$_f$ = 0.34. **HRMS (ESI):** calculated for C$_{24}$H$_{25}$NO$_2$S: 392.1679 [M+H]$^+$, experimental: 392.1686 [M+H]$^+$. **Yield:** 39% (orange powder).

4.4.2 Continuous flow procedures

4.4.2.1 Synthesis of Shi's carbenoid in batch, cyclopropanation in flow

Equipment

The tube reactor was built up from PFA-tubing (internal diameter: 0.020", outer diameter: 1/16") having a total internal volume of about 3 ml. Syringe pumps (Chemyx syringe pump, type Fusion Classic or Fusion Touch) were used to pump the reagent solutions through the reactor. Connection of the PFA-tubing to the glass syringes was performed with an ETFE Luer Lock. Check valves (PEEK) were used to prevent back flow of the solutions and both reagent solutions were mixed in a Y-connector (PEEK). To avoid contact of the solution of $CF_3CO_2ZnCH_2I$ with air, the solution was brought directly from the flask into the syringe through a septum and subsequently to the tube reactor by means of two valves. The reactor was heated to the desired reaction temperature using a water or oil bath.

Experimental procedure

As generic example, the Simmons-Smith cyclopropanation of *N*-styrylmorpholine **158** in flow will be described. For these flow experiments, about 10 ml of each reagent solution was prepared.

- Reagent A: 0.068 M *N*-styrylmorpholine **158** in dry CH_2Cl_2

  0.13 g *N*-styrylmorpholine (0.68 mmol) was dissolved in 10 ml dry CH_2Cl_2.

- Reagent B: 0.2 M $CF_3CO_2ZnCH_2I$ in dry CH_2Cl_2

  2 ml Et_2Zn (1 M in hexanes, 2 mmol) was dissolved in 7.5 ml dry CH_2Cl_2. The reaction mixture was cooled to -78°C and 0.32 ml CH_2I_2 (4 mmol) was added dropwise. The reaction mixture was allowed to warm to 0°C and kept at this temperature for 15 min. A white suspension was formed. Subsequently, 0.15 ml TFA (2 mmol) was added and the reaction mixture was stirred for 15 min at 0°C. A clear, colourless solution was formed.

Before each flow experiment, the tube reactor was rinsed with dry CH_2Cl_2. Both syringes were filled with the reagent solutions and the flow rates were calculated based on the internal volume of the reactor, the desired residence time and stoichiometric ratio of both reagents. Following equations were used:

$$RT \quad = \quad \frac{IV}{F_1 + F_2} \tag{4.4}$$

$$ratio \quad = \quad \frac{C_2 \cdot F_2}{C_1 \cdot F_1} \tag{4.5}$$

with

- RT = residence time (min)
- IV = internal volume (ml)
- F = flow rate (ml/min)
- ratio = stoichiometric ratio
- C = concentration (mmol/ml)

Steady state was assumed after three times the residence time. After reaching steady state, a sample was collected, diluted with CH_2Cl_2 and washed with sat. K_2CO_3. The aqueous phase was extracted with CH_2Cl_2, the combined organic phases were dried ($MgSO_4$) and the solvent was removed under reduced pressure. Subsequently the conversion was determined via ^{1}H-NMR.

4.4.2.2   Synthesis of Shi's carbenoid and cyclopropanation in flow

Equipment

For the generation of Shi's carbenoid, a tube reactor built up from PFA-tubing (internal diameter: 0.020", outer diameter: 1/16") or Teflon AF-2400 tubing (internal diameter: 0.6 mm, outer diameter: 0.8 mm) was used (Figure 4.13). If necessary, the reactor was cooled to 0°C in an ice batch. A Syrris® Reagent Pump was used to mix both reagent solutions in an ETFE T-mixer. The generated solution of $CF_3CO_2ZnCH_2I$ was subsequently mixed with a solution of the enamine in a PEEK Y-connector and transported to the Uniqsis® static mixer in a setup as described earlier (Figure 4.10). An Uniqsis® Binary Pump Module was used to pump the enamine solution. After the static mixer, the reaction mixture was passed through a residence time unit. A BPR of 75 psi (5.2 bar) was used at the end of the reactor and the reaction mixture was collected in sat. K_2CO_3.
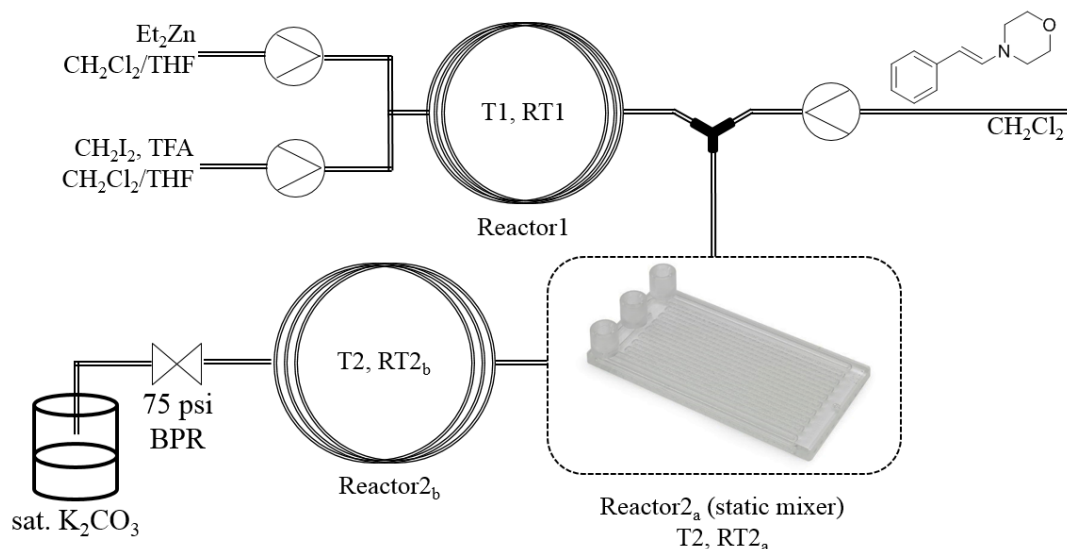
Figure 4.13. Reactor setup

Experimental procedure

The following solutions were prepared in batch:

- Et$_2$Zn in dry CH$_2$Cl$_2$:THF
- CH$_2$I$_2$ and CF$_3$CO$_2$H in dry CH$_2$Cl$_2$:THF
- *N*-styrylmorpholine **158** in dry CH$_2$Cl$_2$

Before starting the flow experiment, the reactor was rinsed with dry MeOH and dry CH$_2$Cl$_2$. Subsequently, the reagent solutions were pumped through the reactor with flow rates corresponding to the desired residence time and stoichiometric ratio. After reaching steady state, a sample was collected in sat. K$_2$CO$_3$ and diluted with CH$_2$Cl$_2$. The aqueous phase was extracted with CH$_2$Cl$_2$, the combined organic phases were dried (MgSO$_4$) and the solvent was removed under reduced pressure. Subsequently the conversion was determined via ^{1}H-NMR.

4.5   Aziridination of bisphosphonoazadienes

4.5.1   Batch procedures

4.5.1.1   Synthesis of tetraethyl *N,N*-dibenzylaminomethylbisphosphonate

Tetraethyl *N,N*-dibenzylaminomethylbisphosphonate was synthesized according to a procedure published by Wechter *et al.*[294] A flask was charged with 11.8 g dibenzylamine (60 mmol, 1 equiv.), 10.6 g triethyl orthoformate (72 mmol, 1.2 equiv.) and 25.6 g diethyl phosphite (186 mmol, 3.1 equiv.). The mixture was place under a N_2-atmosphere and heated at reflux temperature for 5 h. Subsequently, the reaction mixture was cooled to room temperature and the formed EtOH was removed under reduced pressure. The residue was heated to 160°C and stirred at this temperature overnight. The reaction mixture was cooled down to room temperature and $CHCl_3$ was added. The organic phase was washed twice with 2 M NaOH and twice with brine. The organic phase was dried with $MgSO_4$ and the solvent was removed *in vacuo*. The crude reaction product was purified by column chromatography (automated column chromatography, Table 4.3). Tetraethyl *N,N*-dibenzylaminomethylbisphosphonate was obtained as a yellow oil (7.75 g, 16 mmol, 27%). Spectral data corresponded with literature.[294]

Table 4.3: Automated column chromatography

Min	Solvent	Ratio
0.0	PE:EtOAc	85:15
5.0	PE:EtOAc	85:15
20.0	PE:EtOAc	0:100
20.0	EtOAc:MeOH	100:0
25.0	EtOAc:MeOH	100:0
40.0	EtOAc:MeOH	97:3

4.5.1.2   Synthesis of tetraethyl aminomethylbisphosphonate

Tetraethyl aminomethylbisphosphonate **192** was synthesized according to a procedure published by Wechter *et al.*[294] Tetraethyl *N,N*-dibenzylaminomethylbisphosphonate (6 g, 12.4 mmol) was dissolved in MeOH and Pd/C (10%, 1 g) was added. The reaction mixture was stirred overnight at room temperature under a H_2-atmosphere (5.0 - 5.5 bar). After filtration of the solids and removal of the solvent under reduced pressure, tetraethyl aminomethylbisphosphonate **192** was obtained as a colourless oil (3.6 g, 12 mmol, 95%). Spectral data corresponded with literature.[294]

4.5.1.3 Synthesis of 2-chloro-2-phenylpropanal

2-Chloro-2-phenylpropanal was synthesized according to a procedure reported by Stevens *et al.*[295] A flask equipped with an air cooler was charged with 6.7 g 2-phenylpropanal (50 mmol, 1 equiv.) and cooled to 0°C. Subsequently, 4.3 ml SO_2Cl_2 (52.5 mmol, 1.05 equiv.) was added dropwise and the reaction mixture was allowed to warm to room temperature. After 1 h, the reaction mixture was poured in H_2O and the aqueous phase was extracted twice with CH_2Cl_2. The combined organic layers were washed with sat. $NaHCO_3$ and dried with $MgSO_4$. After removal of the solvent under reduced pressure, the crude reaction product was purified via vacuum distillation. 2-Chloro-2-phenylpropanal was obtained as a colourless oil (4.9 g, 29 mmol, 58%).

4.5.1.4 Synthesis of 1,1-bisphosphono-2-aza-1,3-dienes

1,1-Bisphosphono-2-aza-1,3-diene **12d** was synthesized according to a procedure published by Stevens *et al.*[295] Tetraethyl aminomethylbisphosphonate (1.3 g, 4.28 mmol, 1 equiv.) and 2-chloro-2-phenylpropanal (0.7 g, 4.28 mmol, 1 equiv.) were dissolved in dry CH_2Cl_2 and 0.26 g $MgSO_4$ (2.14 mmol, 0.5 equiv.) was added. The reaction mixture was protected from moisture with a $CaCl_2$-tube and was stirred for 4.5 h at room temperature. Subsequently, Et_3N (0.66 ml, 4.71 mmol, 1.1 equiv.) was added an the reaction mixture was stirred for 30 min. The solvent was removed under reduced pressure and the residue was dissolved in dry Et_2O. After filtration of the formed solids, the solvent was removed *in vacuo*. If necessary, this procedure was repeated. The crude product was purified by column chromatography (EtOAc). Spectral data of diethyl (diethoxyphosphoryl)-(2-phenylprop-1-en-1-ylimino)methylphosphonate **201** (1.29 g, 3.1 mmol, 72%) corresponded to literature.[295]

4.5.1.5 Synthesis of CH_2N_2

Caution! Diazomethane is a toxic and explosive compound! The synthesis must be carried out in a properly working hood in special glassware! Dedicated glassware was charged with diazald (5.0 g, 23.3 mmol, 1 equiv.) and dry Et_2O. KOH (1.3 g, 23.3 mmol, 1 equiv.) was dissolved in absolute EtOH and added dropwise to the cooled (0°C) solution of diazald. After complete addition, the reaction mixture was heated to reflux temperature. A solution of CH_2N_2 in Et_2O was distilled off and collected in a flask cooled to 0°C.

4.5.1.6 Synthesis of *N*-vinyl-2,2-bisphosphonoaziridines

1,1-Bisphosphono-2-aza-1,3-diene **12d** was dissolved in dry Et_2O and the required amount of freshly prepared CH_2N_2-solution was added. The reaction mixture was stirred at room temperature and the conversion was determined with ^{31}P-NMR. If needed, an ordinary light bulb (45W) was used to illuminate the reaction mixture.

4.5.2 Flow procedures

Equipment

Flow experiments were performed in a Labtrix® Start microreactor. A detailed description of this microreactor is given in section 4.2 of the experimental part.

Experimental procedure

The microreactor chip was rinsed with dry Et_2O and heated to the desired reaction temperature. If needed, the chip was illuminated with an ordinary light bulb (45W). A freshly prepared CH_2N_2-solution was diluted to the required concentration and a solution of 1,1-bisphosphono-2-aza-1,3-diene **12d** in dry Et_2O was prepared. Both solutions were pumped through the microreactor with a flow rate corresponding to the desired residence time and stoichiometric ratio. After reaching steady state, a sample was collected and the conversion was determined via ^{31}P-NMR.

4.6   Continuous flow Bt-activation of amino acids

4.6.1   Batch procedures

4.6.1.1   Cbz-protection of amino acids

The Cbz-protection of amino acids was published by Abell *et al.*[321] In a typical experiment, 3 g glycine (40 mmol, 1 equiv.) was dissolved in H_2O:acetone (9:1). Subsequently, 11.1 g K_2CO_3 (80 mmol, 2 equiv.) and 3.4 g $NaHCO_3$ (40 mmol, 1 equiv.) were added. The reaction mixture was cooled to 0°C and 7.1 ml CbzCl (50 mmol, 1.25 equiv.) was added dropwise. The reaction mixture was heated to 30°C and stirred at this temperature for 3 h. Subsequently, Et_2O was added and the aqueous phase was separated. 2 M HCl was added to the aqueous phase (pH=2) and the aqueous phase was extracted twice with EtOAc. The combined organic layers were washed with H_2O and dried with $MgSO_4$. After removal of the solvent under reduced pressure, 6.9 g Cbz-Gly was obtained (33 mmol, 83%). The Cbz-protected amino acids are well known compounds and most of them are also commercially available.

4.6.1.2   Synthesis of 1-(methanesulfonyl)benzotriazole (BtMs)

The synthesis of BtMs was published by Katritzky *et al.*[322] A flask of 250 ml was charged with 10 g BtH (84 mmol, 1 equiv.), 10.3 ml pyridine (134.4 mmol, 1.6 equiv.) and 100 ml dry toluene. The reaction mixture was place under a N_2-atmosphere and cooled to 0°C. Subsequently, a solution of 7.8 ml MsCl (117.6 mmol, 1.4 equiv.) in dry toluene was added. The reaction mixture was allowed to warm to room temperature and stirred at this temperature overnight. The solvent was removed *in vacuo* and the residue was dissolved in EtOAc. The organic phase was washed twice with H_2O and once with brine and subsequently dried with $MgSO_4$. After removal of the solvent under reduced pressure, the crude reaction product was recrystallized from MeOH. 1-(Methanesulfonyl)benzotriazole **25** was obtained as colourless crystals (11.3 g, 57 mmol, 68%). Spectral data corresponded with literature.[336]

4.6.1.3   Activation of Cbz-Gly with BtMs

The activation of amino acids with BtMs was based on a procedure published by Katritzky *et al.*[323] A flask of 25 ml was charged with 0.5 g BtMs (2.5 mmol, 1 equiv.), 0.5 ml Et_3N (3.5 mmol, 1.4 equiv.) and 10 ml dry THF. The reaction mixture was placed under a N_2-atmosphere and 0.5 g Cbz-Gly (2.5 mmol, 1 equiv.) was added. Subsequently, the reaction mixture was heated to reflux temperature. After 3 h, the solvent was removed under reduced pressure and the residue was dissolved in 20 ml $CHCl_3$. The organic phase was washed twice

with H_2O and dried ($MgSO_4$). After removal of the solvent *in vacuo*, the crude reaction product was recrystallized from MeOH. Cbz-Gly-Bt was obtained as a white solid (0.44 g, 1.4 mmol, 57%). Spectral data corresponded with literature.[337]

4.6.1.4 Activation of Cbz-Gly with BtH - SOCl₂

The Bt-activation of amino acids with BtH - SOCl₂ was performed according to procedures published by Katritzky *et al.*[302] A flask of 25 ml was charged with 0.5 g BtH (9.87 mmol, 4 equiv.) and 15 ml dry THF. The reaction mixture was placed under a N_2-atmosphere and cooled to 0°C. Subsequently, 0.12 ml SOCl₂ (2.5 mmol, 1.05 equiv.) was added. After 1 h, 0.5 g Cbz-Gly (2.39 mmol, 1 equiv.) was added and the reaction mixture was stirred for 1.5 h at 0°C and for 1 h at reflux temperature. The solvent was removed under reduced pressure and the residue was dissolved in CH_2Cl_2. The organic phase was washed twice with 4 M HCl and once with H_2O and brine. The organic phase was dried ($MgSO_4$) and the solvent was removed *in vacuo*. After recrystallization from hexane:CH_2Cl_2 (1:1), 0.51 g Cbz-Gly-Bt (1.6 mmol, 69%) was obtained. Spectral data corresponded with literature.[337]

4.6.1.5 Coupling of Cbz-L-Trp-Bt and L-Pro-OMe.HCl

Cbz-L-Trp-Bt (300 mg, 0.68 mmol, 1 equiv.) was dissolved in 7 ml dry MeCN:NMP (6:1) and a solution of 119 mg L-Pro-OMe.HCl (0.71 mmol, 1.05 equiv.) and 0.11 ml Et₃N (0.82 mmol, 1.2 equiv.) in dry MeCN:NMP (6:1) was added. The reaction mixture was stirred overnight at room temperature and subsequently diluted with EtOAc. The organic phase was washed with 4 M HCl and brine and dried with $MgSO_4$. After removal of the solvent under reduced pressure, 290 mg Cbz-L-Trp-L-Pro-OMe was obtained (0.64 mmol, 92%). Spectral data corresponded to literature.[338]

4.6.2 Flow procedures

4.6.2.1 Activation of amino acids with BtMs

Equipment

Experiments were performed with a Labtrix® Start microreactor. A detailed description of this microreactor is given in section 4.2 of the experimental part.

Experimental procedure

Two solutions were prepared in advance:

- 0.125 M Cbz-L-Trp and 0.175 M Et$_3$N in MeCN
- 0.156 M BtMs in MeCN

The reactor chip was heated to 90°C and both solutions were pumped through the microreactor with a flow rate of 0.33 μl/min corresponding with a residence time of 15 min and an excess of BtMs (1.25 equiv.). After reaching steady state, a sample was collected an analysed via LC-MS.

4.6.2.2 Activation of amino acids with BtH - SOCl$_2$

Equipment

The activation of amino acids with BtH - SOCl$_2$ was performed with a tube reactor in view of the corrosiveness of the reagents (Figure 4.14).
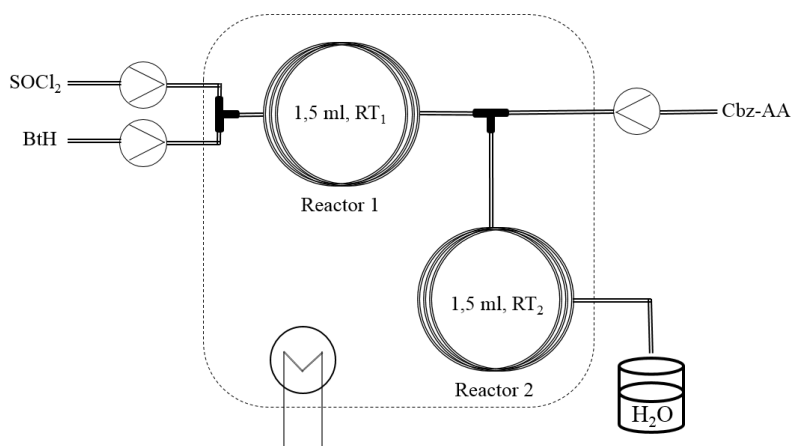
Figure 4.14. Tube reactor

Both tube reactors were built up from PFA-tubing (internal diameter: 0.020", outer diameter: 1/16") having an internal volume of 1.5 ml each. The reagent solutions were pumped through the tube reactor with a Syrris® Reagent Pump (SOCl$_2$ and BtH) and a Uniqsis® Binary Pump Module (Cbz-AA). The mixing of the reagents occurred in a ETFE T-connector. The reactor was cooled to the desired reaction temperature using an ice bath and the reactor output was collected in excess H$_2$O.

Experimental procedure

The reactor was rinsed with dry MeCN:NMP (6:1) and the following solutions were prepared in advance:

- Reagent A: 0.45 M $SOCl_2$ in dry MeCN:NMP (6:1)
- Reagent B: 1.2 M BtH **22** in dry MeCN:NMP (6:1)
- Reagent C: 0.15 M Cbz-AA in dry MeCN:NMP (6:1)

The tube reactor was cooled to 0°C and reagent A was also cooled to prevent degradation of $SOCl_2$. Reagents A and B were pumped through the tube reactor with a flow rate of 0.375 ml/min each, corresponding to a residence time of 2 min in the first tube reactor. The output of the first reactor was mixed with reagent C (0.75 ml/min). Hence a residence time of 1 min and a stoichiometric ratio Cbz-AA:BtH:$SOCl_2$ 1:4:1.5 were obtained in the second tube reactor. After reaching steady state, a sample was collected in excess H_2O over a period of 30 min. A pale white precipitate (Cbz-AA-Bt) was formed which was filtered and subsequently washed with H_2O to remove traces of NMP. Spectral data of the synthesized Cbz-AA-Bt corresponded with literature.[325,337]

4.6.2.3 Coupling of Cbz-D,L-Phe-Bt and 2-aminopyridine

Equipment

Experiments were performed with a KiloFlow® reactor. A detailed description of this reactor is given in section 4.2 of the experimental part. However, a Uniqsis® Binary Pump Module was used to pump the reagent solutions.

Experimental procedure

The reactor was rinsed with dry MeCN:NMP (6:1) and the following solutions were prepared in advance:

- Reagent A: 0.075 M Cbz-D,L-Phe-Bt **18c** in dry MeCN:NMP (6:1)
- Reagent B: 0.09 M 2-aminopyridine **202** in dry MeCN:NMP (6:1)

In order to dissolve all Cbz-D,L-Phe-Bt, the solution was heated to 50°C. The reactor was heated to 130°C and both reagent solutions were pumped through the reactor at a flow rate of 0.11 ml/min each. Hence, a residence time of 29.5 min and a stoichiometric ratio **18c:202** 1:1.2 was obtained. After reaching steady state, a sample was collected and analysed via LC-MS.

4.6.2.4 Coupling of Cbz-L-Trp-Bt and L-Pro-OMe.HCl

Equipment

Optimization was performed in a Labtrix® Start microreactor and the developed procedure was subsequently scaled-up to the KiloFlow® reactor. A detailed description of both reactors is given in section 4.2 of the experimental part. A Uniqsis® Binary Pump Module was used to pump the reagent solutions through the KiloFlow® reactor.

Experimental procedure

The reactor was rinsed with dry MeCN:NMP (6:1) and heated to 130°C and the following solutions were prepared in advance:

- Reagent A: 0.10 M Cbz-L-Trp-Bt in dry MeCN:NMP (6:1)
- Reagent B: 0.105 M L-Pro-OMe.HCl and 0.12 M Et$_3$N in dry MeCN:NMP (6:1)

Both reagent solutions were pumped through the KiloFlow® reactor with a flow rate of 0.11 ml/min each corresponding to a residence time of 29.5 min and a stoichiometric ratio Cbz-L-Trp-Bt:L-Pro-OMe.HCl:Et$_3$N of 1:1.05:1.2. After reaching steady state, a sample was collected over a period of 60 min. The reaction mixture was subsequently washed with 4 M HCl, H$_2$O and brine. The organic phase was dried with MgSO$_4$ and the solvent was removed under reduced pressure. Cbz-Trp-Pro-OMe was obtained as two diastereoisomers in a ratio ~6:1 (264 mg, 0.59 mmol, 89%). Spectral data corresponded to literature.[338]

Chapter 5

Summary and perspectives

Microreactor technology provides a number of specific advantages compared to traditional batch technology, including a better mass and heat transfer, a safer manipulation of toxic and reactive reagents and a straightforward scale-up. Several literature examples illustrate these beneficial characteristics. It is estimated that about 44% of today's chemical reactions can benefit from microreactor technology. In this PhD thesis, a number of generic reactions were fundamentally studied, with a focus on industrially relevant reactions, in order to be able to perform these under microreactor conditions.

As a first example, the catalyst-free, continuous flow condensation of acid chlorides **i** and alcohols **ii** was evaluated (Scheme 5.1).
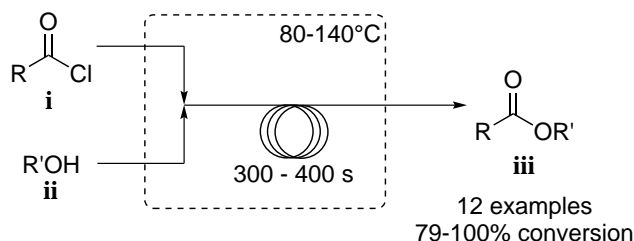
Scheme 5.1. Condensation of acid chlorides **i** and alcohols **ii**

Initial optimization experiments were performed in a Labtrix® Start microreactor with benzoyl chloride and MeOH. Performing the condensation reaction in Et_2O resulted in limited conversions whereas excellent conversions were obtained under solventless conditions. Subsequently, the reaction scope was broadened to other low boiling alcohols (EtOH and *i*PrOH). In all cases, complete conversion was obtained with a residence time of 300 s, a slight excess of the alcohol (1.3 equiv.) and a reaction temperature above the atmospheric boiling point of the alcohol. Using the optimized conditions, other liquid acid chlorides were reacted with the low boiling alcohols with excellent conversions (>91%).

In a second step, the substrate scope was broadened to solid acid chlorides and alcohols. Different solvents (CH_2Cl_2, dioxane and CH_3CN) were evaluated of which CH_3CN appeared to

be the superior solvent. However, the condensation between a solid acid chloride in solution and a neat alcohol failed in every case. On the other hand, condensation of a neat acid chloride with a solid alcohol in solution resulted in excellent conversions (>98%) if the reaction temperature, residence time and excess of alcohol were increased in comparison with the previously optimized reaction conditions. If both the solid acid chloride and solid alcohol were dissolved in CH_3CN, good conversions were obtained (79%).

In a final part of this study, the developed procedure was scaled-up to the KiloFlow® reactor without further optimization. Stable and high isolated yields (>98%) were obtained during the course of the operation and a throughput of 2.2 g/min of methyl benzoate was reached. Moreover, the formed HCl could be partly (46%) captured as an aqueous solution.

The developed procedure is the first catalyst-free continuous flow procedure for the synthesis of esters starting from acid chlorides. Compared to the catalyst-free transesterification reaction using novel process windows, more energy efficient reaction conditions are obtained which reduces the operating cost.[189,190] Other reported continuous flow procedures make use of a catalyst to perform the reaction, making the process less sustainable as more waste is generated. In batch, the reaction can be performed catalyst-free and solventless but with a limited throughput.[206] Moreover, no attempts to recycle the HCl, which is liberated during the condensation reaction, have been reported in the literature. On the other hand, the currently optimized reaction conditions are too harsh for reactive substrates and these substrates are most interesting for industry. Probably, lower temperatures and dilute systems can overcome this problem.

In a second part of this PhD research, the tribromination of methyl sulfones and methane-sulfonates with potassium hypobromite was evaluated. In a first series of experiments, a KOBr-solution was prepared in batch and used as such to optimize the bromination of 4-isopropoxyphenyl methyl sulfone **iv** in two different mesoreactors: (1) a tube reactor and (2) an Uniqsis® static mixer chip (Scheme 5.2).
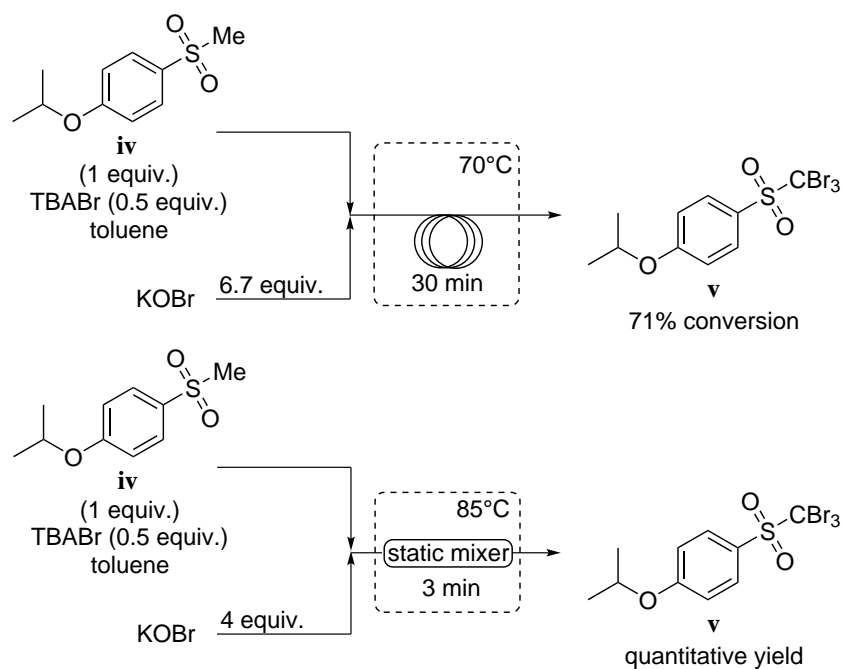
Scheme 5.2. Continuous flow bromination of 4-isopropoxyphenyl methyl sulfone **iv** in a tube reactor and a static mixer chip

The bromination of **iv** in the tube reactor was optimized by varying the reaction temperature, excess KOBr and residence time. Moreover, the influence of the amount of phase transfer catalyst and the type of mixer (T- or Y-connector) was assessed. After optimization, a conversion of 71% was reached. Next to the end product **v**, mainly starting material **iv** and traces of the dibrominated intermediate were detected.

On the other hand, the end product **v** was isolated in quantitative yield after optimization of the bromination reaction in the static mixer setup. In the static mixer chip, an emulsion was formed due to the integrated mixing elements and hence, very efficient contact between the aqueous and organic phase was obtained resulting in full conversion of the starting material. In the tube reactor, a plug flow was observed with a smaller interfacial area compared to the emulsion.

Subsequently, the Uniqsis® static mixer was used to synthesize a small library of tribromomethyl sulfones and the substrate scope was successfully broadened to aryl methanesulfonates. If the developed continuous flow procedure was used for the bromination of aryl methanesulfonamides, bromination of the aromatic system was observed.

Compared to the batch process, a significant decrease of the reaction time was obtained due to the large interfacial area between the aqueous and organic phase resulting in efficient mass transfer. As the reaction was optimized in flow for one compound and subsequently broadened

to other derivatives, sometimes less pure reaction mixtures were obtained in flow compared to the corresponding batch procedure as a higher reaction temperature was used in flow.

In a next part, the synthesis of KOBr in a mesoreactor was evaluated. Attempts to synthesize KOBr in a tube reactor failed due to the large difference in flow rate between both reagent streams. In order to establish a better flow ratio, Br_2 was diluted with a suitable solvent but then, problems in the subsequent bromination reaction were encountered. If a static mixer was used for the generation of KOBr, clogging of the mixer chip was observed due to precipitate formation. At last, a continuous stirred tank reactor was used to synthesize hypobromite under continuous flow conditions. Hence, the formation of hypobromite was successfully coupled with the subsequent bromination reaction in the static mixer (Scheme 5.3). Performing both the synthesis of hypobromite and the subsequent bromination reaction in flow allows the safe handling of bromine and reduces the degradation of the formed hypobromite.
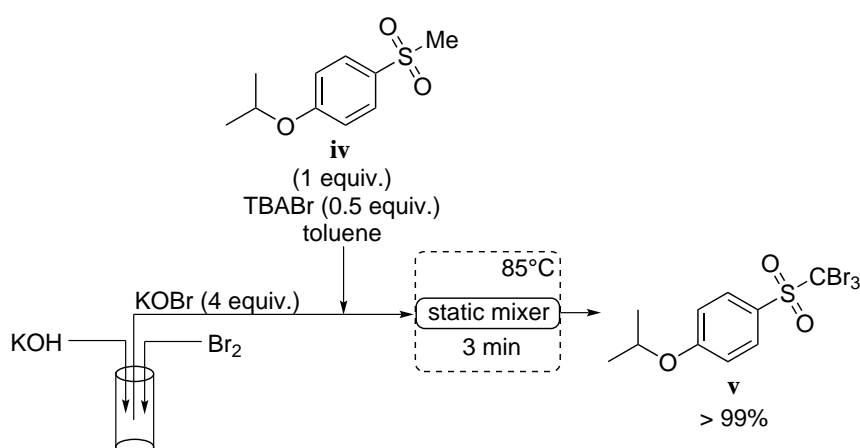
Scheme 5.3. Continuous flow synthesis of hyprobromite and subsequent bromination

A last part of this research topic comprised the deprotection of the isopropyl ether of tribromomethyl 4-isopropoxyphenyl sulfone **v** (Scheme 5.4).
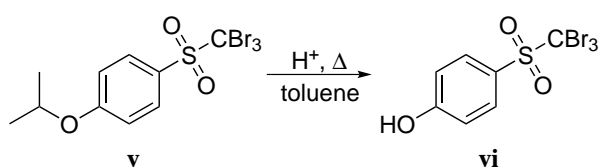
Scheme 5.4. Deprotection of the isopropyl ether group of **v**

Although an efficient batch process was developed using catalytic amounts of CF_3SO_3H, the deprotection was evaluated in a mesoreactor in order to telescope the deprotection step with the

preceding bromination step. The deprotection of ethers with H_3PO_4 is reported in the literature but attempts to use this acid in the mesoreactor failed. On the other hand, use of H_2SO_4 or CH_3SO_3H resulted in good conversions (>81%) if a large excess of the acid was used.

Finally, the continuous flow deprotection was also evaluated with CF_3SO_3H and an excellent conversion (97%) was obtained with stoichiometric amounts of CF_3SO_3H. As the end product **vi** precipitated in toluene, a co-solvent (DMSO) was used in order to avoid clogging of the reactor (Scheme 5.5). However, the original batch process is superior to the developed continuous flow process since catalytic amounts of CF_3SO_3H were used in batch and the end product was easily isolated in high yields.
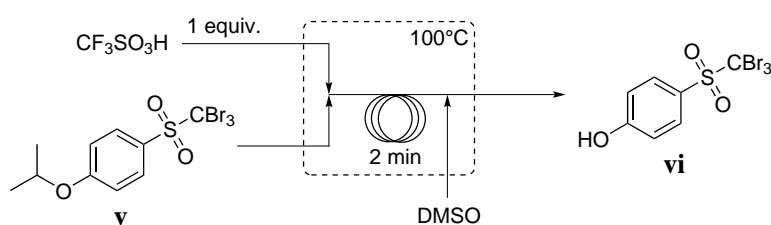
Scheme 5.5. Deprotection of the isopropyl ether group of **v** under continuous flow conditions

In a batch reactor, the formed propene escapes from the reaction mixture and the end product **vi** precipitates. Hence, the equilibrium of the reaction is shifted to the right (Le Chatelier's principle). In flow, homogeneous reaction conditions were obtained and propene stays in solution as no headspace is available in the tubing. Probably, this explains why the reaction does not work in flow with catalytic amounts of CF_3SO_3H whereas in batch, excellent yields were obtained. In order to be able to perform the reaction continuously with catalytic amounts of acid, methods to remove propene from the reaction mixture during the course of the reaction can be evaluated, e.g. gas permeable tubing.

In a third part of this PhD thesis, the Simmons-Smith cyclopropanation of enamines **vii** was evaluated (Scheme 5.6).
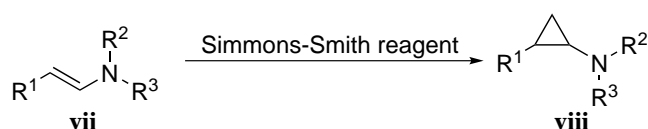
Scheme 5.6. Simmons-Smith cyclopropanation of enamines

The enamines **vii** were synthesized via standard imination procedures and isolated in moderate to good yields (43-90%). Subsequently, different Zn-carbenoids were evaluated in batch and special attention was paid to the solubility of the formed Zn-carbenoids. After screening three different Zn-carbenoids ($Zn(CH_2I)_2$, $Zn(CH_2I)_2$.DME and $CF_3CO_2ZnCH_2I$), $CF_3CO_2ZnCH_2I$ or Shi's carbenoid was selected for the cyclopropanation reaction based on reactivity and solubility. Excellent conversions were obtained in batch with 2 equivalents of $CF_3CO_2ZnCH_2I$ and a reaction time of 2.5 - 5 h. If the enamines were reacted with 3 equivalents of $CF_3CO_2ZnCH_2I$, full conversion was reached within 45 min. Despite the excellent conversions, isolated yields were rather low. Several work up and purification strategies were evaluated, however all of them either failed or resulted in moderate isolated yields.

Subsequently, the cyclopropanation of enamines with an EWG on nitrogen was evaluated in batch. These enamines were less reactive and required a higher excess of the Zn-carbenoid (3 equiv.) and longer reaction times (6 h) in order to reach full conversion. Several tosylated cyclopropylamines were synthesized in moderate to good isolated yields (40-80%).

In a first series of flow experiments, a solution of $CF_3CO_2ZnCH_2I$ was synthesized in batch and used as such for the cyclopropanation reaction in a mesoreactor. Using a residence time of 5 min and 3 equivalents of $CF_3CO_2ZnCH_2I$, excellent to quantitative conversions of the enamines were reached at a reaction temperature of 35°C.

In a subsequent step, the formation of Shi's carbenoid in flow was evaluated. In order to avoid the formation of an intermediate suspension in the synthesis of $CF_3CO_2ZnCH_2I$, the original experimental batch procedure was successfully adapted. Initial attempts to translate the adapted batch procedure to a continuous flow process failed due to clogging of the tube reactor. If a solvent that complexes the generated Zn-carbenoid (THF) was used instead of CH_2Cl_2, no clogging of the tube reactor was observed but either a complex reaction mixture or no conversion was observed.

Finally, a mixture of THF and CH_2Cl_2 was considered in order to find the right balance between reactivity and solubility of the formed Zn-carbenoid. Batch experiments revealed that the more THF was used, the slower the reaction proceeded and the lower the final conversion was. On the other hand, THF was required in order to prevent clogging of the tube reactor. After optimization, both the synthesis of $CF_3CO_2ZnCH_2I$ and the subsequent cyclopropanation reaction were run under continuous flow conditions at a reaction temperature of 35°C with as less as 1.5 equivalents of Shi's carbenoid (Scheme 5.7). Complete conversion

of the starting material was obtained but as with the batch experiments, isolation of the formed cyclopropylamines remained the bottleneck.
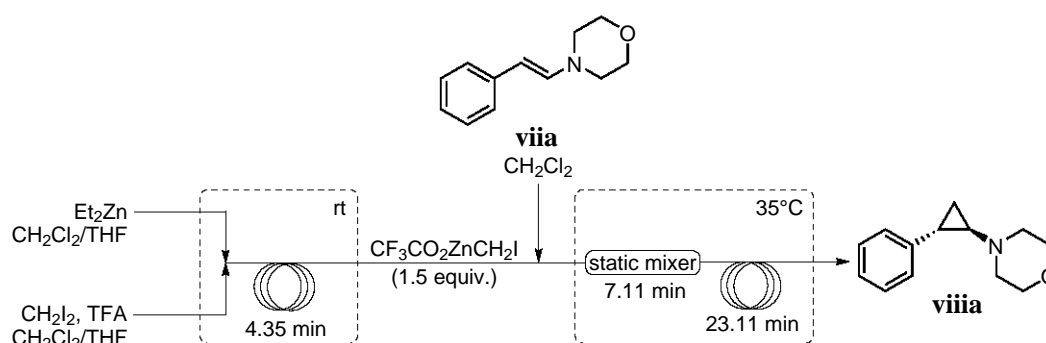
Scheme 5.7. Continuous flow Simmons-Smith cyclopropanation of enamines

Performing the Simmons-Smith reaction in flow has a distinct advantage concerning the safety of the reaction as accidents related to Simmons-Smith cyclopropanations in batch are reported in the literature.[48,49] The excellent heat transfer combined with the small internal volume of the flow reactor allows safer handling of the Simmons-Smith reagent. In batch, the generation of the carbenoid is typically performed at -78°C whereas in flow, the reaction could be performed at room temperature. Hence, significant less energy is required to cool the reaction mixture.

Compared to other methods to synthesize cyclopropylamines, cyclopropanation of enamines forms a straightforward and versatile method to these cyclopropyl derivatives. Enamines can be easily obtained from aldehydes or ketones and secondary amines. The use of dibenzylamine allows efficient generation of the free amino moiety on the cyclopropyl ring after hydrogenolysis. Moreover, the Simmons-Smith reaction is stereospecific and can be performed enantioselective if chiral auxiliaries are used.

One of the major issues related to the cyclopropanation of enamines, was the isolation of the synthesized cyclopropylamines. As the isolation of the cyclopropylamines is difficult, further research has to be performed in order to increase the isolated yields. Purification strategies avoiding the use of water are probably most succesful as a large amount of product is lost during aqueous work up. In order to be industrial relevant, inline purification can be developed.

In a penultimate research topic, the synthesis of *N*-vinyl-2,2-bisphosphonoaziridines **x** starting from the corresponding 1,1-bisphosphono-2-aza-1,3-dienes **ix** was evaluated. Preliminary research at our department revealed the formation of side products if the reaction was performed in batch.

In initial continuous flow experiments with 10 equivalents of diazomethane, only trace amounts of the aziridine were detected. However, if the excess diazomethane was increased to 35 equivalents, combined with illumination of the reactor chip, a selective conversion of 71% was obtained (Scheme 5.8). The developed continuous flow process showed the safe manipulation of diazomethane at higher temperatures (60°C).
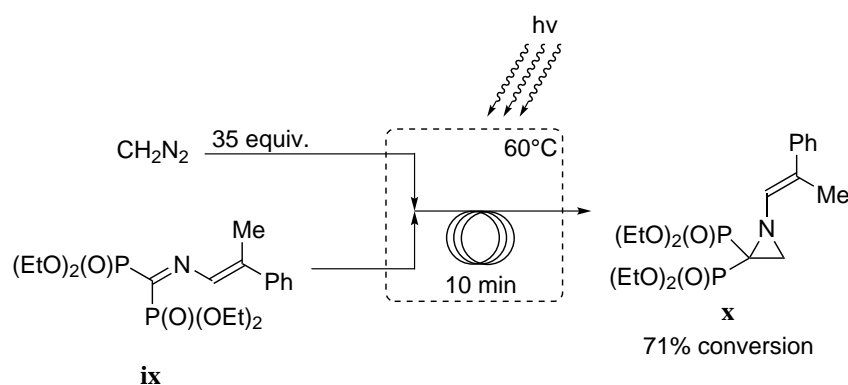
Scheme 5.8. Aziridination of 1,1-bisphosphono-2-aza-1,3-diene **ix**

In further research, the continuous flow process can be elaborated in order to obtain full and selective conversion to the aziridine. Longer residence times, as well as lower reaction temperatures, can be evaluated. At the high reaction temperatures used in this research, substantial diazomethane degradation can occur, explaining the large excess necessary in order to obtain reasonable conversions. Another pathway which can be elaborated is the photodecomposition of the intermediate 1,2,3-triazoline. In this setup, an ordinary light bulb was used to illuminate the reactor chip. However, other light sources can be evaluated in order to increase the efficiency of the photodecomposition.

A last synthesis strategy that can be pursued is the photolysis of diazomethane.[339,340] Photolysis of diazomethane results in the free carbene and hence, another reaction mechanism can be obtained compared to the cycloaddition of diazomethane to the C=N bond. Moreover, the generation of diazomethane under continuous flow conditions, as described by Kappe *et al.*, can be coupled with the subsequent aziridination reaction (Scheme 5.9).[129]
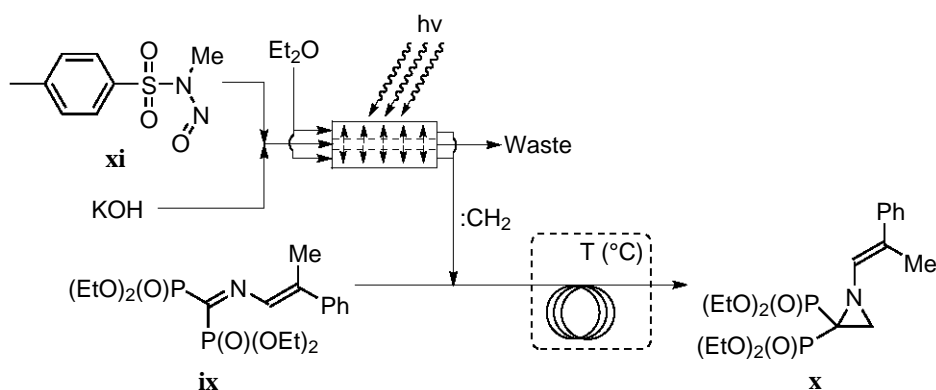
Scheme 5.9. Photolysis of diazomethane and subsequent aziridination of **ix**

In a final research topic, the activation of amino acids with 1*H*-benzotriazole was examined. Two different activation strategies were evaluated: (a) BtMs and (b) BtH - SOCl$_2$ (Scheme 5.10).
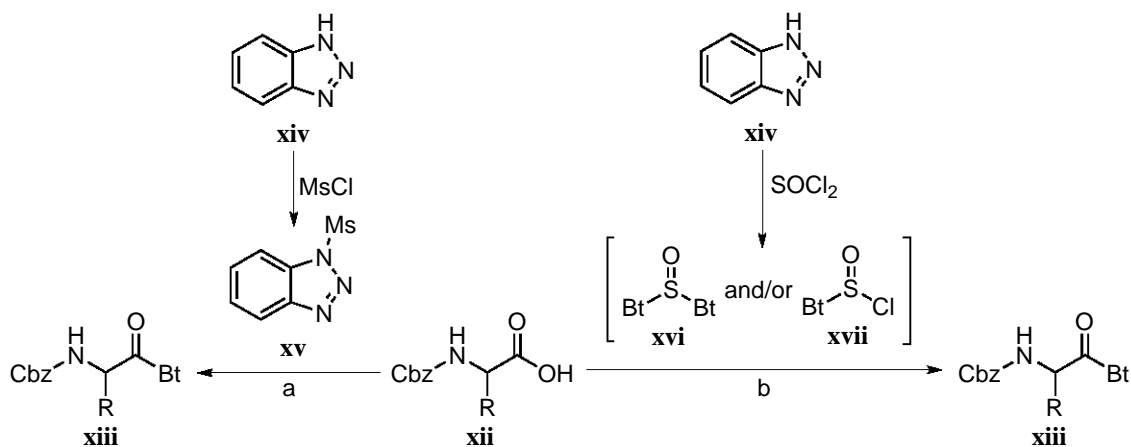
Scheme 5.10. Activation of amino acids with *1H*-benzotriazole **xiv**

If the right solvent was used, both methods could be performed under continuous flow conditions without precipitate formation. After optimization of the Bt-activation of Cbz-L-Trp **xiia** with BtMs, a limited conversion of 81% was reached. However, using BtH - SOCl$_2$ in MeCN:NMP (6:1) resulted in excellent conversions (94%). Moreover, work up of the reaction mixture was very straightforward. Several derivatives were synthesized in good isolated yields (76-99%) (Scheme 5.11).
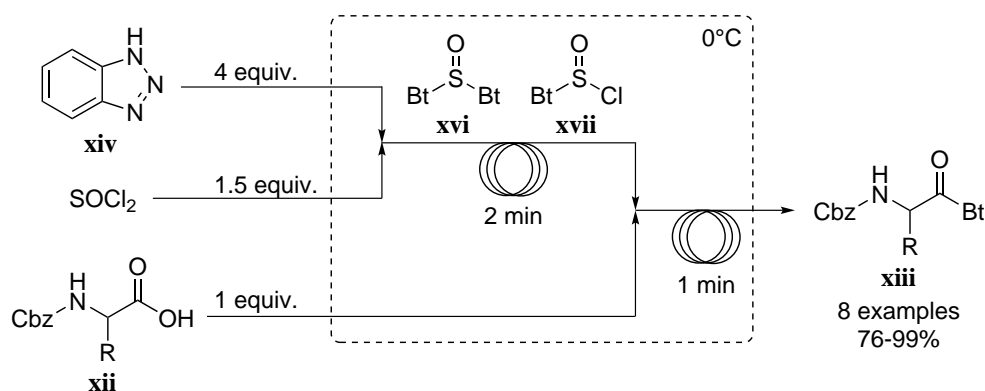
Scheme 5.11. Continuous flow activation of amino acids with 1*H*-benzotriazole **xiv**

Performing the coupling of a Bt-activated amino acid with a heterocyclic amine in MeCN:NMP (6:1) resulted in poorer conversions as compared to previous research in which DMSO was evaluated as solvent. On the other hand, the synthesis of a dipeptide in MeCN:NMP (6:1) went smoothly although racemization was observed.

Solid phase peptide synthesis (SPSS) is a common technique for the synthesis of peptides and has the advantage of easy product purification and automation. However, an expensive polymer support is required and additional steps are necessary to couple the amino acid with the support and finally remove the peptide from the polymer. Typically, a high excess of reagents is used in SPSS. The developed continuous flow protocol generates less waste as no solid support is necessary and only a slight excess of reagents is used. It allows for a flexible peptide synthesis as the reactor output can be split and the obtained peptide can be subsequently coupled with different amino acids leading to a broad array of peptides. Moreover, activation and protection/deprotection steps can be integrated. On the other hand, inline work up and purification strategies have to be developed in order to telescope all the reaction steps and racemization has to be suppressed.

In summary, several industrially relevant reactions were successfully optimized under continuous flow conditions. All the generic reactions considered benefit from the intrinsic characteristics of microreactor technology, i.e. efficient mass and heat transfer, small and closed hold-up volume and excellent control of the reaction time. However, some of the reactions require further elaboration in order to increase the conversion and isolated yield of the desired end product.

Chapter 6

Samenvatting en perspectieven

Microreactortechnologie biedt een aantal specifieke voordelen in vergelijking met traditionele batch chemie. Een verbeterde massa- en warmtetransfer, een veiligere manipulatie van toxische en reactieve reagentia en een eenvoudige opschaling zijn de belangrijkste voordelen. Verschillende voorbeelden in de literatuur illustreren deze eigenschappen van microreactortechnologie. Schattingen geven aan dat ongeveer 44% van de chemische reacties baat kunnen hebben bij het gebruik van microreactortechnologie. In deze doctoraatsthesis werden een aantal reacties fundamenteel bestudeerd met de nadruk op industrieel relevante reacties die voordeel kunnen halen uit de intrinsieke eigenschappen van microreactortechnologie.

Een eerste project betreft de condensatie van zuurchloriden **i** en alcoholen **ii** zonder katalysator in een microreactor (Schema 6.1).
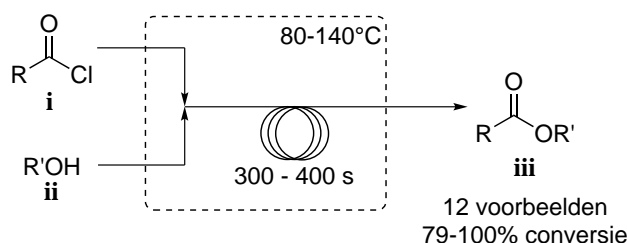
Schema 6.1. Condensatie van zuurchloriden **i** en alcoholen **ii**

De optimalisatie experimenten werden uitgevoerd met benzoylchloride en MeOH in een Labtrix® Start microreactor. Wanneer de condensatiereactie werd uitgevoerd in Et$_2$O, werden beperkte conversies verkregen terwijl uitstekende conversies werden bekomen onder solventvrije condities. Vervolgens werd de reactie uitgebreid naar andere laagkokende alcoholen (EtOH en *i*PrOH). Er werd telkens een volledige conversie waargenomen met een verblijftijd van 300 s, een lichte overmaat van het alcohol (1.3 equiv.) en een reactietemperatuur boven het atmosferisch kookpunt van het alcohol. Vervolgens werden uitstekende conversies (>91%) bekomen wanneer andere vloeibare zuurchloriden werden gecondenseerd met de laagkokende alcoholen.

In een tweede stap werd het substraatbereik uitgebreid naar vaste zuurchloriden en alcoholen. Er werden verschillende solventen (CH_2Cl_2, dioxaan en CH_3CN) geëvalueerd waaruit bleek dat de beste resultaten verkregen werden met CH_3CN. De condensatie van een vast zuurchloride in oplossing met een solventvrij alcohol mislukte. Anderzijds werden uitstekende conversies (>98%) bekomen wanneer een solventvrij zuurchloride reageerde met een vast alcohol in oplossing als de reactietemperatuur, verblijftijd en overmaat alcohol werden verhoogd in vergelijking met de eerder geoptimaliseerde reactiecondities. Als zowel het zuurchloride als het alcohol vast waren en opgelost werden in CH_3CN, werden goede conversies bekomen (79%).

In een laatste deel van deze studie werd de ontwikkelde procedure opgeschaald naar de KiloFlow® reactor zonder verdere optimalisatie. Er werden stabiele en hoge geïsoleerde rendementen bekomen (>98%) en een throughput van 2.2 g/min methylbenzoaat werd bereikt. Bovendien kon het vrijgestelde HCl deels (46%) gerecupereerd worden als een waterige oplossing.

De ontwikkelde procedure is de eerste microreactor procedure voor de synthese van esters zonder katalysator uitgaande van zuurchloriden. In vergelijking met de transesterificatie reactie zonder katalysator via novel process windows, werden energie efficiëntere reactiecondities bekomen wat resulteert in een lagere werkingskost.[189,190] Andere gerapporteerde continue procedures maken gebruik van een katalysator om de verestering uit te voeren waardoor het proces minder duurzaam wordt aangezien meer afval gegenereerd wordt. In batch kan de reactie solventvrij en zonder katalysator uitgevoerd worden maar met een beperkte throughput.[206] Bovendien werden nog geen pogingen gerapporteerd om het vrijgekomen HCl te recycleren. Anderzijds zijn de geoptimaliseerde reactiecondities niet geschikt voor reactieve substraten en deze substraten zijn het meest interessant voor de industrie. Waarschijnlijk kan dit probleem opgelost worden door een lagere reactietemperatuur te gebruiken en de reagentia te verdunnen in een solvent.

In een tweede deel van dit doctoraatsonderzoek werd de tribromering van methylsulfonen en methaansulfonaten met hypobromiet geëvalueerd. In een eerste serie experimenten werd KOBr aangemaakt in batch en werd deze oplossing gebruikt om de bromering van 4-isopropoxy-fenylmethylsulfon **iv** te optimaliseren in twee verschillende mesoreactoren: (1) een buisreactor en (2) een statische menger (Uniqsis®) (Schema 6.2).
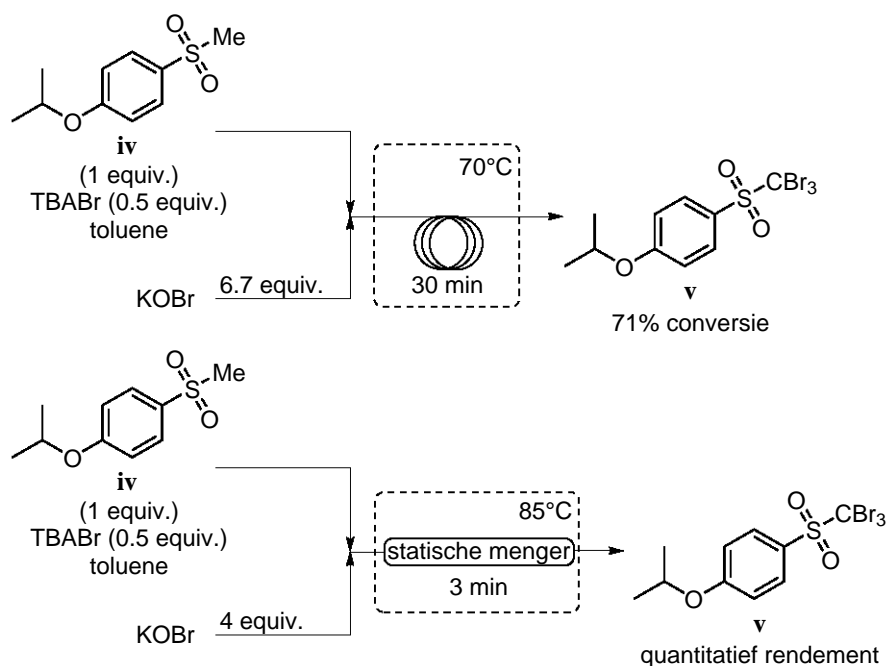
Schema 6.2. Bromering van 4-isopropoxyfenylmethylsulfon **iv** in een buisreactor en een statische menger

De bromering van **iv** in de buisreactor werd geoptimaliseerd door de reactietemperatuur, de overmaat KOBr en de verblijftijd te variëren. Bovendien werd de invloed nagegaan van de hoeveelheid fasetransferkatalysator en het type menger (T- of Y-verbinding). Na optimalisatie werd een beperkte conversie van 71% bereikt. Naast het eindproduct **v**, werden voornamelijk startproduct **iv** en sporen van het gedibromeerde intermediair gedetecteerd.

Anderzijds werd het eindproduct **v** met een quantitatief rendement geïsoleerd na optimalisatie van de bromeringsreactie in de statische menger. De geïntegreerde statische mengelementen zorgden voor de vorming van een emulsie. Op die manier werd een efficiënt contact tussen de organische en waterfase bekomen wat uiteindelijk resulteerde in een volledige conversie van het startmateriaal. In de buisreactor werd een plugstroom waargenomen met een kleinere interfaseoppervlakte in vergelijking met de emulsie.

Vervolgens werd de Uniqsis® statische menger gebruikt om verschillende tribroommethyl-sulfonen te synthetiseren en werd het substraatbereik succesvol uitgebreid naar arylmethaan-sulfonaten. Wanneer de ontwikkelde procedure gebruikt werd voor de bromering van arylmethaansulfonamiden, werd bromering van de aromatische ring vastgesteld.

In vergelijking met het batch proces werd een aanzienlijke afname van de reactietijd bekomen door de efficiënte massatransfer tussen de organische en waterige fase. Aangezien de reactie

geoptimaliseerd werd voor één derivaat en nadien uitgebreid werd naar andere derivaten, werden soms mindere zuivere reactiemengsels bekomen in vergelijking met het batch proces. Dit kan verklaard worden door de hogere reactietemperatuur in het continu proces.

Nadien werd de synthese van KOBr in een mesoreactor geëvalueerd. Verschillende pogingen om KOBr aan te maken in een buisreactor mislukten door het grote debietverschil tussen beide reagensstromen. Om een betere debietverhouding te bekomen, werd Br_2 vervolgens verdund met een geschikt solvent. Hierbij werden echter problemen waargenomen in de daaropvolgende bromeringsreactie. Wanneer een statische menger gebruikt werd om KOBr aan te maken, trad neerslagvorming op waardoor de menger verstopte. Uiteindelijk werd een continu geroerde batch reactor gebruikt om het hypobromiet aan te maken. Op die manier kon de continue synthese van hypobromiet succesvol gekoppeld worden aan de daaropvolgende bromering in de statische menger (Schema 6.3). Door zowel de synthese van hypobromiet en de bromeringsreactie continu uit te voeren, kan broom veiliger gemanipuleerd worden en wordt de degradatie van hypobromiet beperkt.
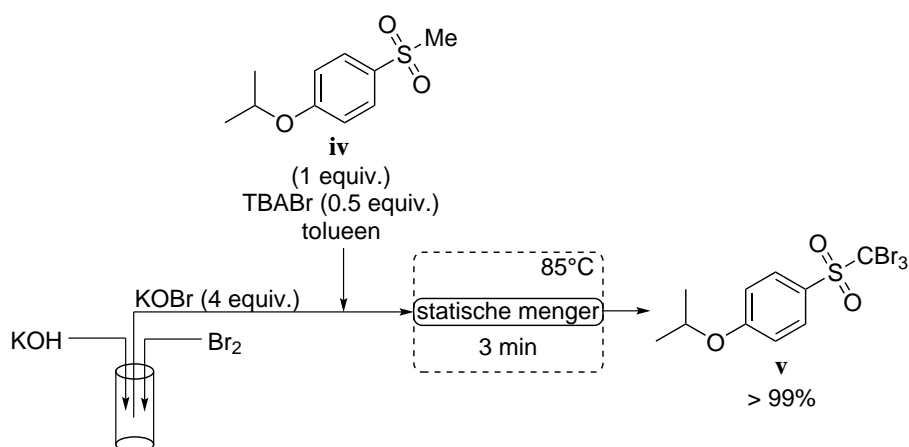
Schema 6.3. Continue synthese van hypobromiet en daaropvolgende bromering in de statische menger

In een laatste deel van dit project werd de ontscherming van de isopropylethergroep van tribroommethyl-4-isopropoxyfenylsulfon **v** onderzocht (Schema 6.4).
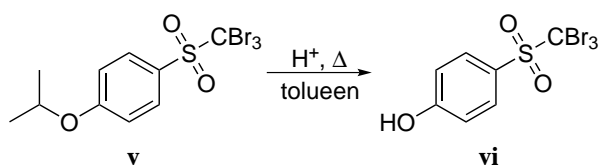
Schema 6.4. Ontscherming van de isopropylethergroep van **v**

Alhoewel reeds een efficient batch proces ontwikkeld was met een katalytische hoeveelheid CF_3SO_3H, werd de ontscherming onderzocht in een mesoreactor om de ontschermingsstap te kunnen koppelen aan de voorgaande bromeringsreactie. De ontscherming van ethers met H_3PO_4 is reeds gerapporteerd in de literatuur maar verschillende pogingen om de ontscherming uit te voeren in een mesoreactor mislukten. Anderzijds resulteerde het gebruik van H_2SO_4 of CH_3SO_3H in goede conversies (>81%) wanneer een grote overmaat van het zuur werd gebruikt.

Uiteindelijk werd de ontscherming ook getest met CF_3SO_3H in een mesoreactor waarbij een uitstekende conversie (97%) bekomen werd met een stoichiometrische hoeveelheid CF_3SO_3H. Aangezien het eindproduct **vi** neerslaat in tolueen, werd DMSO als co-solvent gebruikt om verstopping van de reactor te vermijden (Schema 6.5). Het oorspronkelijke batch proces is beter dan het ontwikkelde continu proces aangezien slechts katalystische hoeveelheden CF_3SO_3H nodig zijn in batch en het product eenvoudig geïsoleerd kan worden met een uitstekend rendement.
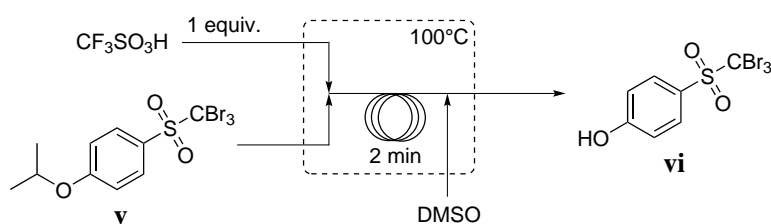
Schema 6.5. Ontscherming van de isopropylethergroep van **v** in een mesoreactor

In een batch reactor slaat het eindproduct **vi** neer en ontsnapt het gevormde propeen uit het reactiemengsel. Op die manier wordt het evenwicht van de reactie naar rechts getrokken (principe van Le Chatelier). In het continu proces werd een homogeen reactiemengsel bekomen en blijft propeen in oplossing aangezien geen headspace aanwezig is in de reactor. Dit verklaart waarschijnlijk waarom de reactie in de mesoreactor niet werkt met katalytische hoeveelheden CF_3SO_3H terwijl in batch uitstekende rendementen bekomen werden. Om de reactie continu uit te voeren met katalytische hoeveelheden zuur, kunnen methoden onderzocht worden om propeen uit het reactiemengsel te verwijderen gedurende de reactie, bv. gasdoorlatende tubing.

In een derde luik van deze doctoraatsthesis werd de Simmons-Smith cyclopropanering van enaminen **vii** onderzocht (Schema 6.6).
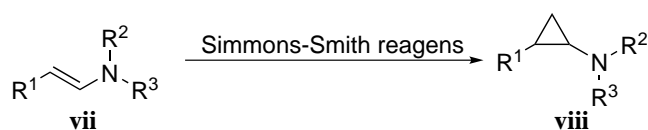
Schema 6.6. Simmons-Smith cyclopropanering van enaminen

De enaminen **vii** werden via standaardmethoden aangemaakt en in matige tot goede rendementen geïsoleerd (43-90%). Nadien werden verschillende Zn-carbenoïden onderzocht in batch waarbij aandacht besteed werd aan de oplosbaarheid van de gevormde Zn-carbenoïden. Drie verschillende Zn-carbenoïden ($Zn(CH_2I)_2$, $Zn(CH_2I)_2.DME$ en $CF_3CO_2ZnCH_2I$) werden geëvalueerd waarbij $CF_3CO_2ZnCH_2I$ of Shi's carbenoïde werd geselecteerd voor de cyclo-propaneringsreactie op basis van reactiviteit en oplosbaarheid. In batch werden uitstekende conversies bekomen met 2 equivalenten $CF_3CO_2ZnCH_2I$ en een reactietijd van 2.5 - 5 h. Wanneer 3 equivalenten $CF_3CO_2ZnCH_2I$ werden gebruikt, waren de enaminen reeds na 45 min volledig omgezet. Ondanks de uitstekende conversies waren de geïsoleerde rendementen eerder laag. Verschillende opwerkings- en opzuiveringsmethoden werden onderzocht maar ofwel mislukte de methode, ofwel werden matige rendementen bekomen.

Vervolgens werd de cyclopropanering van enaminen met een elektronenzuigende groep op het stikstofatoom onderzocht in batch. Deze enaminen waren minder reactief en om een volledige conversie te bereiken, was een grotere overmaat van het Zn-carbenoïde (3 equiv.) en een langere reactietijd (6 h) nodig. Op deze manier werden verschillende getosyleerde cyclopropylaminen gesynthetiseerd in matige tot goede rendementen (40-80%).

In een eerste serie mesoreactor experimenten werd de oplossing van $CF_3CO_2ZnCH_2I$ aangemaakt in batch en als dusdanig gebruikt voor de cyclopropanering van de enaminen in een mesoreactor. Er werden uitstekende conversies bereikt bij een reactietemperatuur van 35°C, een verblijftijd van 5 min en 3 equivalenten $CF_3CO_2ZnCH_2I$.

Vervolgens werd de vorming van $CF_3CO_2ZnCH_2I$ in een mesoreactor onderzocht. De oorspronkelijke batch procedure voor de synthese van $CF_3CO_2ZnCH_2I$ werd succesvol aangepast om de vorming van een intermediaire suspensie te vermijden. De eerste pogingen om de aangepaste batch procedure te vertalen naar een continu proces mislukten door verstopping van de buisreactor. Wanneer er overgeschakeld werd op een solvent dat het Zn-

carbenoïde complexeert (THF) in de plaats van CH_2Cl_2, werd geen verstopping van de reactor waargenomen. In dit geval werd er ofwel een complex reactiemengsel bekomen, ofwel werd er geen conversie van het startproduct vastgesteld.

Om een optimale balans te vinden tussen reactiviteit en oplosbaarheid van het Zn-carbenoïde, werden in een volgende stap solventmengsels van THF en CH_2Cl_2 geëvalueerd. Uit batch experimenten bleek dat hoe meer THF werd gebruikt, hoe trager de reactie verliep en hoe lager de uiteindelijke conversie was. Anderzijds was THF vereist om verstopping van de buisreactor te vermijden. Na optimalisatie konden zowel de synthese van $CF_3CO_2ZnCH_2I$ als de daaropvolgende cyclopropaneringsreactie continu uitgevoerd worden met een reactie-temperatuur van 35°C en slechts 1.5 equivalenten $CF_3CO_2ZnCH_2I$ (Schema 6.7). Met deze reactiecondities werd een volledige conversie bekomen, maar net zoals bij de batch experimenten was de isolatie van de gevormde cyclopropylamines moeilijk.
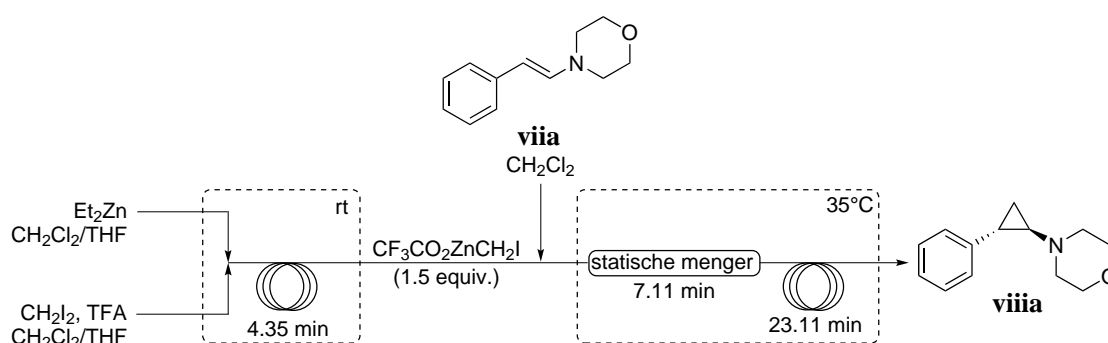
Schema 6.7. Simmons-Smith cyclopropanering van enaminen

In de literatuur worden ongevallen gerapporteerd die betrekking hebben op de Simmons-Smith cyclopropaneringsreactie in batch.[48,49] De uitstekende warmtetransfer in combinatie met het beperkte intern volume maken het mogelijk om het Simmons-Smith reagens veiliger te manipuleren in een microreactor. In batch wordt het carbenoïde typisch aangemaakt bij -78°C terwijl in het continu proces de reactie kon uitgevoerd worden bij kamertemperatuur. Bovendien is op deze manier minder energie vereist om het reactiemengsel te koelen.

In vergelijking met andere methoden om cyclopropylaminen te synthetiseren, is de cyclo-propanering van enaminen een eenvoudige en veelzijdige methode om deze derivaten te bekomen. Enaminen kunnen bekomen worden uit aldehyden of ketonen en secundaire aminen. Bovendien kan door het gebruik van dibenzylamine de vrije aminogroep op de cyclopropylring bekomen worden na hydrogenolyse. Daarnaast is de Simmons-Smith reactie stereospecifiek en kan deze reactie enantioselectief uitgevoerd worden m.b.v. chirale hulpstoffen.

Het voornaamste probleem bij de cyclopropanering van enaminen, was de isolatie van de gesynthetiseerde cyclopropylaminen. De opzuivering van de cyclopropylaminen is moeilijk waardoor verder onderzoek noodzakelijk is om de geïsoleerde rendementen te verbeteren. Opzuiveringsmethoden waarbij geen water gebruikt wordt, genieten de voorkeur aangezien een aanzienlijke hoeveelheid product verloren gaat tijdens de waterige opwerking. Om industrieel relevant te zijn, kan inline opzuivering ontwikkeld worden.

In een voorlaatste project van deze doctoraatsthesis werd de synthese van *N*-vinyl-2,2-bisfosfonoaziridines **x** onderzocht uitgaande van de overeenkomstige 1,1-bisfosfono-2-aza-1,3-diënen **ix**. Uit voorgaand onderzoek aan onze vakgroep bleek dat nevenproducten gevormd werden indien de reactie uitgevoerd werd in batch.

In een eerste reeks microreactorexperimenten met 10 equivalenten diazomethaan, werden enkel sporen van het aziridine gedetecteerd. Wanneer de overmaat diazomethaan verhoogd werd tot 35 equivalenten in combinatie met belichting van de microreactor chip, werd een selectieve conversie naar het gewenste eindproduct waargenomen van 71% (Schema 6.8). Via de ontwikkelde microreactorprocedure kon diazomethaan op een veilige manier gebruikt worden bij hogere temperaturen (60°C).
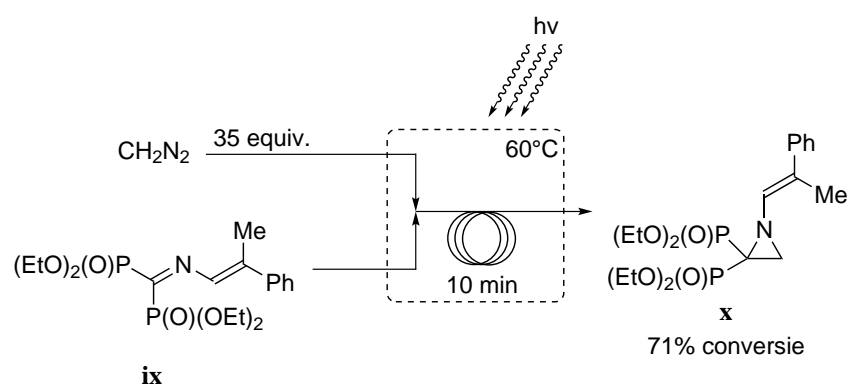
Schema 6.8. Aziridinering van 1,1-bisfosfono-2-aza-1,3-dieen **ix**

In verder onderzoek kan de microreactorprocedure geoptimaliseerd worden om volledige en selectieve conversie te bereiken. Zowel langere verblijftijden als lagere reactietemperaturen kunnen onderzocht worden. De hoge reactietemperaturen die in dit project gebruikt werden, kunnen aanleiding geven tot de afbraak van diazomethaan. Op deze manier kan de grote overmaat diazomethaan verklaard worden die nodig was om een matige conversie te bereiken. Een andere route die verder onderzocht kan worden, is de fotodecompositie van het intermediaire 1,2,3-triazoline. In dit doctoraatsonderzoek werd een eenvoudige lamp gebruikt

om de microreactor te belichten. Om het rendement van de fotodecompositie te verhogen, kunnen andere lichtbronnen onderzocht worden.

Een laaste synthesestrategie die geëvalueerd kan worden, is de fotolyse van diazomethaan.[339,340] Fotolyse van diazomethaan geeft aanleiding tot het vrij carbeen waardoor een ander reactiemechanisme mogelijk is in vergelijking met de cycloaddditie van diazomethaan aan de C=N binding. Bovendien kan de continue synthese van diazomethaan, zoals beschreven door Kappe *et al.*, gekoppeld worden aan de daaropvolgende continue vorming van het aziridine (Schema 6.9).[129]
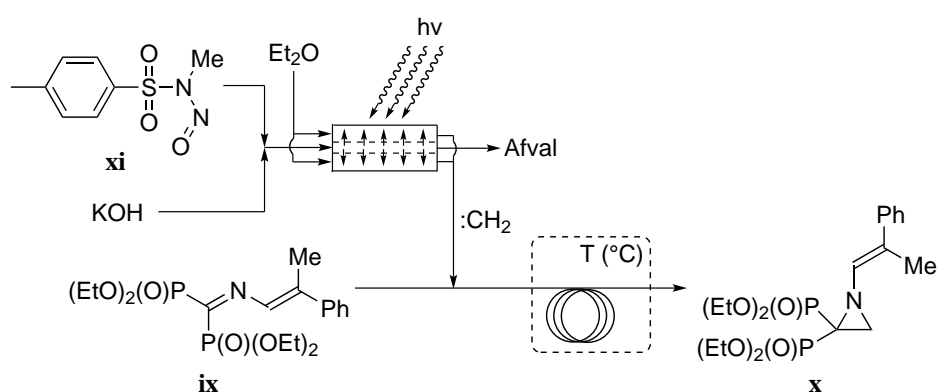
Schema 6.9. Fotolyse van diazomethaan en daaropvolgende aziridinering van **ix**

In een laatste project van deze doctoraatsthesis werd de activering van aminozuren met 1*H*-benzotriazool onderzocht. Er werden twee verschillende activatiestrategieën onderzocht: (a) BtMs en (b) BtH - SOCl$_2$ (Schema 6.10).
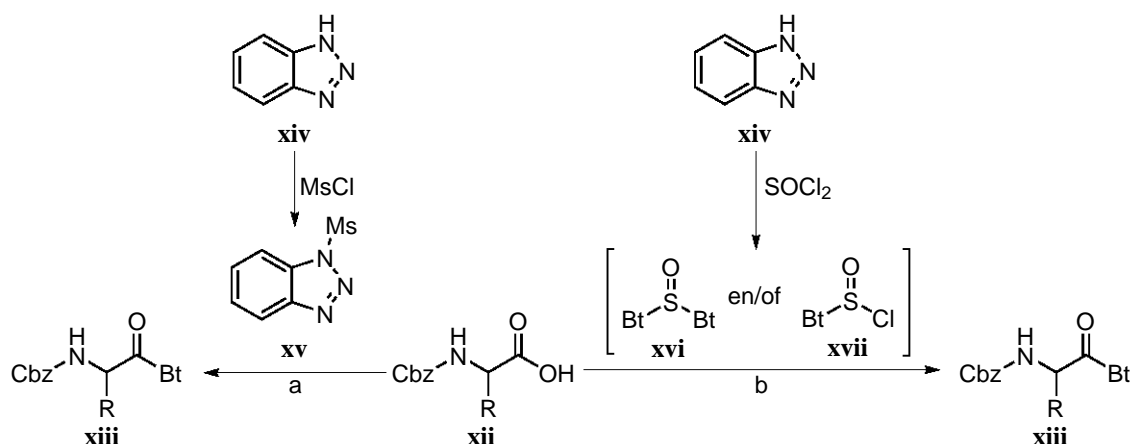
Schema 6.10. Activatie van aminozuren met 1*H*-benzotriazool **xiv**

Indien het juiste solvent gekozen werd, konden beide methoden uitgevoerd worden in een mesoreactor zonder neerslagvorming. Na optimalisatie van de Bt-activering van Cbz-L-Trp **xiia** met BtMs werd een beperkte conversie van 81% bekomen. Anderzijds werd een uitstekende conversie (92%) bekomen wanneer de activatie werd uitgevoerd met BtH - SOCl$_2$ in MeCN:NMP (6:1). Bovendien was de opwerking van het reactiemengsel zeer eenvoudig. Vervolgens werden verschillende derivaten gesynthetiseerd met goede tot uitstekende rendementen (76-99%) (Schema 6.11).
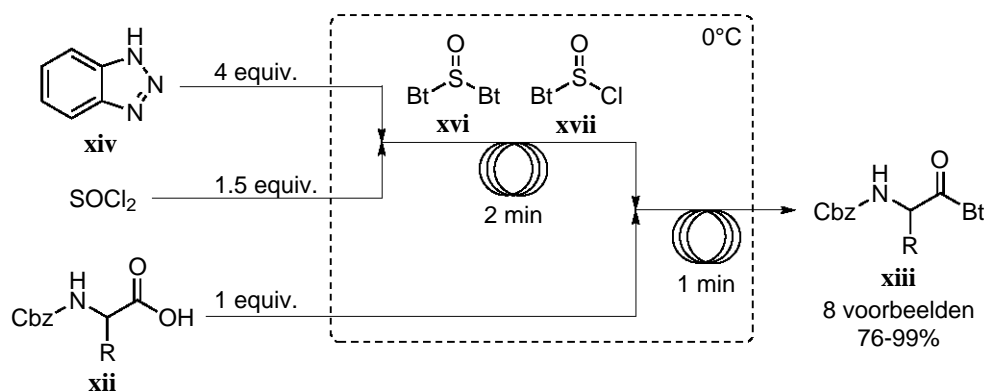
Schema 6.11. Continue activatie van aminozuren met 1*H*-benzotriazool **xiv**

Bij de koppeling van het geactiveerd aminozuur met een heterocyclisch amine in MeCN:NMP (6:1) werden lagere conversies verkregen in vergelijking met vorig onderzoek waarbij DMSO gebruikt werd als solvent. Anderzijds kon MeCN:NMP (6:1) wel aangewend worden voor de synthese van dipeptiden. Hierbij werd echter racemisatie waargenomen.

Vaste fase peptide synthese is een algemene techniek voor de synthese van peptiden waarbij een eenvoudige product isolatie en automatisering de belangrijkste voordelen zijn. Anderzijds is een kostelijk polymeer vereist en zijn bijkomende stappen nodig om het aminozuur met het polymeer te koppelen en uiteindelijk het peptide van de vaste drager los te koppelen. Daarnaast wordt typisch een grote overmaat aan reagentia gebruikt. In de ontwikkelde continue procedure wordt minder afval geproduceerd aangezien geen vaste drager nodig is en slechts een beperkte overmaat aan reagentie gebruikt wordt. Bovendien is een flexibele synthese mogelijk aangezien de uitgang van de reactor opgesplitst kan worden waarbij het bekomen peptide vervolgens gekoppeld kan worden met verschillende aminozuren. Daarnaast kunnen activatie en bescherming/ontscherming in de reactiesequentie geïntegreerd worden. Anderzijds moeten inline opwerking en opzuivering ontwikkeld worden om de verschillende reactiestappen met elkaar te kunnen koppelen en moet racemisatie onderdrukt worden.

Kortom, in deze doctoraatsthesis werden verschillende industrieel relevante reacties succesvol geoptimaliseerd in een micro- of mesoreactor. Alle reacties die onderzocht werden, profiteren van de intrinsieke eigenschappen van microreactortechnologie, waaronder een efficiënte massa- en warmtetransfer, een klein en gesloten reactorvolume en een uitstekende controle over de verblijftijd. Sommige reacties moeten echter verder onderzocht worden om de conversie of het rendement te verhogen.

References

1. C. Wiles, P. Watts, *Eur. J. Org. Chem.* **2008**, *2008*, 1655–1671.

2. V. Hessel, T. Noël in *Ullmann's Encyclopedia of Industrial Chemistry*, Wiley-VCH, **2012**, pp. 1–9.

3. K. Jähnisch, V. Hessel, H. Löwe, M. Baerns, *Angew. Chem. Int. Ed.* **2004**, *43*, 406–446.

4. H. Salimi-Moosavi, T. Tang, D. J. Harrison, *J. Am. Chem. Soc.* **1997**, *119*, 8716–8717.

5. M. Brivio, W. Verboom, D. N. Reinhoudt, *Lab Chip* **2006**, *6*, 329–344.

6. P. D. Fletcher, S. J. Haswell, E. Pombo-Villar, B. H. Warrington, P. Watts, S. Y. Wong, X. Zhang, *Tetrahedron* **2002**, *58*, 4735–4757.

7. X. Feng, S. J. Haswell, P. Watts, *Curr. Top. Med. Chem.* **2004**, *4*, 707–727.

8. H. Pennemann, P. Watts, S. J. Haswell, V. Hessel, H. Löwe, *Org. Process Res. Dev.* **2004**, *8*, 422–439.

9. P. Watts, S. J. Haswell, *Chem. Eng. Technol.* **2005**, *28*, 290–301.

10. B. P. Mason, K. E. Price, J. L. Steinbacher, A. R. Bogdan, D. T. McQuade, *Chem. Rev.* **2007**, *107*, 2300–2318.

11. T. Wirth, *Microreactors in organic synthesis and catalysis*, John Wiley & Sons, **2008**.

12. A. Cukalovic, J.-C. M. Monbaliu, C. V. Stevens in *Synthesis of Heterocycles via Multicomponent Reactions I*, Springer, **2010**, pp. 161–198.

13. D. Webb, T. F. Jamison, *Chem. Sci.* **2010**, *1*, 675–680.

14. C. Wiles, P. Watts, *Chem. Commun.* **2011**, *47*, 6512–6535.

15. J. Wegner, S. Ceylan, A. Kirschning, *Adv. Synth. Catal.* **2012**, *354*, 17–57.

16. P. Watts, C. Wiles, *J. Chem. Res.* **2012**, *36*, 181–193.

17. N. G. Anderson, *Org. Process Res. Dev.* **2012**, *16*, 852–869.

18. L. Protasova, M. Bulut, D. Ormerod, A. Buekenhoudt, J. Berton, C. Stevens, *Org. Process Res. Dev.* **2013**, *17*, 760–791.

19. L. Vaccaro, D. Lanari, A. Marrocchi, G. Strappaveccia, *Green Chem.* **2014**, *16*, 3680–3704.

20. S. G. Newman, K. F. Jensen, *Green Chem.* **2013**, *15*, 1456–1472.

21. N. Kockmann, M. Gottsponer, B. Zimmermann, D. M. Roberge, *Chem. Eur. J.* **2008**, *14*, 7470–7477.

22. J. Wegner, S. Ceylan, A. Kirschning, *Chem. Commun.* **2011**, *47*, 4583–4592.

23. S. Taghavi-Moghadam, A. Kleemann, G. Golbig, *Org. Process Res. Dev.* **2001**, *5*, 652–658.

24. R. L. Hartman, J. P. McMullen, K. F. Jensen, *Angew. Chem. Int. Ed.* **2011**, *50*, 7502–7519.

25. G. Caygill, M. Zanfir, A. Gavriilidis, *Org. Process Res. Dev.* **2006**, *10*, 539–552.

26. Royal Society of Chemistry, *EHSC Note - Safety issue in the scale up of chemical reactions*, website: "http://www.rsc.org/", accessed 02/06/2014.

27. D. Janasek, J. Franzke, A. Manz, *Nature* **2006**, *442*, 374–380.

28. D. M. Roberge, L. Ducry, N. Bieler, P. Cretton, B. Zimmermann, *Chem. Eng. Technol.* **2005**, *28*, 318–323.

29. R. L. Hartman, J. R. Naber, N. Zaborenko, S. L. Buchwald, K. F. Jensen, *Org. Process Res. Dev.* **2010**, *14*, 1347–1357.

30. J. Sedelmeier, S. V. Ley, I. R. Baxendale, M. Baumann, *Org. Lett.* **2010**, *12*, 3618–3621.

31. T. Noël, J. R. Naber, R. L. Hartman, J. P. McMullen, K. F. Jensen, S. L. Buchwald, *Chem. Sci.* **2011**, *2*, 287–290.

32. D. L. Browne, B. J. Deadman, R. Ashe, I. R. Baxendale, S. V. Ley, *Org. Process Res. Dev.* **2011**, *15*, 693–697.

33. C. Jiménez-González, P. Poechlauer, Q. B. Broxterman, B.-S. Yang, D. am Ende, J. Baird, C. Bertsch, R. E. Hannah, P. Dell'Orco, H. Noorman, S. Yee, R. Reintjens, A. Wells, V. Massonneau, J. Manley, *Org. Process Res. Dev.* **2011**, *15*, 900–911.

34. C. Wiles, P. Watts, *Green Chem.* **2012**, *14*, 38–54.

35. S. V. Ley, *Chem. Rec.* **2012**, *12*, 378–390.

36. W. Greene, P. Wuts, *Protective Groups in Organic Synthesis*, Wiley, New York, **2007**.

37. C. Wiles, P. Watts, S. J. Haswell, E. Pombo-Villar, *Tetrahedron* **2003**, *59*, 10173–10179.

38. E. Šinkovec, A. Pohar, M. Krajnc, *Microfluid. Nanofluid.* **2013**, *14*, 489–498.

39. V. Hessel, D. Kralisch, N. Kockmann, T. Noël, Q. Wang, *ChemSusChem* **2013**, *6*, 746–789.

40. S. C. Stouten, T. Noël, X. Wang, V. Hessel, *Aust. J. Chem.* **2013**, *66*, 121–130.

41. V. Hessel, I. Vural-Gürsel, Q. Wang, T. Noël, J. Lang, *J. Chem. Eng. Technol.* **2012**, *35*, 1184–1204.

42. D. D. Zani, M. Colombo, *J. Flow. Chem.* **2012**, *2*, 5–7.

43. J. Jovanovic, W. Hengeveld, E. V. Rebrov, T. A. Nijhuis, V. Hessel, J. C. Schouten, *Chem. Eng. Technol.* **2011**, *34*, 1691–1699.

44. M. Brasholz, K. Von Kaenel, C. H. Hornung, S. Saubern, J. Tsanaktsidis, *Green Chem.* **2011**, *13*, 1114–1117.

45. M. Kashid, A. Gupta, A. Renken, L. Kiwi-Minsker, *Chem. Eng. J.* **2010**, *158*, 233–240.

46. M. N. Kashid, L. Kiwi-Minsker, *Ind. Eng. Chem. Res.* **2009**, *48*, 6465–6485.

47. A.-L. Dessimoz, L. Cavin, A. Renken, L. Kiwi-Minsker, *Chem. Eng. Sci.* **2008**, *63*, 4035–4044.

48. A. B. Charette, S. Prescott, C. Brochu, *J. Org. Chem.* **1995**, *60*, 1081–1083.

49. http://www.aiha.org/get-involved/VolunteerGroups/LabHSCommittee/Incident%20Pages/Lab-Safety-Explosions-Incidents—Chemistry.aspx.

50. P. P. Mortier, F. E. Van Waes, K. G. Masschelein, T. S. Heugebaert, C. V. Stevens, *Tetrahedron Lett.* **2011**, *52*, 4273–4276.

51. P. Scheiner, *J. Org. Chem.* **1965**, *30*, 7–10.

52. P. Scheiner, *Tetrahedron* **1968**, *24*, 2757–2765.

53. P. Scheiner, *J. Am. Chem. Soc.* **1968**, *90*, 988–992.

54. Y. Matsushita, T. Ichimura, N. Ohba, S. Kumada, K. Sakeda, T. Suzuki, H. Tanibata, T. Murata, *Pure Appl. Chem.* **2007**, *79*, 1959–1968.

55. T. Van Gerven, G. Mul, J. Moulijn, A. Stankiewicz, *Chem. Eng. Process.* **2007**, *46*, 781–789.

56. M. Oelgemöller, O. Shvydkiv, *Molecules* **2011**, *16*, 7522–7550.

57. Y. Su, N. J. W. Straathof, V. Hessel, T. Noël, *Chem. Eur. J.* **2014**, *20*, 10562–10589.

58. T. Noël, X. Wang, V. Hessel, *Chimica Oggi* **2013**, *31*, 10–14.

59. A. Cukalovic, *Use of microreactor technology and renewable resources to develop green chemical processes*, PhD dissertation, Ghent University, 2012.

60. W. Löhder, L. Bergann, (Akademie der Wissenschaften der DDR), DD 246257, 1986.

61. W. Ehrfeld, DECHEMA-Monographs, DECHEMA, Frankfurt, 1995, p. 132.

62. P. Rys, *Acc. Chem. Res.* **1976**, *9*, 345–351.

63. P. Rys, *Angew. Chem. Int. Ed.* **1977**, *16*, 807–817.

64. J.-i. Yoshida, A. Nagaki, T. Iwasaki, S. Suga, *Chem. Eng. Technol.* **2005**, *28*, 259–266.

65. P. Petrino, Y. Gaston-Bonhomme, J. Chevalier, *J. Chem. Eng. Data* **1995**, *40*, 136–140.

66. T. Wirth, *Microreactors in organic synthesis and catalysis*, John Wiley & Sons, **2008**.

67. K. D. Nagy, B. Shen, T. F. Jamison, K. F. Jensen, *Org. Process Res. Dev.* **2012**, *16*, 976–981.

68. W. Ehrfeld, K. Golbig, V. Hessel, H. Löwe, T. Richter, *Ind. Eng. Chem. Res.* **1999**, *38*, 1075–1082.

69. V. Hessel, H. Löwe, F. Schönfeld, *Chem. Eng. Sci.* **2005**, *60*, 2479–2501.

70. N.-T. Nguyen, Z. Wu, *J. Micromech. Microeng.* **2005**, *15*, R1–R16.

71. S. Suga, A. Nagaki, J.-i. Yoshida, *Chem. Commun.* **2003**, 354–355.

72. A. Nagaki, M. Togai, S. Suga, N. Aoki, K. Mae, J.-i. Yoshida, *J. Am. Chem. Soc.* **2005**,

127, 11666–11675.

73. J.-C. M. Monbaliu, A. Cukalovic, J. Marchand-Brynaert, C. V. Stevens, *Tetrahedron Lett.* **2010**, *51*, 5830–5833.

74. J. E. Corrie, G. W. Kirby, J. W. Mackinnon, *J. Chem. Soc. Perkin Trans. 1* **1985**, 883–886.

75. G. W. Kirby, J. W. Mackinnon, *J. Chem. Soc. Perkin Trans. 1* **1985**, 887–892.

76. G. W. Kirby, H. McGuigan, J. W. Mackinnon, D. McLean, R. P. Sharma, *J. Chem. Soc. Perkin Trans. 1* **1985**, 1437–1442.

77. G. W. Kirby, H. McGuigan, D. McLean, *J. Chem. Soc. Perkin Trans. 1* **1985**, 1961–1966.

78. D. Zhao, M. Johansson, J.-E. Bäckvall, *Eur. J. Org. Chem.* **2007**, *2007*, 4431–4436.

79. P. Quadrelli, M. Mella, A. Gamba Invernizzi, P. Caramella, *Tetrahedron* **1999**, *55*, 10497–10510.

80. S. F. Martin, M. Hartmann, J. A. Josey, *Tetrahedron Lett.* **1992**, *33*, 3583–3586.

81. F. Leroux, N. Nicod, L. Bonnafoux, B. Quissac, F. Colobert, *Lett. Org. Chem.* **2006**, *3*, 165–169.

82. D. J. Morrison, T. K. Trefz, W. E. Piers, R. McDonald, M. Parvez, *J. Org. Chem.* **2005**, *70*, 5309–5312.

83. A. Nagaki, N. Takabayashi, Y. Tomida, J.-i. Yoshida, *Org. Lett.* **2008**, *10*, 3937–3940.

84. A. Nagaki, N. Takabayashi, Y. Tomida, J.-i. Yoshida, *Beilstein. J. Org. Chem.* **2009**, *5*, 16.

85. D. M. Ratner, E. R. Murphy, M. Jhunjhunwala, D. A. Snyder, K. F. Jensen, P. H. Seeberger, *Chem. Commun.* **2005**, 578–580.

86. K. Geyer, P. H. Seeberger, *Helv. Chim. Acta* **2007**, *90*, 395–403.

87. T. Schwalbe, V. Autze, M. Hohmann, W. Stirner, *Org. Process Res. Dev.* **2004**, *8*, 440–454.

88. J. Pelleter, F. Renaud, *Org. Process Res. Dev.* **2009**, *13*, 698–705.

89. D. M. Roberge, N. Bieler, M. Mathier, M. Eyholzer, B. Zimmermann, P. Barthe, C. Guermeur, O. Lobet, M. Moreno, P. Woehl, *Chem. Eng. Technol.* **2008**, *31*, 1155–1161.

90. H. Wakami, J.-i. Yoshida, *Org. Process Res. Dev.* **2005**, *9*, 787–791.

91. E. Riva, S. Gagliardi, M. Martinelli, D. Passarella, D. Vigo, A. Rencurosi, *Tetrahedron* **2010**, *66*, 3242–3247.

92. L. Ducry, D. M. Roberge, *Org. Process Res. Dev.* **2008**, *12*, 163–167.

93. J.-i. Yoshida, A. Nagaki, T. Yamada, *Chem. Eur. J.* **2008**, *14*, 7450–7459.

94. J.-i. Yoshida, *Chem. Rec.* **2010**, *10*, 332–341.

95. J.-i. Yoshida, Y. Takahashi, A. Nagaki, *Chem. Commun.* **2013**, *49*, 9896–9904.

96. K. Omura, A. K. Sharma, D. Swern, *J. Org. Chem.* **1976**, *41*, 957–962.

97. K. Omura, D. Swern, *Tetrahedron* **1978**, *34*, 1651–1660.

98. A. K. Sharma, D. Swern, *Tetrahedron Lett.* **1974**, *15*, 1503–1506.

99. A. K. Sharma, T. Ku, A. D. Dawson, D. Swern, *J. Org. Chem.* **1975**, *40*, 2758–2764.

100. T. Kawaguchi, H. Miyata, K. Ataka, K. Mae, J.-i. Yoshida, *Angew. Chem. Int. Ed.* **2005**, *44*, 2413–2416.

101. J. J. v. d. Linden, P. W. Hilberink, C. M. Kronenburg, G. J. Kemperman, *Org. Process Res. Dev.* **2008**, *12*, 911–920.

102. P. Nieuwland, K. Koch, N. vanHarskamp, R. Wehrens, J. M. vanHest, F. J. Rutjes, *Chem. Asian J.* **2010**, *5*, 799.

103. H. Usutani, Y. Tomida, A. Nagaki, H. Okamoto, T. Nokami, J.-i. Yoshida, *J. Am. Chem. Soc.* **2007**, *129*, 3046–3047.

104. H. Gilman, R. D. Gorsich, *J. Am. Chem. Soc.* **1956**, *78*, 2217–2222.

105. L. S. Chen, G. J. Chen, C. Tamborski, *J. Organomet. Chem.* **1980**, *193*, 283–292.

106. U. D. G. Prabhu, K. C. Eapen, C. Tamborski, *J. Org. Chem.* **1984**, *49*, 2792–2795.

107. F. Leroux, M. Schlosser, *Angew. Chem. Int. Ed.* **2002**, *41*, 4272–4274.

108. W. E. Parham, Y. A. Sayed, *J. Org. Chem.* **1974**, *39*, 2053–2056.

109. W. E. Parham, L. D. Jones, Y. Sayed, *J. Org. Chem.* **1975**, *40*, 2394–2399.

110. W. E. Parham, L. D. Jones, *J. Org. Chem.* **1976**, *41*, 2704–2706.

111. C. E. Tucker, T. N. Majid, P. Knochel, *J. Am. Chem. Soc.* **1992**, *114*, 3983–3985.

112. A. Nagaki, H. Kim, J.-i. Yoshida, *Angew. Chem.* **2008**, *120*, 7951–7954.

113. A. Nagaki, H. Kim, Y. Moriwaki, C. Matsuo, J.-i. Yoshida, *Chem. Eur. J.* **2010**, *16*, 11167–11177.

114. A. Nagaki, H. Kim, J.-i. Yoshida, *Angew. Chem. Int. Ed.* **2009**, *48*, 8063–8065.

115. A. Nagaki, H. Kim, H. Usutani, C. Matsuo, J.-i. Yoshida, *Org. Biomol. Chem.* **2010**, *8*, 1212–1217.

116. K. Tanaka, S. Motomatsu, K. Koyama, K. Fukase, *Tetrahedron Lett.* **2008**, *49*, 2010–2012.

117. K. Tanaka, K. Fukase, *Org. Process Res. Dev.* **2009**, *13*, 983–990.

118. T. H. Black, *Aldrichimica Acta* **1983**, *16*, 3–10.

119. E. B. LeWinn, *Am. J. Med. Sci.* **1949**, *218*, 556–562.

120. R. Schoental, *Nature* **1960**, *166*, 420–421.

121. T. J. de Boer, H. Backer, *J. Org. Synth.* **1963**, *4*, 250–253.

122. C. E. LEWIS, *J. Occup. Environ. Med.* **1964**, *6*, 91–92.

123. A. J. Warr, L. D. Proctor, *Generation of diazomethane*, **1971**, GB 2,357,501.

124. L. D. Proctor, A. J. Warr, *Org. Process Res. Dev.* **2002**, *6*, 884–892.

125. M. Struempel, B. Ondruschka, R. Daute, A. Stark, *Green Chem.* **2008**, *10*, 41–43.

126. E. Rossi, P. Woehl, M. Maggini, *Org. Process Res. Dev.* **2012**, *16*, 1146–1149.

127. L. J. Martin, A. L. Marzinzik, S. V. Ley, I. R. Baxendale, *Org. Lett.* **2011**, *13*, 320–323.

128. R. A. Maurya, C. P. Park, J. H. Lee, D.-P. Kim, *Angew. Chem. Int. Ed.* **2011**, *50*, 5952–5955.

129. F. Mastronardi, B. Gutmann, C. O. Kappe, *Org. Lett.* **2013**, *15*, 5590–5593.

130. D. R. Acke, C. V. Stevens, *Green Chem.* **2007**, *9*, 386–390.

131. D. R. Acke, C. V. Stevens, B. I. Roman, *Org. Process Res. Dev.* **2008**, *12*, 921–928.

132. T. S. Heugebaert, B. I. Roman, A. De Blieck, C. V. Stevens, *Tetrahedron Lett.* **2010**, *51*, 4189–4191.

133. A. Cukalovic, J.-C. M. Monbaliu, G. J. Heynderickx, C. V. Stevens, *J. Flow. Chem.* **2012**, *2*, 43–46.

134. B. Gutmann, J.-P. Roduit, D. Roberge, C. O. Kappe, *Angew. Chem. Int. Ed.* **2010**, *49*, 7101–7105.

135. B. Gutmann, T. N. Glasnov, T. Razzaq, W. Goessler, D. M. Roberge, C. O. Kappe, *Beilstein. J. Org. Chem.* **2011**, *7*, 503–517.

136. B. Gutmann, D. Obermayer, J.-P. Roduit, D. M. Roberge, C. O. Kappe, *J. Flow. Chem.* **2012**, *2*, 8–19.

137. M. E. Kopach, M. M. Murray, T. M. Braden, M. E. Kobierski, O. L. Williams, *Org. Process Res. Dev.* **2009**, *13*, 152–160.

138. B. Gutmann, J.-P. Roduit, D. Roberge, C. O. Kappe, *Chem. Eur. J.* **2011**, *17*, 13146–13150.

139. E. F. Scriven, K. Turnbull, *Chem. Rev.* **1988**, *88*, 297–368.

140. S. Bräse, C. Gil, K. Knepper, V. Zimmermann, *Angew. Chem. Int. Ed.* **2005**, *44*, 5188–5240.

141. N. Peet, P. Weintraub, *Chem. Eng. News* **1994**, *72*, 4–4.

142. P. Patnaik, *A comprehensive guide to the hazardous properties of chemical substances*, John Wiley & Sons, **2007**.

143. A. G. O'Brien, F. Levesque, Y. Suzuki, P. H. Seeberger, *Chim. Oggi* **2011**, *29*, 57–+.

144. C. J. Smith, C. D. Smith, N. Nikbin, S. V. Ley, I. R. Baxendale, *Org. Biomol. Chem.* **2011**, *9*, 1927–1937.

145. C. J. Smith, N. Nikbin, S. V. Ley, H. Lange, I. R. Baxendale, *Org. Biomol. Chem.* **2011**, *9*, 1938–1947.

146. F. Stazi, D. Cancogni, L. Turco, P. Westerduin, S. Bacchi, *Tetrahedron Lett.* **2010**, *51*, 5385–5387.

147. M. M. Delville, P. J. Nieuwland, P. Janssen, K. Koch, J. van Hest, F. P. Rutjes, *Chem. Eng. J.* **2011**, *167*, 556–559.

148. E. D. Goddard-Borger, R. V. Stick, *Org. Lett.* **2007**, *9*, 3797–3800.

149. I. R. Baxendale, J. Deeley, C. M. Griffiths-Jones, S. V. Ley, S. Saaby, G. K. Tranmer,

Chem. Commun. **2006**, 2566–2568.

150. P. B. Palde, T. F. Jamison, *Angew. Chem. Int. Ed.* **2011**, *50*, 3525–3528.

151. C. D. Smith, I. R. Baxendale, S. Lanners, J. J. Hayward, S. C. Smith, S. V. Ley, *Org. Biomol. Chem.* **2007**, *5*, 1559–1561.

152. I. R. Baxendale, S. V. Ley, A. C. Mansfield, C. D. Smith, *Angew. Chem. Int. Ed.* **2009**, *48*, 4017–4021.

153. R. Tinder, R. Farr, R. Heid, R. Zhao, R. S. Rarig Jr, T. Storz, *Org. Process Res. Dev.* **2009**, *13*, 1401–1406.

154. A. R. Bogdan, N. W. Sach, *Adv. Synth. Catal.* **2009**, *351*, 849–854.

155. S. B. Ötvös, Á. Georgiádes, I. M. Mándity, L. Kiss, F. Fülöp, *Beilstein. J. Org. Chem.* **2013**, *9*, 1508–1516.

156. J. Vandenbergh, T. Tura, E. Baeten, T. Junkers, *J. Polym. Sci. A Polym. Chem.* **2014**, *52*, 1263–1274.

157. H. R. Sahoo, J. G. Kralj, K. F. Jensen, *Angew. Chem.* **2007**, *119*, 5806–5810.

158. M. Baumann, I. R. Baxendale, S. V. Ley, N. Nikbin, C. D. Smith, J. P. Tierney, *Org. Biomol. Chem.* **2008**, *6*, 1577–1586.

159. M. Baumann, I. R. Baxendale, S. V. Ley, N. Nikbin, C. D. Smith, *Org. Biomol. Chem.* **2008**, *6*, 1587–1593.

160. J. C. Brandt, T. Wirth, *Beilstein. J. Org. Chem.* **2009**, *5*, 30.

161. C. F. Carter, H. Lange, S. V. Ley, I. R. Baxendale, B. Wittkamp, J. G. Goode, N. L. Gaunt, *Org. Process Res. Dev.* **2010**, *14*, 393–404.

162. J. Antes, D. Boskovic, H. Krause, S. Loebbecke, N. Lutz, T. Tuercke, W. Schweikert, *Chem. Eng. Res. Des.* **2003**, *81*, 760–765.

163. G. Panke, T. Schwalbe, W. Stirner, S. Taghavi-Moghadam, G. Wille, *Synthesis* **2003**, *2003*, 2827–2830.

164. L. Ducry, D. M. Roberge, *Angew. Chem. Int. Ed.* **2005**, *44*, 7972–7975.

165. R. Halder, A. Lawal, R. Damavarapu, *Catal. Today* **2007**, *125*, 74–80.

166. A. A. Kulkarni, N. T. Nivangune, V. S. Kalyani, R. A. Joshi, R. R. Joshi, *Org. Process Res. Dev.* **2008**, *12*, 995–1000.

167. J. Shen, Y. Zhao, G. Chen, Q. Yuan, *Chin. J. Chem. Eng.* **2009**, *17*, 412–418.

168. A. A. Kulkarni, V. S. Kalyani, R. A. Joshi, R. R. Joshi, *Org. Process Res. Dev.* **2009**, *13*, 999–1002.

169. S. Braune, P. Pöchlauer, R. Reintjens, S. Steinhofer, M. Winter, O. Lobet, R. Guidat, P. Woehl, C. Guermeur, *Chim. Oggi* **2009**, *27*, 26–29.

170. C. E. Brocklehurst, H. Lehmann, L. La Vecchia, *Org. Process Res. Dev.* **2011**, *15*, 1447–

1453.

171. J. R. Gage, X. Guo, J. Tao, C. Zheng, *Org. Process Res. Dev.* **2012**, *16*, 930–933.

172. Z. Yu, Y. Lv, C. Yu, W. Su, *Org. Process Res. Dev.* **2013**, *17*, 438–442.

173. A. A. Kulkarni, *Beilstein. J. Org. Chem.* **2014**, *10*, 405–424.

174. K. Tanaka, S. Motomatsu, K. Koyama, S.-i. Tanaka, K. Fukase, *Org. Lett.* **2007**, *9*, 299–302.

175. K. Tanaka, K. Fukase, *Beilstein. J. Org. Chem.* **2009**, *5*, 40.

176. V. Hessel, C. Hofmann, H. Löwe, A. Meudt, S. Scherer, F. Schönfeld, B. Werner, *Org. Process Res. Dev.* **2004**, *8*, 511–523.

177. M. A. Kousemaker, K. D. Thiele, *Method for Producing an Oxygen-containing Compound used as Fuel Additive*, **2009**, US 0270643.

178. J.-C. M. Monbaliu, M. Winter, B. Chevalier, F. Schmidt, Y. Jiang, R. Hoogendoorn, M. A. Kousemaker, C. V. Stevens, *Bioresour. Technol.* **2011**, *102*, 9304–9307.

179. M. R. Nanda, Z. Yuan, W. Qin, H. S. Ghaziaskar, M.-A. Poirier, C. C. Xu, *Appl. Energy* **2014**, *123*, 75–81.

180. M. R. Nanda, Z. Yuan, W. Qin, H. S. Ghaziaskar, M.-A. Poirier, C. C. Xu, *Fuel* **2014**, *128*, 113–119.

181. A. A. Kulkarni, K.-P. Zeyer, T. Jacobs, A. Kienle, *Ind. Eng. Chem. Res.* **2007**, *46*, 5271–5277.

182. X. Yao, J. Yao, L. Zhang, N. Xu, *Catal. Lett.* **2009**, *132*, 147–152.

183. R. Becker, K. Koch, P. J. Nieuwland, F. P. J. T. Rutjes, *Chim. Oggi* **2011**, *29*, 47–49.

184. J. W. Swarts, P. Vossenberg, M. H. Meerman, A. E. M. Janssen, R. M. Boom, *Biotechnol. Bioeng.* **2008**, *99*, 855–861.

185. L. L. Woodcock, C. Wiles, G. M. Greenway, P. Watts, A. Wells, S. Eyley, *Biocatal. Biotransform.* **2008**, *26*, 501–507.

186. A. Pohar, I. Plazl, P. Znidarsic-Plazl, *Lab Chip* **2009**, *9*, 3385–3390.

187. P. Znidarsic-Plazl, I. Plazl, *Process Biochem.* **2009**, *44*, 1115–1121.

188. T. McCreedy, N. G. Wilson, *Analyst* **2001**, *126*, 21–23.

189. F. Benito-Lopez, R. M. Tiggelaar, K. Salbut, J. Huskens, R. J. M. Egberink, D. N. Reinhoudt, H. J. G. E. Gardeniers, W. Verboom, *Lab Chip* **2007**, *7*, 1345–1351.

190. T. Razzaq, T. N. Glasnov, C. O. Kappe, *Eur. J. Org. Chem.* **2009**, 1321–1325.

191. D. R. Acke, R. V. Orru, C. V. Stevens, *QSAR Comb. Sci.* **2006**, *25*, 474–483.

192. D. R. Acke, C. V. Stevens, *Org. Process Res. Dev.* **2006**, *10*, 417–422.

193. E. Van Meenen, K. Moonen, D. Acke, C. V. Stevens, *Arkivoc* **2006**, *1*, 31–45.

194. D. R. Acke, C. V. Stevens, B. I. Roman, *Org. Process Res. Dev.* **2008**, *12*, 921–928.

195. B. K. Singh, C. V. Stevens, D. R. Acke, V. S. Parmar, E. V. Van der Eycken, *Tetrahedron Lett.* **2009**, *50*, 15–18.

196. J.-C. Monbaliu, J. Jorda, B. Chevalier, C. Stevens, B. Morvan, *Chim. Oggi* **2011**, *29*, 50–52.

197. K. Ishihara, H. Kurihara, H. Yamamoto, *J. Org. Chem.* **1993**, *58*, 3791–3793.

198. A. R. Hajipour, G. Mazloumi, *Synth. Commun.* **2002**, *32*, 23–30.

199. B. P. Bandgar, V. T. Kamble, V. S. Sadavarte, L. S. Uppalla, *Synlett* **2002**, 735–738.

200. V. K. Yadav, K. G. Babu, M. Mittal, *Tetrahedron* **2001**, *57*, 7047–7051.

201. S. Paul, P. Nanda, R. Gupta, *Molecules* **2003**, *8*, 374–380.

202. V. K. Yadav, K. G. Babu, *J. Org. Chem.* **2004**, *69*, 577–580.

203. M. A. Pasha, K. Manjula, *Indian J. Chem. B* **2008**, *47*, 597–600.

204. R. Ghosh, S. Maiti, A. Chakraborty, *Tetrahedron Lett.* **2004**, *45*, 6775–6778.

205. P. Strazzolini, A. G. Giumanini, G. Verardo, *Tetrahedron* **1994**, *50*, 217–254.

206. B. C. Ranu, S. S. Dey, A. Hajra, *Green Chem.* **2003**, *5*, 44–46.

207. A. J. Crovetti, D. S. Kenney, R. B. Hasbrouck, *Antimicrobial coatings and method using diiodomethyl sulfones*, **1971**, US 3,615,745.

208. F. C. Becker, J. P. Li, *N-substituted maleimides in liquid concentrates*, **1981**, US 4,247,559.

209. R. Baum, H. Schmidt, T. Wunder, C. Savides, *Biocide compositions comprising 3-methylisothiazolin-3-one and a haloalkyl sulphone*, **2010**, US 0,189,811.

210. http://www.dow.com/microbial/applications/ma_t_products.htm.

211. A. Smith, *Topical treatment of fungal or yeast infections using p-tolyl diiodomethyl sulfone*, **1980**, US 4,185,120.

212. W. E. Craig, W. F. Hester, *3,4-dichlorophenylsulfonyl tribromomethane*, **1947**, US 2,484,489.

213. S. Shigematsu, Y. Yamada, I. Kimura, *Herbicide composition*, **1983**, JP 58,128,305.

214. Y. Oishi, T. Watanabe, K. Kusa, M. Kazama, K. Konya, *Diphenylamine derivative and aquatic adhesive life-controlling agent containing said derivative*, **1988**, JP 63,243,067.

215. S. Kondo, T. Higashi, *Photopolymerizable composition and image recording material*, **2005**, EP 1,510,865.

216. R. K. Barr, C. O'Connor, *Imaging methods*, **2007**, US 0,117,042.

217. A. Williamson, C. Geukens, H. Van Aert, K. Heylen, *Method of making a lithographic printing plate*, **2009**, WO 063,024.

218. A. Williamson, J. Loccufier, S. Wynants, K. Heylen, *A lithographic printing plate*, **2008**, EP 2,186,637.

219. M. Suda, C. Hino, *Tetrahedron Lett.* **1981**, *22*, 1997–2000.

220. D. J. Burton, D. M. Wiemers, *J. Fluorine Chem.* **1981**, *18*, 573–582.

221. A. K. Saikia, S. Tsuboi, *J. Org. Chem.* **2001**, *66*, 643–647.

222. W. Farrar, *J. Chem. Soc.* **1956**, 508–513.

223. Z. Ochal, R. Kaminski, *Pol. J. Chem.* **2005**, *49*, 215.

224. K. M. Borys, M. D. Korzyński, Z. Ochal, *Tetrahedron Lett.* **2012**, *53*, 6606–6610.

225. K. M. Borys, M. D. Korzyński, Z. Ochal, *Beilstein. J. Org. Chem.* **2012**, *8*, 259–265.

226. M. Jafarpour, A. Rezaeifard, T. Golshani, *Phosphorus Sulfur Silicon Relat. Elem.* **2011**, *186*, 140–148.

227. B. Li, M. Berliner, R. Buzon, C. K.-F. Chiu, S. T. Colgan, T. Kaneko, N. Keene, W. Kissel, T. Le, K. R. Leeman, B. Marquez, R. Morris, L. Newell, S. Wunderwald, M. Witt, W. J, Z. J. Zhang, Z. L. Zhang, *J. Org. Chem.* **2006**, *71*, 9045–9050.

228. L. A. Wessjohann, W. Brandt, T. Thiemann, *Chem. Rev.* **2003**, *103*, 1625–1647.

229. A. Asai, A. Hasegawa, K. Ochiai, Y. Yamashita, T. Mizukami, *J. Antibiot.* **2000**, *53*, 81–83.

230. A. Asai, T. Tsujita, S. V. Sharma, Y. Yamashita, S. Akinaga, M. Funakoshi, H. Kobayashi, T. Mizukami, *Biochem. Pharm.* **2004**, *67*, 227–234.

231. H. Yamaguchi, A. Asai, T. Mizukami, Y. Yamashita, S. Akinaga, S. Ikeda, Y. Kang, *Proteasome inhibitors*, **2002**, EP 1,166,781.

232. T. Mizukami, A. Asai, Y. Yamashita, R. Katahira, A. Hasegawa, K. Ochiai, S. Akinaga, *UCK14 compounds*, **1997**, US 5,663,298.

233. S. Wang, X. D. Jia, M. L. Liu, Y. Lu, H. Y. Guo, *Bioorg. Med. Chem. Lett.* **2012**, *22*, 5971–5975.

234. D. Sriram, P. Yogeeswari, J. S. Basha, D. R. Radha, V. Nagaraja, *Bioorg. Med. Chem.* **2005**, *13*, 5774–5778.

235. R. Wise, J. M. Andrews, L. J. Edwards, *Antimicrob. Agents Chemother.* **1983**, *23*, 559–564.

236. H. Frieling, S. Bleich, *Eur. Arch. Psy. Clin. N.* **2006**, *256*, 268–273.

237. R. Csuk, M. J. Schabel, Y. von Scholz, *Tetrahedron-Asymmetry* **1996**, *7*, 3505–3512.

238. C. Kaiser, C. L. Zirkle, B. M. Lester, L. Zirngibl, A. Burger, T. J. Della, C. S. Davis, *J. Med. Pharmaceut. Chem.* **1962**, *5*, 1243–&.

239. C. L. Zirkle, C. Kaiser, R. E. Tedeschi, D. H. Tedeschi, *J. Med. Pharmaceut. Chem.* **1962**, *5*, 1265–&.

240. J. Finkelstein, E. Chiang, J. Lee, *J. Med. Chem.* **1965**, *8*, 432–&.

241. J. Finkelstein, E. Chiang, F. M. Vane, J. Lee, *J. Med. Chem.* **1966**, *9*, 319–&.

242. P. Riederer, L. Lachenmayer, G. Laux, *Curr. Med. Chem.* **2004**, *11*, 2033–2043.

243. T. L. Macdonald, K. Zirvi, L. T. Burka, P. Peyman, F. P. Guengerich, *J. Am. Chem. Soc.* **1982**, *104*, 2050–2052.

244. C. L. Shaffer, S. Harriman, Y. M. Koen, R. P. Hanzlik, *J. Am. Chem. Soc.* **2002**, *124*, 8268–8274.

245. G. Wittig, F. Wingler, *Chem. Ber. Recl.* **1964**, *97*, 2146–&.

246. E. P. Blanchard, H. E. Simmons, J. S. Taylor, *J. Org. Chem.* **1965**, *30*, 4321–&.

247. M. E. Kuehne, J. C. King, *J. Org. Chem.* **1973**, *38*, 304–311.

248. Z. L. Song, T. Lu, R. P. Hsung, Z. F. Al-Rashid, C. H. Ko, Y. Tang, *Angew. Chem. Int. Ed.* **2007**, *46*, 4069–4072.

249. P. Valenta, P. J. Carroll, P. J. Walsh, *J. Am. Chem. Soc.* **2010**, *132*, 14179–14190.

250. M. Asano, K. Hashimoto, B. Saito, Z. Shiokawa, H. Sumi, M. Yabuki, M. Yoshimatsu, K. Aoyama, T. Hamada, N. Morishita *et al.*, *Bioorg. Med. Chem.* **2013**, *21*, 5725–5737.

251. D. L. Muck, E. R. Wilson, *J. Org. Chem.* **1968**, *33*, 419–&.

252. V. K. Aggarwal, J. de Vicente, R. V. Bonnert, *Org. Lett.* **2001**, *3*, 2785–2788.

253. G. Mass, A. Müller, *J. Prak. Chem.-Chem. Ztg.* **1998**, *340*, 315–322.

254. M. Wang, M. A. Wang, B. F. Hu, *Chin. Chem. Lett.* **1995**, *6*, 557–558.

255. K. Paulini, H. U. Reissig, *Liebigs. Ann. Chem.* **1991**, 455–461.

256. B. Martin-Vaca, T. Durand-Reville, M. Audouin, H. Rudler, *Synthesis* **1998**, 1534–1538.

257. B. Martín-Vaca, H. Rudler, M. Audouin, M. Nicolas, T. Durand-Réville, B. Vissière, *J. Organomet. Chem.* **1998**, *567*, 119–126.

258. H. Bieräugel, J. M. Akkerman, J. C. Lapierre Armande, U. K. Pandit, *Tetrahedron Lett.* **1974**, 2817–2820.

259. H. Bieräugel, J. M. Akkerman, J. C. Lapierre Armande, U. K. Pandit, *Recl. Trav. Chim. Pays-Bas* **1976**, *95*, 266–269.

260. J. Asunskis, H. Shechter, *J. Org. Chem.* **1968**, *33*, 1164–&.

261. R. P. Wurz, A. B. Charette, *J. Org. Chem.* **2004**, *69*, 1262–1269.

262. T. N. Riley, C. G. Brier, *J. Med. Chem.* **1972**, *15*, 1187–&.

263. C. G. Overberger, T. Nishiyama, *J. Polym. Sci. Pol. Chem.* **1981**, *19*, 311–330.

264. A. Armstrong, J. N. Scutt, *Org. Lett.* **2003**, *5*, 2331–2334.

265. S. Mangelinckx, N. De Kimpe, *Tetrahedron Lett.* **2003**, *44*, 1771–1774.

266. J. Kang, K. S. Kim, *J. Chem. Soc. Chem. Commun.* **1987**, 897–898.

267. S. Bénard, L. Neuville, J. Zhu, *Chem. Commun.* **2010**, *46*, 3393–3395.

268. W. B. Motherwell, G. Begis, D. E. Cladingboel, L. Jerome, T. D. Sheppard, *Tetrahedron* **2007**, *63*, 6462–6476.

269. G. Bégis, D. E. Cladingboel, L. Jerome, W. B. Motherwell, T. D. Sheppard, *Eur. J. Org. Chem.* **2009**, 1532–1548.

270. S. Ishikawa, T. D. Sheppard, J. M. D'Oyley, A. Kamimura, W. B. Motherwell, *Angew. Chem. Int. Ed.* **2013**, *52*, 10060–10063.

271. S. Mangelinckx, N. De Kimpe, *Synlett* **2005**, 1521–1526.

272. B. Denolf, S. Mangelinckx, K. W. Tornroos, N. De Kimpe, *Org. Lett.* **2007**, *9*, 187–190.

273. S. Mangelinckx, S. T. Kadam, E. Semina, G. Callebaut, F. Colpaert, D. De Smaele, N. De Kimpe, *Tetrahedron* **2013**, *69*, 3728–3735.

274. A. de Meijere, S. I. Kozhushkov, A. I. Savchenko, *J. Organomet. Chem.* **2004**, *689*, 2033–2055.

275. C. C. Tsai, I. L. Hsieh, T. T. Cheng, P. K. Tsai, K. W. Lin, T. H. Yan, *Org. Lett.* **2006**, *8*, 2261–2263.

276. D. Declerck, S. Josse, A. N. Van Nhien, D. Postel, *Tetrahedron Lett.* **2009**, *50*, 2171–2173.

277. A. de Meijere, V. Chaplinski, H. Winsel, M. Kordes, B. Stecker, V. Gazizova, A. I. Savchenko, R. Boese, F. Schill, *Chem. Eur. J.* **2010**, *16*, 13862–13875.

278. M. I. Burguete, A. Cornejo, E. Garcia-Verdugo, J. Garcia, M. J. Gil, S. V. Luis, V. Martinez-Merino, J. A. Mayoral, M. Sokolova, *Green Chem.* **2007**, *9*, 1091–1096.

279. M. I. Burguete, A. Cornejo, E. Garcia-Verdugo, M. J. Gil, S. V. Luis, J. A. Mayoral, V. Martinez-Merino, M. Sokolova, *J. Org. Chem.* **2007**, *72*, 4344–4350.

280. L. Delhaye, C. Stevens, A. Merschaert, P. Delbeke, W. Brione, U. Tilstam, A. Borghese, G. Geldhof, K. Diker, A. Dubois, M. Barberis, L. Casarubios, *Org. Process Res. Dev.* **2007**, *11*, 1104–1111.

281. G. Bélanger, M. Doré, F. Ménard, V. Darsigny, *J. Org. Chem.* **2006**, *71*, 7481–7484.

282. N. De Kimpe, R. Verhé, L. De Buyck, N. Schamp, *Chem. Ber.* **1983**, *116*, 3846–3857.

283. H. E. Simmons, R. D. Smith, *J. Am. Chem. Soc.* **1958**, *80*, 5322–5324.

284. H. E. Simmons, R. D. Smith, *J. Am. Chem. Soc.* **1959**, *81*, 4256–4264.

285. J. Furukawa, N. Kawabata, J. Nishimur, *Tetrahedron Lett.* **1966**, 3353–&.

286. S. E. Denmark, J. P. Edwards, *J. Org. Chem.* **1991**, *56*, 6974–6981.

287. J. C. Lorenz, J. Long, Z. Q. Yang, S. Xue, Y. Xie, Y. Shi, *J. Org. Chem.* **2004**, *69*, 327–334.

288. K. Fujii, K. Shiine, T. Misaki, T. Sugimura, *Appl. Organomet. Chem.* **2013**, *27*, 69–72.

289. H. Neville-Webbe, I. Holen, R. Coleman, *Cancer Treat. Rev.* **2002**, *28*, 305–319.

290. M. Caraglia, D. Santini, M. Marra, B. Vincenzi, G. Tonini, A. Budillon, *Endocr. Relat. Cancer* **2006**, *13*, 7–26.

291. A. J. Roelofs, K. Thompson, S. Gordon, M. J. Rogers, *Clin. Cancer Res.* **2006**, *12*, 6222s–6230s.

292. V. Stresing, F. Daubiné, I. Benzaid, H. Mönkkönen, P. Clézardin, *Cancer Lett.* **2007**, *257*, 16–35.

293. D. Santini, S. Galluzzo, B. Vincenzi, G. Schiavon, E. Fratto, F. Pantano, G. Tonini, *Ann. Oncol.* **2007**, *18*, vi164–vi167.

294. D. Kantoci, J. K. Denike, W. J. Wechter, *Synth. Commun.* **1996**, *26*, 2037–2043.

295. K. G. Masschelein, C. V. Stevens, *Tetrahedron Lett.* **2008**, *49*, 4336–4338.

296. O. Marder, F. Albericio, *Chimica Oggi* **2003**, *21*, 35–42.

297. S.-Y. Han, Y.-A. Kim, *Tetrahedron* **2004**, *60*, 2447–2467.

298. C. A. Montalbetti, V. Falque, *Tetrahedron* **2005**, *61*, 10827–10852.

299. E. Valeur, M. Bradley, *Chem. Soc. Rev.* **2009**, *38*, 606–631.

300. A. El-Faham, F. Albericio, *Amino Acids Peptides and Proteins in Organic Chemistry: Building Blocks Catalysis and Coupling Chemistry Volume 3* **2011**, 407–444.

301. A. El-Faham, F. Albericio, *Chem. Rev.* **2011**, *111*, 6557–6602.

302. A. R. Katritzky, X. Lan, J. Z. Yang, O. V. Denisko, *Chem. Rev.* **1998**, *98*, 409–548.

303. S. S. Panda, C. D. Hall, E. Scriven, A. R. Katritzky, *Aldrichimica Acta* **2013**, *46*, 43–55.

304. A. R. Katritzky, T. Narindoshvili, B. Draghici, P. Angrish, *J. Org. Chem.* **2008**, *73*, 511–516.

305. A. R. Katritzky, P. Angrish, E. Todadze, *Synlett* **2009**, *2009*, 2392–2411.

306. A. R. Katritzky, N. E. Abo-Dya, S. R. Tala, K. Gyanda, Z. K. Abdel-Samii, *Org. Biomol. Chem.* **2009**, *7*, 4444–4447.

307. A. R. Katritzky, S. Rachwal, *Chem. Rev.* **2009**, *110*, 1564–1610.

308. A. R. Katritzky, S. Rachwal, *Chem. Rev.* **2011**, *111*, 7063–7120.

309. J. G. Conway, R. C. Andrews, B. Beaudet, D. M. Bickett, V. Boncek, T. A. Brodie, R. L. Clark, R. C. Crumrine, M. A. Leenitzer, D. L. McDougald, B. J. Han, K. Hedeen, P. Y. Lin, M. Milla, M. Moss, H. Pink, M. H. Rabinowitz, T. Tippin, P. W. Scates, J. Selph, S. A. Stimpson, J. Warner, J. D. Becherer, *J. Pharmacol. Exp. Ther.* **2001**, *298*, 900–908.

310. M. H. Rabinowitz, R. C. Andrews, J. D. Becherer, D. M. Bickett, D. G. Bubacz, J. G. Conway, D. J. Cowan, M. Gaul, K. Glennon, M. H. Lambert, M. A. Leesnitzer, D. L. McDougald, M. L. Moss, D. L. Musso, M. C. Rizzolio, *J. Med. Chem.* **2001**, *44*, 4252–4267.

311. C. L. Hinkle, M. J. Mohan, P. Lin, N. Yeung, F. Rasmussen, M. E. Milla, M. L. Moss, *Biochemistry* **2003**, *42*, 2127–2136.

312. S. Schnatterer, D. W. Hawkins, D. Jans, M. Maier, A. Kuhlmann, E. F. Sanwald, M.-T. Thönessen, K. Seeger, *Pesticidal 5-(acylamino) pyrazole derivatives*, **2004**, WO 2004/049803.

313. F. R. Pinacho Crisóstomo, Y. Feng, X. Zhu, K. Welsh, J. An, J. C. Reed, Z. Huang, *Bioorg. Med. Chem. Lett.* **2009**, *19*, 6413–6418.

314. J. Lee, S. Bae, S.-h. Lee, H. Choi, Y. H. Kim, S. J. Kim, G. T. Park, S. K. Moon, D.-H. Kim, S. Lee, S. K. Ahn, N. S. Choi, K. J. Lee, *Bioorg. Med. Chem. Lett.* **2010**, *20*, 6327–6330.

315. W. Shi, H. Ma, Y. Duan, K. Aubart, Y. Fang, R. Zonis, L. Yang, W. Hu, *Bioorg. Med. Chem. Lett.* **2011**, *21*, 1060–1063.

316. A. R. Katritzky, B. E.-D. M. El-Gendy, E. Todadze, A. A. Abdel-Fattah, *J. Org. Chem.* **2008**, *73*, 5442–5445.

317. I. R. Baxendale, S. V. Ley, C. D. Smith, G. K. Tranmer, *Chem. Commun.* **2006**, 4835–4837.

318. P. Watts, C. Wiles, S. J. Haswell, E. Pombo-Villar, P. Styring, *Chem. Commun.* **2001**, 990–991.

319. P. Watts, C. Wiles, S. J. Haswell, E. Pombo-Villar, *Tetrahedron* **2002**, *58*, 5427–5439.

320. O. Flögel, J. D. Codée, D. Seebach, P. H. Seeberger, *Angew. Chem. Int. Ed.* **2006**, *45*, 7000–7003.

321. A. D. Pehere, A. D. Abell, *Tetrahedron Lett.* **2011**, *52*, 1493–1494.

322. A. R. Katritzky, H.-Y. He, K. Suzuki, *J. Org. Chem.* **2000**, *65*, 8210–8213.

323. A. R. Katritzky, M. Wang, H. Yang, S. Zhang, N. G. Akhmedov, *Arkivoc* **2002**, *8*, 134–142.

324. A. R. Katritzky, K. Suzuki, S. K. Singh, *Synthesis* **2004**, 2645–2652.

325. A. R. Katritzky, P. Angrish, K. Suzuki, *Synthesis* **2006**, *2006*, 411–424.

326. M. Peyronneau, M.-T. Boisdon, N. Roques, S. Mazieres, C. Le Roux, *Eur. J. Org. Chem.* **2004**, *2004*, 4636–4640.

327. K. Jayalakshmi, B. T. Gowda, *Z. Naturforsch. A* **2004**, *59*, 491–500.

328. B. Kaboudin, Y. Abedi, *Synthesis* **2009**, *2009*, 2025–2028.

329. M. Barbero, I. Degani, S. Dughera, R. Fochi, P. Perracino, *Synthesis* **1999**, *1999*, 90–93.

330. D. C. Johnson II, T. S. Widlanski, *Tetrahedron Lett.* **2004**, *45*, 8483–8487.

331. S. E. Gibson, K. A. Kaufmann, P. R. Haycock, A. J. White, D. J. Hardick, M. J. Tozer, *Organometallics* **2007**, *26*, 1578–1580.

332. F. Tamaddon, A. Nasiri, S. Farokhi, *Catal. Commun.* **2011**, *12*, 1477–1482.

333. A. Tillack, H. Trauthwein, C. G. Hartung, M. Eichberger, S. Pitter, A. Jansen, M. Beller, *Monatsh. Chem.* **2000**, *131*, 1327–1334.

334. A. R. Katritzky, Q.-H. Long, P. Lue, A. Jozwiak, *Tetrahedron* **1990**, *46*, 8153–8160.

335. M. Nakanishi, C. Minard, P. Retailleau, K. Cariou, R. H. Dodd, *Org. Lett.* **2011**, *13*, 5792–

5795.

336. A. R. Katritzky, N. Shobana, J. Pernak, A. Afridi, W.-Q. Fan, *Tetrahedron* **1992**, *48*, 7817–7822.

337. A. R. Katritzky, P. Angrish, D. Hür, K. Suzuki, *Synthesis* **2005**, *2005*, 397–402.

338. A. Coste, M. Toumi, K. Wright, V. Razafimahaléo, F. Couty, J. Marrot, G. Evano, *Org. Lett.* **2008**, *10*, 3841–3844.

339. D. B. Richardson, M. Simmons, I. Dvoretzky, *J. Am. Chem. Soc.* **1960**, *82*, 5001–5002.

340. G. Taylor, J. Simons, *Can. J. Chem.* **1970**, *48*, 1016–1018.

Curriculum Vitae

Personalia

Van Waes Frederik   °05/05/1987, Gent

Kraaigemstraat 33

9968 Bassevelde

frederikvanwaes@gmail.com

0476 301 245

Education

2005 - 2010   Master in Bioscience Engineering - chemistry and bioprocess technology

Ghent University - greatest distinction

Master thesis:

"*Synthese van tricyclische methanoproline analogen met potentiële antifeedant eigenschappen*"

Promoter: Prof. dr. ir. C. Stevens

1999 - 2005   Mathematics - Sciences

College O.-L.-V.-ten-Doorn - Eeklo

Experience

2014 - ...   R&D Project Leader at Taminco, Gent

2010 - 2014   Doctoral researcher (Aspirant FWO)

"*Micro- and millireactor technology for difficult batch reactions in organic chemistry*"

Promoter: Prof. dr. ir. C. Stevens

Publications in international journals with peer review (A1)

Van Waes, F.E.A.; Seghers, S.; Stevens, C.V., Efficient continuous flow bromination of methyl sulfones and methanesulfonates and continuous synthesis of hypobromite, *J. Flow Chem.*, in press. (IF 2012: 4.09)

Van Waes, F.E.A.; Debrouwer, W.; Heugebaert, T.S.A.; Stevens, C.V., On the discovery and development of tandem 1,4- and 1,2-addition of phosphites to 1-azadienes, *Arkivoc*, **2014**, i, 386-427. (IF 2012: 1.06)

Van Waes, F.E.A.; Drabowicz, J.; Cukalovic, A.; Stevens, C.V., Efficient and catalyst-free condensation of acid chlorides and alcohols using continuous flow, *Green Chem.*, **2012**, 14(10), 2776-2779. (IF 2012: 6.83)

Mortier, P.P.J.; Van Waes, F.E.A.; Masschelein, K.G.R.; Heugebaert, T.S.A.; Stevens, C.V., Synthesis of *N*-vinyl-2,2-bisphosphonoaziridines from 1,1-bisphosphono-2-aza-1,3-dienes, *Tetrahedron Lett.*, **2011**, 52(33), 4273-4276. (IF 2011: 2.40)

Conferences and seminars

14th Belgian Organic Synthesis Symposium (BOSS XIV), July 13-18, **2014**, Louvain-la-Neuve, Belgium

> Poster presentation: Frederik Van Waes, Jeroen De Visscher, Christian V. Stevens.
> *Benzotriazole activation of amino acids using microreactor technology.*

13th International Conference on Microreaction Technology (IMRET13), June 23-25, **2014**, Budapest, Hungary

> Oral presentation: Frederik E.A. Van Waes, Christian V. Stevens.
> *Continuous flow technology for reactions difficult to scale-up.*

17th Sigma-Aldrich Organic Synthesis Meeting, December 5-6, **2013**, Blankenberge, Belgium

13th Belgian Organic Synthesis Symposium (BOSS XIII), July 15-20, **2012**, Leuven, Belgium
> Poster presentation: Frederik Van Waes, Jozef Drabowicz and Christian V. Stevens.
> *Efficient and catalyst-free condensation of acid chlorides and alcohols using continuous flow.*

Flow Chemistry Workshop, May 21-22, **2012**, Dinslaken, Germany

16th Sigma-Aldrich Organic Synthesis Meeting, December 6-7, **2012**, Spa, Belgium

15th Sigma-Aldrich Organic Synthesis Meeting, December 1-2, **2011**, Spa, Belgium

14th Sigma-Aldrich Organic Synthesis Meeting, December 2-3, **2010**, Spa, Belgium